SUBSEA PIPELINE INTEGRITY AND RISK MANAGEMENT

YONG BAI

QIANG BAI

ELSEVIER

Amsterdam • Boston • Heidelberg • London
New York • Oxford • Paris • San Diego
San Francisco • Sydney • Tokyo

Gulf Professional Publishing is an imprint of Elsevier

Gulf Professional Publishing is an imprint of Elsevier
225 Wyman Street, Waltham, MA 02451, USA
The Boulevard, Langford Lane, Kidlington, Oxford, OX5 1GB, UK

First edition 2014

Library of Congress Cataloguing-in-Publication Data
Bai, Yong, author.
Subsea pipeline integrity and risk management / by Yong Bai, Qiang Bai. – First edition.
pages cm
Summary: "In most subsea developments, oil and gas productions are transported from subsea well to platform in multiphase flow without separation process. Corrosion represents increasing challenges for the operation of subsea pipelines. Corrosion can be defined as a deterioration of a metal, due to chemical or electrochemical between the metal and its environment. The tendency of a metal to corrode depends on a given environment and the metal type"– Provided by publisher.
Includes bibliographical references and index.
ISBN 978-0-12-394432-0 (hardback)
1. Underwater pipelines–Corrosion. 2. Underwater pipelines–Design and construction. 3. Offshore structures–Design and construction. 4. Offshore oil well drilling–Safety measures. 5. Offshore oil industry–Risk management. I. Bai, Qiang, author. II. Title.
TC1800.B354 2014
621.8'67209162–dc23
2013047933

British Library Cataloguing in Publication Data
A catalogue record for this book is available from the British Library

For information on all Gulf Professional publications
Visit our web site at store.elsevier.com

Printed and bound in USA
14 15 16 17 18 10 9 8 7 6 5 4 3 2 1

ISBN: 978-0-12-394432-0

FOREWORD

I am delighted to write a brief Foreword to this extensive handbook for subsea pipeline integrity and risk management. It is often a challenge to find a single book that discusses all aspects of subsea pipeline integrity and risk management in sufficient detail that the practicing engineer can have this book or volume of books as a desk reference for a large range of subsea topics, instead of the engineer having to search for specific subject matter in Conference Proceedings. And the authors have succeeded in accomplishing just that. The effort it took in writing well over a 450 pages of text and formulae and cross-checking was truly a labor of love and dedication to the profession of subsea pipeline engineers, and for those readers who wish to know more about a particular subject, the list of references at the end of each chapter is truly outstanding.

Frans Kopp, January 2014

PREFACE

It has been 8 years since our book "Subsea Pipelines and Risers" (SPR) was published by Elsevier. As a new sister book of "Subsea Pipeline Design, Analysis and Installation", this new book "Subsea Pipeline Integrity and Risk Management" reflects upon the new pipeline technologies in integrity and risk management developed by the oil and gas industry, where the authors apply them in design, consulting and integrity management. This book is written for engineers who work in the field of subsea pipeline engineering.

Pipeline integrity management has become matured and applied to the operation and maintenance. Risk and reliability management of pipelines became ever more critical in the subsea industry for QRA assessment, risk and environmental impact study as well as preparation of emergency response plans. The risk and reliability assessment has also been successfully applied for the determination of partial safety factors in design criteria.

The industry has been seeking new tools for subsea pipeline inspection and integrity management, whether the pig launchers are available or not. The authors have been also involved in the development of new tools for non-piggable pipelines, flexible pipelines and composite RTP pipelines.

We hope that these two books (Subsea Pipeline Design, Analysis and Installation, and Subsea Pipeline Integrity and Risk Management) are useful reference sources of subsea pipeline design, analysis, installation, integrity management and risk management for subsea engineers.

The authors would like to thank our graduate students, PhD and post-doctoral fellows at Zhejiang University and Harbin Engineering University, who provided editing assistance (Mr. Jiwei Tang, Mr. Carl Bai & Mr. Akira Bai) and initial technical writing (Mr. Gao Tang, Ms. Yin Zhang, Mr. Shiliang He, Mr. Hongdong Qiao, Mr. Weidong Ruan, Mr. Hui Shao, and Ms. Shahirah Abu Baka), thank Zhejiang University for their support for publishing this book.

Thanks to all the persons involved in reviewing and updating the books, particularly Ms. Anusha Sambamoorthy of Elsevier, who provided editory assistance. We specially thank our families and friends for their supports.

Dr. Qiang Bai & Prof. Yong Bai
Houston, USA

CHAPTER 1

Corrosion and Corroded Pipelines

Contents

1. Introduction 3
2. Corrosion Defect Prediction 4
   - Introduction 4
   - Sweet: Carbon Dioxide Corrosion 5
   - Sour: Hydrogen Sulfide Corrosion 6
   - Inspection for Corrosion Defects 7
   - Corrosion Defect Growth 7
   - Corrosion Predictions 8
     - *CO_2 Corrosion Models Comparison* 10
     - *Sensitivity Analysis for CO_2 Corrosion Calculation* 11
3. Remaining Strength of Corroded Pipe 18
   - NG-18 Criterion 18
   - B31G Criterion 19
     - *Maximum Allowable Design Pressure* 19
     - *Maximum Allowable Defect Length and Depth* 20
     - *The Safe Maximum Pressure Level* 20
   - Evaluation of Existing Criteria 21
   - Corrosion Mechanism 21
     - *Spiral Corrosion* 22
     - *Pits Interaction* 23
     - *Groove Interactions* 23
     - *Corrosion in Welds* 23
     - *Effect of Corrosion Width* 24

References 24

1. INTRODUCTION

In most subsea developments, oil and gas production is transported from the subsea well to a platform in multiphase flow without a separation process. Corrosion represents increasing challenges for the operation of subsea pipelines. *Corrosion* can be defined as a deterioration of a metal due to chemical or electrochemical reactions between the metal and its environment. The tendency of a metal to corrode depends on a given environment and the metal type.

The presence of carbon dioxide (CO_2), hydrogen-sulfide (H_2S), and free water in the production fluid can cause severe corrosion problems in oil and

Subsea Pipeline Integrity and Risk Management
ISBN 978-0-12-394432-0
http://dx.doi.org/10.1016/B978-0-12-394432-0.00001-9

gas pipelines. Internal corrosion in wells and pipelines is influenced by temperature, CO_2 and H_2S content, water chemistry, flow velocity, oil or water wetting, and the composition and surface condition of the steel. Corrosion-resistant alloys, such as 13% Cr steel and duplex stainless steel, are often used in downhole piping of subsea equations and structures. However, for long-distance pipelines, carbon steel is the only economically feasible alternative and corrosion has to be controlled and the flowline protected from the corrosion both internally and externally.

This chapter develops prediction models of corrosion defects and the reliability based design and requalification criteria for assessing corroded pipelines. This evaluation focuses on the following interrelated issues:

- Corrosion defect growth.
- Checking burst strength (allowable versus maximum internal service pressure).
- Checking bending capacity (allowable versus maximum external service pressure, bending moment, and axial load).
- Checking adequacy of residual corrosion allowance for remaining service life.
- Inspecting corrosion defects.
- Updated inspection and maintenance programs.

2. CORROSION DEFECT PREDICTION

Introduction

Two types of corrosions may occur in the oil and gas pipeline system when CO_2 and H_2S are present in the hydrocarbons fluid: sour corrosion and sweet corrosion. Sweet corrosion occurs in systems containing only carbon dioxide or a trace of hydrogen sulfide (H_2S partial pressure < 0.05 psi). Sour corrosion occurs in systems containing hydrogen sulfide above a partial pressure of 0.05 psia (0.34 kPa) and carbon dioxide.

When corrosion products are not deposited on the steel surface, very high corrosion rates of several millimeters per year (mm/yr) can occur. This "worst case" corrosion is the easiest type to study and reproduce in the laboratory. When CO_2 dominates the corrosivity, the corrosion rate can be reduced substantially under conditions where iron carbonate can precipitate on the steel surface and form a dense and protective corrosion product film. This occurs more easily at high temperatures or high pH values in the water phase. When H_2S is present in addition to CO_2, iron sulfide films are formed rather than iron carbonate, and protective films can be formed at

lower temperatures, since iron sulfide precipitates much more easily than iron carbonate. Localized corrosion with very high corrosion rates can occur when the corrosion product film does not give sufficient protection, and this is the most feared type of corrosion attack in oil and gas pipelines.

Sweet: Carbon Dioxide Corrosion

Carbon dioxide is composed of one atom of carbon with two atoms of oxygen. It is a corrosive compound found in natural gas, crude oil, condensate, and produced water. It is one of the most common environments in the oil field industry where corrosion occurs. The CO_2 corrosion is enhanced in the presence of both oxygen and organic acids, which can dissolve iron carbonate scale and prevent further scaling.

Carbon dioxide is a weak acidic gas and becomes corrosive when dissolved in water. However, CO_2 must hydrate to carbonic acid, H_2CO_3, which is a relatively slow process, before it becomes acidic. Carbonic acid causes a reduction in the pH of water and results in corrosion when it comes in contact with steel.

Areas where CO_2 corrosion is most common include flowing wells, gas condensate wells, areas where water condenses, tanks filled with CO_2, saturated produced water, and pipelines, which are generally corroded at a slower rate because of lower temperatures and pressures. The CO_2 corrosion is enhanced in the presence of both oxygen and organic acids, which can act to dissolve iron carbonate scale and prevent further scaling.

The maximum concentration of dissolved CO_2 in water is 800 ppm. When CO_2 is present, the most common forms of corrosion include uniform corrosion, pitting corrosion, wormhole attack, galvanic ringworm corrosion, heat affected corrosion, mesa attack, raindrop corrosion, erosion corrosion, and corrosion fatigue. The presence of carbon dioxide usually means no H_2 embrittlement.

Rates of CO_2 corrosion are greater than the effect of carbonic acid alone. Corrosion rates in a CO_2 system can reach very high levels (thousands of millions per year), but it can be effectively inhibited. Velocity effects are very important in the CO_2 system: Turbulence is often a critical factor in pushing a sweet system into a corrosive regime. This is because it either prevents formation or removes a protective iron carbonate (siderite) scale.

Products of CO_2 corrosion include iron carbonate (siderite, $FeCO_3$), iron oxide, and magnetite. Corrosion product colors may be green, tan, or brown to black. This can be protective under certain conditions. Scale itself can be soluble. Conditions favoring the formation of a protective scale are

elevated temperatures, increased pH as occurs in bicarbonate-bearing waters, and lack of turbulence, so that the scale film is left in place. Turbulence is often the critical factor in the production or retention of a protective iron carbonate film. Iron carbonate is not conductive. Therefore, galvanic corrosion cannot occur. Therefore, corrosion occurs where the protective iron carbonate film is not present and is fairly uniform over the exposed metal. Crevice and pitting corrosion occur when carbonate acid is formed. Carbon dioxide can also cause embrittlement, resulting in stress corrosion cracking.

Sour: Hydrogen Sulfide Corrosion

Hydrogen sulfide is a flammable and poisonous gas. It occurs naturally in some groundwater. It is formed from decomposing underground deposits of organic matter, such as decaying plant material. It is found in deep or shallow wells and also can enter surface water through springs, although it quickly escapes to the atmosphere. Hydrogen sulfide often is present in wells drilled in shale or sandstone or near coal or peat deposits or oil fields.

Hydrogen sulfide gas produces an offensive "rotten egg" or "sulfur water" odor and taste in water. In some cases, the odor may be noticeable only when the water is initially turned on or when hot water is run. Heat forces the gas into the air, which may cause the odor to be especially offensive in a shower. Occasionally, a hot water heater is a source of hydrogen sulfide odor. The magnesium corrosion control rod present in many hot water heaters can chemically reduce naturally occurring sulfates to hydrogen sulfide.

Hydrogen sulfide (H_2S) occurs in approximately 40% of all wells. Wells with large amounts of H_2S are usually labeled *sour*; however, only wells with 10 ppm or above can be labeled *sour*. Partial pressures above 0.05psi H_2S are considered corrosive. The amount of H_2S appears to increase as the well grows older. The H_2S combines with water to form sulfuric acid (H_2SO_4), a strongly corrosive acid. Corrosion due to H_2SO_4 is often referred to as *sour corrosion*. Since hydrogen sulfide combines easily with water, damage to stock tanks below water levels can be severe.

Water with hydrogen sulfide alone does not cause disease. However, hydrogen sulfide forms a weak acid when dissolved in water. Therefore, it is a source of hydrogen ions and is corrosive. It can act as a catalyst in the absorption of atomic hydrogen in steel, promoting sulfide stress cracking (SSC) in high strength steels. Polysulfides and sulfanes (free acid forms of polysulfides) may be formed when hydrogen sulfide reacts with elemental sulfur.

The corrosion products are iron sulfides and hydrogen. Iron sulfide forms a scale at low temperatures and can act as a barrier to slow corrosion. The absence of chloride salts strongly promotes this condition, and the absence of oxygen is absolutely essential. At higher temperatures, the scale is cathodic in relation to the casing, and galvanic corrosion starts. The chloride forms a layer of iron chloride, which is acidic and prevents the formation of FeS layer directly on the corroding steel, enabling the anodic reaction to continue. The hydrogen produced in the reaction may lead to hydrogen embrittlement. A nuisance associated with hydrogen sulfide includes its corrosiveness to metals such as iron, steel, copper, and brass. It can tarnish silverware and discolor copper and brass utensils.

Inspection for Corrosion Defects

The scope of the assessment for corrosion defects consists of a proper characterization of defects by thickness profile measurements and an initial screening phase to decide whether detailed analysis is required.

The assessment of a single isolated defect is to be based on a critical profile defined by the largest measured characteristic dimensions of the defect (e.g., depth, width, length) and properly calibrated safety and uncertainty factors, to account for uncertainties in the assessment and thickness measurements.

A distance equivalent to the normal pipe wall thickness may be used as a simple criterion of separation for colonies of longitudinally oriented pits separated by a longitudinal distance or parallel longitudinal pits separated by a circumferential distance. For longitudinal grooves inclined to the pipe axis,

- If the distance, x, between two longitudinal grooves of length L_1 and L_2 is greater than either L_1 or L_2, then the length of corrosion defect L is L_1 or L_2, whichever is greater. It can be assumed that there is no interaction between the two defects.
- If the distance, x, between two longitudinal grooves of length L_1 and L_2 is less than either L_1 or L_2, it is assumed that the two defects are fully interacted and the length of the corrosion defect L is to be taken as $L = L_1 + L_2 + x$.

Corrosion Defect Growth

The corrosion defect depth, d, after the time, T, of operation may be estimated by using an average corrosion rate, V_{cr}:

$$d = d_0 + V_{cr} \cdot T \qquad [1.1]$$

where d_0 is defect depth at present time.

The defect length may be assumed to grow in proportion with the depth, hence:

$$L = L_0\left(1 + \frac{V_{\text{cr}} \cdot T}{d_0}\right) \qquad [1.2]$$

where L and L_0 are defect lengths at the present time and the time T later.

Corrosion Predictions

The CO_2 corrosion of carbon steel used in oil production and transportation, when liquid water is present, is influenced by a large number of parameters, some of which follow:

- Temperature.
- CO_2 partial pressure.
- Flow (flow regime and velocity).
- pH.
- Concentration of dissolved corrosion product ($FeCO_3$).
- Concentration of acetic acid.
- Water wetting.
- Metal microstructure (welds).
- Metal prehistory.

The detailed influence of these parameters is still poorly understood and some of them are closely linked to each other. A small change in one of them may influence the corrosion rate considerably.

Various prediction models have been developed and are used by different companies. Among them are the de Waard et al. model (Shell), CORMED (Elf Aquitaine), LIPUCOR (Total), and a new electrochemically based model developed at IFE. Due to the complexity of the various corrosion controlling mechanisms involved and a built-in conservatism, the corrosion models often overpredict the corrosion rate of carbon steel.

The Shell model for CO_2 corrosion is most commonly used in oil and gas industry. The model is mainly based on the de Waard et al.'s equation published in 1991 [1]. Starting from a "worst case" corrosion rate prediction, the model applies correction factors to quantify the influence of environmental parameters and corrosion product scale formed under various conditions. However, the first version of the model was published in 1975, and it has been revised several times to make it less conservative by including new knowledge and information. The original formula of de

Waard and Milliams implied certain assumptions that necessitated the application of correction factors for the influence of environmental parameters and for the corrosion product scale formed under various conditions.

Rates of CO_2 corrosion in pipelines made of carbon steel may be evaluated using industry accepted equations, which preferably combine contributions from flow-independent kinetics of the corrosion reaction at the metal surface, with the contribution from flow-dependent mass transfer of dissolved CO_2.

The corrosion rate calculated from the original formula with its correction factors is independent of the liquid velocity. To account for the effect of flow, a new model was proposed, which takes the effect of mass transport and fluid velocity into account by means of a so-called resistance model:

$$V_{cr} = \frac{1}{\frac{1}{V_r} + \frac{1}{V_m}} \quad [1.3]$$

where the corrosion rate V_{cr} is in mm/year; V_r is the flow-independent contribution, denoted the reaction rate; and V_m is the flow-dependent contribution, denoted the mass transfer rate.

In multiphase turbulent pipeline flow, V_m depends on the velocity and the thickness of the liquid film, while V_r depends on the temperature, CO_2 pressure, and pH. For example, for pipeline steel containing 0.18% C and 0.08% Cr, the equations for V_r and V_m for liquid flow in a pipeline are

$$\log(V_r) = 4.93 - \frac{1119}{T_{mp} + 273} + 0.58 \cdot \log\left(p_{CO_2}\right) \quad [1.4]$$

where T_{mp} is pipeline fluid temperature in °C, and the partial pressure p_{CO_2} of CO_2 is in bar. The partial pressure p_{CO_2} can be found by

$$p_{CO_2} = n_{CO_2} \cdot p_{opr} \quad [1.5]$$

where n_{CO_2} is the fraction of CO_2 in the gas phase, and p_{opr} is the operating pressure in bar.

The mass transfer rate V_m, is approximated by

$$V_m = 2.45 \cdot \frac{U^{0.8}}{d^{0.2}} \cdot p_{CO_2} \quad [1.6]$$

where U is the liquid flow velocity in m/s, and d is the inner diameter in m.

CO_2 Corrosion Models Comparison

The corrosion caused by the incidences of CO_2 represents the greatest risk to the integrity of carbon steel equipment in a production environment and is more common than damage related to fatigue, erosion, or stress corrosion cracking. NORSOK, Shell, as well as other companies and organizations have developed models to predict the corrosion degradation.

NORSOK's standard M-506 may be used to calcuate the CO_2 corrosion rate which is an empirical model for carbon steel in water containing CO_2 at different temperatures, pH, $CO_{2fugacity}$, and wall shear stress. The NORSOK model covers only the corrosion rate calculation where CO_2 is the corrosive agent. It does not include additional effects of other constituent, which may influence the corrosivity, such as H_2S, which commonly appears in the production flowlines. If such constituent is present, the effect must be evaluated separately. None of the de Waard et al. models includes the H_2S effect.

Figure 1.1 shows an example of corrosion rate prediction in a subsea gas condensate pipeline. Here, two of the most commonly used corrosion prediction models were combined with a three-phase fluid flow model to calculate corrosion rate profiles along a pipeline. This can help identify locations where variation in flow regime, flow velocity, and water accumulation may increase the risk of corrosion damage. For this pipeline, the temperature was 90°C at the inlet and 20°C at the outlet, and the decrease in predicted corrosion rates toward the end of the pipeline is mainly a result of the decreasing temperature. The lower corrosion rates close to the

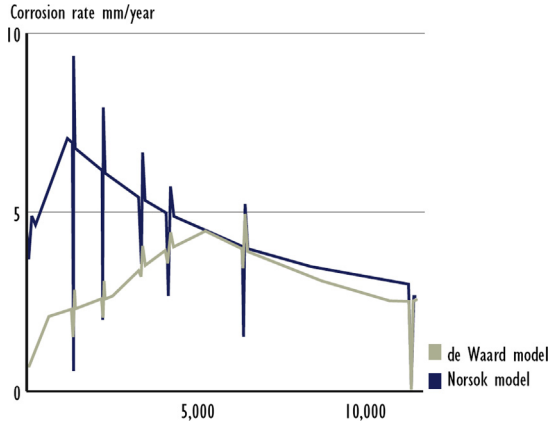

FIGURE 1.1 ***Predicted Corrosion Rate in a Subsea Pipeline.*** *Source: Nyborg [2].* (For color version of this figure, the reader is referred to the online version of this book.)

pipeline inlet are due to the effect of protective corrosion films at high temperatures, which is predicted differently by the two corrosion models used. The peaks in predicted corrosion rates result from variation in flow velocity due to variations in the pipeline elevation profile.

Sensitivity Analysis for CO_2 Corrosion Calculation

Table 1.1 presents the base case for the following sensitivity analysis. These data are based on the design operating data for a 10 in. production flowline.

Total System Pressure and CO_2 Partial Pressure

An increase in total pressure leads to an increase in corrosion rate because p_{CO_2} increases in proportion. With increasing the pressure, the CO_2 fugacity f_{CO_2}, should be used instead of the CO_2 partial pressure, p_{CO_2}, since the gases are not ideal at high pressures. The real CO_2 pressure can be expressed as

$$f_{CO_2} = a * p_{CO_2} \quad [1.7]$$

where a is fugacity constant, which depends on pressure and temperature, such as the following:

$$a = 10^{P(0.0031-1.4/T)} \text{ for } P \leq 250 \text{ bar}$$

$$a = 10^{250(0.0031-1.4/T)} \text{ for } P > 250 \text{ bar}$$

Figures 1.2 and 1.3 present the effect of total pressure and CO_2 partial pressure on the corrosion rate, respectively. With increasing the total pressure and CO_2 partial pressure, the corrosion rate is greatly increased.

Table 1.1 Base Case for Sensitivity Analysis

Parameter	Units	Base Case
Total pressure	bar	52
Temperature	°C	22.5
CO_2 in gas	Mole %	0.5
Flow velocity	m/s	2.17
H_2S	ppm	220
pH	[—]	4.2
Water cut	[—]	50%
Inhibitor availability	[—]	50%

System Temperature

Temperature has the effect of the formation of protective film. At lower temperatures, the corrosion product can be easily removed by flowing liquid. At higher temperatures, the film becomes more protective and less

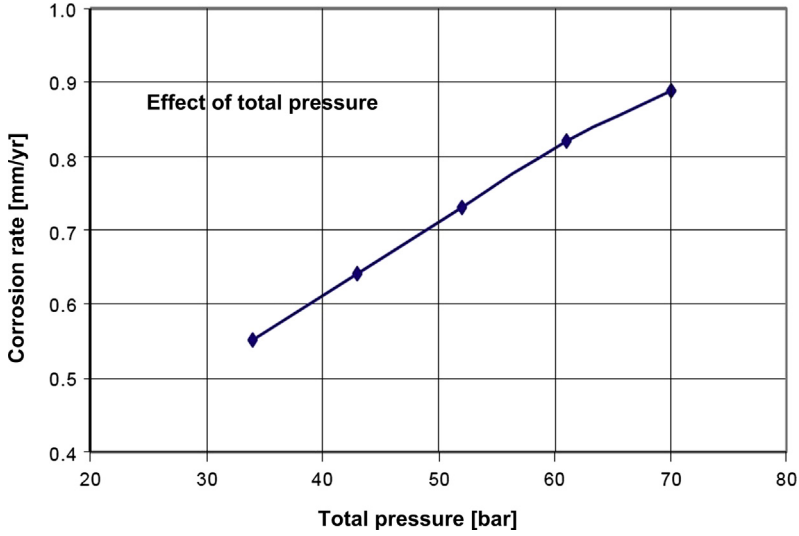

FIGURE 1.2 ***Effect of Total Pressure on the Corrosion Rate.*** (For color version of this figure, the reader is referred to the online version of this book.)

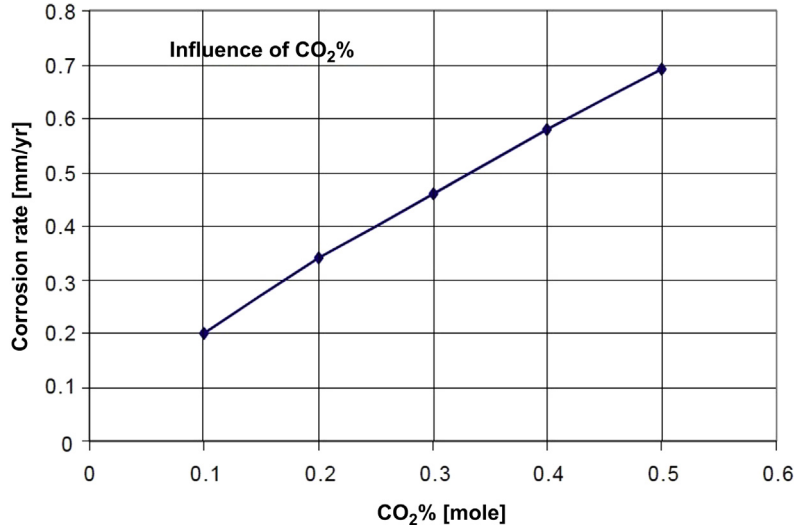

FIGURE 1.3 ***Effect of CO_2 on the Corrosion Rate.*** (For color version of this figure, the reader is referred to the online version of this book.)

easily washed away. Further increase in temperature results in a lower corrosion rate and the corrosion rate goes through a maximum [1]. This temperature is referred as the scaling temperature. At this temperature, pH and Fe++ concentration form at the steel's surface. At temperatures exceeding the scaling temperature, the corrosion rates tend to decrease to close to zero, according to De Waard et al. Tests in IFE Norway reveal that the corrosion rate is still increasing when the design temperature is beyond the scaling temperature [3].

Figure 1.4 shows the effect of temperature on the corrosion rate, where the total pressure is 48 bar and the pH is equal to 4.2. The corrosion rate increases with increasing the temperature, when the temperature is lower than the scaling temperature.

H_2S

Hydrogen sulfide can depress pH when it dissolves in a CO_2 aqueous solution. The presence of H_2S in CO_2-brine systems can reduce the corrosion rate of steel when compared to the corrosion rate without H_2S at temperatures less than 80°C, due to the formation of a meta-stable iron sulfide film. At higher temperatures, the combination of H_2S and chlorides produce higher corrosion rates than just the CO_2-brine system, since the protective film is not formed.

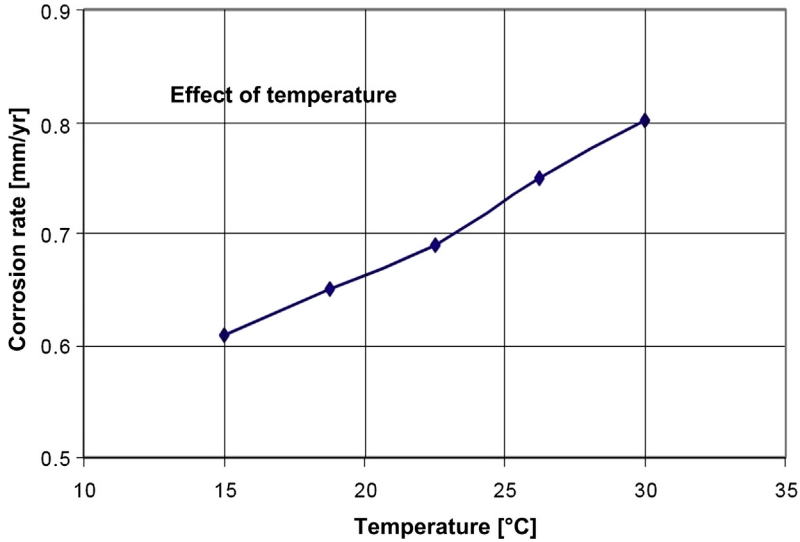

FIGURE 1.4 ***Effect of Temperature on the Corrosion Rate.*** (For color version of this figure, the reader is referred to the online version of this book.)

The H_2S at levels below the NACE criteria for sulfide stress corrosion cracking (per MR0175, NACE publication) reduces general metal loss rates but can promote pitting. The pitting proceeds at a rate determined by the CO_2 partial pressure and therefore CO_2-based models are still applicable at low levels of H_2S. Where the H_2S concentration is greater or equal to the CO_2 value or greater than 1 mol %, the corrosion mechanism may not be controlled by CO_2 and therefore CO_2-based models may not be applicable.

pH

The pH affects the corrosion rate by affecting the reaction rate of cathodes and anodes, therefore, the formation of corrosion products. The contamination of a CO_2 solution with corrosion products reduces the corrosion rate. The pH has a dominant effect on the formation of corrosion films, due to its effect on the solubility of ferrous carbonate. An increase in pH slows down the cathodic reduction of H^+. Figure 1.5 presents the relationship between the pH and corrosion rate. In a solution with a pH less than 7, corrosion rate decreases with increasing pH.

Inhibitors and Chemical Additives

Inhibitors can reduce the corrosion rate by presenting a protective film. The presence of the proper inhibitors with optimum dosage can maintain the

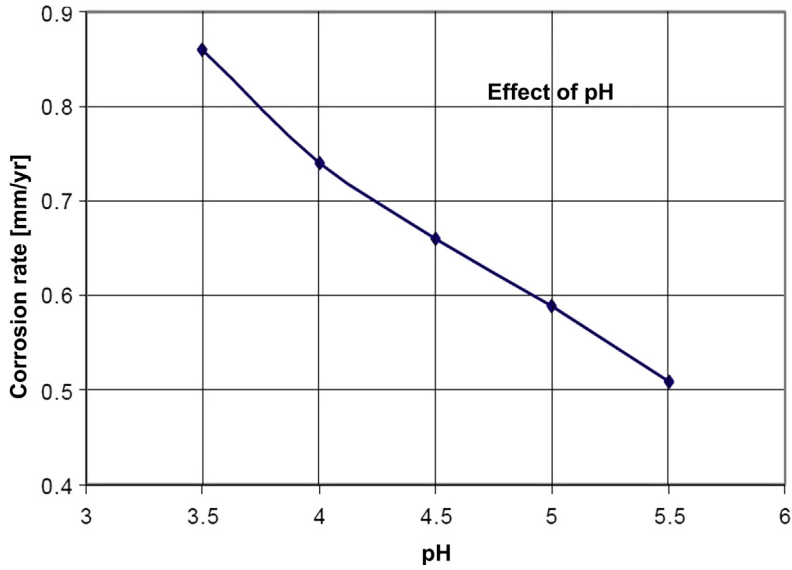

FIGURE 1.5 ***Effect of pH on Corrosion Rate.*** (For color version of this figure, the reader is referred to the online version of this book.)

corrosion rate at 0.1 mm/year. Use of inhibitors can greatly decrease corrosion rate and, therefore, increase pipeline life.

The impingement of sand particles can destroy the inhibitor film and, therefore, reduce the inhibitor efficiency. Inhibitors also perform poorly in low-velocity lines, particularly if the fluids contain solids, such as wax, scale, or sand. Under such circumstances, deposits inevitably form at the 6 o'clock position, preventing the inhibitor from reaching the metal surface. Flow velocities below approximately 1.0 m/s should be avoided if inhibitors are expected to provide satisfactory protection, and this is critical in lines containing solids.

Inhibitor Efficiency versus Inhibitor Availability

When inhibitors are applied, there are two ways to describe the extent to which an inhibitor reduces the corrosion rate, the use of inhibitor efficiency (IE) and the use of the inhibitor availability (IA). A value of 95% for IE is commonly used. However, inhibitors are unlikely to be constantly effective throughout the design life. For instance, increased inhibitor dosage or better chemicals increase the inhibitor concentration. It may be assumed that the inhibited corrosion rate is unrelated to the uninhibited corrosivity of the system, and all systems can be inhibited to 0.1 mm/year. The corrosion inhibitor is not available 100% of the time and therefore corrosion will proceed at the uninhibited rate for some periods.

Figure 1.6 shows the inhibited corrosion rate under different inhibitor availability. The lines are based on the assumed existence of corrosion inhibitors that can protect the steel to a corrosion rate CRmit (typically 0.1 mm/year) regardless of the uninhibited corrosion rate CRunmit, taking into consideration the percentage of time IA the inhibitor is available.

Chemical Additives

Glycol (or methanol) is often used as the hydrate preventer on a recycled basis. If glycol is used without the addition of a corrosion inhibitor, there is some benefit from the glycol. De Waard et al. produced a glycol correction factor. However, if glycol and inhibitor are both used, little additional benefit accrues from the glycol and it should be ignored for design purpose.

Methanol is batch injected during startup until the flowline temperatures rise above the hydrate formation region and during extended shutdown.

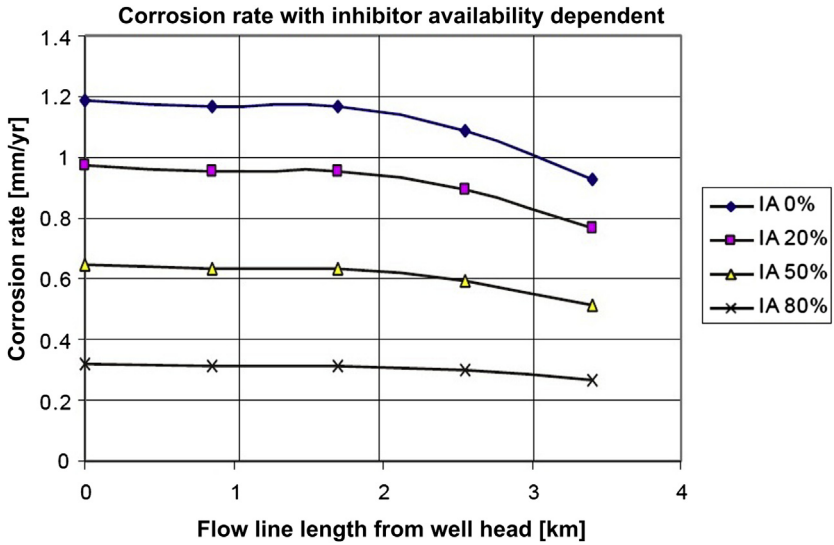

FIGURE 1.6 ***Inhibited Corrosion Rate under different Inhibitor Availabilities.*** (For color version of this figure, the reader is referred to the online version of this book.)

Single-Phase Flow Velocity

Single-phase flow refers to a flow with only one component, normally oil, gas, or water through a porous media. Fluid flow influences corrosion by affecting mass transfer and the mechanical removal of solid corrosion products. The flow velocity used in corrosion model is identified as the true water velocity. Figure 1.7 shows that the corrosion rate increases consistently with increased flow rate at low pH values.

Multiphase Flow

Multiphase flow refers to the simultaneous flow of more than one fluid phase through a porous media. Most oil wells ultimately produce both oil and gas from the formation and often produce water. Consequently, multiphase flow is common in oil wells. The multiphase flow in a pipeline is usually studied by flow regime and corresponding flow rate. Because of the various hydrodynamics and the corresponding turbulence, multiphase flow further influences the internal corrosion rate, in a significantly different way than the influence of single-phase flow in the pipeline.

Water Cut

Water cut means the ratio of water produced compared to the volume of total liquid produced. Corrosion from CO_2 is mainly caused by water in contact with the steel surface. The severity of the CO_2 corrosion is proportional to

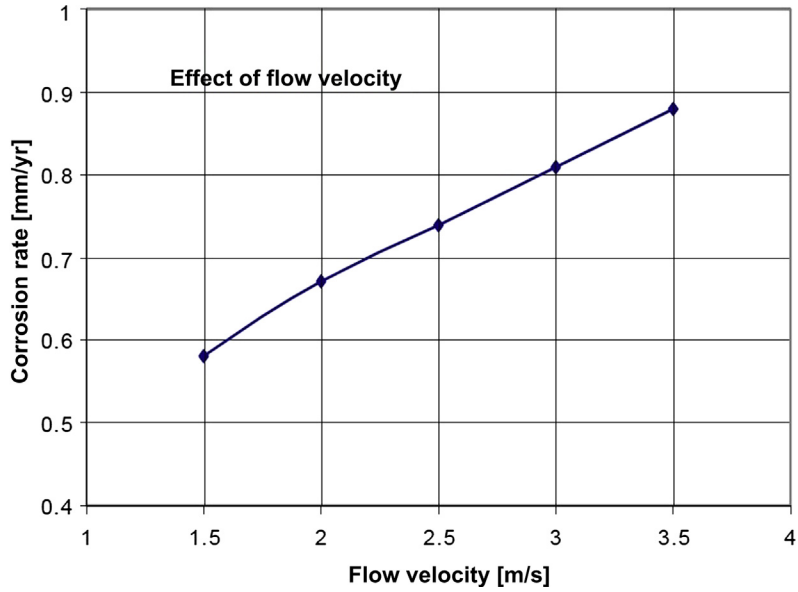

FIGURE 1.7 ***Effect of Flow Velocity on the Corrosion Rate.*** (For color version of this figure, the reader is referred to the online version of this book.)

the time during which the steel surface is wet in the water phase. Thus, the water cut is an important factor to influence the corrosion rate. However, the effect of the water cut cannot be separated from the flow velocity and the flow regime.

Free-Span Effect

Pipeline spanning can occur on a rough seabed or a seabed subjected to scouring. The evaluation of allowable free-span length should be considered to avoid the excessive yielding and fatigue. The localized reduction of wall thickness influences the strength capacity of the pipeline, therefore, the allowable free-span length. This is discussed in many reports and papers. It is not within the scope of work for this chapter to assess yielding and fatigue of free spans. Instead, a qualitative discussion is given on possible development or acceleration of the development of corrosion.

Figure 1.8 shows at the middle point of the free spans. Additional accumulated waters and marine organism may accelerate corrosion development. The flow regime and flow rates change. The corrosion defect depth in the region close to the middle point is most likely deeper.

These three corrosion models were developed based on the results of tests using water-only, that is, a 100% water cut, system in the laboratory.

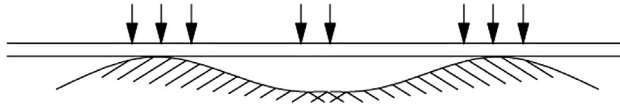

FIGURE 1.8 *Effect of Free Spans on Corrosion Defect Development.*

Therefore, the corrosion rate predicted with these models represents the worst case corrosion rates. For comparison, the corrosion rate under the flow condition with smaller water cut is generally lower than the worst case rate. Therefore, the predictoion of corrosion rates with these models is very conservative compared to the real corrosion rate in the field. With more corrosion data from pipeline pigging, the accuracy of corrosion rate prediction can be improved. However, the accuracy of corrosion rate prediction still cannot be exaggerated, since the internal corrosion is influenced by numerous parameters, as already discussed. The combination of the corrosion rate prediction method and the pipeline pigging method can provide a benchmark to pinpoint the weakest links in the pipeline, predict the remaining life, and maintain the pipeline integrity.

3. REMAINING STRENGTH OF CORRODED PIPE

The design criteria for corroded pipelines are generally expressed as equations to determine the operating parameters:

- Maximum allowable length of defects.
- Maximum allowable design pressure for uncorroded pipelines.
- Maximum safe pressure.

A number of criteria exist to determine these operating parameters.

NG-18 Criterion

The NG-18 criterion developed in the late 1960s and early 1970s is used to evaluate the remaining strength of corroded pipe [4]. It was developed for a pipe with a longitudinal surface flaw:

$$S_p = S_{flow}\frac{1-\left(\mathrm{AREA}/\mathrm{AREA}_0\right)}{1-M^{-1}\left(\mathrm{AREA}/\mathrm{AREA}_0\right)} \qquad [1.8]$$

where

S_p = predicted hoop stress level at failure

S_{flow} = flow stress of the material

AREA = area of through thickness profile of flaw
$AREA_0 = Lt$
L = maximum axial extent of the defect
t = nominal wall thickness of the pipe
M = Folias factor, which is determined by

$$M = \sqrt{1 + \frac{2.51\left(L/2\right)^2}{Dt} - \frac{0.054\left(L/2\right)^4}{\left(Dt\right)^2}} \quad [1.9]$$

where
D = nominal outside diameter of the pipe. Equation [1.9] can be further simplified as [5]

$$M = \sqrt{1 + \frac{0.8L^2}{Dt}} \quad [1.10]$$

The calculation of AREA is simplified by assuming the shape of corroded area is parabolic for short corrosions and rectangular for long corrosions [5]. The maximum allowable length, L_{allow}, and the failure pressure P is solved from a formula which equates predicted bursting hoop stress S_p to 1.1 SMYS (specified minimum yield stress) assuming that the flow stress is 1.1 SMYS (Bai and Mørk, 1994 [6]).

B31G Criterion

The B31G criterion [7] is widely used to assess corroded pipelines for evaluation of fitness for purpose. The main equations in the ASME B31G criteria (1993) can be summarized as follows.

Maximum Allowable Design Pressure

The maximum allowable design pressure, P, in B31G is expressed as

$$P = \frac{2\text{SMYS}}{D} Ft \quad [1.11]$$

where
P = the maximum allowable design pressure
SMYS = the specified minimum yield strength
F = the design factor, which is normally 0.72

Maximum Allowable Defect Length and Depth

In B31G [7], a criterion for the acceptable corroded length is given as follows for a corroded area having a maximum depth, d, in the range of $0.1 < d/t < 0.8$, where t is the nominal wall thickness:

$$L_{\text{allow}} = 1.12B\sqrt{Dt} \qquad [1.12]$$

where

L_{allow} = the maximum allowable axial extent of the defect

$$B = \sqrt{\left(\frac{d/t}{1.1d/t - 0.15}\right)^2 - 1} \qquad [1.13]$$

The maximum allowable operating pressure (MAOP) is defined to be less or equal to the maximum allowable design pressure, P, given by Eq. [1.11]:

$$\text{MAOP} \leq P \qquad [1.14]$$

Equating the safe maximum pressure level, P', to the maximum allowable operating pressure, the maximum allowable defect depth d_{allow} is, for $A \leq 4$,

$$d_{\text{allow}} = \frac{3t}{2}\left[\frac{1 - \frac{\text{MAOP}}{1.1P}}{1 - \frac{\text{MAOP}}{1.1P\sqrt{A^2+1}}}\right] \qquad [1.15]$$

and for $A > 4$,

$$d_{\text{allow}} = \left[1 - \frac{\text{MAOP}}{1.1P}\right]t \qquad [1.16]$$

The Safe Maximum Pressure Level

The safe maximum pressure level, P', for the corroded area is

$$P' = 1.1P\left(\frac{1 - \frac{2}{3}\left[\frac{d}{t}\right]}{1 - \frac{2}{3}\left(\frac{d}{t\sqrt{A^2+1}}\right)}\right); \qquad P' \leq P; \qquad A \leq 4 \qquad [1.17]$$

$$P' = 1.1P\left(1 - \frac{d}{t}\right); \qquad P' \leq P \text{ and } A > 4 \qquad [1.18]$$

where

$$A = 0.893\left(\frac{L}{\sqrt{Dt}}\right) \qquad [1.19]$$

Evaluation of Existing Criteria

The existing criterion, ASME B31G for corroded pipelines, was established based on the knowledge developed over 20 years ago. This criterion is re-examined to develop an improved criterion based on current knowledge. This evaluation is conducted based on the corrosion mechanisms, parameters in the existing criterion, and applications that are not included in the existing criterion.

Corrosion Mechanism

Figure 1.9 shows the types of corrosion defects. For marine pipelines, internal corrosion is a major problem, Mandke (1990) [8], Jones et al. (1992) [9]. Many forms of internal corrosion occur, for example, girth weld corrosion, massive general corrosion around the whole circumference, and long plateau corrosion at about the 6 o'lock position. External corrosion, on the other hand, is normally thought of as being local, covering an irregular area of the pipe. However, when the protective coating fails, external corrosion may tend to be in the pattern of a long groove.

The B31G criterion has several problems for corrosion defects in real applications. It cannot be applied to spiral corrosion, pits and grooves interaction, or the corrosion in welds. For very long, irregularly shaped corrosion, the B31G criterion may lead to overly conservative results. It also ignores the beneficial effects of closely spaced corrosion pits.

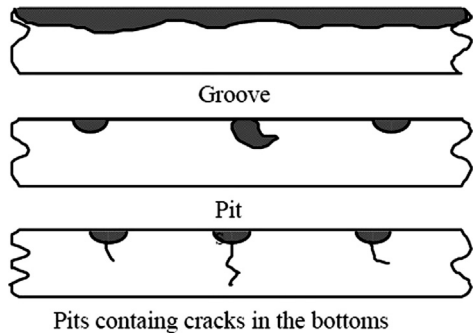

FIGURE 1.9 *Type of Corrosion Defects.*

Spiral Corrosion

For defects in other orientations, the B31G criterion recommends that the defects projected on the longitudinal axis of the pipe be treated as a longitudinal defect. This recommendation appears to be adequate for short defects. It is conservative for long, spiral defects [6].

Mok et al. (1990 [10], 1991 [11]) conducted extensive tests in the applicability of the B31G criteria to long, spiral corrosion. For spiral defects with spiral angles other than 0° or 90°, the study found that B31G underpredicted the burst pressure by as much as 50%. The effect of a spiral angle is illustrated in Figure 1.10 [10].

Based on the experimental and numerical studies, Mok et al. [10] recommend the spiral correction factor in determining the burst pressure for $W/t \leq 32$ as

$$Q = \frac{1 - Q_1}{32}\frac{W}{t} + Q_1 \qquad [1.20]$$

in which W is the defect width, and the coefficient Q_1 is a function of the spiral angle ϕ ($\phi = 90°$ for longitudinal corrosion, $\phi = 0$ for circumferential corrosion):

$$Q_1 = \begin{cases} 0.2 & \text{for} \quad 0° < \phi < 20° \\ 0.02\phi - 0.2 & \text{for} \quad 20° < \phi < 60° \\ 1.0 & \text{for} \quad \phi > 60° \end{cases} \qquad [1.21]$$

for $W/t > 32$, the value of Q must be taken as 1.0.

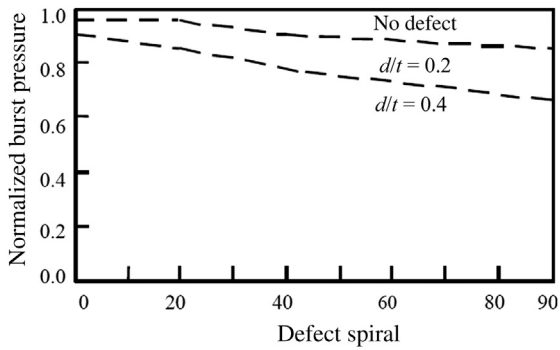

FIGURE 1.10 ***Effect of a Spiral Angle.***

Pits Interaction

Corrosion in pipelines often results in colonies of pits over an area of the pipe. For closely spaced corrosion pits, a distance of t (wall thickness) is used as a criterion of pit separation for a colony of longitudinally oriented pits separated by a longitudinal distance or parallel longitudinal pits separated by a circumferential distance.

For circumferentially spaced pits separated by a distance longer than t, the burst pressure can be accurately predicted by the analysis of the deepest pits within the colonies of pits. For longitudinally oriented pits separated by a distance less than t, the failure stress of interacting defects can be predicted by neglecting the beneficial effects of the noncorroded area between the pits. For parallel longitudinal pits separated by a circumferential distance, experiments suggested that pits could be treated as interacting pits if the circumferential spacing is less [6].

Groove Interactions

For the interaction of longitudinal grooves, if the defects are inclined to the pipe axis and the distance x between two longitudinal grooves of length L_1 and L_2 is larger than L_1 and L_2, the length of corrosion L is the maximum of L_1 and L_2 . If the defects are inclined to the pipe axis and the distance x between two longitudinal grooves of lengths L_1 and L_2 is less than L_1 and L_2, the length of corrosion L is the sum of x, L_1, and L_2; $L = L_1 + L_2 + x$.

Corrosion in Welds

One of the major corrosion damages for marine pipelines is the effects of the localized corrosion of welds on the fracture resistance. Figure 1.11 shows a typical pattern of weld corrosion. The B31G criteria do not cover the

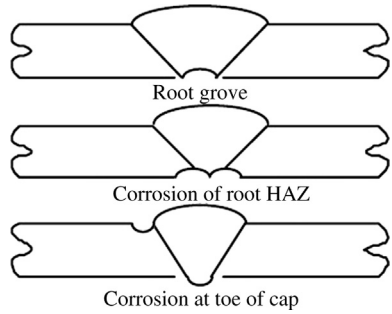

FIGURE 1.11 ***Typical Patterns of Weld Corrosion.***

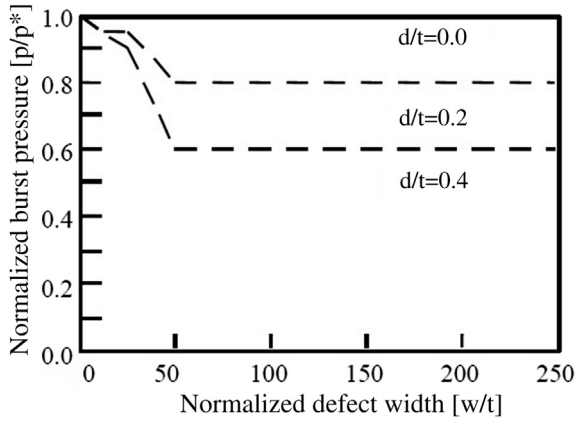

FIGURE 1.12 ***Effect of Defect Width.***

assessment of corroded welds. The existing fracture assessment procedures [12] are recommended.

Effect of Corrosion Width

Figure 1.12 shows the of defect width on burst pressure with a longitudinal defect [11], for the case of X52, OD = 508 mm, $t = 6.1$ mm, $d/t = 0.4$. Mok et al.'s studies conclude that the width effect is negligible on the burst pressure of pipe with long longitudinal defects.

REFERENCES

[1] De Waard C, Lotz U, Milliams DE. Predictive model for CO_2 corrosion engineering in wet natural gas pipelines. Corrosion 1991;47(2):976–85.
[2] Nyborg R. Controlling internal corrosion in oil and gas pipelines. Exploration Prod Oil Gas Rev 2005;I(2).
[3] Dugstad A, Lunde L, Videm K. Parametric study of CO_2 corrosion of carbon steel. Corrosion 1994.
[4] Maxey WA, Kiefner JF, Eiber RJ, Duffy AR. Ductile fracture initiation, propagation and arrest in cylindrical vessels, fracture toughness. In: Proceedings of the 1971 National Symposium on Fracture Mechanics, Part II, ASTM STP 514. Philadelphia: American Society for Testing and Materials; 1971. pp. 70–81.
[5] Kiefner JF. Corroded pipe strength and repair methods. Symposium on Line Pipe Research, Pipeline Research Committee, American Gas Association; 1974.
[6] Bai Y, Mørk KJ. Probablistic assessment of dented and corroded pipeline. International Conference on Offshore and Polar Engineering. Japan: Osaka; 1994.
[7] ASME. B31G. Manual for assessing remaining strength of corroded pipes. New York: American Society of Mechanical Engineers; 1996.
[8] Mandke JS. Corrosion causes most pipeline failure in the Gulf of Mexico. Oil Gas J October 29, 1990.

[9] Jones DG, Turner T, Ritchie D. Failure behaviour of internally corroded linepipe; 1992. OMAE'92.
[10] Mok DHB, Pick RJ, Glover AG. Behaviour of line pipe with long external corrosion. Mater Perform 1990;29(5):75–9.
[11] Mok DHB, Pick RJ, Glover AG, Hoff R. Bursting of line pipe with long external corrosion. Int J Pressure Vessel and Piping 1991;46:159–216.
[12] BSI. PD6493. Guidance on Methods for assessing the acceptability of flaws in fusion welded structures. London: British Standards Institute; 1991.

CHAPTER 2

Buckling and Collapse of Corroded Pipes

Contents

1. Introduction 27
2. Moment Capacity of Pipe Under Combined Loads 27
   General 27
   Case 1: Corroded Area in Compression 28
   The Fully Plastic Neutral Axis 30
   Bending Moment Capacicity 31
      Corrosion in Compression *31*
   Discussion of the Equations 32
3. Collapse Due to External Pressure 35
4. Modification to Timoshenko and Gere's Equations 38
5. Interaction of Bending and Pressure 39
   Analytical versus Finite Element Results 39
   Guidelines for Bending Strength Calculations 44
   Maximum Allowable Bending Moment 45
      Limit Bending Moment for External Overpressure Cases *45*
      Collapse Pressure for External Overpressure Cases *47*
      Limit Bending Moment for Internal Overpressure Cases *47*
6. Conclusions 49

References 50

1. INTRODUCTION

The purpose of this chapter is to derive analytical equations for the capacity of corroded pipes under combined loads. The derived capacity equations are compared with the results from finite element analysis. The derived analytical capacity equations may be used to extend applicability of the existing pipeline rules/guidelines.

2. MOMENT CAPACITY OF PIPE UNDER COMBINED LOADS

General

In this section, an analytical solution is given for the calculation of the moment capacity for corroded pipes subjected to internal pressure, bending,

Subsea Pipeline Integrity and Risk Management
ISBN 978-0-12-394432-0
http://dx.doi.org/10.1016/B978-0-12-394432-0.00002-0

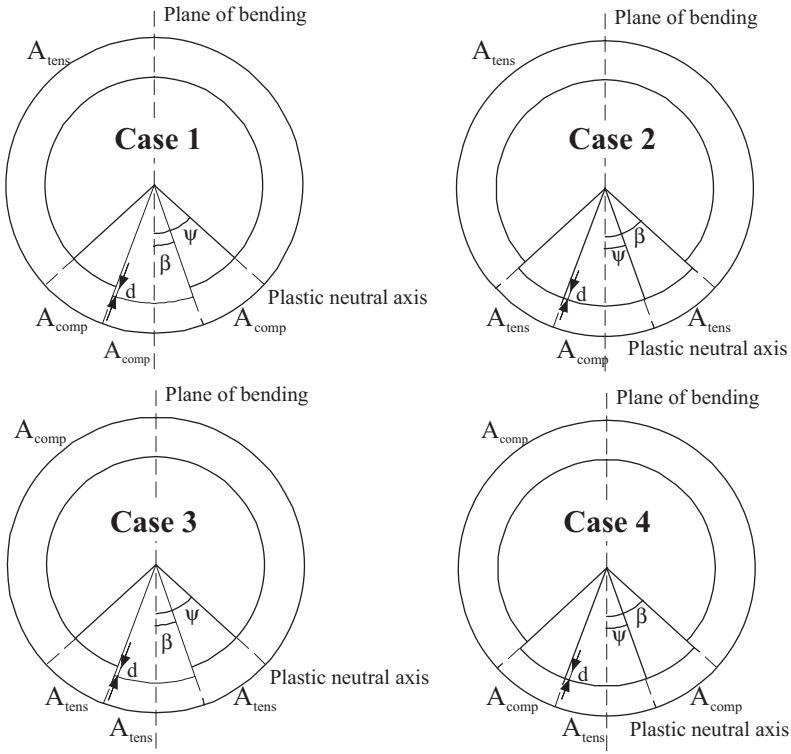

FIGURE 2.1 ***Four Discussed Combination of Defect and Bending.***

and axial force. The corrosion defect is assumed to be symmetrical to the plane of bending, which represents the worst case. For simplicity, initial out of roundness is not included in the solution. The rationality of this is that the influence of initial out of roundness is small (for thick-walled pipes with practical out of roundness). The *moment capacity* is defined as the moment at which the entire pipe cross section yields.

The solution presented in this section takes the following configurations into account: corroded area in compression (case 1), in compression and some in tension (case 2), in tension (case 3), in tension and some in compression (case 4). The four cases are shown in Figure 2.1. Only case 1 is fully discussed here, but the final solutions for cases 2–4 are given in the guideline at the end of the chapter.

Case 1: Corroded Area in Compression

To keep the complexity of the equations on a reasonable level, the following assumptions have been made:

- Diameter/wall-thickness (D/t) ratio 15–45.

- No initial out of roundness and no diameter expansion.
- Cross sections remain circular throughout deformation.
- Entire cross section in yield due to applied loads.
- Material model is elastic and perfectly plastic.
- Defect region is symmetric around plane of bending.
- Corrosion defect is of infinite length and does not cause local stress concentrations.

In general, the Von Mises yield criterion can be expressed as

$$\sigma_l^2 - \sigma_l\sigma_\theta + \sigma_\theta^2 = \sigma_Y^2 \qquad [2.1]$$

where σ_l is the longitudinal stress, σ_θ is the circumferential/hoop stress, and σ_Y is the material yield stress. Solving the second-degree equation for the longitudinal stress σ_l gives

$$\sigma_l = \frac{1}{2}\sigma_\theta \pm \sigma_Y\sqrt{1 - \frac{3}{4}\left(\frac{\sigma_\theta}{\sigma_Y}\right)^2} \qquad [2.2]$$

If compression is defined as negative and σ_{comp} as the longitudinal compressive stress that causes the pipe material to yield, then σ_{comp} is equal to σ_l as just determine with a negative sign in front of the square root. In the same way, σ_{tens} is equal to σ_l with a positive sign in front of the square root:

$$\sigma_{comp} = \frac{1}{2}\sigma_\theta - \sigma_Y\sqrt{1 - \frac{3}{4}\left(\frac{\sigma_\theta}{\sigma_Y}\right)^2} \qquad [2.3]$$

$$\sigma_{tens} = \frac{1}{2}\sigma_\theta + \sigma_Y\sqrt{1 - \frac{3}{4}\left(\frac{\sigma_\theta}{\sigma_Y}\right)^2} \qquad [2.4]$$

The hoop stress in the pipe at a given pressure may be found based on the following equation, Kiefner and Vieth [1]:

$$\sigma_\theta = p\frac{D}{2t}\frac{1 - d\Big/\left[t\sqrt{1 + 0.8\left(L/\sqrt{Dt}\right)^2}\right]}{1 - d/t} \qquad [2.5]$$

Here, D is the average diameter, t is the wall thickness, d is the defect depth, L is the defect length, and p is the resulting pressure acting on the pipe. As may be noted, the defect width is not included in the equation. This is mainly because, for all practical applications, the width has only

a minor influence on the pressure capacity. For small defect widths in particular, it may though be favorable to replace Eq. [2.5] with hoop stress based on, say, finite element analysis. For further details on the influence of corrosion width on pressure containment, see Mok et al. [2].

The Fully Plastic Neutral Axis

For case 1, the true longitudinal force, F, can be expressed as

$$F = A_{\text{comp1}}\sigma_{\text{comp}} + A_{\text{comp2}}\sigma_{\text{comp}} + A_{\text{tens}}\sigma_{\text{tens}} \quad [2.6]$$

$$A_{\text{comp1}} = 2(\Psi - \beta)r_{\text{av}}t \quad [2.7]$$

$$A_{\text{comp2}} = 2\beta r_{\text{av}}\left(1 + \frac{d}{2r_{\text{av}}}\right)t\left(1 - \frac{d}{t}\right) \quad [2.8]$$

$$A_{\text{tens}} = 2(\pi - \Psi)r_{\text{av}}t \quad [2.9]$$

where A_{comp1} is the compressed part of the nondefect cross section, A_{comp2} is the compressed part of the defect cross section, and A_{tens} is the part of the cross section in tension, see Figure 2.2. Here, r_{av} is the average radius, β is half the defect width, and Ψ is the angle from the plane of bending to the plastic neutral axis.

Inserting Eqs. [2.7]–[2.9] into Eq. p2.6 and solving for Ψ gives

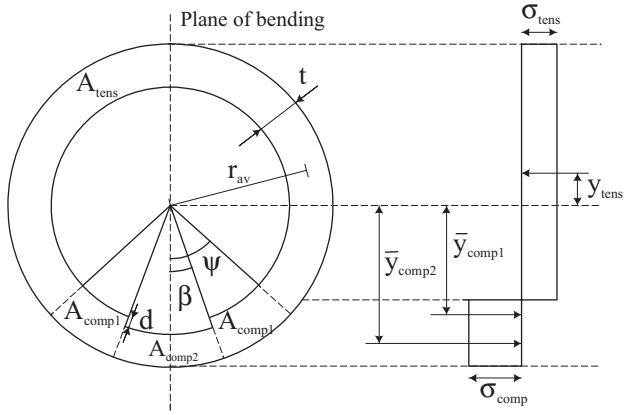

FIGURE 2.2 ***Pipe Cross Section and Idealized Stress Diagram for Fully Plasticized Cross Section.***

$$\Psi = \frac{F - 2r_{av}t\left(\pi\sigma_{tens} - k_1\beta\sigma_{comp}\right)}{2r_{av}t\left(\sigma_{comp} - \sigma_{tens}\right)} \quad [2.10]$$

$$k_1 = 1 - \left(1 - \frac{d}{t}\right)\left(1 + \frac{d}{2r_{av}}\right) \quad [2.11]$$

Now, inserting Eq. [2.3] for σ_{tens} and Eq. [2.4] for σ_{comp} in Eq. [2.10] gives

$$\Psi = \frac{\pi + k_1\beta}{2} - 2\frac{(\pi - k_1\beta)\left(\frac{F}{F_Y} - \frac{1}{2}\frac{\sigma_0}{\sigma_Y}\right)}{\sqrt{1 - \frac{3}{4}\left(\frac{\sigma_0}{\sigma_Y}\right)^2}} \quad [2.12]$$

where F_Y: is the plastic axial force for a corroded pipe:

$$F_Y = 2(\pi - k_1\beta)r_{av}t\sigma_Y \quad [2.13]$$

Bending Moment Capacicity

Corrosion in Compression

The bending moment capacity, M_C, of the pipe can now be calculated as

$$M_C = -\left(A_{comp1}\overline{y}_{comp1} + A_{comp2}\overline{y}_{comp2}\right)\sigma_{comp} + A_{tens}\overline{y}_{tens}\sigma_{tens} \quad [2.14]$$

where A_{comp1}, A_{comp2}, and A_{tens} are as defined previously and $\overline{y}$ is the perpendicular distance from the bending axis to the mass center of each area, see Figure 2.2:

$$\overline{y}_{comp1} = r_{av}\frac{\sin(\Psi) - \sin(\beta)}{\Psi - \beta} \quad [2.15]$$

$$\overline{y}_{comp2} = r_{av}\left(1 + \frac{d}{2r_{av}}\right)\frac{\sin(\beta)}{\beta} \quad [2.16]$$

$$\overline{y}_{tens} = r_{av}\frac{\sin(\Psi)}{\pi - \Psi} \quad [2.17]$$

Inserting Eqs. [2.15]–[2.17] into Eq. [2.14], one gets the following expression for the bending moment capacity:

$$M_C = -2tr_{av}^2[\sin(\Psi) - k_2\sin(\beta)]\sigma_{comp} + 2tr_{av}^2\sin(\Psi)\sigma_{tens} \quad [2.18]$$

$$k_2 = 1 - \left(1 - \frac{d}{t}\right)\left(1 + \frac{d}{2r_{av}}\right)^2 \quad [2.19]$$

Substituting the expressions for the tensile and compressive stress, Eqs. [2.3] and [2.4], into Eq. [2.18] gives the final expression for the bending moment capacity for case 1:

$$M_C = 2tr_{av}^2\sigma_Y\left[k_2\sin(\beta)\left(\frac{1}{2}\frac{\sigma_\theta}{\sigma_Y} - \sqrt{1 - \frac{3}{4}\left(\frac{\sigma_\theta}{\sigma_Y}\right)^2}\right) + 2\sin(\Psi)\sqrt{1 - \frac{3}{4}\left(\frac{\sigma_\theta}{\sigma_Y}\right)^2}\right] \quad [2.20]$$

where the angle to the plastic neutral axes is given by Eq. [2.12], the plastic yield force for a corroded pipe by Eq. [2.13], and the constants k_1 and k_2 by Eqs. [2.11] and [2.19], respectively.

Based on the limitation that the expression under the squarer root must be positive and that the angle to the plastic neutral axes between 0° and 180°, the moment equation is mathematically valid for the following range of hoop stress and axial force:

$$\frac{-2}{\sqrt{3}} \le \frac{\sigma_\theta}{\sigma_Y} \le \frac{2}{\sqrt{3}} \quad [2.21]$$

$$\frac{1}{2}\frac{\sigma_\theta}{\sigma_Y} - \sqrt{1 - \frac{3}{4}\left(\frac{\sigma_\theta}{\sigma_Y}\right)^2} \le \frac{F}{F_Y} \le \frac{1}{2}\frac{\sigma_\theta}{\sigma_Y} + \frac{\pi + k_1\beta}{\pi - k_1\beta}\sqrt{1 - \frac{3}{4}\left(\frac{\sigma_\theta}{\sigma_Y}\right)^2} \quad [2.22]$$

Discussion of the Equations

To demonstrate the consistency of the equations and the influence of different input parameters, some examples are shown in Figures 2.3 to 2.6. For all the examples, the D/t ratio is 25, d/t is equal to 30%, and σ_Y is equal to 450 MPa. It is common to the four figures that the areas where each of the four cases given in Figure 2.1 is governing is plotted with a different line type. The line types are marked Case 1 to 4, respectively.

In Figures 2.3 and 2.4, the axial tension is $0.3 \times \pi \times D \times t \times \sigma_y$ and the internal overpressure is $0.6 \times \sigma_y \times 2 \times t/D$. In Figure 2.5, the axial

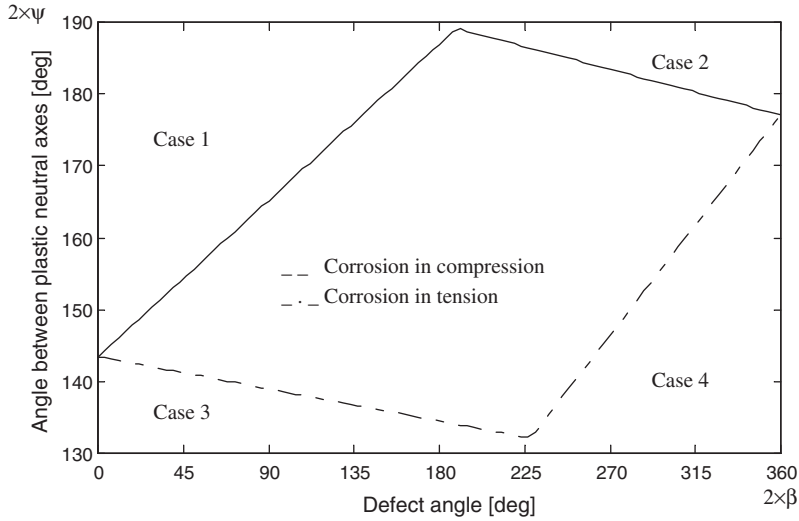

FIGURE 2.3 ***Angle between the Plane of Bending and Plastic Neutral Axis as a Function of the Defect Width.***

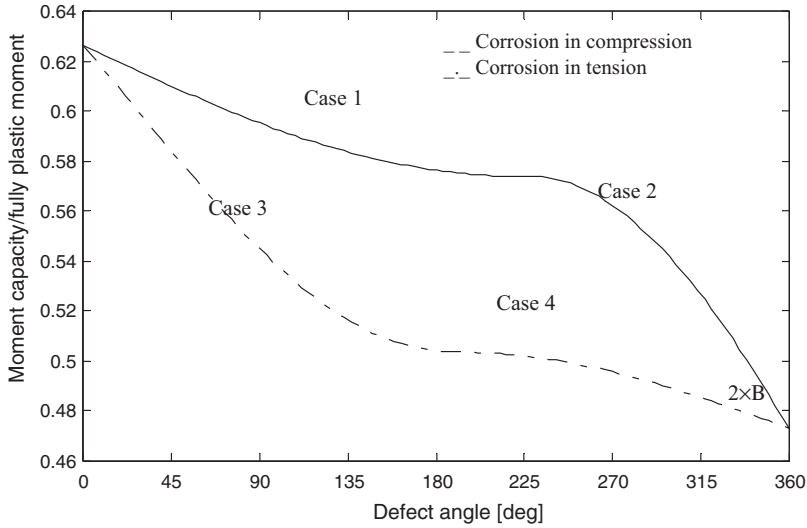

FIGURE 2.4 ***Normalized Moment Capacity as a Function of the Defect Width.***

force for internal pressure equal to [0, 0.2, 0.4, 0.6] × p_y, starting from the left. $p_y = 2 \times t/D \times \sigma_y$ and $2 \times \beta = 90°$. In Figure 2.6, the axial forces equal to [–0.6, –0.3, 0, 0.3, 0.6] × F_Y, starting from the left; $F_y = \pi D t \sigma_y$, $2 \times \beta = 90°$ and $P_{plastic} = 2 \times \sigma_y \times (t - d)/D$.

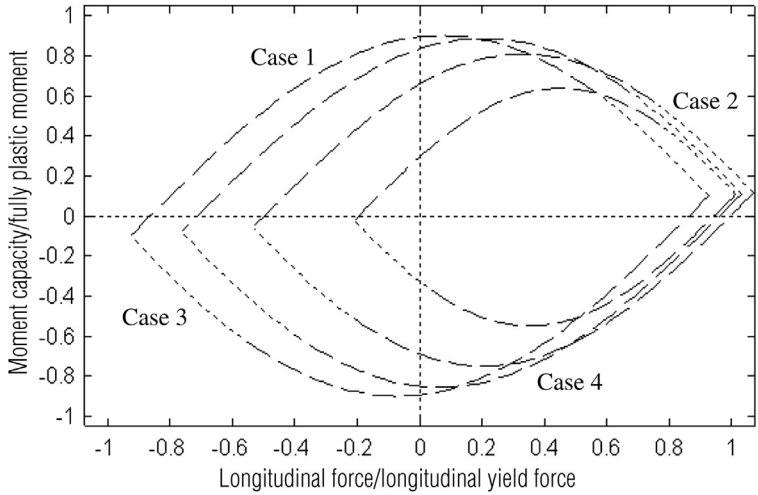

FIGURE 2.5 ***Interaction between Bending and Axial Force.***

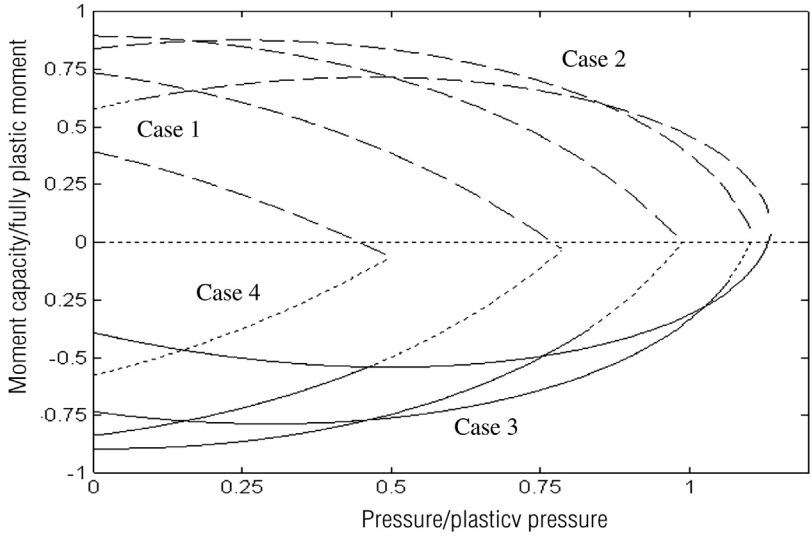

FIGURE 2.6 ***Interaction between Bending and Differential Pressure.***

Figure 2.3 demonstrates that the equations giving the angle between the plastic neutral axis and the bending plan together form a continuous path.

Figure 2.4 shows an example of reduction in moment capacity as a function of the defect width. For the present axial force, the dashed line

representing the corroded area in tension gives the limit state. The gain by including the defect width in the calculations of the moment capacity increases with decreasing width and increasing d/t ratio. Note that, for $2 \times \beta = 0$ and $d = 0$, the equations provides $M/M_p = 0.85$ and not 0.62, as shown in Figure 2.4. The difference is due to the definition of the hoop stress, which does not account for the defect width. This conservatism though applies only to small angles, up to 10–20°, as demonstrated for the collapse pressure in Figure 2.10. Due to the uncertainties normally related to estimating the defect size of especially small defects, the authors find no engineering reasons for extending this study to reduce the conservatism in the hoop stress equation for small defect widths.

Figure 2.5 demonstrates the influence of axial force on the moment capacity. For the non- and fully corroded pipe, symmetry is obtained both about the x-axis and the y-axis and hence a simpler equation can be used for calculating the moment capacity for a given longitudinal force, see Mohareb et al. [3]. When a defect is included in the calculations, this symmetry is no longer present. Due to the unsymmetrical reduction in the pipe wall thickness, a bending moment is introduced in the pipe when it is subjected to longitudinal force. Therefore, to find the minimum moment capacity for a partly corroded pipe, two calculations are required, one for a positive and one for a negative moment.

Figure 2.6 shows that, for the cycle where the longitudinal force is zero, symmetry about the x-axis is seen, and one calculation for a given pressure gives the moment capacity for the pipe. It is noted that the maximum pressure capacity for this case is the same as given by Eq. [2.5]. When longitudinal force is applied, an additional moment comes into being and two calculations, as described, are needed to find the moment capacity.

All the figures show that the equations are consistent for the entire mathematically valid range of variables. The equations have also been compared with Miller's equations [4], for calculating the moment capacity of corroded nonpressurized pipes and good agreement has been found. The comparison is not given here.

3. COLLAPSE DUE TO EXTERNAL PRESSURE

Initial out of roundness and corrosion defects are the two major types of imperfections influencing the collapse capacity of pipes. In the following, the work by Timoshenko and Gere [5] is extended to account for the effect of a corrosion defect.

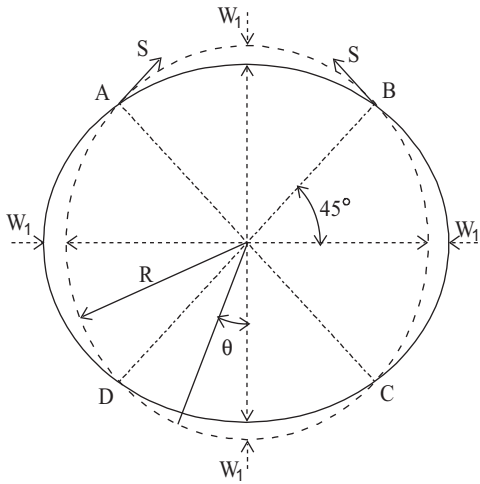

FIGURE 2.7 ***Circular and Elliptic Pipe Sections.***

The deviation of an initial ellipticity form from a perfect circular form can be defined by a radial deflection, w_i, which for the purpose of simplification is assumed to be given by the following equation:

$$w_i = w_1 \cos(2\theta) \qquad [2.23]$$

where w_1 is the maximum initial radial deviation from a circle and θ is the central angle measured as shown in Figure 2.7.

Under the action of external uniform pressure, p_e, there is an additional flattening of the pipe, and the corresponding additional radial displacement, w, is calculated using the differential equation:

$$\frac{d^2w}{d\theta^2} + w = -\frac{12\left(1-\nu^2\right)Mr_{av}^2}{Et^3} \qquad [2.24]$$

where M is the pipe wall bending, ν is Poisson's ratio, and E is Young's modulus. The decrease in the initial curvature as a consequence of the external pressure introduces a positive bending moment in sections AB and CD and a negative bending moment in sections AD and BC. At points A, B, C, and D, the bending moment is zero, and the actions between the parts are represented by the forces S tangential to the dotted circle represent the ideal circular shape.

The circle can be considered a funicular curve for the external pressure, p_e, and the compressive force along this curve remains constant and equal

to S. Thus, the bending moment at any cross section is obtained by multiplying S by the total radial displacement, $w_1 + w$, at the cross section. Therefore,

$$M = p_e r_{av}[w + w_1 \cos(2\theta)] \quad [2.25]$$

Substituting in Eq. [2.24],

$$\frac{d^2w}{d\theta^2} + w = -\frac{12(1-\nu^2)}{Et^3} p_e r_{av}^3 [w + w_1 \cos(2\theta)] \quad [2.26]$$

or

$$\frac{d^2w}{d\theta^2} + w\left[1 + \frac{12(1-\nu^2)}{Et^3} p_e r_{av}^3\right] = -\frac{12(1-\nu^2)}{Et^3} p_e r_{av}^3 w_1 \cos(2\theta) \quad [2.27]$$

The solution to this equation satisfying the conditions of continuity at the points A, B, C, and D is

$$w = \frac{w_1 p_e}{p_{el} - p_e} \cos(2\theta) \quad [2.28]$$

in which p_{el} is the elastic buckling pressure, given as

$$p_e = \frac{E}{4(1-\nu^2)} \left(\frac{t}{r_{av}}\right)^3 \quad [2.29]$$

It is seen that, at the points A, B, C, and D, w and $d^2w/d\theta^2$ are zero. Hence, the bending moment at these points is zero, as assumed earlier. The maximum moment, M_{max}, occurs at $\theta = 0$ and at $\theta = \pi$, where

$$M_{max} = p_e r_{av}\left(w_1 + \frac{w_1 p_e}{p_{el} - p_e}\right) = p_e r_{av} \frac{w_1}{1 - p_e/p_{el}} \quad [2.30]$$

The initial yielding condition for a rectangular cross section with height of wall thickness and width of unity (1) can be expressed as

$$\sigma_y = \sigma_a + \sigma_b \quad [2.31]$$

where σ_a is the stress induced by the external pressure and σ_b is the stress induced by the bending moment. The pressure-induced hoop stress per unit length is defined as

$$\sigma_a = \frac{p_e r_{av}}{t} \quad [2.32]$$

The relationship between bending stress and moment in the elastic region is as follows:

$$\sigma_b = \frac{\eta}{1+\eta/r_{av}} \cdot \frac{M_{max}}{I} \approx \frac{t/2}{1} \cdot \frac{M_{max}}{t^3/12} = 6\frac{M_{max}}{t^2} \qquad [2.33]$$

where η is the distance from the center for moment of inertia (centre of pipe wall) to the outer fiber, r_{av} is the initial curvature, and I is the moment of inertia. From Eq. [2.30], it is seen that, for small values of the ratio p_e/p_{el}, the change in the ellipticity of the pipe due to pressure can be neglected, and the maximum bending moment is obtained by multiplying the compressive force $p_e \times r_{av}$ by the initial deflection w_1. When the ratio p/p_{el} is not small, the change in the initial ellipticity of the pipe should be considered and Eq. [2.30] must be used in calculating M_{max}. Thus, it is found that

$$\sigma_{max} = \frac{p_e r_{av}}{t} + \frac{6p_e r_{av}}{t^2}\frac{w_1}{1-p_e/p_{el}} \qquad [2.34]$$

Assuming that this equation can be used with sufficient accuracy up to the yield point stress of the material, the following equation can be obtained for the uniform external overpressure p_Y, at which yielding in the extreme fibers begins:

$$p_Y^2 - \left[\frac{\sigma_Y t}{r_{av}} + \left(1 + 6\frac{w_1}{t}\right)p_{el}\right]p_Y + \frac{\sigma_Y t}{r_{av}}p_{el} = 0 \qquad [2.35]$$

It should be noted that the pressure P_Y determined in this manner is smaller than the pressure at which the collapse of the pipe, P_c, occurs, and it becomes equal to the latter only in the case of a perfectly round pipe. Hence, by using the value of p_Y calculated from Eq. [3.35] as the ultimate value of pressure, the results are on the safe side.

4. MODIFICATION TO TIMOSHENKO AND GERE'S EQUATIONS

Buckling is an equilibrium problem and occurs when external loads are higher than or equal to internal resistance over the cross section. The cross section here means a rectangular one, with height of t or $t - d$ and length along the pipe longitudinal direction of (1) unit.

The external loads acting on the cross section are the moment and compression and the weakest cross-sectional point describes the internal resistance. The term p_{el} describes the amplification of the external loads due

to a combination of imperfection (i.e., w_1) and axial compression acting on the pipe wall. The amount of amplification is minimally affected by a local corrosion defect unless the defect is very wide or deep. The internal resistance is reduced significantly though by the corrosion defect and therefore the reduced wall thickness $t - d$ is used for terms describing the internal resistance. Based on this discussion, Eq. [2.35] is modified to Eq.[2.36]:

$$p_Y^2 - \left[\frac{\sigma_Y(t-d)}{r_{av}} + \left(1 + 6\frac{w_1}{(t-d)}\right)p_{el}\right]p_Y + \frac{\sigma_Y(t-d)}{r_{av}}p_{el} = 0 \quad [2.36]$$

where the elastic pressure is unaffected by the corrosion defect:

$$p_{el} = \frac{E}{4(1-\nu^2)}\left(\frac{t}{r_{av}}\right)^3 \quad [2.37]$$

In the following, P_Y is conservatively used as the characteristic collapse pressure P_c.

5. INTERACTION OF BENDING AND PRESSURE

The interaction between moment capacity for a nonpressurised pipe and the external collapse pressure may be expressed according to Eq. [2.36], [6, 7], which also is the relation used by the DNV [8] in its rules for submarine pipeline systems:

$$\left(\frac{M}{M_c}\right)^2 + \left(\frac{p_e}{p_c}\right)^2 \leq 1 \quad [2.38]$$

Analytical versus Finite Element Results

Due to lack of available results from tests of corroded pipes in the literature, it has been necessary to use finite element analyses to verify the analytical solution. A shell model, see Hauch and Bai [9], has been developed and the following input data are used:

- $D/t = 25$, $d/t = 0.3$.
- Initial out of roundness $f_0 = 1.5\%$, $f_0 = (D_{max} - D_{min})/D$.
- Material yield strength = 450 MPa.
- Material ultimate tensile strength = 530 MPa.

A Ramberg-Osgood material curve was used as input to the analyses, and the model represents one quarter of a pipe section with a model length of 3 times the pipe diameter.

Several comparisons between the equations presented at the end of this section and finite element analyses were made and some of the results are presented in Figures 2.8 to 2.12, where $P_{\text{plastic}} = 2 \times \sigma y \times (t - d)/D$. Defect width $(2 \times \beta) = 90°$.

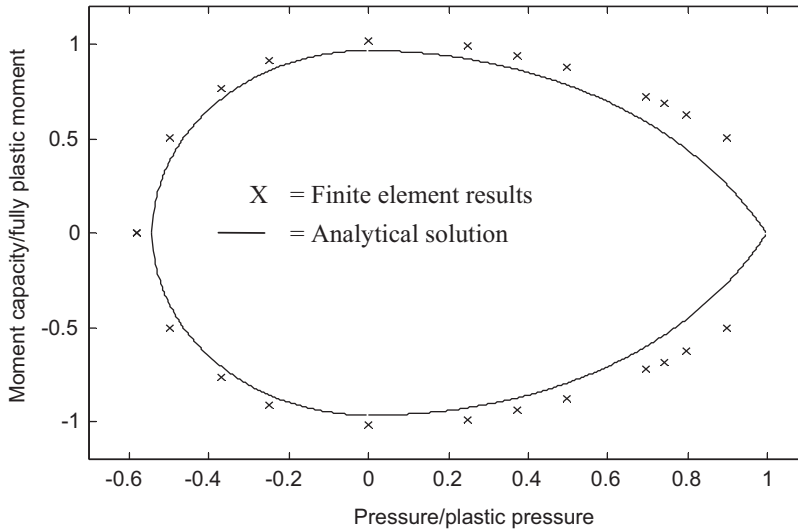

FIGURE 2.8 ***Moment Capacity Versus Pressure.***

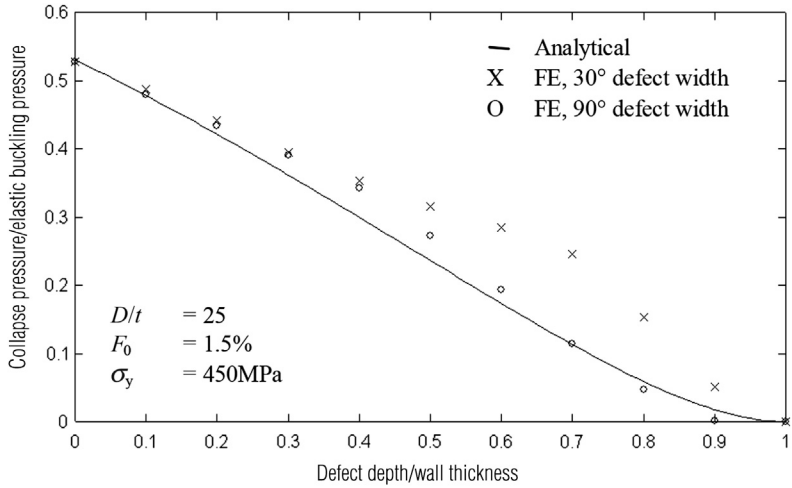

FIGURE 2.9 ***Collapse Pressure as a Function of the Defect Depth.***

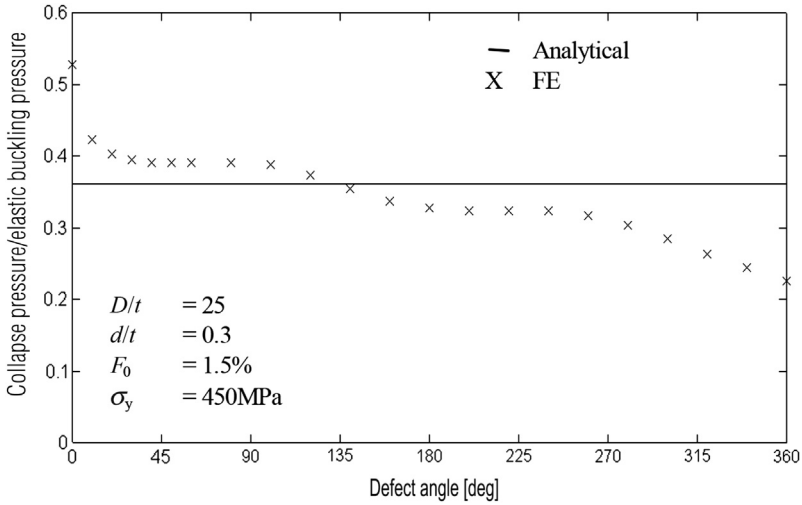

FIGURE 2.10 ***Collapse Pressure as a Function of the Defect Width.***

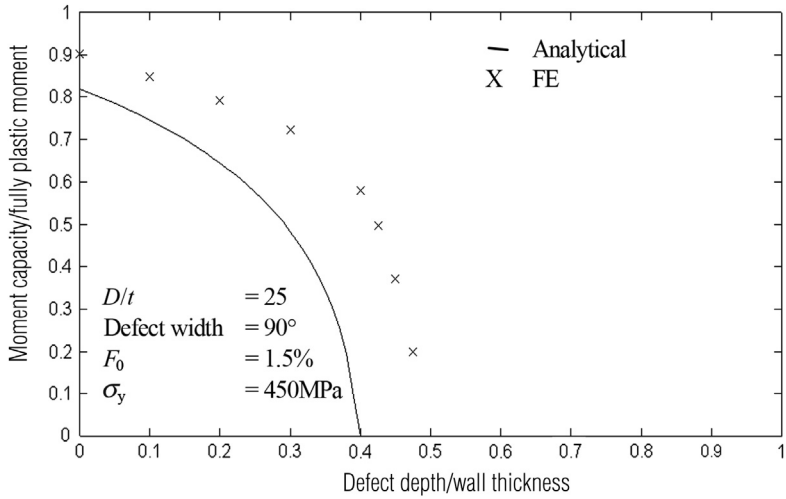

FIGURE 2.11 ***Moment Capacity as Function of the Defect Depth.***

From Figure 26.8, it is seen that, for external overpressure, the analytical solution is in good agreement with the FE results. It seems though that the accuracy of the analytical solution decreases conservatively with increasing internal overpressure, which is due to interaction between failure modes caused by bending and pressure, respectively.

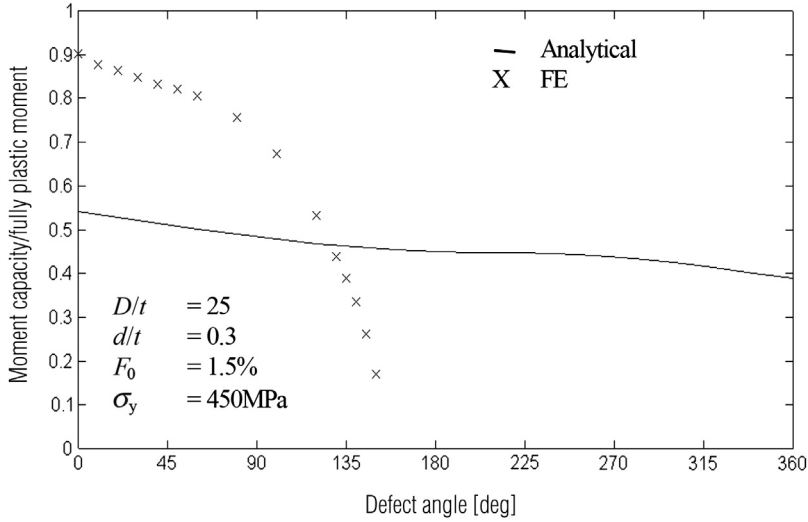

FIGURE 2.12 ***Moment Capacity as Function of the Defect Width.***

Pressure forces the pipe to expand, while bending collapses the cross section. That the two failure modes operate in opposite directions causes the average stress in the pipe at collapse to be higher than the material yield strength, σ_Y, which has been assumed in the previous deduction. The interaction between failure modes can be taken partly into account by using a higher value for the maximum hoop stress at failure, see also Hauch and Bai [9].

Figures 2.9 to 2.12 present some of the results from a parametric study. Here, the influence of defect depth and defect width has been investigated and analytical results compared with results obtained by the finite element method.

Figure 2.9 shows the collapse pressure as a function of defect depth. In the derivation of the analytical solution, it was assumed that the defect width is of minor importance for the calculation of the collapse pressure. This assumption is confirmed by a series of finite element analyses, where the results from a 30° and a 90° defect width are plotted in the same figure. In Figure 2.10, the collapse pressure is given as a function of defect width for a pipe with a defect depth of 30% of the wall thickness. The finite element results presented in this figure demonstrate that the main reduction in collapse strength occurs when the defect is introduced, and thereafter decreases only slowly with increased defect width. In general, the agreement between the analytical results and the finite element results seems good for the entire range of defect depths and width.

The results presented in Figures 2.11 and 2.12 are for a pipe exposed to an external overpressure of 75% of the collapse pressure for a noncorrode pipe then subjected to increased bending until the maximum bending capacity is reached.

Figure 2.11 gives the moment capacity as a function of defect depth and demonstrates a good agreement between the analytical results and results obtained by the finite element method. The conservatism in the analytical solution demonstrated in Figure 2.11 is mainly introduced through the collapse term. The same good agreement is not found when the defect width is varied.

The moment equation and the collapse equation have each demonstrated to be in good agreement with results obtained through the finite element method and previous analytical results, like those presented by Miller (1988) [4]. Based on Figures 2.9 and 2.10, it was concluded that the defect width has minor effect on the collapse strength and that the simplification in the derivation of the collapse equation therefore is acceptable. Nevertheless, this simplification causes the poor agreement in Figure 2.12.

Collapse strength (even a little higher than the external overpressure) gives a significant moment capacity. Going back to Figure 2.10, it is seen that, after the initial strength reduction, the collapse capacity drops slowly with the defect width. The result in Figure 2.12 is based on a pipe subjected to an external overpressure of 75% of the collapse pressure for a similar pipe without a defect.

This pressure level is reached at a defect width of approximately 150°, after which no bending strength is left. From Figure 2.9, it is seen that the analytical equation predicts collapse strength that is 5–10% higher than that given by the finite element model, which in this case gives the difference in moment capacity shown in Figure 2.12.

If the external overpressure is decreased or the defect depth is less, the agreement increases dramatically. This is seen from Figure 2.13, for which the input data, except defect depth, are identical to the input data for Figure 2.12. Said in other terms, the equations presented in this paper provide the best predictions for load scenarios that are not dominated by the external pressure collapse failure mode.

Based on this discussion, it is concluded that, if the external overpressure is well below the collapse pressure, the equations presented in this chapter are in good agreement with finite element results. If the external overpressure, on the other hand, is close to the collapse pressure for the corroded pipe, it is recommended that more comprehensive finite element analyses be

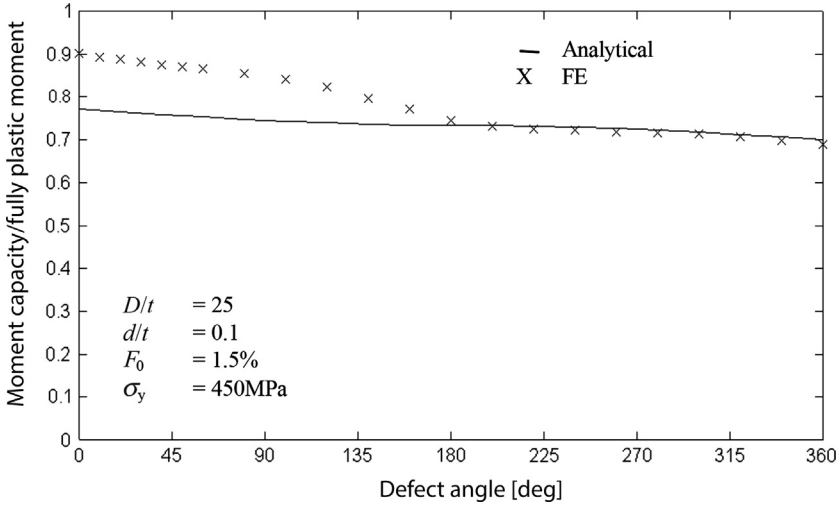

FIGURE 2.13 ***Moment Capacity as Function of the Defect Width.***

performed. In general, the equations demonstrate that, for conditions with high pressure, the defect width has little influence on the capacity compared to the defect depth.

Guidelines for Bending Strength Calculations

The guidelines can be list as follows:

- **Local buckling and collapse:** For pipelines subjected to combined pressure, longitudinal force, and bending, local buckling or collapse may occur. The failure mode may be collapse of the cross section or buckling on the compressive side of the pipe. The check given in this guideline provides the tools to estimate the maximum allowable bending moment for local buckling of corroded pipes with an initial out of roundness. It is noted that, to find the maximum allowable bending moment for a pipe, the fracture limit state also needs to be checked.
- **Local buckling and accumulative out of roundness:** Increased out of roundness due to installation and cyclic operating loads may aggravate local buckling and is to be considered. To estimate the out of roundness induced over the life cycle of the pipeline, it is recommended that ratcheting analyses be performed.
- **Load- and displacement-controlled situations:** The local buckling check can be separated into a check for load-controlled situations (bending moment) and one for displacement-controlled situations

(strain level). Due to the relation between applied bending moment and maximum strain in a pipe, a higher allowable strength for a given safety level can be achieved by using a strain-based criterion rather than the bending moment criterion. In this guideline, only the bending moment criterion is given.

Maximum Allowable Bending Moment

The following are a partial safety factor methodology given by the DNV [8], the allowable bending moment for local buckling under load controlled situations can be expressed as

$$\left(\frac{\gamma_F \cdot \gamma_C \cdot M_{F,c} + \gamma_E \cdot M_{E,c}}{\frac{M_c}{\gamma_R}}\right)^2 + \left(\frac{P_e}{\frac{P_c}{\gamma_R}}\right)^2 \leq 1 \qquad [2.39]$$

where

$M_{F,c}$ = characteristic functional bending moment
$M_{E,c}$ = characteristic environmental bending moment
M_c = characteristic limit bending moment
γ_F = load safety factor for functional loads
γ_E = load safety factor for environmental loads
γ_C = condition load factor
γ_R = strength resistance safety factor
P_e = characteristic external overpressure
P_c = characteristic collapse pressure (P_c is equal to infinity for internal overpressure)

The partial safety factors γ_F, γ_E, γ_C, and γ_R are still to be calibrated, but until then the following safety factors, according to DNV 1996 [8], are suggested, see Table 2.1.

Limit Bending Moment for External Overpressure Cases

The characteristic limit bending moment, M_C, for external overpressure cases should be calculated as follows. If $\Psi \geq \beta$,

$$\Psi = \frac{\pi + k_1\beta}{2} + \frac{(\pi - k_1\beta)}{2}\frac{\gamma_F\gamma_C|F|}{F_y} \qquad [2.40]$$

then

$$M_C = 0.5D^2 t\sigma_y[k_2 \sin(\beta) - 2\sin(\Psi)] \qquad [2.41]$$

Table 2.1 Tentative Safety Factors According to DNV 1996

	Safety Factors							
	γ_F[1]		γ_E[1]	γ_C[2]				γ_R
Safety Classes	Load Comb.[a]	Load Comb.[b]	Load Comb.[c]	Uneven Seabed	Pressure Test	Stiff Supported	Else	
Low	1.20	1.10	1.30	1.07	0.91	0.82	1.00	1.19
Normal	1.20	1.10	1.30	1.07	0.91	0.82	1.00	1.32
High	1.20	1.10	1.30	1.07	0.91	0.82	1.00	1.52

[1]Load combinations:
[a]is to be applied for external overpressure and load combination.
[b]is for both internal and external overpressure.
[c]the lowest value of load combination a and b is to be used.
[2]Load condition factors may be combined, e.g., the load condition factor for pressure test of pipelines resting on an uneven seabed, $1.07 \times 0.91 = 0.97$.

Otherwise, if $\Psi < \beta$,

$$\Psi = \frac{\pi - k_1\beta}{2(1-k_1)} + \frac{(\pi - k_1\beta)}{2(1-k_1)}\frac{\gamma_F\gamma_C|F|}{F_y} \qquad [2.42]$$

then

$$M_C = 0.5D^2t\sigma_y[-k_2\sin(\beta) - 2(1-k_2)\sin(\Psi)] \qquad [2.43]$$

where

$$F_y = (\pi - k_1\beta)Dt\sigma_y$$

$$k_1 = 1 - \left(1 - \frac{d}{t}\right)\left(1 + \frac{d}{D}\right), \qquad k_2 = 1 - \left(1 - \frac{d}{t}\right)\left(1 + \frac{d}{D}\right)^2 \qquad [2.44]$$

D = nominal outer diameter
t = nominal wall thickness
d = corrosion depth
σ_Y = material yield strength
β = half the corrosion width
Ψ = angle from plane of bending to plastic neutral axis
F_y = true longitudinal yield force
F = true longitudinal force

Collapse Pressure for External Overpressure Cases

The characteristic capacity for external pressure, p_c, is calculated as

$$p_c^2 - \left[2\frac{\sigma_y(t-d)}{D} + \left(1 + 6\frac{w_1}{t-d}\right)p_{el}\right]p_c + 2\frac{\sigma_y(t-d)}{D}p_{el} = 0 \quad [2.45]$$

in which

$$p_{el} = \frac{2E}{1-\nu^2}\left(\frac{t}{D}\right)^3, \qquad w_1 = \frac{f_0 D}{4}, \qquad f_0 = \frac{D_{max} - D_{min}}{D} \quad [2.46]$$

where

E = Young's modulus
ν = Poisson's ratio
h = remaining wall thickness
f_0 = out of roundness, not to be taken less than 0.5%
p_{el} = elastic buckling pressure

Note that

1. Out of roundness caused during the construction phase is to be included in the out of roundness, while out of roundness due to external water pressure or moment in as-laid position is not.
2. For internal overpressure cases, the collapse pressure is set to infinity.

Limit Bending Moment for Internal Overpressure Cases

The characteristic limit bending moment, M_C, for internal overpressure cases should be chosen as the minimum of the following two scenarios:

For a corroded area in the compressive side of the pipe, if $\Psi \geq \beta$,

$$\Psi = \frac{\pi - k_1\beta}{2} - \frac{\gamma_F\gamma_C(\pi - k_1\beta)\left(\frac{F}{F_Y} - \frac{1}{2}\frac{\sigma_\theta}{\sigma_y}\right)}{2\sqrt{1 - \frac{3}{4}\left(\frac{\sigma_\theta}{\sigma_y}\right)^2}} \quad [2.47]$$

then

$$M_C = M_p\left\{k_2\sin(\beta)\left[\frac{1}{2}\frac{\sigma_\theta}{\sigma_y} - \sqrt{1 - \frac{3}{4}\left(\frac{\sigma_\eta}{\sigma_y}\right)^2}\right] + 2\sin(\Psi)\sqrt{1 - \frac{3}{4}\left(\frac{\sigma_\eta}{\sigma_y}\right)^2}\right\} \quad [2.48]$$

otherwise, if $\Psi < \beta$,

$$\Psi = \frac{\pi - k_1\beta}{2k_3} - \frac{\gamma_F\gamma_C(\pi - k_1\beta)\left(\frac{F}{F_Y} - \frac{1}{2}\frac{\sigma_\theta}{\sigma_y}\right)}{2k_3\sqrt{1 - \frac{3}{4}\left(\frac{\sigma_\theta}{\sigma_y}\right)^2}} \quad [2.49]$$

then

$$M_C = M_p\left\{k_2\sin(\beta)\left[\frac{1}{2}\frac{\sigma_\theta}{\sigma_y} + \sqrt{1 - \frac{3}{4}\left(\frac{\sigma_\theta}{\sigma_y}\right)^2}\right] + 2k_4\sin(\Psi)\sqrt{1 - \frac{3}{4}\left(\frac{\sigma_\theta}{\sigma_y}\right)^2}\right\} \quad [2.50]$$

For the corroded area in the tensile side of the pipe, if $\Psi \geq \beta$,

$$\Psi = \frac{\pi + k_1\beta}{2} + \frac{\gamma_F\gamma_C(\pi - k_1\beta)\left(\frac{F}{F_Y} - \frac{1}{2}\frac{\sigma_\theta}{\sigma_y}\right)}{2\sqrt{1 - \frac{3}{4}\left(\frac{\sigma_\theta}{\sigma_y}\right)^2}} \quad [2.51]$$

then

$$M_C = M_p\left\{k_2\sin(\beta)\left[\frac{1}{2}\frac{\sigma_\theta}{\sigma_{fail}} + \sqrt{1 - \frac{3}{4}\left(\frac{\sigma_\theta}{\sigma_y}\right)^2}\right] - 2\sin(\Psi)\sqrt{1 - \frac{3}{4}\left(\frac{\sigma_\theta}{\sigma_y}\right)^2}\right\} \quad [2.52]$$

otherwise, if $\Psi < \beta$,

$$\Psi = \frac{\pi - k_1\beta}{2k_3} + \frac{\gamma_F\gamma_C(\pi - k_1\beta)\left(\frac{F}{F_Y} - \frac{1}{2}\frac{\sigma_\theta}{\sigma_y}\right)}{2k_3\sqrt{1 - \frac{3}{4}\left(\frac{\sigma_\theta}{\sigma_y}\right)^2}} \quad [2.53]$$

then

$$M_C = M_p \left\{ k_2 \sin(\beta) \left[\frac{1}{2}\frac{\sigma_\theta}{\sigma_y} + \sqrt{1 - \frac{3}{4}\left(\frac{\sigma_\theta}{\sigma_y}\right)^2} \right] - 2k_4 \sin(\Psi) \sqrt{1 - \frac{3}{4}\left(\frac{\sigma_\theta}{\sigma_y}\right)^2} \right\} \quad [2.54]$$

The following values are to be used in the preceding equations:

$$M_p = 0.5 \cdot D \cdot t \cdot \sigma_y, \qquad F_Y = (\pi - k_1 \beta) D \cdot t \cdot \sigma_Y$$

$$\sigma_\theta = (p_i - p_e)\frac{D + d}{2(t - d)}$$

$$k_1 = 1 - \left(1 - \frac{d}{t}\right)\left(1 + \frac{d}{D}\right), \qquad k_2 = 1 - \left(1 - \frac{d}{t}\right)\left(1 + \frac{d}{D}\right)^2, \quad [2.55]$$

$$k_3 = 1 - k_1, \qquad k_4 = 1 - k_2$$

where

σ_h = hoop stress in thinnest part of the pipe wall

p_i = characteristic internal overpressure

The lowest bending moment capacity of these expressions for a corrosion defect in the compressive and tensile sides of the pipe, respectively, is to be used as the maximum allowable bending moment for local buckling and plastic collapse.

6. CONCLUSIONS

The following conclusions may be made on the buckling and collapse strength of corroded pipes subjected to combined pressure, axial force, and bending:

- Analytical moment capacity equations have been derived for corroded pipes subjected to pressure, bending, and axial force, by extending the equations by Timoshenko and Gere and Mohareb et al. for noncorroded pipes.
- The analytical solution is in agreement with Miller's moment capacity equations for nonpressurized corroded pipes.

- For external overpressure well below the collapse pressure for the corroded pipe, the equations presented in this chapter are in good agreement with finite element results. If, on the other hand, the external overpressure is close to the collapse pressure, it is recommended that more comprehensive finite element analyses be performed.
- For internal overpressure, the results agree well with results obtained using the finite element method, even though they may be a little conservative.

REFERENCES

[1] Kiefner JF, Vieth PH. A modified criterion for evaluating the remaining strength of corroded pipe. RSTRENG Project PR 3–805 Pipeline Research Committee. Battelle, Ohio: American Gas Association; 1989.
[2] Mok DHB, Pick RJ, Glover AG, Hoff RA. Bursting of line pipe with long external corrosion. Int J Press Vessel Piping 1991.
[3] Mohareb ME, Elwi AE, Kulak GL, Murray DW. Deformational behaviour of line pipe. Structural Engineering Report No. 22. Edmonton, Canada: University of Alberta; 1994.
[4] Miller AG. Review of limit loads of structures containing defects. Int J Press Vessel Piping 1998;32:197–327.
[5] Timoshenko SP, Gere JM. Theory of elastic stability. New York: McGraw-Hill; 1961.
[6] Bai Y, Igland R, Moan T. Tube collapse under combined pressure, tension and bending. Int J Offshore Polar Eng 1993;3(2):121–9.
[7] Bai Y, Igland R, Moan T. Tube collapse under combined external pressure, tension and bending. J Mar Structures 1997;10(5):389–410.
[8] DNV. Rules for submarine pipelines. Det Norske Veritas 1996.
[9] Hauch S, Bai Y. Bending moment capacity of pipes. In: Proc. of OMAE'99. St. John's, Canada; 1999.

CHAPTER 3

Dented Pipelines

Contents

1. Introduction 52
2. Limit-State Based Criteria for Dented Pipes 52
   - General 52
   - Serviceability Limit State (Out of Roundness) 53
   - Bursting Criterion for Dented Pipes 53
   - Fracture Criterion for Dented Pipes with Cracks 54
   - Fatigue Criterion for Dented Pipes 54
   - Moment Criterion for Buckling and Collapse of Dented Pipes 55
     - *Collapse Criterion* *55*
     - *Buckling/Collapse of Dented Pipe* *55*
3. Fracture of Pipes with Longitudinal Cracks 56
   - Failure Pressure of Pipes with Longitudinal Cracks 56
   - Burst Pressure of Pipes Containing Combined Dent and Longitudinal Notch 57
     - *Toughness Modification* *58*
     - *Compliance Modification* *58*
     - *Geometry Function* *59*
     - *Bending Moment, M, and Uniaxial Tensile Stress, σ, in a Dented Pipe* *60*
     - *Flow Stress Modification* *61*
   - Burst Strength Criteria 61
4. Fracture of Pipes with Circumferential Cracks 62
   - Fracture Condition and Critical Stress 62
   - Material Toughness, K_{mat} 62
   - Net Section Stress, σ_n 62
   - Maximum Allowable Axial Stress 63
5. Reliability-Based Assessment 63
   - Design Format versus LSF 63
     - *Design Format* *63*
     - *Limit State Function* *64*
   - Uncertainty Measure 64
6. Design Examples 64
   - Case Description 65
   - Parameter Measurements 65
   - Reliability Assessments 65
   - Sensitivity Study 66

References 70

Subsea Pipeline Integrity and Risk Management
ISBN 978-0-12-394432-0
http://dx.doi.org/10.1016/B978-0-12-394432-0.00003-2

1. INTRODUCTION

With the increased use of pressure vessels, pipelines, and piping systems, more and more pipes are being put into use. Mechanical damages in the form of dents and cracks occur frequently. These damages are mainly caused by third party or operation activities, fabrication errors, and so forth. Leakage of gas and oil from pipes due to structural failure may lead to reduced operating pressure or stopped production, human and environmental hazards, and the significant economic loss, consequently. Since the existence of dents especially at weld seams is one of the causes of leakage, it is important to arrive at a basis for assessing the structural integrity of dented pipe with cracks.

The first part of the chapter deals with the burst strength criteria of dented pipes with longitudinal and circumferential cracks. Subsequently, fracture assessment of damaged pipes is studied. Uncertainties involved in loading, strength, and modeling are assessed. In the third part of the chapter, fracture reliability model of dented pipes with cracks is developed. Reliability-based calibration of the safety factor and uncertainty modeling is performed. Conclusions and recommendations are also outlined.

2. LIMIT-STATE BASED CRITERIA FOR DENTED PIPES

General

Pipeline systems are more and more are used for transportation of gas and oil. They are usually unprotected when resting on the seabed and exposed to cyclic loading and corrosive fluids and gases. Typical defects that may found in the pipeline systems include

- Dents due to impact or local buckling.
- Corrosion.
- Cracks.

Failure modes for the pipeline systems in service may be categorized as

- Serviceability limit state (out of roundness).
- Ultimate limit state.

The remaining strength evaluation based on a limit state approach includes assessment against the following failure modes:

- Out of roundness.
- Fracture.
- Fatigue.
- Bursting.

- Collapse.
- Local buckling.

When damages have been found in the pipeline systems, possible actions are

- None.
- Seabed intervention.
- Reduced operating pressure and pressure fluctuation.
- Repair.
- Replacement of pipe sections.

In this section, a set of limit state design equations are developed for dented pipe, including bursting, buckling or collapse, fatigue, and fracture for

- Deepwater pipelines under combined loads.
- Metallic risers in deep water.
- High-strength steel.
- Different safety levels.

In particular, buckling and collapse equations for dented pipe have been newly developed for combined pressure, axial force, bending, and torsional moment. Some of these limit states are discussed in more detail in the following text.

Serviceability Limit State (Out of Roundness)

Out of roundness is a serviceability limit state mainly dictated by the operation of the pigging tools. The maximum allowable out of roundness is between 2.5 and 5%, while fabrication tolerance is between 0.5 and 1.5%.

A detected out of roundness significantly higher than what is assumed in the design influences the predicted collapse pressure and the bending moment capacity for external pressure load conditions.

Bursting Criterion for Dented Pipes

The bursting criterion is an ultimate limit state, which for design normally is given in form of a maximum allowable internal overpressure. The bursting limit state is often used in wall thickness design for pipes where internal pressure is the dominating load. The detection of cracks, corrosion as well as their size, number, and orientation have high influence on the capacity. The bursting criterion for dented pipe may be summarized as follows:

- The bursting strength of a dented pipe is close to that for a new pipe if there is no crack in the dented area.
- A crack in the dented area may reduce bursting strength due to stress concentration at the crack tip.

- Bursting of a dented pipe with a crack is actually a fracture failure mode.
- A dented pipe with cracks must be assessed.

Fracture Criterion for Dented Pipes with Cracks

The fracture criterion is an ultimate limit state normally in the form of a maximum allowable tensile strain. In pipeline design, the fracture limit state is based on wall thickness and minimum detectable crack size, given by pipe dimensions and the measuring method.

A detected crack larger than assumed in the design or a corrosion defect deeper than an included corrosion allowance changes the predicted fracture strength and the fracture calculations should be updated in accordance with the measured values.

Fatigue Criterion for Dented Pipes

The fatigue criterion is a limit state normally given in form of a maximum allowable stress range derived based on the S-N curve approach or fracture mechanics approach. The fatigue limit state is based on the design life and assumed load cycles during the life cycle of the pipeline. High plastic deformation of the pipe caused by a dent may reduce the fatigue life dramatically. A severe reduction in cross-sectional area due to cracks or corrosion also reduces the fatigue life.

The fatigue criterion may be divided into fatigue due to cyclic internal pressure and fatigue due to cyclic longitudinal forces and bending. The fatigue damage is influenced by detection of dents, cracks and corrosion.

In fatigue-dented pipes due to cyclic pressure loads,

- The fatigue of dented pipe without a crack is to be calculated using S-N curve approach, where stress concentration due to the dent is included. The design is to estimate allowable cycles of stress range.
- The fatigue of dented pipe with crack is to be based on fracture mechanics approach, which accounts for crack growth and final fracture. It is important to define correct input data on material and defects in the fracture mechanics assessment.

In the fatigue of dented pipes due to cyclic longitudinal force and bending,

- The fatigue strength of dented pipe without a crack is close to the fatigue strength of new pipes.
- Stress concentration due to dents should be accounted for, and this is similar to the design of new pipes.

Moment Criterion for Buckling and Collapse of Dented Pipes

Collapse Criterion

The collapse criterion is an ultimate limit state, which for design normally is given in form of a maximum allowable external overpressure. The collapse limit state is often used in wall thickness design for pipes where external pressure is the dominating load. Cracks, corrosion as well as their size, number, and orientation have high influence on the capacity.

Buckling/Collapse of Dented Pipe

The moment capacity equations for dented pipe are based on the following mechanism:

- The stress distribution is a fully plastic yielding problem.
- Integrating stress over the cross section to get a fully plastic interaction equation for pipes under the combined internal pressure, axial force, and bending as well as torsion.
- The derived interaction equations are to be validated using finite element models, see Hauch and Bai [1, 2].
- The effect of torsion may be included using plastic interaction equations, derived by Fujikubo et al. [3].

When the dent angle is less than the angle to the plastic neutral axis, the moment capacity of dented pipes may be expressed as follows. For a dent in the tensile side of the cross section,

$$M_{\text{dented}} = M_{\text{allowable}}(F,p) - 0.5\frac{\eta_{\text{RM}}}{\gamma_{\text{C}}}M_{\text{l}}[\sin(\beta) - \beta\cos(\beta)] \left[\alpha\frac{p}{\eta_{\text{RP}}p_{\text{l}}} + \sqrt{1-(1-\alpha^2)\left(\frac{p}{\eta_{\text{RP}}p_{\text{l}}}\right)^2}\right] \quad [3.1]$$

For a dent in the compressive side of the cross section,

$$M_{\text{dented}} = M_{\text{allowable}}(F,p) - 0.5\frac{\eta_{\text{RM}}}{\gamma_{\text{C}}}M_{\text{l}}[\beta\cos(\beta) - \sin(\beta)] \left[\alpha\frac{p}{\eta_{\text{RP}}p_{\text{l}}} + \sqrt{1-(1-\alpha^2)\left(\frac{p}{\eta_{\text{RP}}p_{\text{l}}}\right)^2}\right] \quad [3.2]$$

where

M_{C} (F, p) = Hauch and Bai [2]

M_{l} = limit moment (plastic moment capacity as for a pipe without damage)

F_l = longitudinal limit force (longitudinal force capacity as for a pipe without damage)

p_l = limit pressure (the external limit pressure is given by Thimoshenko or Haagsma, including high out of roundness and reduction in cross-sectional area due to cracks, see Bai and Hauch [4]

For a dented pipe under external pressure, the collapse strength of a dented pipe may be obtained by a curve between

- The collapse pressure for pipes without dent (e.g., Timoshenko's equations).
- The collapse pressure for pipes with very deep dents or buckles propagation pressure.

The alpha factor is an important factor that affects the accuracy of the derived equations. Ideally, its value should be calibrated against experimental and numerical tests. Tentatively, it is suggested that $\alpha = 0.25(P_l/F_l)$.

It may be concluded that

- A new set of equations for calculating the bending moment strength are newly suggested for metallic pipes with corrosion defects or dent damage (and cracks).
- The finite element method provides good predictions of the load versus deflection behavior of pipes.
- Results from the developed analytical equations and finite element analyses are in good agreement for the range of variables studied.
- Load and usage factors have been suggested for safety class low, normal, and high.
- A full set of design criteria for corroded pipe, dented pipe, are presented as an extension to Hauch and Bai [2].

3. FRACTURE OF PIPES WITH LONGITUDINAL CRACKS

The following assumptions are made for the analysis:

- The elastic-plastic fracture mechanics method is applied.
- The dent is assumed to be continuous and have a constant length.
- The stress concentrator is considered to be a notch located at the deepest point of the dent (infinite length, constant depth). The notch is longitudinal of length $L = 2c$ and depth a.

Failure Pressure of Pipes with Longitudinal Cracks

Longitudinal surface cracks can occur as isolated cracks or in colonies of numerous closely spaced and parallel cracks. A procedure based on Maxey et al. [5] for calculating the failure stress of longitudinal

flaws is as follows.The Folias factor, M_T, is determined from Kiefner and Veith [6]:

$$M_T = \sqrt{1 + 0.6275x^2 - 0.003375x^4} \text{ for } x \leq 7.07 \quad [3.3]$$

$$M_T = 0.032x^2 + 3.3 \text{ for } x > 7.07 \quad [3.4]$$

where:

$x = L/(Dt)^{0.5}$

L = total length of the crack ($L = 2c$)

D = pipe nominal outside diameter

t = pipe wall thickness.

The failure pressure of pipes with longitudinal flaws is calculated as

$$P_c = \frac{4t\sigma_{flow}}{\pi D M_s}\cos^{-1}[\exp(-B)] \quad [3.5]$$

where σ_{flow} is the material flow stress, and auxiliary parameters M_s and B are given as follows:

$$M_s = \frac{M_T t - a}{M_T(t - a)} \quad [3.6]$$

$$B = \frac{\pi}{4L}\left(\frac{K_{mat}}{\sigma_{flow}}\right)^2 \quad [3.7]$$

where

a = crack depth

K_{mat} = material toughness, estimated from Charpy impact energy tests, as shown later

By applying a safety factor, γ, the allowable pressure can be calculated from

$$P = \frac{P_c}{\gamma} \quad [3.8]$$

The safety factor, γ, can be calibrated by reliability methods, as discussed in the following section. If no calibration is conducted, it is suggested that $\gamma = 2.0$.

Burst Pressure of Pipes Containing Combined Dent and Longitudinal Notch

The fracture condition for the Bilby-Cottrell-Swinden dislocation model [7] is given as [8]

$$\sigma = \frac{2\sigma_p}{\pi}\cos^{-1}\left[\exp\left(-\frac{\pi K_{mat}^2}{8a\sigma_p^2}\right)\right] \quad [3.9]$$

where

σ = stress at failure (bursting)

σ_p = collapse stress for a pipe with an infinitely long defect notch of depth a

This model has been used successfully to describe the failure of part-wall defects in pipes, but modifications are needed before it can be used for dented pipes with defects, as discussed below.

Toughness Modification

Pipe toughness is measured in terms of the Charpy energy, C_v. This measure has been shown to be a good qualitative measure for pipe toughness but has no theoretical relation with the fracture toughness parameter, K_{mat}. It is, therefore, necessary to use an empirical relationship between K_{mat} and C_v.

The Battelle K_{mat}-C_v relationship has been derived based on nonlinear regression on full-scale tests of mechanical damaged pipes. But the deterioration of the fracture toughness caused by the material deformation as a result of denting has not been taken into account. The K_{mat}-C_v relationship has been modified in Nederlanse Gasunie as

$$K_{mat}^2 = 1000\frac{E}{A}(C_v - 17.6) \qquad [3.10]$$

where

K_{mat} = material toughness (N/mm$^{(3/2)}$)

C_v = Charpy energy (J)

E = Young's modulus (N/mm^2)

A = section area for Charpy test (mm^2), normally $A = 80$ mm^2

Compliance Modification

The Bilby-Cottrell-Swinden dislocation model is for an embedded crack in an infinite body. For other geometry and crack shapes, it is necessary to introduce the elastic compliance factor, Y (also called geometry function Y). Rearranging the equation and introducing Yas described by Heald et al. [8], the stress intensity factor (SIF), K, can be written as

$$K = Y\sigma_p\left\{\frac{8a}{\pi}\ln\left[\sec\left(\frac{\sigma}{\sigma_p}\frac{\pi}{2}\right)\right]\right\}^{1/2} \qquad [3.11]$$

In this chapter, geometry functions for a surface crack in plates by Newman and Raju [9] are used. For the wide plate under combined tension

and bending, the stress intensity factor, K, is the sum of tension and bending terms:

$$K = \frac{F}{\sqrt{Q}}\sigma\sqrt{\pi a} + H\frac{F}{\sqrt{Q}}\frac{6M}{t^2}\sqrt{\pi a} \qquad [3.12]$$

where the factors F, Q, and bending correction factor H are given by Newman and Raju.

Geometry Function

Geometry correction factors Q, F, and H are given by the following:

$$Q = 1 + 1.464\left(\frac{a}{c}\right)^{1.65} \text{ for } \frac{a}{c} \leq 1 \qquad [3.13]$$

where

c = half length of the dent

$$F = \left[M_1 + M_2\left(\frac{a}{t}\right)^2 + M_3\left(\frac{a}{t}\right)^4\right] f_\phi g f_w \qquad [3.14]$$

where

$$M_1 = 1.13 - 0.09\frac{a}{c}$$

$$M_2 = -0.54 + \frac{0.89}{0.2 + \left(\frac{a}{c}\right)}$$

$$M_3 = 0.5 - \frac{1}{0.65 + \left(\frac{a}{c}\right)} + 14\left(1 - \frac{a}{c}\right)^{24}$$

$$g = 1 + \left[0.1 + 0.35\left(\frac{a}{t}\right)^2\right](1 - \sin\phi)^2$$

where

ϕ = parametric angle of the elliptical crack

The function f_ϕ, an angular function from the embedded elliptical crack solution, is

$$f_\phi = \left[\left(\frac{a}{c}\right)^2 \cos^2\phi + \sin^2\phi\right]^{1/4} \qquad [3.15]$$

The function f_w, a finite-width correction factor, is

$$f_w = \left[\sec\frac{c}{D}\cdot\sqrt{\frac{a}{t}}\right]^{1/2} \quad [3.16]$$

The function H has the form:

$$H = H_1 + (H_2 - H_1)\sin^p \phi$$

where

$$p = 0.2 + \left(\frac{a}{c}\right) + 0.6\left(\frac{a}{t}\right)$$

$$H_1 = 1 - 0.34\left(\frac{a}{t}\right) - 0.11\left(\frac{a}{c}\right)\left(\frac{a}{t}\right)$$

$$H_2 = 1 + G_1\frac{a}{t} + G_2\left(\frac{a}{t}\right)^2$$

and

$$G_1 = -1.22 - 0.12\left[\frac{a}{c}\right]$$

$$G_2 = 0.55 - 1.05\left(\frac{a}{c}\right)^{0.75} + 0.47\left(\frac{a}{c}\right)^{1.5}$$

Bending Moment, M, and Uniaxial Tensile Stress, σ, in a Dented Pipe

Solutions for bending moment, M, and uniaxial tensile stress, σ, in a dented pipe are given by Shannon [10]. These complex functions can be approximately represented by the following relationships:

$$\sigma = \sigma_H\left(1 - 1.18\frac{D_d}{D}\right) \quad [3.17]$$

$$M = 0.85\sigma_H t D_d \quad [3.18]$$

where

σ_H = nominal hoop stress

D_d = dent depth.

Substituting σ and M into Eq, [3.16],

$$K = \frac{F}{\sqrt{Q}}\left[1 - 1.8\left(\frac{D_d}{D}\right) + 5.1H\left(\frac{D_d}{t}\right)\right]\sigma_H\sqrt{\pi a} \quad [3.19]$$

Therefore, the geometry function Y can be expressed as

$$Y = \frac{F}{\sqrt{Q}}\left[1 - 1.8\left(\frac{D_d}{D}\right) + 5.1H\left(\frac{D_d}{t}\right)\right] \quad [3.20]$$

The material fails when the following critical condition is satisfied:

$$K = K_{mat} \quad [3.21]$$

in which K_{mat} is related to the Charpy energy, C_v.

Flow Stress Modification

A more accurate measure of the plastic failure stress is the collapse stress with a defect present. Following the B31G, collapse stress for a rectangular defect in a pipe is

$$\sigma_p = \sigma_f \frac{t - a}{t - aM_T^{-1}} \quad [3.22]$$

in which σ_f is the flow stress for intact pipe and can be estimated from API 5L [11]as

$$\sigma_f = \alpha\sigma_y \quad [3.23]$$

where σ_y is the pipe yield strength and parameter α is around 1.25, α decreases when σy increases.

Burst Strength Criteria

The critical stress at failure is obtained from Eqs. [3.11] and [3.21] as

$$\sigma = \frac{2\sigma_p}{\pi}\cos^{-1}\left[\exp\left(-\frac{\pi K_{mat}^2}{Y^2 8a\sigma_p^2}\right)\right] \quad [3.24]$$

Burst strength is given by

$$P = 2\sigma\frac{t}{D} \quad [3.25]$$

Based on a failure assessment diagram (FAD), the aforementioned burst strength can also be obtained by use of the procedure presented in the BSI's PD6493 [12], in which iteratively solving the equation of assessment involves including safety factors, as described for the case for circumferential cracks.

4. FRACTURE OF PIPES WITH CIRCUMFERENTIAL CRACKS

It is assumed that the stress concentrator is a notch located at the deepest point of the dent, it is continuous (infinite length, constant depth) and has circumferential length $2c$ and depth a.

Fracture Condition and Critical Stress

Based on PD6493, the equation of the fracture failure assessment curve is given by

$$K_r = S_r \left\{ \frac{8}{\pi^2} \ln \left[\sec \left(\frac{\pi}{2} S_r \right) \right] \right\}^{-1/2} \quad [3.26]$$

in which

$$K_r = \frac{K_I}{K_{mat}} + \rho \quad [3.27]$$

where

ρ = plasticity correction factor

K_I = stress intensity factor, determined from the following equation:

$$K_I = Y\sigma\sqrt{\pi a} \quad [3.28]$$

where Y_σ is divided to primary stress term and secondary stress term as:

$$Y_\sigma = (Y\sigma)_p + (Y\sigma)_s \quad [3.29]$$

The stress ratio, S_r, is defined as the ratio of net section stress, σ_n, to flow stress σ_{flow}:

$$S_r = \frac{\sigma_n}{\sigma_{flow}} \quad [3.30]$$

Material Toughness, K_{mat}

Several statistical correlations exist between standard full-size C_v (the Charpy V notch) and K_{mat}. Rolfe [13] developed the following correlation for upper-shelf toughness in steel:

$$K_{mat} = \sigma_y \sqrt{\frac{0.6459 C_v}{\sigma_y} - 0.25} \quad [3.31]$$

with K_{mat} in MPa(mm)$^{1/2}$, C_v in mm-N, and σ_y in MPa.

Net Section Stress, σ_n

Following PD6493, the net section stress for pipes with a surface flaw is

$$\sigma_n = \frac{\sigma_b + \sqrt{\sigma_b^2 + 9\sigma_m^2(1-\alpha)^2}}{3(1-\alpha)^2} \quad [3.32]$$

where

σ_b = bending stress

σ_m = membrane stress

$$\alpha = \left(\frac{2a}{t}\right) \Big/ \left(1 + \frac{t}{c}\right)$$

$$\sigma_b = M / \frac{t^2}{6}$$

where M is given by Eq. [3.18], substituting σ_H with nominal axial stress, σ_{AX}.

Maximum Allowable Axial Stress

The critical stress at failure is obtained by iteratively solving the Level-2 FAD of PD6493 (Eq. [3.26]) including safety factors.

5. RELIABILITY-BASED ASSESSMENT

Design Format versus LSF

Design Format

If only internal pressure is considered, the partial safety factor approach given by Eq. [3.8] leads to the design format as

$$P_c \geq \gamma P_L \quad [3.33]$$

where

P_c = characteristic strength of the pipe according to a criterion

P_L = characteristic load (internal pressure)

γ = safety factor

The new design equation for dented pipes with cracks in operation with respect to fracture criterion can be formulated by substituting Eqs. [3.24] and [3.25] into Eq. [3.33]:

$$P_L \leq \frac{1}{\gamma} \cdot 2\frac{t}{D} \cdot \frac{2\sigma_p}{\pi} \cos^{-1}\left[\exp\left(-\frac{\pi K_{mat}^2}{Y^2 8a\sigma_p^2}\right)\right] \quad [3.34]$$

All the parameters in the new design format can be referred to the aforementioned sections. Note that characteristic values of those parameters are used to estimate the design pressure.

Limit State Function

The limit state function (LSF) can be formed based on failure criteria for the specified case. Pipes burst at the uncontrolled tearing point if the equivalent stress exceeds the flow stress. The bursting failure leads to pipe rupture. The LSF based on the new fracture criterion can be formulated as

$$g(Z) = 2\frac{t}{D}\cdot\frac{2\sigma_{\mathrm{p}}}{\pi}\cos^{-1}\left[\exp\left(-\frac{\pi K_{\mathrm{mat}}^2}{Y^2 8a\sigma_{\mathrm{p}}^2}\right)\right] - P_{\mathrm{L}} \qquad [3.35]$$

where Z is the set of random variables involved in the new design format. By introducing the normalized random variables, including a model error, as discussed in details later, the new LSF is given by

$$g(Z) = \frac{4t_{\mathrm{c}}\sigma_{\mathrm{fc}}}{\pi D_{\mathrm{c}}} X_{\mathrm{M}} X_{\mathrm{i}} X_{\mathrm{f}} X_{\mathrm{s}}^{-1} \cos^{-1}\left[\exp\left(\frac{-\pi M_{\mathrm{s}}^2 K_{\mathrm{mat}}^2}{\sigma_{\mathrm{fc}}^2 Y^2 8a X_{\mathrm{Y}}^2 X_{\mathrm{f}}^2}\right)\right] \qquad [3.36]$$

where P_d, the design pressure, can be estimated from new design Eq. [3.34]; parameters M_{s} and K_{mat} are given by Eqs. [3.6] and [3.10], respectively, by introducing uncertainties into the corresponding random variables; and the subscript c indicates the characteristic values of corresponding variables.

Uncertainty Measure

Considering uncertainties involved in the design format, each random variable X_{i} can be specified as

$$X_{\mathrm{i}} = B_{\mathrm{X}} \cdot X_{\mathrm{C}} \qquad [3.37]$$

where X_{C} is the characteristic value of X_{i}, and B_{X} is a normalized variable reflecting the uncertainty in X_{i}. The statistical values for these biases are given in the next section.

6. DESIGN EXAMPLES

Cited from a practical evaluation of an existing dented pipe, an example is given to verify the presented model and demonstrate its application in assessing structural integrity of damaged pipes.

Case Description

The analysis is based on the data given in Table 3.1 from an existing pipe.

Parameter Measurements

A complete list of uncertainties parameters for reliability analysis is given in Table 3.2.

Reliability Assessments

Fracture reliability assessment is performed by use of STRUREL [14] and PROBAN [15], respectively.

The influence of dent depth on fracture reliability is given in Figure 3.1, from which it is seen that no obvious changes can be observed if the dent depth is not serious. But, failure probability increases dramatically with the increase of dent depth.

Table 3.1 Basic Input Data of Pipe

Pipe outside diameter, D	1066.8 mm
Pipe yield strength, σ_y	413.7 N/mm^2
Material	API 5L60
Pipe wall-thickness, t	14.3 mm
Design pressure, P	1.913 MPa
Dent depth, D_d	45 mm
Hydrostatic test pressure	30 kg/cm^2

Table 3.2 Basic Probabilistic Parameters Description

Random Variable	Distribution	Mean	cov
Wall thickness factor, X_t	Normal	1.04	0.02
Flow stress factor, X_f	Normal	1.14	0.06
Flow stress model, X_M	Normal	0.92	0.11
Max. pressure factor, X_P	Gumbel	1.05	0.02
Crack length factor, X_L	Normal	1.00	0.10
Crack depth, a	Exponential	0.10	1.00
Dent depth factor, X_D	Normal	0.90	0.05
Y function factor, X_Y	Log normal	1.00	0.10
Charpy energy, C_v	Log normal	63.0	0.10
Young's modulus, E	Normal	210	0.03

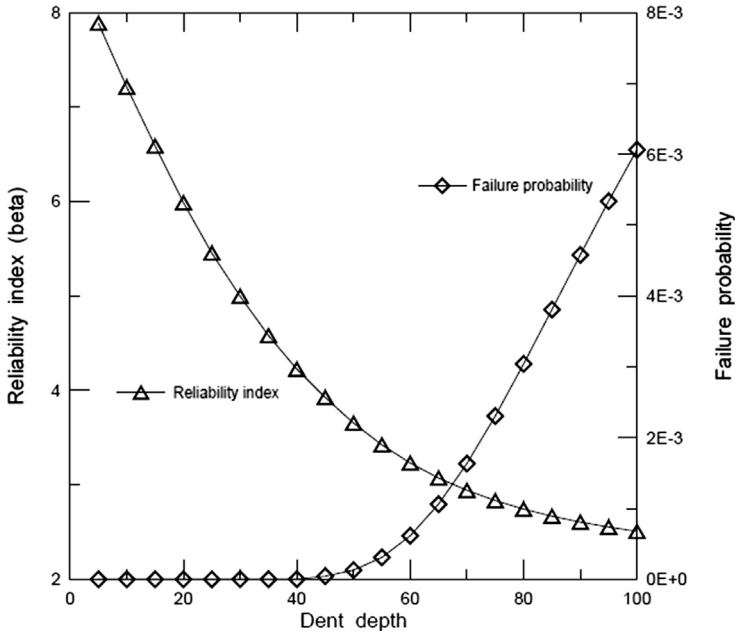

FIGURE 3.1 *Effect of Dent Depth, D_d.*

Figure 3.2 gives the results of the changes of failure probability and reliability index versus dent depth to wall thickness ratio, D_d/t. It is interesting to note that this ratio is a key factor affecting pipe fracture strength, since the stress concentration in the bottom of the dent is proportional to the dent depth.

Parametric study results of dent depth to outside diameter D_d/D is shown in Figure 3.3, from which it is observed that failure probability increases rapidly when the ratio of D_d/D exceeds a certain value, say 4%. Care should be taken for the case of a large D_d/D.

The effect of crack depth to pipe wall thickness ratio, a/t, on fracture reliability is studied and shown in Figure 3.4, from which it is observed that the ratio a/t is quite an influential on the fracture reliability. As the crack depth increases, the reliability decreases rapidly.

Sensitivity Study

From Figure 3.1, it is seen that some dominating factors are very influential to the reliability index. Their effect on different target safety levels are studied and the results are shown in Table 3.3 [16]. In addition to those parameters discussed previously, other major parametric study results are

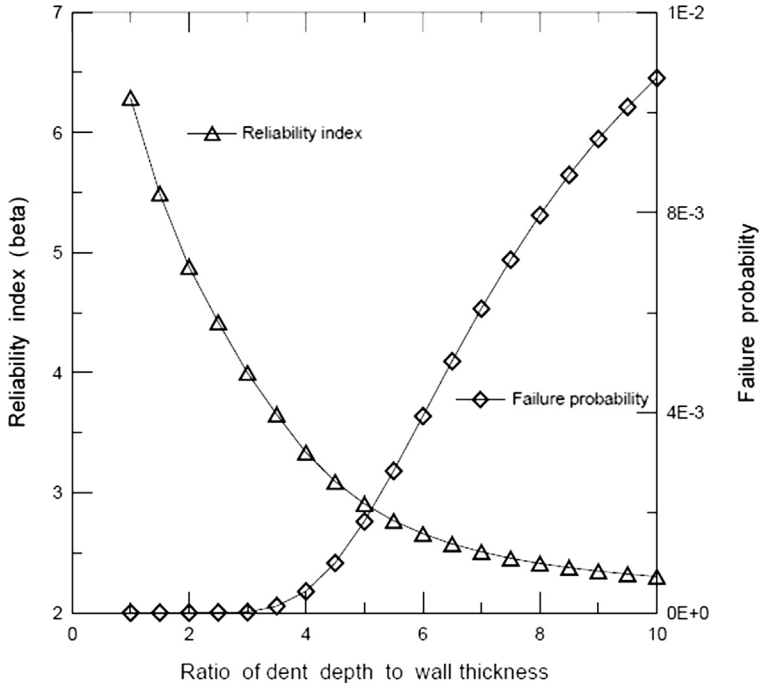

FIGURE 3.2 *Effect of Dent Depth to Thickness (D_d/t).*

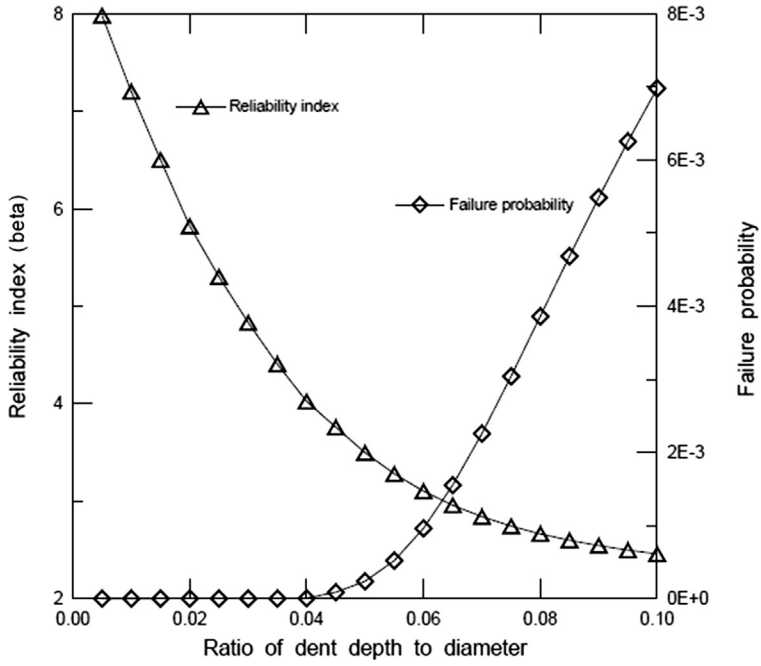

FIGURE 3.3 *Effect of Dent Depth to Diameter Ratio (D_d/D).*

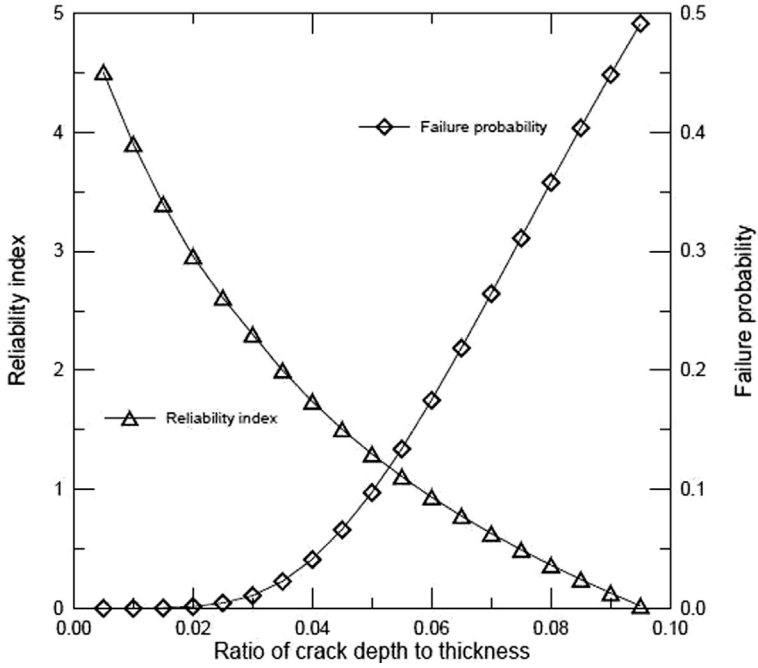

FIGURE 3.4 *Effect of Crack Depth to Thickness Ratio (a/t).*

listed in this table, in which the variations of the safety factor are set to $\gamma = 1.6$ to ~ 2.2 (Figure 3.5) and the investigation is performed based on the basic input parameters given in Table 3.3. The different parameters between the investigated case and the basic case are indicated in the table with given distribution type, mean, and covariance. A clearer picture of the parametric studies can be obtained from Table 3.3. It is important to note, from Table 3.3, that crack depth, a, is very influential to the reliability index. In practical engineering, crack depth varies from case to case due to the measurability of the pressure vessels. Different crack sizes have a corresponding calibrated safety factor. Also, log-normal distribution may be applied to fit the crack size [17]. In this case, it is noted from the comparison in Table 3.3 that the reliability index increases a great deal, so that it is essential to choose a suitable crack depth based on a practical considered case to have rational results. It is observed from Table 3.3 that the estimated reliability index is very sensitive to model uncertainty. In the interpretation of this result, it is important to be aware of that the results depend heavily on the chosen uncertainty model. Even a small change in X_M leads to a big change in the reliability index. Therefore, further study including tests and

Table 3.3 Parameter Studies

Parametric studies		$\gamma = 1.6$		$\gamma = 1.8$		$\gamma = 2.0$		$\gamma = 2.2$	
		β	P_F	β	P_F	β	P_F	β	P_F
X_M	N(0.92, 0.11)	3.048	.115E-02	3.516	.219E-03	3.926	.432E-04	4.293	.882E-05
	N(1.0, 0.1)	3.298	.487E-03	3.768	.824E-04	4.183	.144E-04	4.557	.260E-05
	N(1.0, 0.2)	2.140	.162E-01	2.457	.700E-02	2.712	.334E-02	2.921	.174E-02
a	EXP(0.1)	3.048	.115E-02	3.516	.219E-03	3.926	.432E-04	4.293	.882E-05
	EXP(0.18)	2.436	.742E-02	2.861	.211E-02	3.241	.595E-03	3.588	.167E-03
	LN(0.09, 1.0)	3.664	.124E-03	4.297	.868E-05	4.812	.747E-06	5.240	.806E-07
X_d	N(0.9, 0.05)	3.048	.115E-02	3.516	.219E-03	3.926	.432E-04	4.293	.882E-05
	N(0.9, 0.10)	2.990	.139E-02	3.440	.291E-03	3.833	.632E-04	4.186	.142E-04
	N(0.9, 0.15)	2.909	.185E-02	3.334	.428E-03	3.708	.105E-03	4.043	.264E-04
X_t	N(1.04, 0.02)	3.048	.115E-02	3.516	.219E-03	3.926	.432E-04	4.293	.882E-05
	N(1.04, 0.05)	2.910	.181E-02	3.355	.397E-03	3.742	.912E-04	4.088	.218E-04
	N(1.04, 0.10)	2.508	.608E-02	2.881	.198E-03	3.197	.694E-03	3.474	.257E-03
X_Y	LN(1.0, 0.10)	3.048	.115E-02	3.516	.219E-03	3.926	.432E-04	4.293	.882E-05
	LN(1.0, 0.20)	2.808	.249E-02	3.197	.695E-03	3.536	.204E-03	3.838	.621E-04
	LN(1.0, 0.30)	2.624	.435E-02	2.991	.139E-02	3.317	.454E-03	3.613	.151E-03
C_v	LN(63.0, 0.1)	3.048	.115E-02	3.516	.219E-03	3.926	.432E-04	4.293	.882E-05
	LN(63.0, 0.2)	2.843	.223E-02	3.251	.574E-03	3.605	.156E-03	3.917	.448E-04
	LN(63.0, 0.3)	2.530	.570E-02	2.845	.222E-02	3.102	.962E-03	3.313	.462E-03

Note: Distribution types used in the table include N = normal, LN = log normal, EXP = exponential.

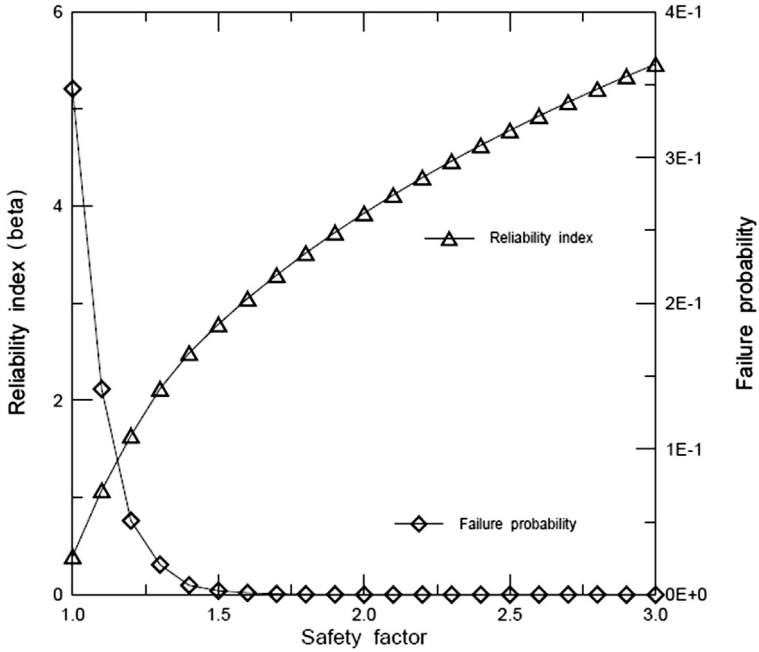

FIGURE 3.5 ***Safety Factor*** γ ***Versus*** β ***and*** P_f.

additional information from inspection are needed. Also note, from this table, the uncertainty of pipe wall thickness is quite influential to the reliability index. This is just as expected, since wall thickness is an important design parameter of pipes.

REFERENCES

[1] Hauch S, Bai Y. Use of finite element analysis for local buckling design of pipelines; 1998. OMAE'98.
[2] Hauch S, Bai Y. Bending moment capacity of pipes; 1999. OMAE'99.
[3] Fujikubo M, Bai Y, Ueda Y. Dynamic elastic-plastic analysis of offshore framed structures by plastic node method considering strain hardening effects. Int J Offshore Polar Eng 1991;1(3):220–7.
[4] Bai Y, Hauch S. Analytical collapse of corroded pipes; 1998. ISOPE'98.
[5] Maxey WA, et al. Ductile fracture initiation, propagation and arrest in cylindrical pressure vessels. ASTM STP 514. Philadelphia: American Society of Testing and Materials; 1972.
[6] Kiefner JF, Vieth PH. A modified criterion for evaluation the remaining strength of corroded pipe. RSTRENG, Project PR-3–805 Pipeline Research Committee. Ohio: American Gas Association; 1989.
[7] Bilby BA, Cottrell AH, Swinden KH. The spread of plastic yield from a notch. Proc R Soc 1963;A272:304.

[8] Heald PT, et al. Fracture initiation toughness measurement methods. Mater Sci Eng 1971;10:129.
[9] Newman JC. RajuIS. An empirical stress-intensity factor equation for the surface crack. Eng Fracture Mech 1981;15:85–191.
[10] Shannon RWE. Failure behaviour of line pipe defects. International Journal of Pressure Vessels and Piping 1974;2(3):243–55.
[11] API. 5L specifications. Washington, DC: America Petroleum Institutes; 1993.
[12] BSI. PD6493. Guidance on methods of assessing the acceptability of flaws in fusion welded structures. London: British Standard Institute; 1991.
[13] Rolfe ST. Slow bend KIC testing of medium strength high toughness steels. ASTM STP 463. Philadelphia: American Society of Testing and Materials; 1970.
[14] STRUTEL. A structural reliability analysis program system. Munich: Germany: RCP Consult; 1996.
[15] PROBAN. General purpose probabilistic analysis program. Bærum, Norway: Det Norske Veritas; 1996.
[16] Bai Y, Song R. Fracture assessment of dented pipes with cracks and reliability-based calibration of safety factors. Int J Press Vessels Piping 1997;74:221–9.
[17] Kirkemo F. Application of probabilistic fracture mechanics of offshore structures. Houston, TX: Proc. of OMAE; 1988.

CHAPTER 4

Pipeline Inspection and Subsea Repair

Contents

1. Pipeline Inspection 73
   - Introduction 73
   - Metal Loss Inspection Techniques 76
     - *General* 76
     - *Magnetic Flux Leakage* 76
     - *Ultrasonics Pig* 80
     - *High-Frequency Eddy Current* 82
     - *Remote Field Eddy Current* 83
   - Intelligent Pigs for Purposes Other than Metal Loss Detection 84
     - *General* 84
     - *Crack Detection* 84
     - *Calipering* 85
     - *Route Survey* 85
     - *Free-Span Detection* 86
     - *Leak Detection* 86
2. Pipeline Repair Methods 86
   - Conventional Repair Methods 86
   - General Maintenance Repair 88
     - *Corrosion Coating Repair* 88
     - *Submerged Weight Rectification* 88
     - *Cathodic Protection Repairs* 90
     - *Pipeline Span Rectification* 92
3. Deepwater Pipeline Repair 93
   - Introduction 93
   - Diverless Repair Research and Development 95
   - Intelligent Plugs for Deepwater Pipeline Repair 96

References 98

1. PIPELINE INSPECTION

Introduction

Pipeline inspection is a part of pipeline integrity management for keeping the pipeline in good condition. The rules governing inspection are the pipeline safety regulations. In most cases, the pipeline is inspected regularly.

Subsea Pipeline Integrity and Risk Management
ISBN 978-0-12-394432-0
http://dx.doi.org/10.1016/B978-0-12-394432-0.00004-4

The pipeline safety regulations [1] require that the operator ensure that a pipeline is maintained in an efficient state, in efficient working order, and in good repair. In fact, the pipeline operator has a vested interest in the pipeline being operated effectively and safely to satisfy the appropriate authority and save the failure costs in environment, loss of production, and repair. The pipeline inspection includes external inspection and internal inspection. The subsea pipeline external inspection looks at the pipeline's external condition, such as concrete weight coating, trench and concrete mattress losses, marine growth, anode wastage and corrosion, free spans and global buckling condition, and damages due to external loads through visual observation. The subsea pipeline internal inspection is normally carried out through nondestructive testing techniques and technologies by intelligent pigs, such as magnetic-flux leakage technology in axial and circumferential conditions, ultrasound technologies, eddy-current technologies, and other technologies.

Table 4.1 summarizes the common types of survey and inspection methods for subsea pipelines. The abbreviations in the table are defined as

- RATs: Rope access technicians; rope access is a means of working at heights or depths in locations that would be difficult or dangerous to reach by other means.
- GI: General imaging, inspection using side scan sonar.
- GVI: General visual imaging, using cameras.
- NDT: Nondestructive testing.
- FMD: Flooded member detection.
- CP: Cathodic protection.
- ROTV: Remotely operated towed vehicle.
- WROV: Work-class remotely operated vehicle.

The use of intelligent pigs has increased from, on average, about 2% of the pipelines per year at the beginning of the 1980s to about 8% in the 1990s. The inspection capabilities of intelligent pig contractors have continuously improved by developments in sensor technology and data processing, storage, and analysis. Despite all the developments in the mechanical design of pigs and the inspection technology, intelligent pigs should not be seen as infallible. Each tool has inherent limitations to inspection capabilities that should be realized. Various experiences within the industry, where unsatisfactory inspection results were obtained, emphasize this point. The main causes for unsatisfactory results have been no philosophy and the nature and operational risks of the pipeline. Indeed, many pipelines are not designed to be or have never been intelligently pigged [4].

Table 4.1 Pipeline Inspection Methods [2], [3]

Inspection	Survey Platform	Type/Method	Component	Notes/Restrictions
RATS	Platform based	Visual - cameras, NDT techniques	Riser	Down to splash zone, weather
Diver	Platform or Dynamic positioning (DP) vessel based	Visual cameras, NDT techniques	Riser, pipeline, point structures, landfalls	Depth, current, weather, sea state, Health and safety Executive (HSE)
Landfall GI	Inshore survey vessel	Hull mounted, acoustic, CP snake	Pipelines	Inshore only, weather, tides, sea state @ 1 m, fishing gear
Structural GVI	Oil platform or DP survey vessel, 3 × eyeball ROVs	Visual cameras, NDT techniques, FMD	Legs, structural members, risers	Weather, sea state @ 2 m, current, visibility
Pipeline GI	Survey vessel, ROTV	Towed Side Scan Sonart (SSS), acoustic	Pipelines, structures	Seafloor structures only, cannot stop , current restrictions, sea state @ 2 m
Pipeline GVI	Dynamic positioning (DP) survey vessel, WROV	Dynamic positioning (DP) follow sub, visual cameras, CP	Riser, pipeline, structures	Current restrictions, visibility; sea state @ 4.5–5 m

The external inspections of subsea pipelines are not detailed in this chapter, because the reasons and solutions for the evidence of things going wrong in external inspections have been discussed in most chapters of this book. In this chapter, the use of intelligent pigs to conduct internal inspections of subsea pipelines is described. The different types of pigs available and their various capabilities and limitations are summarized.

Metal Loss Inspection Techniques

General

Several techniques are available for the inspection of pipelines using pigging technology; however, each technique and tool has inherent limitations in inspection capabilities that should be realized. The type of pig chosen depends on the purpose of the inspection and the nature of the inspection data required.

Although, on occasion, the objectives of pipeline inspection using an intelligent pigging tool may vary, in general, it is the requirement to detect metal loss that concerns most operators of oil and gas pipelines.

Several techniques are applied in metal loss intelligent pigs [5]:

- Magnetic flux leakage.
- Ultrasonics.
- High-frequency eddy current.
- Remote field eddy current.

Magnetic Flux Leakage

Principle

About 90% of all metal loss inspections are performed with magnetic flux leakage (MFL) pigs. Hence, the MFL technology can be regarded as the most important technique for detecting metal loss (such as corrosion and pitting) inspections of pipelines.

The magnetic flux leakage technique is based on magnetizing the pipe wall and sensing the MFL of metal loss defects and other features. From the MFL signal patterns, it is possible to identify and recognize metal loss corrosion defects and other features, such as girth welds, seam welds, valves, fittings, adjacent metal objects, gouges, dents, mill defects, girth weld cracks, and large nonmetallic inclusions.

Magnetism

MFL pigs are equipped with large magnetic yokes to magnetize the pipe wall in the axial direction. The magnetic yoke consists of a backing bar,

permanent magnets, pole shoes, and brushes, as shown in Figure 4.1. The combination of the magnetic yoke and pipe wall is called the *magnetic circuit*. The magnetic resistance, called *reluctance*, in the magnetic circuit should be minimized to obtain a high magnetic flux density, also referred to as the *level of magnetism*, through the pipe wall. Minimization of the magnetic reluctance is achieved by optimizing the design of the magnetic yoke and using steels with a high magnetic permeability. The magnetic power is given by the strength of the permanent magnets. The strongest permanent magnets applied today are made of Nd-Fe-B. Alternatively, an electromagnet can be applied as the magnetic power source instead of a permanent magnets.

Pipe wall magnetism depends on wall thickness, tool velocity, and pipe material, except for the design of the magnetic yoke. The minimum pipe wall magnetism required to obtain good flux leakage signals is 1.6 Tesla. Lower pipe wall magnetism levels make the measurement sensitive to all sorts of disturbances. The best performance is achieved at higher magnetization levels, that is, in excess of 1.7 Tesla. A magnetic field moving through a pipeline induces eddy currents in the pipe wall. At high velocities, these eddy currents lead to a lower pipe wall magnetization and a distorted MFL field from a defect. In thick-walled pipe or high tool speed, there comes a point where the pipe wall is no longer sufficiently magnetized.

Sensors and Resolution As an MFL tool navigates the pipeline, a magnetic circuit is created between the wall of pipe and the tool. Brushes typically act as a transmitter of magnetic flux from the tool into the wall of pipe, and as the magnets are oriented in opposing directions, a flow of flux is created in an elliptical pattern. High-field MFL tools saturate the wall of pipe with magnetic flux until the wall of pipe can no longer hold any more flux. The remaining flux leaks out of the wall of pipe and strategically placed

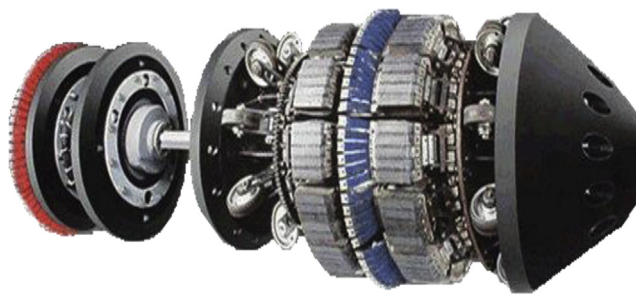

FIGURE 4.1 ***A Typical MFL Pig.*** (For color version of this figure, the reader is referred to the online version of this book.)

triaxial Hall effect sensor heads can accurately measure the three-dimensional vector of the leakage field.

Two types of sensors are applied to sense the magnetic flux leakage fields. In the past, mostly coil sensors were used, since they could be shaped in all geometries and need no power. The disadvantages are that they require a minimum tool speed and a time differential signal of the absolute flux leakage fields is obtained, which requires integration. Nowadays, more and more MFL pigging contractors apply Hall effect sensors, which have the advantage that they measure the absolute magnetic field, are sensitive and small (i.e., make a point measurement), and have no limit on minimum tool speed. The major disadvantage of Hall effect sensors is that they require power.

A measurement grid is made over the pipeline, both in the circumferential and axial directions. The resolution of the grid plays an important role on the detectability and sizing performance of small defects; hence, the best performance can be obtained only with a fine grid. The grid spacing circumference is determined by the circumferential sensor spacing and, in the axial direction, by the sampling frequency. The sensor spacing varies between 8 and 100 mm for the various MFL pigs. The axial sampling distance varies between 2.5 and 5 mm. The smallest defect to be detected and properly sized has a width equal to the sensor spacing and a length equal to about three times the axial sampling distance.

Within the intelligent pigging industry, a distinction is made between low-resolution and high-resolution MFL pigs, referring to the quality of measurement. However, note that a proper definition on low and high resolution is nonexistent. Therefore, the fact that an MFL pig is called *high resolution* does not guarantee a good performance.

Many MFL pigs contain additional sensors to discriminate between internal and external defects and to get a measure of wall thickness changes. Internal-external discrimination is done by means of sensors that are sensitive to only internal defects. Most contractors apply weak magnets combined with a magnetic field sensor placed in a second sensor ring outside the magnetic yoke that measures the decrease in magnetic field when the liftoff distance of the magnet to the pipe wall increases by internal metal loss defects. Some contractors use eddy current proximity probes that may be placed within the magnetic yokes.

A measure of the wall thickness is obtained by measuring the axial background magnetic field by means of Hall effect sensors. The axial background magnetic field is related to pipe wall magnetization and thus pipe wall thickness.

Data Analysis

MFL pigs record a large amount of data that needs to be analyzed. Most contractors have developed software that automatically analyzes the data and detects the relevant features. However, manual analysis and data checks are still necessary to obtain the most accurate defect data.

The relation between MFL signals and defect dimensions is indirect and nonlinear. Consequently, good data analysis algorithms are of importance. Defect length can be accurately determined from the start and end of the MFL signals. Defect width can be determined with limited accuracy from the circumferential signal distribution as measured by adjacent sensors. Defect depth is related to the integrated signal amplitudes, but corrections have to be made for defect length and length/width aspect ratios. For defects with a length above $3t$ (t = wall thickness) or 30 mm, this relation tends to become linear. The relationship between metal loss defect depth and MFL signals becomes more nonlinear and length dependent below a defect length of $3t$ or 30 mm, for which reason defect sizing accuracy is of lower quality.

Capabilities and Limitations

Defect detectability levels depend highly on the magnetization level in the pipe wall, the MFL noise as generated by the pipe, and the geometry metal loss defect. The pipe material influences magnetic noise levels. In particular, a seamless pipe creates a high magnetic noise level, while on the other hand, the Electric resistance welding (ERW) manufacturing process gives relatively low MFL noise levels. In addition the quality of the line pipe steel in terms of the number of nonmetallic inclusions also influences magnetic noise levels.

The geometry of the defect plays an important role on defect detectability. Mainly, the defect depth and width, that is, the cross-sectional area of metal loss normal to the pipe axis, have a strong influence on detectability. Defect length has a secondary effect on defect detectability. In general, the detectability and sizing performance reduce for very short defects (pinhole pitting, circumferential cracks) and for very long, smooth defects (axial grooves, general corrosion). Hall effect sensors that measure the absolute axial magnetic field are better suited to measure smooth grooves than coil sensors.

Under optimal conditions, the MFL pigs can detect pits as small as 5% wall thickness loss; however, most MFL pigging contractors specify pit detectability between 10% and 40% wall loss, when the large influence of pipe wall magnetization and line pipe manufacturing process has been taken into account. Under optimal circumstances, the depth sizing accuracy of

general and pitting defects are about 10% of the pipe wall thickness at 80% confidence.

Depth sizing of axial pits and grooves requires a good length/width correction factor on data analysis and an accurate measurement of defect width. In general, depth sizing of axial pits are less accurate. It has been found that the depth of defects with a length/width aspect ratio above 2 and a width smaller than the sensor spacing can be severely undersized. Under optimal conditions, the accuracy of depth sizing of axial pits are +10% and -20% of pipe wall thickness at 80% confidence. Depth sizing of circumferential pits and grooves requires a good length/width correction factor on data analysis. Under optimal conditions, the sizing accuracy can be as good as that of general and pitting defects.

Applicability

MFL pigs can be used under the following conditions:

- Up to velocities of 5 m/s but preferably between 0.5 and 3 m/s.
- $D/t > 15$, but in case $D/t < 30$, precautions may be required to ensure sufficient magnetization and good reliability of measurement.
- Pipe diameter range from 4 to 60 in.
- All sorts of product.

Ultrasonics Pig

Principle

Ultrasonic pig, as shown in Figure 4.2, utilizes ultrasonic transducers that have a standoff distance to the pipe wall. A fluid coupling is required between the transducer and pipe wall. The transducers emit sound pulses that are reflected at both the inner and outer surface of the pipe wall. The time elapsed detection of these two echoes gives a direct measure of the remaining wall thickness of the pipe. The time elapsed between pulse emittance and the first echo is used to determine the standoff distance. Any

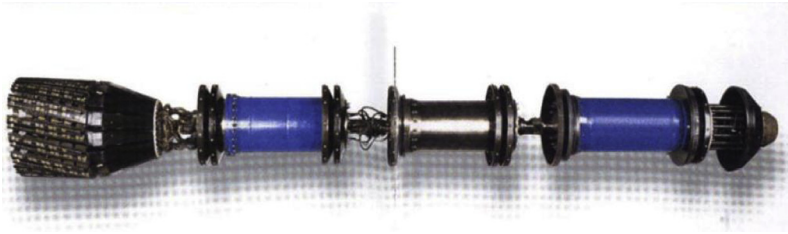

FIGURE 4.2 ***A Typical Ultrasonic Pig.*** (For color version of this figure, the reader is referred to the online version of this book.)

increase in standoff distance in combination with a decrease in wall thickness indicates internal metal loss. A decrease in wall thickness, while the standoff distance keeps constant, indicates external metal loss, laminations, or inclusions. The outer wall echo cannot be distinguished from the inner wall echo for too thin (remaining) wall thickness.

Sensors

Ultrasonic pigs utilize piezoelectric ultrasonic transducers that emit 5-MHz sound pulses. The transducers are placed a standoff distance to the pipe wall. Normally, the transducer and standoff are chosen such that the ultrasonic beam at the pipe wall has a spread of below 10 mm. The circumferential sensor spacing of the state-of-the-art ultrasonic pigs is a little under 10 mm. Consequently the smallest detectable pits have a diameter of about 10 mm. A number of measurements, about four or five, must be made in the axial direction for a pit to be recognized. The sampling frequency depends on the firing frequency of the ultrasonic transducers and the speed of the pig. Under optimal circumstances, the axial sampling distance is about 3 mm.

For accurate metal loss monitoring in heavy-wall pipelines, the ultrasonic technique is better suited than the MFL technique. In gas or multiphase lines, this can be achieved by running the ultrasonic tool in a batch of liquid, such as glycol. In view of the maximum allowable speed of an ultrasonic tool, the velocity excursions of the gas-driven pig-slug train needs to be properly controlled. The dynamics of a pig-slug train in a gas pipeline has been extensively studied to determine the optimum parameter settings to avoid the pig-slug train from stopping during the survey and subsequently shooting off at high velocities. The maximum allowable speed of the ultrasonic tool is determined by the firing frequency of the ultrasonic sensors and was in the past limited to about 1 m/s. However, due to the improved electronics, the firing frequency has been increased, which now allows a maximum velocity of around 3 m/s.

Data Analysis

Interpretation of ultrasonic signals is more straightforward than MFL signals. The standoff and wall thickness signals give a direct mapping of the pipe wall, showing all corrosion defects. A rough surface and internal debris may lead to loss of signal and can be recognized as such. In addition, laminations, inclusions, girth welds, valves, and tees can be easily recognized. Nowadays, defect detection and sizing is fully automated; however, the data are still often checked manually.

Capabilities and Limitations

Ultrasonic pigs have the advantage that they provide a better quantification of the defect sizes than MFL pigs. Detection of defects starts at lengths of 10 mm. The probability of detection becomes high at surface lengths of about 20 mm. Depth sizing accuracy of the remaining wall thickness is on the order of ± 1 mm for pits and ± 0.5 mm for general corrosion at a confidence level of about 80%. Small pits can be missed. This performance is achieved by the state-of-the-art tools.

The depth sizing error is absolute and independent of the nominal pipe wall thickness. The relative error however, increase significantly for smaller wall thickness. Most pipeline operators conclude that ultrasonics are better suited for thick-walled pipe than for thin-walled pipe. A threshold wall thickness of 7 mm is generally chosen, below which ultrasonic pigs are not recommended for use.

The amplitudes of the inner and outer wall echoes must exceed preset threshold values to be detected. The echo signal can be attenuated by fouling, roughness of surfaces, tilting of the probe, and curvature of the surface profile. Dirt at the bottom of the line during a survey may mask the most critical defects.

A rough internal pipe surface, such as due to corrosion, may result in a double inner wall reflection, causing the tool to ignore the second reflection coming from the outer wall. When this shortcoming is not realized, the metal loss is reported to be external with a completely wrong depth.

Applicability

Ultrasonic pigs can be applied under the following conditions:

- Diameter range from 6 to 60 in.
- Velocities from 1 m/s through to 3 m/s.
- For pipe wall thickness above 7 mm.
- Only for liquid products unless the tool is run in a batch of liquid.

High-Frequency Eddy Current

Principle

High-frequency eddy current (HFEC) technology has been developed for monitoring internal corrosion in heavy-walled, small-diameter pipelines.

HFEC proximity sensors are mounted on a polyurethane sensor carrier and applied for two types of measurement, so-called global and local. The local sensors measure the distance from the sensor to the pipe wall. The global sensor is used to measure the distance from the center of the carrier to

the local sensors. The combination of the measurements from local and global sensors provides the internal profile of the pipeline, by which both internal pitting and general corrosion can be determined.

The principle of eddy current is based on the phenomenon that an alternating current in a transmitter coil induces alternating currents, or eddy currents, in any nearby conductor through inductive electromagnetic coupling. The eddy currents in the conductor in turn induces currents in other nearby conductors, establishing an indirect electromagnetic coupling from the transmitter coil via the first conductor to the second conductor. Hence, a receiver coil can be indirectly coupled to a transmitter coil via the pipe wall. By designing the receiver coil in a figure 8 shape, the direct electromagnetic coupling between transmitter and receiver coil is canceled out and the receiver coil is responsive to only the indirect electromagnetic coupling via the pipe wall. The phase and amplitude of receiver coil signal are highly sensitive to the distance between the coils and the pipe wall. By a proper selection of frequency and phase of the eddy currents, the signals have been made insensitive to pipe wall material properties.

Capabilities and Limitations

The sensor geometry has been optimized so that internal pitting and general corrosion with a length exceeding 10 mm and a depth exceeding 1 mm should be detected and sized with an accuracy of ± 1 mm up to a maximum depth of 8 mm. Furthermore, the technique can accurately measure ID reductions such as dents and ovalities.

The HFEC technique can measure only internal defects, no measurement is obtained from external defects. The measurement is insensitive to the pipeline product and to debris.

Applicability

HFEC pigs can be applied under the following conditions:

- Diameter range from 6 to 12 in.
- Velocities up to 5 m/s.
- All sorts of products.
- When only internal corrosion is of concern.

Remote Field Eddy Current

The remote field eddy current (RFEC) dates back to the 1950s (well bore inspection) but use of the technique for pipeline inspection has not passed the experimental stage.

The RFEC technique utilizes a relatively large solenoidal exciter coil, internal to and coaxial with the pipe, which is energized with a low-frequency alternating current to generate eddy currents in the pipe wall. Located at two to three pipe diameters distance (remote field), one or more receivers detect those eddy currents that have penetrated the pipe wall twice (outward at exciter, inward at receiver). Both the amplitude of the received signal and the phase lag between the remote field and the exciter field provide information on wall loss and changes in material properties (electrical conductivity and magnetic permeability). Because of the double wall transit, the RFEC technique has equal sensitivity to internal and external wall loss.

Detection and sizing performance depend on pipeline diameter, wall thickness, magnetic permeability, and tool speed. Tool speed is limited to less than 0.5 m/s, due to the low frequency applied to generate the eddy currents. The maximum wall thickness that can be inspected with a RFEC tool depends on the test frequency in combination with pipe magnetic permeability. For carbon steel pipes, the maximum inspectable thickness is approximately 10–12 mm.

Intelligent Pigs for Purposes Other than Metal Loss Detection

General

If one excludes metal loss detection, then, broadly speaking, pipeline inspection by intelligent pigging can be categorized into the following five groups of inspection capability:

- Crack detection.
- Calipering.
- Route surveying.
- Free-span detection.
- Leak detection.

The purpose of this section is to briefly describe the tools and techniques that are currently available with respect to these inspection requirements.

Crack Detection

British Gas developed a crack detection pig based on ultrasonic wheel probes. This pig, called the *elastic wave inspection vehicle*, can be operated in both gas and liquid pipelines. The first prototype was a 36-in. pig that contained 32 wheel probes. In addition, a 30-in. pig was built. The main difficulties with this technology have been on data interpretation with regard to minimizing the rate of false calls. However, in recent years, much work has been carried out by British Gas on data analysis algorithms to

discriminate real cracks from spurious indications. British Gas claims that the number of false calls has decreased significantly by its recent improvements in data analysis.

PTX developed an ultrasonic crack detection pig that aims to detect both internal and external longitudinal cracks in clean liquid pipelines. The tool can also detect potential fatigue cracks in the longitudinal weld seam. Note that this pig cannot be run in gas pipelines unless this is done in a liquid slug. The key to the concept is the complete coverage of the pipe by a large number of ultrasonic piezoelectric transducers (512 for a 24-in. pig).

Calipering

Caliper pigs measure internal profile variations like dents, ovality, and internal diameter transitions with the primary objective being to detect mechanical damage and ensure that a less flexible metal loss inspection pig can pass through the pipeline. Caliper pigs are normally designed to be flexible and can pass 25% ID reductions.

Most of the caliper pigs are equipped with mechanical sensors (fingers) that follow the inner profile of the pipe wall. Typically, these pigs can detect dents and ID reductions of between 1% and 2% of the pipe diameter. A drawback of the mechanical caliper pig is that false readings can be obtained from debris or solid wax. Established contractors that offer services with mechanical caliper pigs are Pipetronix, Enduro Pipeline Services, and TD Williamson (TDW). Some tools have the additional capability to measure the bend radii.

H Rosen Engineering (HRE) offers a service with a caliper pig that uses eddy current proximity probes and is called the *electronic gauging pig* (EGP). The eight probes are mounted in a conical nose at the front or rear of the pig. This pig has the advantage that it is very rugged and insensitive to debris or wax. When required, the EGP can be mounted with a larger cone, by which the sensitivity can be increased from about 1.5% ID reduction to about 0.5% ID reduction, at the expense of the pig's flexibility.

Route Survey

The Geopig of BJ Pipeline Services (formally Nowsco) is the market leader for route surveying. The Geopig was developed by Pulsearch, Canada, in the mid-1980s with the aim to measure subsidence in the Norman Wells pipelines in Canada, which lie in an active permafrost region. The Geopig is capable of determining the latitude, longitude, height, bend location and curvature, and center point of a complete pipeline in a single run. The heart

of the Geopig is a strap-down inertial measurement unit, giving accuracy on location of 0.5 m/km and a curvature with a radius up to 100 m. Two fixed rings with ultrasonic probes are mounted to measure the internal profile of the pipeline. In liquid pipelines, undamped and unfocused 2.5 MHz transducers are used. The sensors for gas service operate at 250 KHz and require a minimum internal pressure of 10 bar. A footprint of the sonar on the wall has a diameter of 10 mm. The accuracy of the sonar to measure dent depths is ± 2.5 mm.

Some pipeline operators have made good use of the Geopig to assess the pipeline profile for upheaval buckling and the necessity for rock dumping. An alternative to the Geopig is offered by Pipetronix in the form of its scout pig, which uses inertial navigation by means of builtin gyroscopes.

Free-Span Detection

British Gas developed the burial and coating assessment (BCA) pig based on neutron backscattering, which aims to detect free spans. However, the BCA pig has not become a commercial success because of its limited competitiveness with respect to remotely operated vehicle (ROV) inspection.

HRE recently developed a free-span detection pig based on gamma ray technology. BJ Pipeline Services claims that its Geopig (see the previous section) can detect free spans by measuring the vibrations of the pipeline when the pig passes an unsupported section; however, this capability has not yet been field proven.

Leak Detection

Two types of pig are available for leak detection.

The first type aims to acoustically detect leaks in onstream liquid pipelines by means of the escaping noise. Acoustic pigs are offered by Maihak and recently by TUV Osterreich. With this type of pig, it is considered feasible to detect leaks at a leak rate of about 10 liters per hour.

The second type of pig aims to detect leaks in shutin pipelines by measuring the flow or differential pressure over the pig. Service with this type of pig is offered by Pipetronix and H Rosen Engineering.

2. PIPELINE REPAIR METHODS

Conventional Repair Methods

Damage to a subsea pipeline can be repaired in different ways, depending on the water depth and the type and extent of the damage. This section

describes the various types of conventional methods currently available for repairing a damaged subsea pipeline in water depths of less than 300 m. This maximum depth limitation is one that is realistically imposed as a result of diver constraints. Nonconventional pipeline repairs are considered to be those carried out diverless and in water depths exceeding 300 m. Table 4.2 summarizes the various repair methods and their applicable water depths.

The various types of conventional repair methods can be summarized as follows [7]:

- Noncritical repair work.
- Minor repair requiring the installation of a pinhole type repair clamp.
- Medium repair requiring the installation of a split sleeve type repair clamp.
- Major repair requiring the installation of a replacement spool.

Noncritical intervention work, such as free span correction, retrofitting of anode sleds, and rock dumping, can usually be considered as planned preventive measures to reduce the risk of an emergency. For the localized repair of nonleaking minor and intermediate pipeline damage, repair clamps are likely to be utilized, without the necessity of an emergency shutdown to the pipeline system. For major pipeline damage resulting in, or likely to result in, product leakage, immediate production shutdown and depressurization is invariably required, allowing the damaged pipe section to be cut out and replaced by a spool using surface or hyperbaric welding techniques or mechanical connectors. In the case of surface welding, this procedure relies on the requirement for the damaged section of the line to

Table 4.2 Repair Methods Versus Applicable Water Depths

	Water Depth		
Repair Method	**0—50 m**	**50—300 m**	**>300 m**
Repair clamp	↣	↣	↣ (note 1)
Hyperbaric welding	↣ (note 2)	↣	N/A
Mechanical connectors	↣	↣	↣ (note 1)
Surface welding	↣ (note 3)	N/A	N/A

Notes:
[1]Technology exists for the diverless installation (by ROV) and the diverless installable hardware, such as repair clamps and mechanical connectors.
[2]Hyperbaric welding in water depths less than 20 m is not practical, and other repair solutions are required.
[3]Water depth limitation for surface welding is governed by the size of the pipeline, the weight of the pipeline, and the vessel lifting capabilities.
Source: Bai and Bai [6].

be located in shallow water, typically no greater than 30 m. This should allow the pipeline to be raised to the surface using suitably equipped attendant vessels and thereby permit the repairs to be performed in a dry environment.

General Maintenance Repair

This section deals with those noncritical repairs that, in the short term, do not jeopardize the safety of the pipeline and, hence, can form part of a planned maintenance program. Examples include

- Corrosion coating repair.
- Submerged weight rectification.
- Cathodic protection repair.
- Span rectification procedures.
- Installation of an engineered backfill (rock dumping).

Corrosion Coating Repair

Repairs carried out on the corrosion coat of a subsea pipeline may be undertaken under two environments, as follows:

- Marine conditions, coating applied in seawater.
- Hyperbaric conditions, coating applied in dry conditions inside a habitat.

The need for any major repairs at a particular site usually dictates the conditions in which the coating repair is carried out. Repair to a subsea pipeline that involves only repairs to the corrosion coating is unlikely.

Submerged Weight Rectification

In a submerged pipeline system, the concrete weight coating provides negative buoyancy. If a loss of concrete weight coating occurs at locations where a pipeline is exposed on the seabed, the stability and structural integrity of the system may be affected. If the condition worsens, some rectification measures may be necessary to stabilize and protect the pipeline system. These remedial measures may include

- Installation of concrete sleeves.
- Installation of engineered backfill.
- Installation of sand or grout bags.
- Installation of stabilization mattresses or saddles.

For each situation that arises, the requirements for stabilization and protection of the pipeline due to its exposure or loss of weight coating should be analyzed to assess its weight rectification requirements.

Installation of Concrete Sleeves

If concrete sleeves are utilized, the damaged concrete weight coating may be replaced in situ. Fabric sleeves, which are prefabricated, may be zipped and strapped around the damaged section of pipe and subsequently pumped full of grout via the relevant facilities located on board the surface vessel. Refer to Figure 4.3.

The sleeves may be manufactured to suit the pipe size and coating and provide sufficient flexibility to adapt to uneven surfaces of the pipe. Typically, they may be provided in lengths of up to 6 m. The underside of the pipe has to be made accessible to enable the installation of the sleeve. This option may be used for local or one-off type repair but is expensive for more extensive repair requirements.

Installation of Engineered Backfill

If this method is adopted, the engineered backfill material is positioned so as to bury completely the damaged section of weight coating and thus provide the requisite protection and stability. Refer to Figure 4.4.

Installation of Sand or Grout Bags

Sand or grout bags may be employed in a similar manner to the engineered backfill to provide local cover and burial of the damaged section of the pipeline. Divers are used to place the bags around the pipeline system. Refer to Figure 4.3. Comparatively, the operation is more labor intensive than a similar operation using engineered backfill; hence, the financial ramifications may be restrictive for extensive repairs to the pipeline weight coating.

Methods similar to these are frequently used as an integral part of localized span rectification.

Installation of Stabilization Mattresses or Weight Saddles

When this method is employed, flexible mattresses or concrete saddles are positioned over the pipeline system to provide the required stability and protection. In each case, the actual positioning operation is usually completed using a subsea handling frame located over the exposed pipeline. In general, the flexible mattresses are considered to be more suitable than the concrete saddle due to their greater ability to adapt to transient seabed conditions. Refer to Figure 4.5.

This option may be used for a considerable number of situations and provides a versatile facility for one-off or the more extensive type of repair.

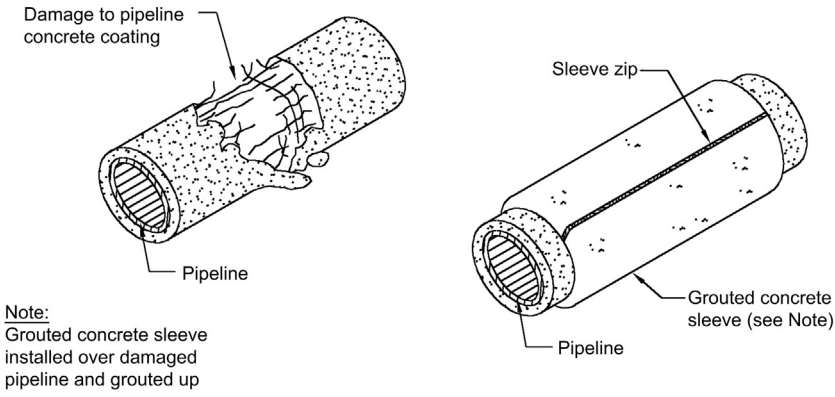

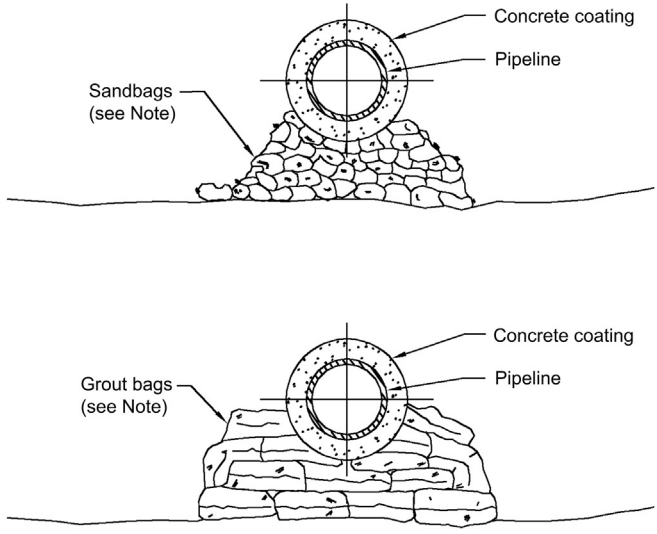

FIGURE 4.3 ***Typical Methods of Concrete Sleeves Grout Bags and Sandbags.***

Cathodic Protection Repairs

The cathodic protection facilities of the pipeline system may need to be repaired or enhanced if the system performance is shown to be inadequate This ineffectiveness may be due to a the anodes being damaged or

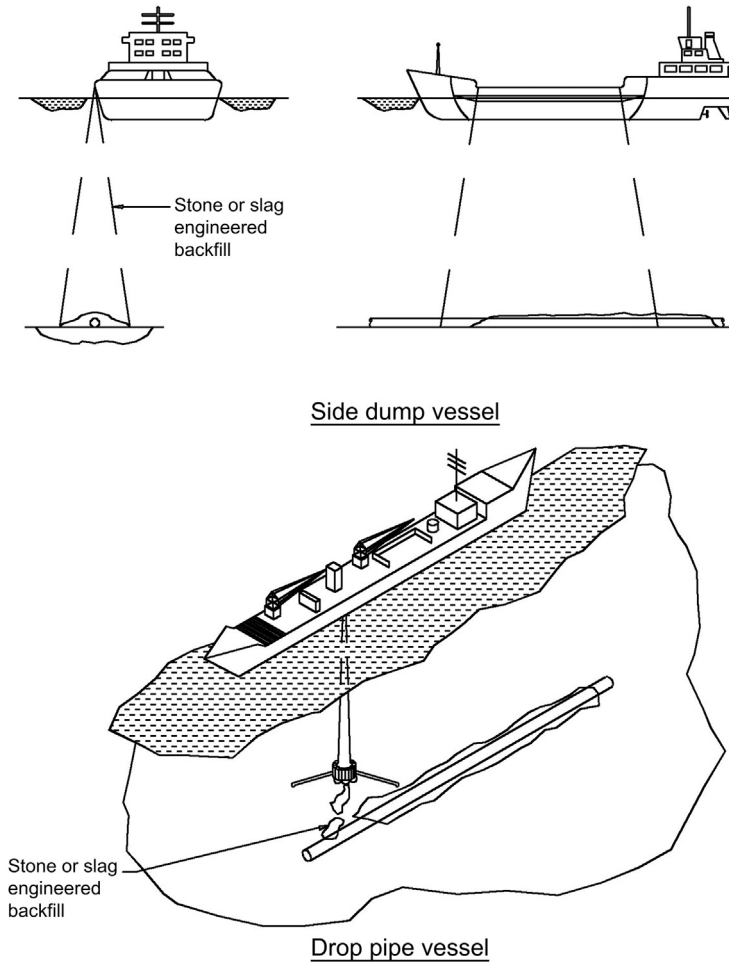

FIGURE 4.4 ***A Typical Methods of Rock Dumping.***

prematurely depleted as a result of bad CP design or unexpected and severe corrosion coating breakdown.

The introduction and connection of anode "sledges" may be utilized to achieve extra cathodic protection. These anode "sledges" are connected at specified intervals along the pipeline system and at a minimum standoff distance from the line, both requirements being optimized for a given situation.

The electrical connection between the end of the anode "sledge" cable and the pipeline is typically achieved by employing mechanical screws or by

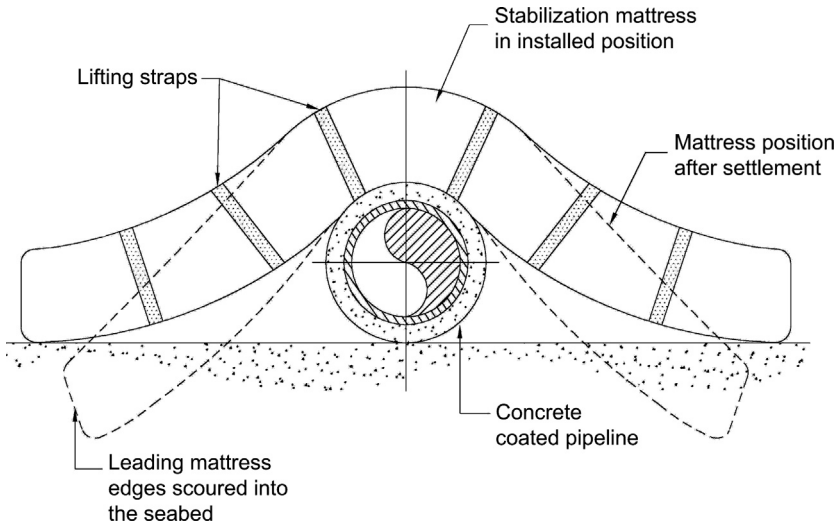

FIGURE 4.5 ***Stabilization Mattress Type Stability Method.***

"wet" welding onto an in-situ doubler plate from an original anode. Screwed connections, although simpler in concept, have been known to lose their electrical contact over time. The technique of wet welding onto an in-situ doubler plate or strap is therefore recommended as the preferred method of providing electrical contact.

Pipeline Span Rectification

Within the pipeline system's design life, unacceptable free spans may develop due to a number of factors, which include scouring action or the passage of sand waves. It is usual practice, during the pipeline design phase, to calculate the permitted spans of the system for all phases of installation and operation. With the pipeline full of water, air, or gas, allowable spans are calculated for the both static and dynamic conditions. Accordingly, a worst case envelope can be developed, which may be used as a basis for designating the allowable span criteria.

Any spans that exist may be detected by a subsequent regular inspection program. The span assessment and method of support should also take into account any proposed changes in the submerged weight of the pipeline.

Span rectification measures are employed if the pipeline span exceeds the allowable span criteria. Generally, span rectification measures take the form of installing discrete supports within the length of the unacceptable pipeline span, thus reducing the actual free span length. The installation of an

engineered backfill may also be necessary to fill in the voids between the supports and to ensure a smooth contour over the pipeline system.

Before the surface support vessel is mobilized, the repair contractor should, in consultation with the company, propose a design for span supports and the method of installing them. Design calculations should be undertaken so that the supports conform to the following requirements:

- The supports are positioned such that all relevant spanning conditions of the pipeline are satisfied.
- Realistic installation tolerance is to be included for the horizontal positioning of the calculated spacing of the supports.
- The supports are to be stable and fully support the pipeline over its remaining design life period.
- The support system is not susceptible to scouring action.
- Lateral movement of the pipeline is prevented by the support installation.

Supports may be developed by placing numerous individual sand or grout bags under the pipeline. An alternative to this is to install an empty fabric formwork under the pipeline and subsequently fill it with grout. This technique is considered to provide a more reliable and complete structural support than using sand or grout bags and, for larger supports, may be comparatively faster to install. Refer to Figure 4.6. The grouted fabric formwork may be shaped to match the contours of the pipe and may be provided with straps to ensure a permanent connection with the pipeline. Additionally, these units may be designed such that, during the grouting operation, the injection pressure may provide an upward lifting mechanism to the pipeline. This feature may provide a useful facility for stress relief in the pipeline span, if they are not within acceptable limits. Alternatively, if required, other equipment may be installed to temporarily lift the pipeline during the support installation.

3. DEEPWATER PIPELINE REPAIR

Introduction

In the last decade, the world's hydrocarbon industry has moved into deep waters and the underwater pipeline repair technology is continuously developing to keep pace. In general, a well-proven capability exists to conduct repairs on pipelines up to a water depth of about 300 m, beyond which divers cannot realistically work in saturation. However, the use of ROVs has undergone significant advancement, enhanced by experience gained in the past 20 years in the field of pipeline repair in deep waters [8].

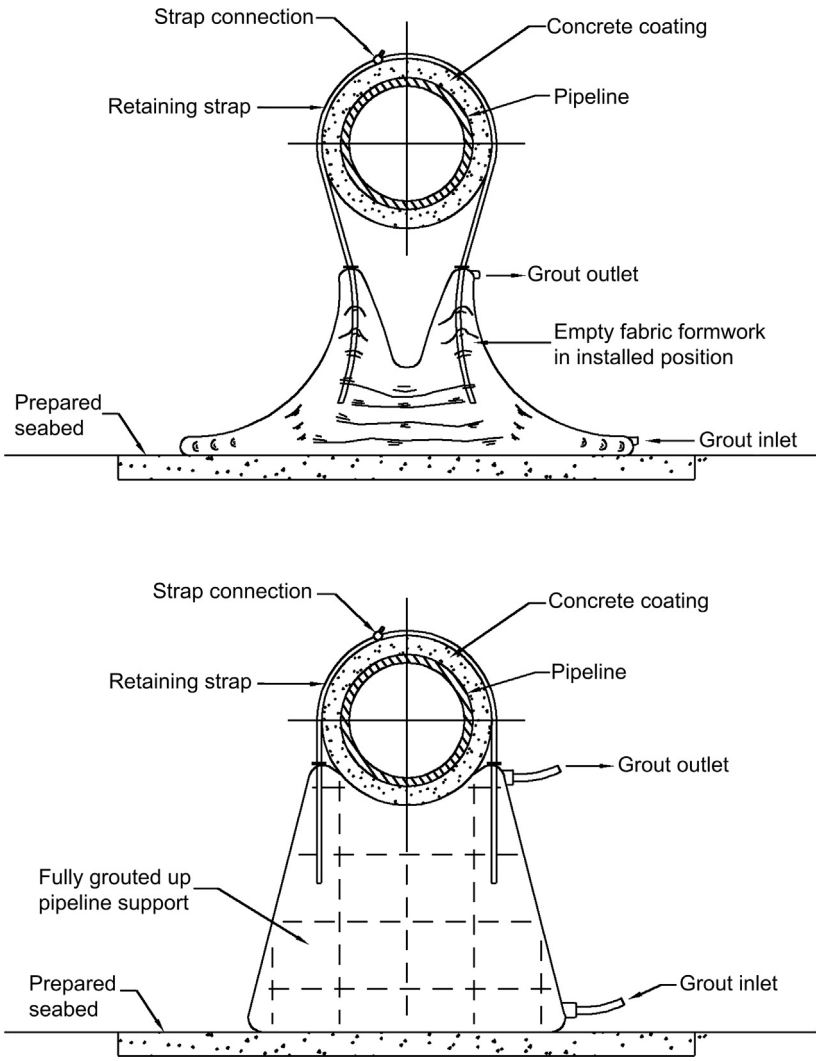

FIGURE 4.6 ***Typical Methods of Using Formwork for Grouting.***

Typically, any deepwater repair procedure requiring the replacement of a pipe section is based on the concept of a spool piece installation using diverless mechanical connectors to attach onto the free ends of the pipeline. End connector hardware capable of being installed without divers has been developed by Hydratight of the United Kingdom and HydroTech of the United States. The basic concept remains the same regardless of whether divers are employed to carry out the tasks, as in more conventional repair

operations (refer to Figure 4.7). Unfortunately, the problems associated with physically accomplishing each task as a diverless operation remain significant.

Notwithstanding this, there is a growing consensus that various ROV contractors could collectively perform virtually all the tasks required with a minimum amount of special support equipment having to be constructed.

This section outlines the progress made in the art of deepwater repair, presents guidelines for new repair technology, and discusses different ways to approach and solve a diverless repair task.

Diverless Repair Research and Development

Diverless repair systems had been considered since 1971, with two significant studies being performed as joint industry studies, one sponsored by Exxon Production Research and the other by Shell. The aims of these studies were twofold; first, to allow pipeline repairs at water depths beyond diver capabilities; second, to have a cost effective diverless repair system that could compete with diver-assisted repair systems. Some of the earlier studies were a little too ambitious, in that they attempted, optimistically, to solve all problems for both small- and large-diameter pipe sizes and in water depths reaching 1300 m. As a result, although the studies identified many of the major problem areas, they did not lead to the development of actual repair capabilities, since at that point in time, the conclusions and

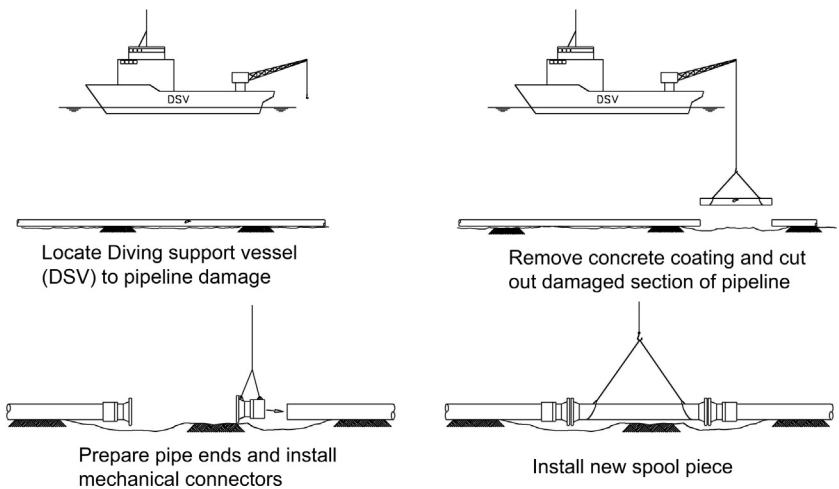

FIGURE 4.7 ***Replacement of a Pipe Section.***

recommendations were considered to be either impractical or too expensive to implement. Also, these earlier studies were prompted by the industry anticipating, in the very near future (at that time), the need to repair large-diameter, concrete-coated pipelines in water depths to 1300 m [9].

Intelligent Plugs for Deepwater Pipeline Repair

The SmartPlug is a remotely controlled and operated (umbilicalless) pipeline isolation system used for isolation of oil and gas pipelines in all dimensions. They are designed, manufactured, and tested to withstand MAOP. This allows repairs, maintenance, and intervention to be carried out, while maintaining pipeline pressure [10].

Figure 4.8 illustrates a remote control and communication system, which consists of the tool itself, the surface control center (SCC), acoustic modems, an ELF communication link (ECL), and remote actuation system. Communication with the tool for typical subsea applications is done from a surface vessel, via acoustic signals to a subsea module, then through the pipeline wall via extremely low-frequency (ELF) electromagnetic waves. Therefore, power and control are provided from the vessel and are remotely operated. This means that there is no limit as to where in the line the isolation pig can be used.

The standard tool is designed to seal against 200 bar operating pressure. Figure 4.9 shows the plug modules used with the remote control and communication system. Two plug modules perform the seal and lock

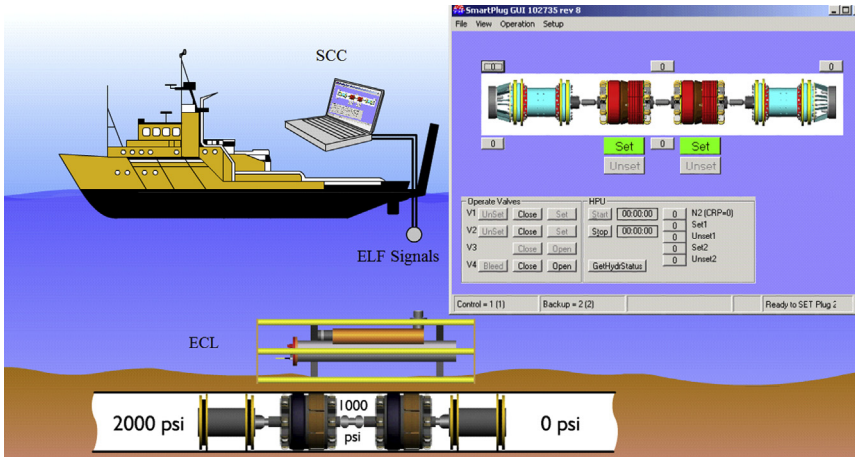

FIGURE 4.8 ***Remote-Controlled Pipeline Isolation System.*** (For color version of this figure, the reader is referred to the online version of this book.)

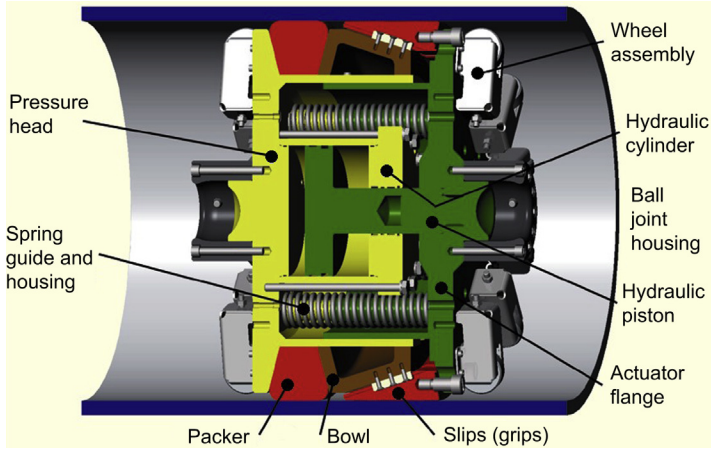

FIGURE 4.9 ***Plug Module.*** *Source: TDW Offshore Services [11].* (For color version of this figure, the reader is referred to the online version of this book.)

function, and each of the modules provides the function independent of the other. The plug modules, linked together by ball joints, have two primary functions:

- Set and lock to the inner pipe wall via the threaded metal segments or slips.
- Apply differential pressure sealing with the large-volume packer.

The plug modules are self-locking; that is, once they have been expanded against the pipe wall, a continued application of differential pressure maintains or intensifies their sealing and gripping ability.

The SmartPlug tool has resolved a range of operational problems caused by faulty pipeline valves and fittings. Figure 4.10 illustrates a midline

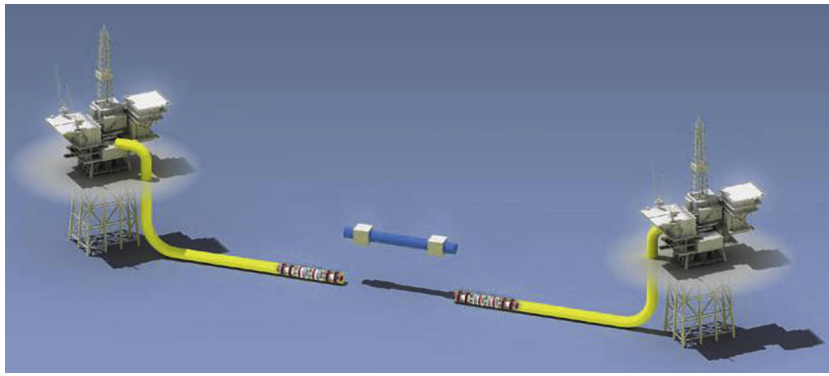

FIGURE 4.10 ***Midline Replacement on a Pipeline at Operating Pressure.*** (For color version of this figure, the reader is referred to the online version of this book.)

replacement on a pipeline at operating pressure. Recent other subsea applications include [12]

- **Pipeline valve repairs or change-outs:** By far the most common use of the SmartPlug is for valve repairs or change-outs. The SmartPlug can be pigged onto position against pipeline pressure and set upstream of the faulty valve yet downstream of the production tee. This allows production to continue while replacement or repair work is carried out.
- **Riser replacement or repairs:** The instrument allows pipelines with multiple downstream platforms to remain in production while risers are replaced or repaired.
- **Pressure testing and leak detection of risers or repaired pipelines:** Testing is possible immediately upon completion of the isolation.
- **Midline pipeline repair and tie-ins:** Cost is reduced and downtime and loss of pipeline contents are prevented.
- **Flood prevention during deepwater pipe laying:** The intelligent plug system is fitted with pressure and water sensors that are automatically activated if water or heavy mist ingress occurs or if pressure builds up in the pipeline.
- **Tie-in of deepwater flowlines and pipelines:** Tie-ins can be performed without shutting down the flowline or pipeline, without watering the line, and without environmental impact or cleanup.
- **Jumper replacement:** The isolation tools allow jumper replacement without wetting the system.

REFERENCES

[1] A guide to the pipelines safety regulations. HSE Books. Available at: www.hse.gov.uk; 1996.
[2] Anderson C. Pipeline inspection. HydroFest. Aberdeen: Scotland; 2005. Available at: www.ths.org.uk/.
[3] Blinco L. Survey operations—Pipeline inspection. HydroFest. Available at: www.ths.org.uk; 2011.
[4] Kiefner JF, Hyatt RW, Eiber RJ. NDT needs for pipeline integrity assurance. Columbus, OH: Battelle/AGA; 1986.
[5] Jackson L, Wilkins R. The development and exploitation of British Gas pipeline inspection technology. Institution of Gas Engineers 55th Autumn Meeting; 1989.
[6] Bai Y, a Bai Q. Subsea pipelines and risers. second ed. Oxford, UK: Elsevier Science Ltd.; 2005.
[7] Manelli G, Radicioni A. Deepwater pipeline repair technology: A general overview; 1994. Houston, U.S.A. OMAE'1994.
[8] Oil and Gas Journal. South East Asia oil directory. Tulsa, OK: PennWell Publishing; 1997.

[9] Diverless pipe repair system set for deepwater trials. Offshore J August 1995.
[10] Aleksandersen J, Tveit E. The SmartPlug: A remotely controlled pipeline isolation system. In: Proceedings of the 11th International Offshore and Polar Engineering Conference. Norway: Stavanger; June 2001.
[11] TDW. Offshore Services. SmartPlug system. Available at: www.tdwoffshore.com.
[12] Oceaneering International. Inc. New technology applications for gas pipelines. ANGDA Contract 06–0425. Oceaneering International, Inc; 2006.

CHAPTER 5

Integrity Management of Flexible Pipes

Contents

1. Introduction 102
   - General 102
   - Failure Statistics 103
   - Risk Management Methodology 104
2. Failure Modes 105
   - End Fitting 105
   - Internal Carcass 105
   - Internal Pressure Sheath 106
   - Pressure Armor 107
   - Tensile Armor 107
   - External Sheath 107
   - Bend Stiffener 109
3. Failure Drivers and Mechanisms 109
   - Corrosion 109
   - Fatigue 110
   - Erosion 112
   - Temperature 112
   - Pressure 113
   - Composition of Production Fluid 114
   - Service Loads 114
   - Pipe Blockage or Flow Restriction 114
   - Accidental Damage 114
4. Integrity Management Strategy 115
   - Integrity Management System in Design Stage 115
   - Integrity Management System in Manufacturing Stage 116
   - Integrity Management System in the Installation and Commissioning Stages 116
5. Inspection and Monitoring, in General 117
   - Inspection and Monitoring Methods 117
   - General Visual Inspection and Close Visual Inspection 117
   - Eddy Current 119
   - Radiography 120
   - Ultrasonic Techniques 120
   - Acoustic Emission 121
   - RAMS and MAPS 121
   - Bore Fluid Parameter Monitoring 122
6. Testing and Analysis Measures 122

Subsea Pipeline Integrity and Risk Management
ISBN 978-0-12-394432-0
http://dx.doi.org/10.1016/B978-0-12-394432-0.00005-6

Coupon Sampling and Analysis 122
Vacuum Testing of a Riser Annulus 123
References 123

1. INTRODUCTION

General

Unbonded flexible pipes have found wide applications in subsea production systems from shallow to intermediate water depths. Figure 5.1 shows a layout of two 6 in. flexible flowlines in the Marin field, connecting the Marlin subsea development to the Marlin TLP 1 mile away, in a water depth of 1000 m.

The increased use of flexible pipes in subsea and high-pressure and high-temperature (HPHT) applications demands operators to adopt an integrity management program to safeguard their assets and avoid reduction of production. The composite construction of unbonded flexible pipes makes the failure modes complex, and the risks of failure and the way to mitigate them becomes an important aspect in system selection. The cost of a failure may be many times over the cost of the implementation of an integrity management program that may prolong the operating life through the use of preventive maintenance procedures.

A high risk generally requires the implementation of some form of predictive inspection or monitoring measure. A medium risk generally

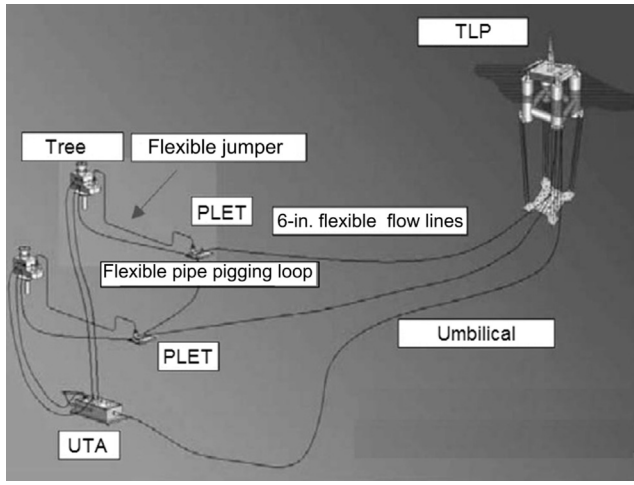

FIGURE 5.1 ***Flexible Flowlines and Jumpers in the Marlin Field.*** *Source: Lecome et al. [1].*

requires an inspection or monitoring measure to detect any sign of initiation of failure due to the particular failure mode or to ascertain that no significant defect leading to this particular failure is present in the pipe. Low risk levels require no quantitative inspection or monitoring procedures nor any specific integrity management procedures.

Flexible pipe integrity management programs with definite methodologies have been established in the industry in the last decades. One of the main standards for flexible pipe integrity management was developed by MCS, and details of this methodology may be found in various publications, such as UKOOA (2001 and 2002). In 2010, MCS Kenny updated the 2002 report in the SureFlex joint industry project (JIP), with the current industry practices in the worldwide area on flexible riser integrity management [2]. This revision extended the scope of the report to include all unbonded flexible pipes used in oil and gas production systems in all global area, resulting in a database that includes 1900 flexible risers, 1400 static flexible flowlines and covers 130 production facilities worldwide. The database includes 315 individual damage and failure incidents from around the world [3].

This chapter deals mainly with the risk assessment and integrity management of flexible pipes. The methodology for formulating an integrity management plan involves carrying out a risk assessment and determining the risks inherent for the flexible pipes. Once risks are determined, specific integrity management measures can be identified to mitigate these risks.

Failure Statistics

From a total of 106 flexible pipe failure or damage incidents reported by UKCS operators, 20% of flexible pipes were found to have experienced some form of damage or failure. Of this 20%, two thirds occurred during installation and one third during normal operation. Of these 106 failure and damage incidents, a total of 32 incidents required the flexible pipes to be replaced. In this book, *failure* is defined as an incident resulting in the loss of containment of the flexible pipe and requiring the pipe to be replaced, while *damage* is defined as an incident resulting in damage to the flexible pipe, where the flexible pipe can remain in service following mitigation measures taking place.

Figure 5.2 shows the spread of failure and damage incidents for flexible pipe in operation. The figure plots the percentage of failure or damage incidents against damage and failure types. The percentage number is the

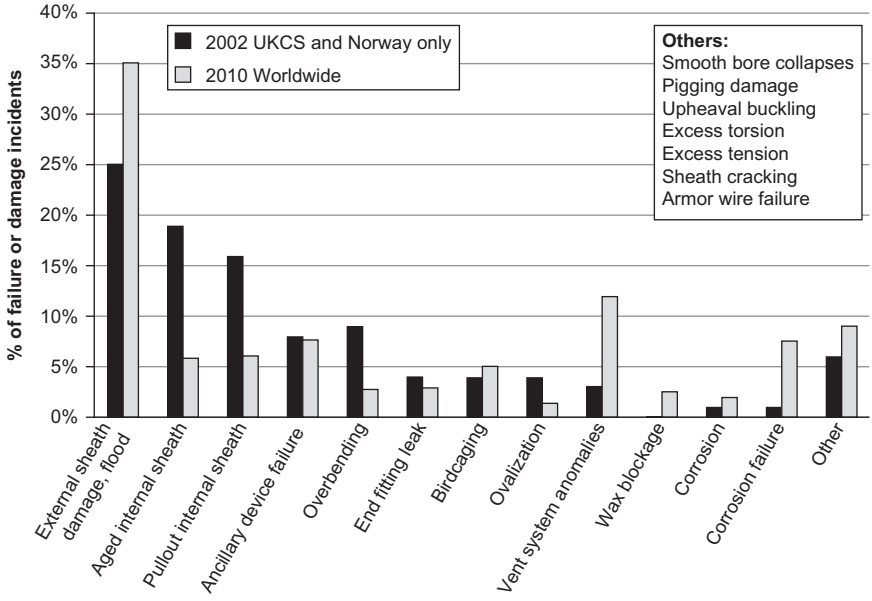

FIGURE 5.2 ***Statistics on Flexible Pipe Failure and Damage.*** *Source: O'Brien et al. [3].*

percentage of the total number of incidents in the failure and damage database. In the figure, the data from the current work are printed in gray, and those determined from the work performed in 2001 are in black. The external sheath damage remains the most common failure mode and is shown to have increased since 2001. There has been a significant decrease in aged internal sheath and PVDF internal sheath pull-out failures. Vent system anomalies and carcass collapse failure have also shown a big increase since the 2001 work, respectively [3].

Risk Management Methodology

Risk is often quantified as a product of a probability of failure and a consequence rating. Risk management takes all possible failure modes into consideration, through an analysis of failure drivers (such as temperature and pressure) and general failure modes (such as fatigue, corrosion, erosion, accidental damage, and ancillary equipment) [4].

The probability of failure is a scale that determines the probability of a failure mode occurring. It is estimated through in-service data and statistics of past failure occurrences. The consequence rating is an integer that describes the severity of a failure occurring due to a particular failure mode.

2. FAILURE MODES

The failure mode describes one possible process by which a flexible pipe can fail due to bursting or leakage. A single failure mode typically represents a succession of pipe defects that have the potential to culminate in pipe failure. Flexible pipe consists of a large number of components. Each of these components has its own failure modes. The identification of relevant failure modes should be based on a detailed knowledge of flexible pipe behavior [5]. From the statistical results of failure and damage incidents worldwide for flexible pipe in operation, damage of the external sheath is the most common failure mode. Table 1 of the document by Out [6] presents a summary of the failure modes likely to lead to bursting or leaking of flexible pipe. The details of these failure modes are described in the catalogue of components of unbonded flexible pipes in the following sections.

End Fitting

The end fitting of a flexible pipe is a critical component to terminate the ends of each flexible pipe layer and provide the required connection to mate with the production facilities. It also has a transition function from the low bending stiffness of the flexible pipe to a stiff end. A proper bending stiffener or restrictor-bellmouth is required to prevent kinking. Failure modes of the end fitting include [7]

- Internal pressure sheath pullout.
- Tensile armor pullout.
- Outer sheath pullout.
- Vent valve blockage or leakage.
- Failure of sealing system.
- Crack or rupture of tensile armor.
- Structural failure of end-fitting body or flange.

Internal Carcass

Figure 5.3 shows a failure mode of carcass collapse due to hydrostatic pressure, which is caused by gases diffusing from the pipe bore through the internal polymer sheath and into the annulus. The gases cause a pressure buildup in the annulus. In the case of rapid depressurization and evacuation of the pipe bore (e.g., through an emergency shutdown), the pressure in the annulus could exceed the pressure in the pipe bore.

Another failure model of the internal carcass is wire severing, which interrupts the continuous ring and locally reduces the collapse resistance.

FIGURE 5.3 ***Collapsed Carcass due to Hydrostatic Pressure.*** *Source: Out [6].* (For color version of this figure, the reader is referred to the online version of this book.)

A circumferential crack disables the interlocking function and leads to a gap. Other failure models include

- Collapse or ovalization.
- Unlocking deformation or interlocking lip failure.
- Circumferential cracking or wear fatigue.

The failure modes of the internal carcass are mainly due to erosion, corrosion, mechanical problems, fatigue, and hydrostatic pressure.

Internal Pressure Sheath

The internal pressure sheath follows any ridges of the interlocking carcass or the interlocking pressure armor and cracks at these locations. This is a main issue for a single PVDF pressure sheath. If there is a single sheath, the bore pressure leaks into the annulus, which likely results in the bursting of the flexible pipe. Figure 5.4 shows an internal sheath crack. Other failure models include

- Hole or crack.
- Rupture.
- Collapse.
- Ageing embrittlement.
- Excess creep of polymer into the metallic layer.
- Blistering.
- Wear, nibbling, and fatigue.

FIGURE 5.4 ***Internal Sheath Crack.*** *Source: O'Brien [7].* (For color version of this figure, the reader is referred to the online version of this book.)

Pressure Armor

The pressure armor is to withstand the hoop stress in the pipe wall caused by the inner bore fluid pressure. The pressure armor is wound around the internal polymer sheath and is made of interlocking wires. The common failure modes are

- Rupture.
- Unlocking or failure of interlocking lips.
- Collapse or ovalization.
- Longitudinal wire crack due to underdesigned presence of a flaw or corrosion.

Tensile Armor

If any of the main loading parameters, such as internal pressure, bending moment, or effective axial tension, is underestimated, the wire of a tensile armor may fail, which causes bursting. Other failure modes, as shown in Figures 5.5 and 5.6, include

- Birdcaging or clustering, the radial buckling mode of the tensile wires, which results from the local deformation of individual wires about wire's "weaker" axis under high compression loads or bending.
- Multiple wire rupture.
- Kinking.
- Individual wire rupture.

External Sheath

A serious form of corrosion fatigue damage could take place in case of a tear in the external sheath of a flexible riser, as shown in Figure 5.7. Such a hole

permits the ingress of seawater into the annulus, which causes an accelerated rate of corrosion and a reduction in the fatigue life of the steel armor wires. Other failure modes of the external sheath include

- A hole, tear, rupture, or crack due to damage during installation.
- A leak, ingress of seawater due to lack of venting system, or pinhole from manufacturing.

FIGURE 5.5 ***Tensile Armor Layers' Failure Modes,*** *Source: O'Brien [7].* (For color version of this figure, the reader is referred to the online version of this book.)

FIGURE 5.6 ***Birdcaging.*** *Source: Clevelario [8].* (For color version of this figure, the reader is referred to the online version of this book.)

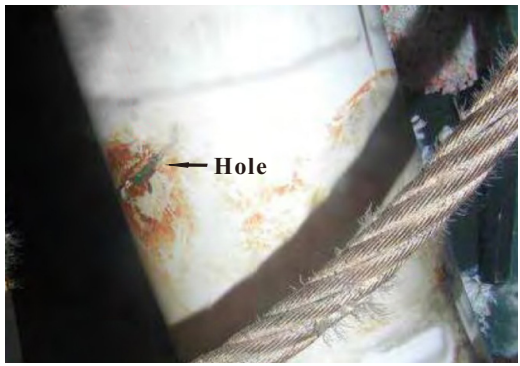

FIGURE 5.7 ***Hole in the Outer Sheath.*** *Source: Kaye [9].* (For color version of this figure, the reader is referred to the online version of this book.)

Bend Stiffener

When the bend stiffener is too stiff or too compliant due to improper specification or design, the bending curvature of flexible pipe exceeds the MBR. The failure modes include:

- Failure of connection to structural support;
- Stiffener crack / rupture;
- Stiffener support structure failure;
- Bellmouth deformation or inadequate size.

3. FAILURE DRIVERS AND MECHANISMS

Corrosion

The steel carcass and steel armor wires of a flexible pipe are susceptible to corrosion due to the presence of water, CO_2, O_2, and H_2S. If the external sheath is damaged, then the armor wires are exposed to seawater and corrode if not protected efficiently by anodes in the vicinity [10]. Some oxygen corrosion is observed in flexible pipes with damage to the external sheath, even when the pipe ends are connected to anodes. This is believed to be related to a possible problem of protecting shielded steel a certain distance away from the damage, where the steel is not directly exposed to seawater.

Figure 5.8 shows a subset of external sheath damage due to general and extensive armor wire corrosion. For external sheath damage at the splash

FIGURE 5.8 ***Corrosion of Armor Wire.*** *Source: Boschee [11].* (For color version of this figure, the reader is referred to the online version of this book.)

zone area, where the cathodic protection system can have limited or no effect and there is access to oxygen, the major corrosion damage can occur rapidly and endanger the pipe's integrity. In the splash zone, the constant wetting and drying of this zone combined with defects in the coating are the usual contributors to corrosion [12].

External sheath damage and flooded annulus are the most common damage mechanisms for unbonded flexible pipes. The external sheath damages occur during installation of the flexible pipes, causing annulus flooding and increasing H_2S levels. This may set up a corrosive environment in combination with oxygen from the outside or CO_2 or H_2S permeating from the bore. Corrosion may take the form of metal loss or a significant deterioration of the fatigue resistance. In this case, corrosion fatigue of armor wires may become an issue. Charlesworth et al. [13] show that generally, in their stufy, the condition of both the polymer and metallic layers was good and the introduction of the corrosion inhibitor into the annulus of the pipe had a positive effect. They also present the fatigue testing program, and the S-N curves generated using the wires from the decommissioned riser are compared against curves for as-manufactured wire. This indicates a significant level of conservatism in current fatigue life prediction methods.

Fatigue

In "wet" fatigue (fatigue in case of wet annulus), the corrosion-fatigue damage is higher than in the case of "dry" fatigue [14], and the increase is very substantial. This conclusion was based on testing with a continuously replenished solution and caused a stir a few years ago. The suppliers and JIPs performed recent testing with better representation of the annulus environment, characterized by low free volume to surface area ratio and a nearly stagnant electrolyte. This condition results in a solution quickly saturated with corrosion product, hence, a highly reduced corrosion rate and reduced corrosion-fatigue damage.

Normally, wave and riser motions cause fatigue damage to the steel armor wires of dynamic flexible pipes during operating condition. A detailed fatigue life analysis is always carried out before the pipe installation. The manufacturer needs to prove that the fatigue life of the pipe is 10 times the pipe's service life. Due to a high damping factor, flexible risers are not susceptible to vortex-induced vibrations (VIVs). However, manufacturing and installation are also likely to introduce a certain amount of fatigue damage.

For the fatigue analysis, the critical location and fatigue damage there need to be determined. Often the location is at the top and inside the bend

stiffener. Fatigue in a corrosive environment (for example, seawater, or CO_2, O_2, and H_2S) is more severe than that in air. The relevant mechanism becomes corrosion fatigue if the free annulus space becomes filled with an electrolyte, seawater from a breach of the external sheath, or fresh water from condensed water vapor permeating from the bore and corrosive agents have permeated, notably CO_2 or H_2S.

Figure 5.9 shows typical corrosion fatigue curve compared to the dry fatigue curve. The S-N curve that applies is dependent upon not only the material, but also the precise environment. The fatigue threshold appears to no longer apply in certain conditions, which means that the multitude of small variations will contribute, and the level of the sloping section may be lower. Prediction of fatigue is therefore difficult, unless the S-N curve for the annulus conditions is available.

If corrosion fatigue needs to be considered, the annulus environment is required in terms of partial pressures of the corrosive agents and S-N curves to match. These curves may not be available, and curves for a roughly comparable environment may be used. If the calculated corrosion-fatigue life is critical, especially if not conservative, it is advised to cover this by commissioning the S-N curves for corrosion fatigue for the particular application [6].

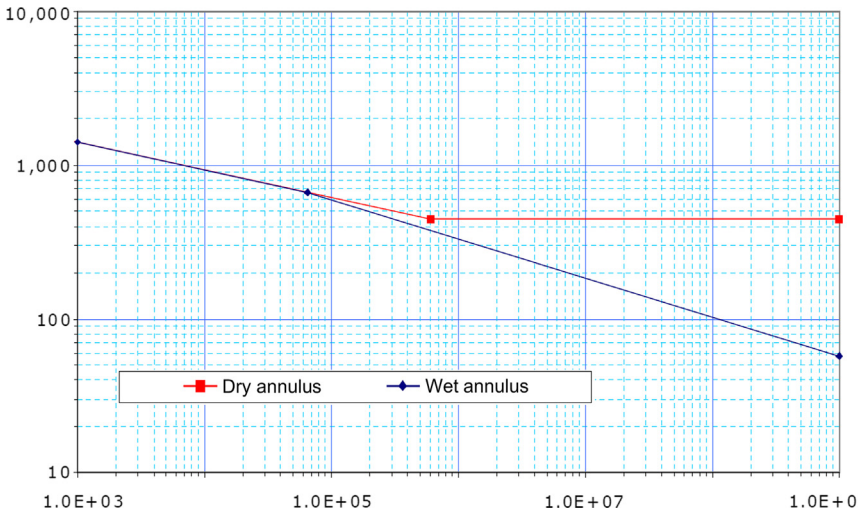

FIGURE 5.9 ***A Typical Corrosion-Fatigue Curve compared to the Dry Fatigue Curve.*** *Source: Picksley et al. [4].* (For color version of this figure, the reader is referred to the online version of this book.)

Erosion

Figure 5.10 shows picture of erosion of a collapsed carcass. Carcass or internal polymer sheath erosion takes place when sand particles impact against the materials. This failure mode is relevant to pipe sections that are curved. Erosion becomes more prominent when gas production risers become more common, as the flow velocities there tend to be high. Traditionally, a velocity limit of 20 m/s is used, but the basis of this is unclear in the context of sand erosion. The chief parameters for erosion of the carcass of a flexible pipe include [6]

- Gas flow velocity.
- Mass flow of sand.
- Size and sharpness of sand grains.
- Radius of the global bend.
- Carcass material.
- Presence of liquid.

Temperature

The most likely failure mode with temperature as a failure driver is cracking or ageing of the internal polymer sheath. Polyamide PA-11 is the main polymer used in the flexible pipe industry, performing many important functions in inner sheath, outer sheath, and other applications. According to API RP 17B [5], the maximum allowable temperature of PA-11 is 900°C if

FIGURE 5.10 ***Erosion of a Collapsed Carcass.*** *Source: Out [6].* (For color version of this figure, the reader is referred to the online version of this book.)

the water cut is 0%, and 650°C if any water is present. Repeated temperature cycling also causes increased stress in the polymer material. Figure 5.11 shows the statistics on design temperature for flexible pipes in operation worldwide. For more detailed guidance on the use and limitations of PA-11, refer to API TRI7RUG [15].

Pressure

Excessive pressure in the pipe bore causes failure of the pressure armor wires. However, internal pressure is usually carefully monitored and controlled, unless it exceeds the design limits. Thus, failure due to pressure is not considered as a high risk. Thermal and pressure cycling, however, could play a significant role in fatigue damage of the pipe and cause significant upheaval buckling in a buried flexible flowline. The risk of pressure surges always exists during well shutdown, and these pressure surges need to be carefully monitored and assessed to ensure they do not cause an unexpected failure of the pressure armor wires.

Hydrostatic collapse also could be a potential failure mode for pipes. However, the pipes are designed with a factor of safety, so it is unlikely for pipes to suffer hydrostatic collapse, especially if the external sheath remains intact. Should the external sheath be breached, water could enter the pipe annulus, and the pressure in the annulus could cause the internal polymer sheath to collapse. The presence of a carcass provides much more safety against this failure mode.

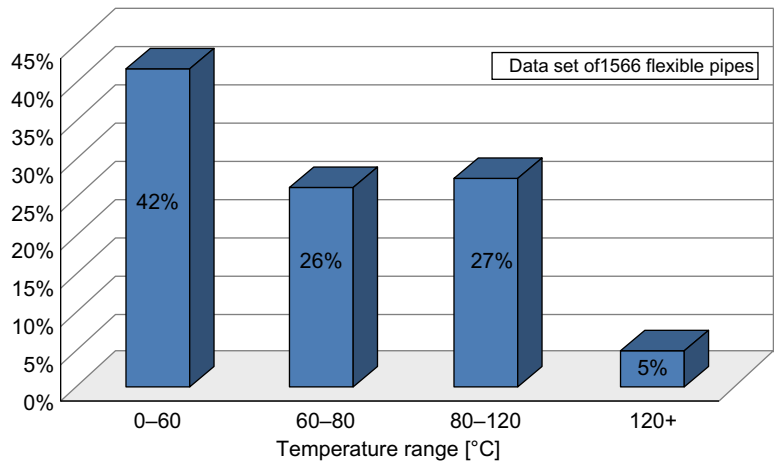

FIGURE 5.11 ***Statistics on Design Temperature for Flexible Pipes.*** *Source: O'Brien et al. [3].* (For color version of this figure, the reader is referred to the online version of this book.)

Composition of Production Fluid

The production fluid in the pipe bore could have a deleterious effect on the pipe wall materials. The presence of water, CO_2, and H_2S in the production may cause pitting, hydrogen-induced cracking (HIC), and sulfur stress cracking (SSC) corrosion. These chemicals not only attack the carcass but diffuse through the internal polymer sheath into the annulus and can cause corrosion of the pressure and tensile armor steel wires. The diffusion of water into the annulus also has a negative effect on the fatigue life of the steel armor wires.

The production transported, including inhibitors and acids, could cause the accelerated degradation of the polymer material of the internal sheath. The presence of sand could also cause erosion of the carcass and internal polymer sheath, particularly in curved sections of the pipe.

Service Loads

Excessive tension in a flexible riser could cause tensile armor wire failure, leading to collapse of the pipe. The loads experienced during installation are often the highest loads that a riser sustains during its lifetime.

Another mode of failure is overbending of the pipe. This causes unlocking of the pressure armor layer and leads to collapse of the pipe wall. Bend stiffeners, bellmouths, and bend restrictors are used to protect a pipe from overbending in its most critical regions.

A failure mode that can occur at the touchdown point of a riser is compression of the riser. This occurs when the effective tension in the pipe wall becomes negative. A high value of compression can result in buckling of the pipe wall.

Pipe Blockage or Flow Restriction

Oil and gas pipelines are susceptible to the formation of hydrate deposits. This normally occurs when the high-pressure, low-temperature production fluid meets with water in the pipe. The formation of hydrate deposits could cause a blockage in the pipe, restrict the flow of fluid, and lead to a pressure increase in the pipe bore, which could eventually cause rupture of the pressure armor layer and collapse of the flexible pipe.

Accidental Damage

Subsea pipelines are susceptible to impacts due to dropped objects from vessels, anchors, interference with other pipes, and trawl boards. Excessive

motions of a pipeline could also cause impacts on the seabed. If these impacts are severe, they could cause damage to the external sheath of the flexible pipe, such as a hole in the external sheath and ingress of water into the pipe annulus. An extremely severe impact to an unbonded flexible pipe could also cause the pressure armor layer to unlock or the tensile armor wires to rupture. Hence, a strict dropped object reporting protocol is required for any installation or vessel operating in the vicinity of flexible pipes. A dropped object must always be reported and an ROV should be deployed to determine the location of the dropped object on the seabed and examine the surrounding pipes for any potential damage. Deck lifting and handling procedures are intended to prevent dropped object incidents from occurring in the first place.

4. INTEGRITY MANAGEMENT STRATEGY

The preservice integrity management strategy of flexible pipe includes methods in the design stage, manufacturing stage, installation stage, and commissioning stage. The service integrity management strategy includes a number of inspection and monitoring measures and testing and analysis methods that are listed in Sections 5 and 6, respectively. It is important for flexible pipes that a risk assessment and an integrity management strategy are defined in the design stage to ensure that the pipes suffer no unnecessary damage during all stages of its life.

Integrity Management System in Design Stage

The integrity management of flexible pipe starts with the design specifications [6]. It is necessary to emphasize that a flexible pipe is a pipeline that contains nonmetals and is built up in a number of layers. Therefore, the following items should be noted:

- The polymer pressure sheath's ageing.
- The pressure sheath's pressure and temperature limitations.
- The steel armoring wires susceptibility to corrosion.

Design of the cross section starts with the material selection of the pressure sheath, which should be based on reasonably worst case design conditions. For dynamic flexible risers, the sheath is made of either PA-11/12 (polyamide or nylon), PVDF, HDPE, or XLPE. Specifying a design temperature too high, for example, may lead to deselection of PA-11/-12 or XLPE as the pressure sheath material and unnecessarily in favor of PVDF, in spite of PVDF's higher cost and relative vulnerability [6].

When a project has requirements that are outside the experience base, the challenge is to anticipate the failure modes and cover them by a comprehensive qualification program, generally with the manufacturer. Before this is complete, the likelihood rating should be regarded as high and due attention given to the issue.

Design of the cross section further involves a permeation analysis to arrive at the expected annulus environment, including CO_2, H_2S, and H_2O; the corrosive condition; and the selection of grade of armoring steels. The permeation analysis carries an uncertainty. Once the materials are chosen, the sizing of wires is relatively easy. To size the collapse carcass against erosion, assumptions have to be made on the sand production.

Design of the riser system involves making global design assumptions, including the metocean conditions, vessel behavior, expected marine growth, operational scenarios with gas density at operating and ambient pressure, required insulation, and increasing the external diameter, all of which have inherent uncertainties.

Integrity Management System in Manufacturing Stage

At the manufacturing stage of flexible pipes, rigorous quality assurance (QA) procedures should be in place and rigorous quality control (QC) should be exercised, especially for the extrusion of the pressure sheath and the construction of the end fitting. With regard to the latter, QA and QC should adequately cover all elements that seal or provide strength, even if they are apparently nominal, such as the welds that anchor the collapse carcass in the axial direction. The operator challenges the manufacturer via an audit process and is further advised to engage an experienced, vigilant, and independent third party to witness to the production of the pipe, especially during the end-fitting construction [6].

For polymeric pressure sheath failure modes, it is believed that better control of the dimensional tolerances (such as OD, thickness, and ovality) should be exercised. API Spec 17J requires the dimensional variations to be such that the utilization values do not rise by more than 3%.

Integrity Management System in the Installation and Commissioning Stages

A number of installation incidents have been documented, and in some cases, expensive mitigation measures had to be taken following these incidents to enable the pipes to remain fit for service. Installation has the potential of damaging the flexible pipe through overbending, excessive tension loading,

and clashing, which might damage the external sheath. Hence, strict installation procedures need to be adhered to in order to prevent damage to the flexible pipes before operational use. Installation requires detailed and robust procedures to prevent damage by impact or interference between hard edges and the flexible pipe outer sheath, and overbending and the like. During execution, the proceedings on the installation vessel should be carefully monitored, likewise by ROV in the water, and proper management of change is to be exercised in spite of the inevitable pressure to complete the installation in a timely manner. Damage should be detected at the earliest possible stage and repaired immediately or in time, depending on the inherent risk.

Commissioning of the flexible pipe system presents the opportunity to test the complete annulus venting system, including the small bore piping downstream from the valves on the end fitting toward the final venting location. The operator should designate this system a safety critical element (SCE) and is best advised to tie in at least two of the valves on the end fitting [6].

5. INSPECTION AND MONITORING, IN GENERAL

Inspection and Monitoring Methods

During the SureFlex JIP, a comprehensive review of existing and emerging techniques for flexible pipe inspection and monitoring was performed. The outcome of this work has been summarized in detail in a state-of-the-art document [2]. Table 5.1 was created within the state-of-the-art document.

Table 5.1 provides insight to the range of techniques described in the state-of-the-art document. It is also noted in the document [2] that no single inspection or monitoring technique can provide a complete picture of the integrity of any flexible pipeline system, and many of the techniques in Table 5.1 fall into the category of specialist solutions to meet specific needs. It is observed from Table 5.1 that visual inspection, annulus monitoring, and FPU (floating production unit) excursion and environmental monitoring have had the highest take-up by the industry to date. Most other techniques as shown in the table have had limited take-up [3].

General Visual Inspection and Close Visual Inspection

As shown in Table 5.1, this measure is one of the most important and commonly used measures for ensuring the integrity of flexible pipes. Visual inspection is used to observe marine growth levels and detect major interference by dropped objects, anchors, fishing gear, and the like, both as a

Table 5.1 Inspection and Monitoring Techniques for Flexible Pipe

Method or Technique	Takeup[1]	JIP Feedback[2]
Visual inspection	(5)	(4) Anomaly tracking , gross defects
Eddy current	(1)	(2) New tool under development
Radiography	(2) Historically limited to topsides	(3) Digital method under development
Ultrasonic techniques	(2) Some examples to detect annulus flooding	(3) Unproven at detecting wire defects, access to critical region may be problematic
Acoustic emission	(1)	(2) Not field proven
Sonar monitoring (riser and anchor chain monitoring system)	(1) Limited use to date	(4) Has detected bend stiffener loss
Magnetic anisotropy and permeability system (MAPS)	(1) Offshore trials ongoing	(2)
Polymer coupons	(3) Commonly used for high-temperature applications	(4) Limited implementation but can provide assurance for PA11
Annulus monitoring (various techniques)	(4) Significant increase in recent years	(3)/(4) Can detect flooding, though dependent on access
Proof pressure testing	(2) Some examples	(3) Short term assurance only, ad-hoc method
Intelligent pigging	(1)	(1)
Torsion monitoring	(1) Focused on deepwater applications	(1) Alternative systems under development
Curvature monitoring	(1) Focused on fatigue	(2) No operational feedback
FPU excursion, environment monitoring	(4)	(3) Several systems failed to properly record and log excursion data
Fiber optic monitoring	(2) Embedded in tensile amour wires to detect strain cycling	(2) No operational feedback

[1]limited, specific application and 5 is a common practice.
[2]Ratesd 1–5, where 1 is underdeveloped, unproven and 5 is reliable.
Source: MCS Kenny and WGIM [2].

topside measure and subsea. As a measure at topside, the end-termination and vent valves of the flexible risers are inspected. Bend stiffeners are inspected for any evidence of damage, and the general condition of the hang-off basket is documented.

Subsea inspection has the aim of determining any damage or anomalies to the flexible pipes, such as buckling, kinking, and holes or tears in the eternal sheath. The touchdown zone should be examined thoroughly to determine the extent of trenching and any evidence of damage or pipe configuration outside the design limits. Evidence of clashing with other risers or objects, including the seabed, should also be documented. Excessive marine growth should be controlled and cleaned if necessary. Subsea ancillary equipment should similarly be examined for any signs of damage. An important point to remember is that small holes in the eternal sheath of operational flexible pipes are difficult to detect by visual inspection; hence, other testing and inspection measures are employed to complement visual inspection and lessen the risk of damage being undetected.

In addition, the cathodic protection survey is normally employed as part of a general visual inspection. The condition of the anodes should be examined at regular intervals to ensure that adequate cathodic protection is available at all times for the flexible pipes and other ancillary equipment.

Eddy Current

The principle of eddy current inspection is shown in Figure 5.12. A coil is placed above a conducting material. When the coil is excited by an alternating current, eddy currents are generated in the conductor. The penetration and

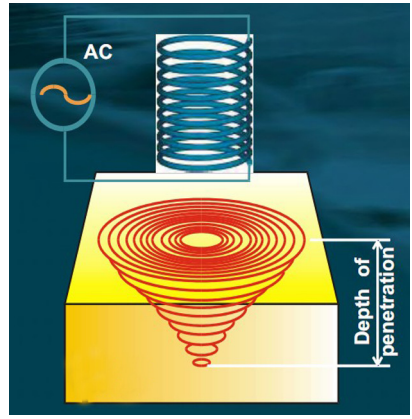

FIGURE 5.12 ***Eddy Current Distribution.*** *Source: Boenisch and Reber [17].* (For color version of this figure, the reader is referred to the online version of this book.)

distribution of eddy currents in the conductor are determined by the geometry and dimension of the probe, frequency of excitation, and resistivity and magnetic permeability of the metallic material. The depth at which eddy current density has decreased to $1/e$, or about 37% of the surface density, is called the *standard depth of penetration*. The eddy current may be tuned to penetrate through a layer of stainless steel, such as the carcass, and go into an underlying structure of carbon steel, such as the interlocked wire [16].

$$\delta = \frac{1}{\sqrt{\sigma \mu_0 \mu_r f}} \qquad [5.1]$$

where

δ = standard depth of the penetration
σ = electrical conductivity
μ_0 = absolute permeability
μ_r = relative permeability
f = frequency

The eddy current technique can be applied unaffected by the content of the pipe, e.g. oil, gas, liquid, from the inside and the outside of the pipe. Magnetic or conducting deposits may influence the eddy current signal. Deposits causing irregular lift-off may also give erroneous indications [16].

Radiography

Within a certain bandwidth, electromagnetic waves (X rays) are absorbed by dense materials (metals) and transmitted by less dense materials (polymers). Radiation from a point source through a structure thus gives a pattern of shades reflecting the through thickness density of the structure. The radiography of a flexible pipe may be configured as double wall, single wall, panoramic and tangential exposures [16].

The radiography method is most applicable for "verification of manufacturing," either as a fabrication QC method or inspection prior to or even after installation. End fittings are of particular interest, while major defects in steel components also are detectable. The method also is suitable for the investigation of damage after accidental loading, such as. to inspect for permanent deformation of steel components.

Ultrasonic Techniques

In ultrasonic techniques, a transmitter-receiver system for high-frequency acoustic (ultrasonic) waves is utilized. An ultrasonic tool was deployed for a number of flexible risers along the outside of a flexible riser via ROV. The

ultrasonic tool is used to detect annulus flooding from the outside of the flexible riser. The liquid-flooded annulus provides an acoustic couplant that enables the ultrasonic waves to travel from the outside of the flexible pipe further into the pipe cross section. Hence, the ability to scan the tensile armor wires is determined by a flooded annulus—no signal is detected if the annulus is dry. Further on the theme of annulus monitoring, an online system, RACS [18], was developed to enable continuous permeated gas flow rate annulus monitoring. As seen from Table 5.1, these techniques, together with armor wire fiber optic monitoring, have seen increased take-up by the industry in recent times and, as such, are rated (2) and above [3].

Acoustic Emission

Many damage mechanisms in materials cause the emission of a burst of high-frequency acoustic waves. Acoustic waves may be transmitted over relatively long distances in metals. A possible strategy is to obtain "signatures" of acoustic emission during stages of a progressing fatigue failure to separate the emission due to failure modes from the background noise. The identifications of damage processes are by observation of

- Changes in acoustic emission pattern over time.
- Occurrence of new acoustic emission sources.
- Steady rise in acoustic emission activity.
- Correlation of acoustic emission activity with external parameters, such as load level, local strain or displacement, and wave motions [16].

RAMS and MAPS

The riser and anchor chain monitoring system (RAMS) system is deployed within the turret of a floating production vessel below the bend stiffener level of the flexible riser system. The RAMS tool emits a horizontal sonar beam through 360° to generate and record sonar images of the spatial positions of the risers (and mooring chains). RAMS has been successfully and reliably used on a North Sea floating production facility and successfully identified the slippage of a bend stiffener, allowing corrective action to fix the problem.

The magnetic anisotropy and permeability system (MAPS) was developed for armor wire stress monitoring [19]. Sensors are permanently attached to the outside of the flexible riser in the bend stiffener region and sense into the tensile armors of the flexible pipe. The technique works by calibrating a change in the magnetic field around the armor wire to changes in applied wire stress [3].

Bore Fluid Parameter Monitoring

Various bore fluid parameters should be continuously monitored, because changes in these parameters could exceed certain design limits and cause damage to the flexible pipe. The parameters that require monitoring are temperature, pressure, volume flow rate, and the bore fluid composition.

Temperature is monitored to ensure it does not exceed the internal polymer temperature and cause accelerated ageing of the internal sheath. Temperature cycling could also cause ratcheting of pipes, and temperature variations could cause a different gas diffusion rate from the pipe bore to the annulus, which alters the corrosion and fatigue life of the annulus armor wires. Pressure is monitored, because excessive pressure or pressure surges could cause damage to the pressure armor layer. Rapid depressurization and evacuation of the pipe bore could cause pipe collapse. Pressure variations could have an effect on the fatigue life of the pipe and cause ratcheting or buckling of the pipe. The volume flow rate is also monitored to give an indication of a depressurization event and ensure that erosion calculations performed during the design stage remain valid throughout the lifetime of the pipe.

The bore fluid parameters are monitored to ensure that gas diffusion calculations are based on valid data.

6. TESTING AND ANALYSIS MEASURES

Coupon Sampling and Analysis

This testing method involves the use of coupon samples, which are ideally obtained from the same polymer extrusion, run as the internal polymer sheath of the flexible pipe. The coupons are placed in a holder in line with the transported bore fluid. The coupons are retrieved at regular intervals and tested to ensure that they do not suffer a worse rate of degradation than has been calculated for the internal polymer sheath during design calculations.

A more reliable method for determining the degradation of the internal polymer sheath is through the use of frequency-dependent electromagnetic sensing (FDEMS). FDEMS involves keeping the coupon samples in their holder and having an electromagnetic online system for monitoring the degradation rate of the coupons. This method is more expensive to implement than coupon sampling and analysis and normally is justified only if the rate of degradation of the internal polymer sheath is estimated to be high and the risk rating for internal pressure sheath failure is high.

Vacuum Testing of a Riser Annulus

Vacuum testing of a riser annulus is the most reliable method in the industry to determine the presence of water in the riser annulus.

Vacuum testing normally involves two separate procedures. Initially, a vacuum is drawn from the vent valves at the end termination of the riser. If the vacuum is stabilized, this is usually a good indication that there is no breach of the outer sheath. However, a further procedure is carried out following the drawing of a vacuum. The next procedure involves the injection of a known volume of nitrogen gas, which creates an inert atmosphere inside the annulus and, hence, has a protective effect on the steel armor wires. The volume of nitrogen gas injected into the annulus is carefully measured; and since the free volume of the annulus would be known from preinstallation tests, the free volume of the annulus at the time of the test can be examined.

REFERENCES

[1] Lecome H, Hogben S, Smith J, Bednar J, Palmer M. BP Marlin: First flexible pipelay with new build deepwater pipeline vessel. Houston: Offshore Technology Conference; 2002. OTC 14185.

[2] Kenny MCS, WGIM. State of the art report on flexible pipe integrity and guidance note on monitoring methods and integrity assurance for unbonded flexible pipes. Available at: http://www.oilandgasuk.co.uk/publications; 2010. code OP010.

[3] O'Brien P, Overton C, Picksley J, Anderson K, MacLeod I, Meldrum E. Outcomes from the SureFlex joint industry project—An international initiative on flexible pipe integrity assurance. Houston: Offshore Technology Conference; 2011. OTC 21524.

[4] Picksley JW, Kavanagh K, Garnham S, Turner D. Managing the integrity of flexible pipe field systems: Industry guidelines and their application. Houston: Offshore Technology Conference; 2002. OTC 14064.

[5] API RP 17B. Recommended practice for flexible pipe. fourth ed.; July 2008.

[6] Out JMM. Integrity management of flexible pipe: Chasing failure mechanisms. Houston: Offshore Technology Conference; 2012. OTC 23670.

[7] O'Brien P. Flexible pipe integrity and design—Current issues. SUT Evening Meeting; October 2005.

[8] Clevelario J. Introduction to unbonded flexible pipe design and manufacturing. USP course on flexible pipes, Wellstream do Brasil; 2012.

[9] Kaye D. Flexible riser integrity management experience west of Shetland. UK Industry Seminar; November, 2008.

[10] Muren J. Failure modes, inspection, testing and monitoring of flexible pipes. P5996-RPT01-REV02, Seaflex for PSA.

[11] Boschee P. Best practices for flexible pipe integrity evolve. Oil Gas Facilities 2012;1(1):2012.

[12] Joel J. Reinforcing wire corrosion in flexible pipe. Health Saf Lab (HSL) 2009.

[13] Charlesworth D, D'All B, Zimmerlin C, Remita E, Langhelle N, Wang T. Operational experience of the fatigue performance of a flexible riser with a flooded annulus. Houston: Offshore Technology Conference; 2011. OTC 22398.

[14] Berge S, et al. Environmental effects on fatigue strength of armour wire for flexible risers. Honolulu, USA; 2009. OMAE2009–80262.
[15] Grove S S, et al. The Rilsan User Group and API TRI7RUG. Houston: Offshore Technology Conference; 2002. OTC 14062.
[16] Berge S S, et al. Handbook on design and operation of flexible pipes. Trondheim, Norway; 1992. STF70 A92006.
[17] Boenisch A A, Reber K. Flexible riser inspection tool, seminar integrity management of unbonded flexible pipelines. Inverurie November 2008.
[18] Binet E, Tuset P, Mjoen S. Monitoring of offshore pipe. Houston: Offshore Technology Conference; 2003. OTC 15163.
[19] Roques J, Balague B, Dion D, Audouin A. Flexible pipe integrity monitoring: A new system to assess the flexible pipe annulus condition. Houston: Offshore Technology Conference; 2010. OTC 20973.

CHAPTER 6

Leak Detection Systems

Contents

1. Introduction 125
2. Leak Detection Methods 127
   General 127
   External Leak Detection Systems 128
      Vacuum Annulus Monitoring *129*
      Hydrocarbon Vapor Sensing Systems *129*
      Fiber Optic Cables *129*
   Internal Leak Detection Systems 130
      Mass Balance with Line Pack Compensation *130*
      Pressure Trend Monitoring *131*
      Real-Time Transient Modeling *131*
      Change of Flow Rate or Pressure *132*
      Pressure Trend Monitoring *133*
      Acoustic Emission Detectors *133*
3. Key Attributes of Different Methods 134
4. Principles of Leak Detection 135
   Gradient Intersection Method 135
   Mass Balance Method 137
   Statistical Leak Detection Systems 138
      Introduction *138*
      Leak Detection Algorithm *139*
      Sequential Probability Ratio Test *140*
   Negative Pressure Wave Method 141

References 143

1. INTRODUCTION

As subsea pipelines are being installed in the arctic or deeper water, there is increased interest in improving leak detection system capabilities throughout the pipeline industry. The consequences of a pipeline leak is significant. Pipeline internal or external corrosion, third-party damage, external loads, and natural disasters can cause pipeline leakage. A leak in subsea pipelines can cause a serious problem. For instance, the leak can significantly delay offshore oil and gas production and contaminate marine environments and ecosystems, threatening hundreds of species of fish, birds,

Subsea Pipeline Integrity and Risk Management
ISBN 978-0-12-394432-0
http://dx.doi.org/10.1016/B978-0-12-394432-0.00006-8

and other wildlife along the coast, ultimately resulting in a serious economic loss. With increasing public awareness and concern for the environment, recent pipeline leak incidents have shown that the cost to a company can be far more than the downtime and clean up expenses. As more stringent statutory regulations are introduced in the developed countries, cost-effective and reliable leak detection techniques play a more important role in the pipeline transportation of gas and oil [1, 2].

From an engineering and technical viewpoint, detection of a leak in a pipeline, often many miles long, is a complicated task unless the leak is caused by a catastrophic rupture or blowup of a pipeline system. The importance of leak detection and prevention of oil spills has also been a hot issue in remote areas, including Alaska. However, with the development of control theory and signal process techniques, the leak detection methods based on software are widely used because of their advantages, such as a high performance to price ratio, easy updating, and good expansibility.

Many factors make the leak detection process complicated and challenging. The fluid produced from offshore reservoirs normally is a multiphase flow of gas, oil, and water, together with a number of impurities. Although the upstream separation of the produced fluid at offshore treatment facilities can separate oil and gas, the fluid in long pipelines essentially undergoes significant changes in pressure and temperature because of heat transfer. In addition to the presence of both highly compressible gas phases and slightly compressible liquid phases, the adaptation of such an active and dynamic mass exchange into a model or simulator should be properly handled.

The primary purpose of leak detection systems is to assist pipeline operators in detecting and locating leaks. In this chapter, the fundamental principles of common pipeline leak detection methods are described. For example, using the negative pressure wave method combined with the flow method to detect and locate pipeline leaks. In this method, the wavelet analysis is chosen as signal processing for the pipeline pressure and flow, in which, the wavelet denoising method is used to filter away noise from the original pressure and flow signals, and the wavelet singularity analysis is used to detect catastrophe points of pipeline pressure and flow signals for pipeline leak detection and location. The acoustic emission leak detection system detects acoustic emission signals generated by leaks.

Normally, the pipeline leak detection systems have the following functions:

- Detect the pipeline leak.
- Locate and identify the leak.

The selection of leak detection system for a pipeline depends on a variety of factors, such as pipeline characteristics, product characteristics, instrumentation and communication capabilities, coatings, thermal insulation, burial depth, operating temperature, background noise, operating conditions, and economics. The instruments are normally located at the ends of a pipeline, far away from an actual leak. Instrument inaccuracies also introduce error in the measured parameters. Selecting the alarm settings of the leak detection systems for very small leaks may result in an unacceptable number of false alarms, due to their achievable sensitivity, and this inherent error. However, leaks that are smaller than the alarm settings may continue undetected by these systems.

2. LEAK DETECTION METHODS

General

Different leak detection methods have been applied to monitor the integrity of a pipeline in last several decades. The leak detection systems are varied and uniquely applicable to specific pipeline applications. However, leak detection technologies can be classified according to the physical principles involved in the leak detection. The leak detection technologies can be classified into three groups: biological methods, hardware-based methods, and software-based methods, as shown in Figure 6.1 [3].

Biological methods use experienced personnel or trained dogs to detect and locate a leak by visual inspection, odor, or sound. The biological methods are traditional leak detection methods, which use experienced personnel who walk along a pipeline looking for unusual patterns near the pipeline, smelling substances that could be released from the pipeline, or listening to noises generated by product escaping from a pipeline hole.

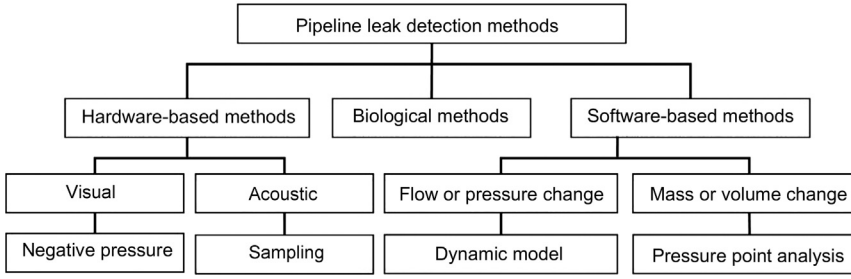

FIGURE 6.1 ***Leak Detection Methods.***

The results of such leak detection methods depend on individuals' experience and whether a leak develops before or after the inspection [3]; however, it is hard to do with a pipeline including H_2S or a deepwater pipeline.

Hardware-based methods use hardware sensors to directly detect the occurrence of a leak and assist the localization of the leak. Typical devices used include acoustic emission detectors, fiber optic sensors, negative pressure detectors, ultrasonic technologies, and infrared thermograph.

Software-based methods use computer software packages to constantly monitor data of pressure, temperature, and flow rate for detecting leaks in a pipeline. The complexity and reliability of these packages vary significantly. Examples of these methods are flow and pressure change detection, mass-volume balance, dynamic-model based systems, and pressure point analysis.

The leak detection methods may also be divided into two categories, external-based detection systems and internal-based detection systems. External-based methods detect leaking product outside the pipeline and include traditional procedures such as right-of-way inspection by line patrols as well as technologies like hydrocarbon sensing via fiber optics. Internal-based methods, which are similar to software-based methods, use instruments to monitor internal pipeline parameters such as pressure, temperature, density, and flow rate, which are inputs for inferring a product release [4].

The following is a summary of the leak detection methods that are considered suitable for subsea leak detection applications.

External leak detection systems include

- Vacuum annulus monitoring.
- Hydrocarbon vapor sensing systems.
- Distributed temperature sensing (DTS) fiber optic cable systems.
- Distributed acoustic sensing (DAS) fiber optic cable systems.
- Distributed strain sensing (DSS) fiber optic cable monitoring systems.

Internal leak detection systems include

- Mass balance with line pack compensation.
- Pressure trend monitoring.
- Real-time transient monitoring.
- Pressure safety low (PSL).
- Periodic shut-in pressure tests.
- Pressure wave and acoustic wave monitoring.

External Leak Detection Systems

External leak detection systems rely on detecting fluids, gases, temperatures, or other data that may only be present outside a pipeline during a leak event.

Vacuum Annulus Monitoring

Vacuum annulus monitoring involves monitoring the vacuum pressure within the annulus between an inner and outer pipe for a pipe-in-pipe (PIP) pipeline. To minimize the number of sensors, sensor connections, and cabling along the length of an offshore pipeline, monitoring of a continuous annulus at one end of the pipeline is desired. While this system does not have a limiting leak detection threshold, the application of this technology is limited by distance and the ability to lift and install larger pipe-in-pipe pipelines, which may be bundled to other pipelines.

Hydrocarbon Vapor Sensing Systems

If the product inside a pipeline is highly volatile, a vapor monitoring system can be used to detect the level of hydrocarbon vapor in the pipeline surroundings. This is usually done by vapor sensing. The method can be used for single-phase gas, single-phase oil, or multicomponent or multiphase flow to estimate the location and size of the leak by concentration measurements. The sampling can be done by carrying the device along a pipeline or using a sensor tube buried parallel to the pipeline. The response time of the detection system is usually from several hours to days. For application to offshore pipelines, a hydrocarbon detector can be used with a ROV. Pipeline leaks result in hydrocarbon anomalies in surrounding sediments and seawater, which can be detected by the hydrocarbon or chemical detector.

The LEOS system is a vapor sensing leak detection system, which has been installed on one arctic subsea pipeline project (BP Northstar). However, while it is very sensitive in detecting very small, chronic leaks, the water depth limitation and the above-water access requirement for both ends of the LEOS system generally limit applications to near-shore, shallow water pipelines.

Fiber Optic Cables

Fiber optic technologies rely on the fiber optic cable to act as a continuous, distributed sensor along the length of a pipeline. This is different than using discrete, single-point instruments spaced along a pipeline [4]. The optical characteristics of fibers alter with temperature changes, mechanical stress, and surface coating or absorption of chemicals. The substances to be measured come into contact with the cable when a leak occurs, changing the temperature of the cable. The distributed fiber-optical temperature-sensing technique offers the possibility to measure temperature along the

pipeline. Scanning the entire length of the fiber, the temperature profile along the pipeline is determined, leading to leak detection. However, it may not detect leaks in unburied subsea pipelines.

Two other distributed fiber optic technologies are available for monitoring a pipeline:

- Distributed acoustic sensing.
- Distributed temperature sensing.
- Distributed strain sensing.

Internal Leak Detection Systems

Internal leak detection systems rely on internal pressure, temperature, flow rate, or density measurements. They are sometimes referred to as *computational leak detection systems*. However, some external leak detection systems also rely on computations to monitor pipelines for leaks.

Mass Balance with Line Pack Compensation

Mass balance with line pack compensation (MBLPC) relies on the principle of conservation of mass. For a normal pipeline, the flow entering and leaving the pipe can be metered. The mass of fluid in the pipe section can be calculated from the pipe dimensions and measurement of state variables of the fluid such as pressure and temperature.

The sensors required for this technique can be categorized as flow rate, pressure, and temperature of the production fluid. Flow meters are required at all inlets and outlets of the pipeline. In addition, some systems use density meters in their monitoring. [5].

If the difference of mass between upstream and downstream are larger than an established tolerance, a leak alarm is generated. This method allows the detection of a leak that does not necessarily generate a high rate of change in pressure or flow. The methods can be based on flow rate difference only, which would generate a mass or volume balance scheme or on mass balance compensated by pressure or temperature changes and inventory fluctuations in a pipeline.

The sensitivity of the mass balance technique depends on the accuracy of the estimate of pipe contents. The accuracy can be increased by considering the flow into and out of the pipe section over a long enough time period, when the mass that has flowed in and out of the pipeline is very large compared to the mass resident in the pipe. Over a long enough time period, detection is limited only by the accuracy of the flow instrumentation. Generally, the method can detect small leaks over a long

time, assuming steady state line conditions. A wide range of flow variations can be accommodated without masking the leak detection process, and pipeline transients are normally filtered out by long-term averaging.

Pressure Trend Monitoring

Pressure trend monitoring uses pressure measurements to monitor operating trends in the pipeline. If a set of parameters does not match historical trends, an alarm is triggered. Pressure trend monitoring systems tend to catch larger leaks faster than MBLPC on single-phase liquid pipelines, but pressure trend monitoring systems may have a larger (worse) leak rate detection threshold limits than MBLPC systems for single-phase pipelines. EFA technologies' pressure point analysis (PPA) is an example of pressure trend monitoring. It is used in combination with MBLPC and supplemented by the LEOS vapor sensing system.

Real-Time Transient Modeling

The real-time transient modeling (RTTM) systems monitor the pipeline at every block valve site and collect pipeline data over the entire pipeline length, including metering stations at the end. It also called a *dynamic model-based system*. The data give the operator a real-time view of pipeline conditions. The data collected can also be utilized for leak detection, usually within a dedicated computer connected to the SCADA computer [5]. Figure 6.2 shows a pipeline leak detection system. The total release from a pipeline depends on the response of the line leak detection system and the closure time of the valve.

This technique attempts to mathematically model the one-dimensional hydraulic behavior of the pipeline. Mathematically, this is an initial-boundary value problem. which is completely defined by boundary conditions taken from sampled measurements of pipeline pressure, flow, and temperature. Given pressure and flow at the pipeline inlet, the equations solve for outlet pressure and flow. Leaks are determined as discrepancies between predicted and measured values [6].

The hydraulic governing equations used to simulate the fluid flow in the model-based system are

- Conservation of mass.
- Conservation of momentum.
- Conservation of energy.
- Equation of state for the fluid.

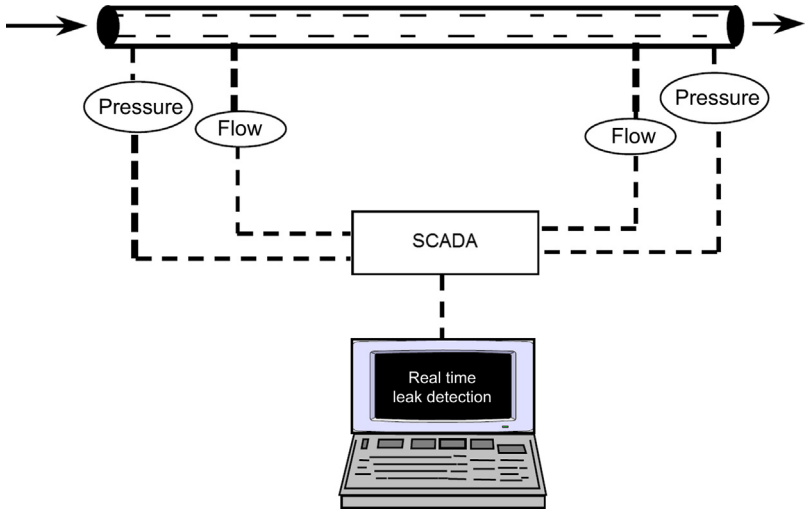

FIGURE 6.2 ***Pipeline Leak Detection System.***

The conservation laws are described by nonsteady partial differential equations in which the hydraulic parameters of pressure, temperature, and flow are functions of time and distance along the pipe. The partial differential equations are solved by a variety of computational techniques, depending on the choices of suppliers. The alternative methods currently in use in commercial software packages include

- Finite difference.
- Finite element.
- Method of characteristics.
- Frequency response or spatial discretization.

The method requires flow, pressure, and temperature measurements at the inlet and outlet of a pipeline. It will be better if the pressure and temperature measurements at several points along the pipeline could be carried out.

Change of Flow Rate or Pressure

This technique relies on the assumption that a high rate of change in flow rate or pressure at the inlet or outlet of a pipe indicates the occurrence of a leak. If the change of flow rate or pressure is higher than a predefined value within a specific time period, then a leak alarm is generated. The system is designed to detect the sudden change in pressure or flow rate that would arise in rupture situations. A sudden change in flow rate due to a leak

propagates as a wave at acoustic velocity and quickly settles down to a new steady state position [7].

The main drawback in is the loss of signal definition due to background events and noise. The major problem is the false alarm rate. The change in flow rate or pressure systems can estimate leak size but cannot locate a leak because of insufficient signal intelligence from one monitor only.

The effectiveness of these systems depends on line length and, crucially, where the leak occurs. The maximum response and sensitivity are obtained when the leak is at the downstream end of the pipe close to the monitor.

Pressure Trend Monitoring

Pressure trend monitoring is based on an assumption that, if a leak occurs in a pipeline, the pressure in the line drops. Using statistical analysis of the pressure measurements, a decrease in the mean value of a pressure measurement may indicate a leak. If the decrease is more than a predefined level, then a leak alarm is generated.

Pressure trend monitoring detects leaks by monitoring pipeline pressures at single pressure transmitter points along the line and comparing them against a running statistical trend constructed from previous pressure measurements. The combination of selective filtering and software thresholds determines if the behavior of successive measurements contains evidence of a leak.

The advantages of this method are

- A low level of instrumentation and low installation costs.
- A combined pressure trend monitoring and mass balance system is complementary.

The disadvantages of this method are

- A fall in pipeline pressure is not unique to a leak situation. There is a high probability of generating a false alarms when unforeseen transients occur. Relatively leak alarm free operation limits the system to detection of medium to large leaks. However, it can detect these leaks relatively rapidly, compared to other systems.
- Leak location is determined by the time stamped pressure data between measurements at two pressure transmitter locations.

Acoustic Emission Detectors

When a leak occurs, an acoustic vibration energy signal is generated as the fluid escapes from the pipeline. The wave of the signal propagates

with a speed determined by the physical properties of the fluid in the pipeline. The intensity of emitted sound is proportional to the eighth power of the turbulent flow velocity and increases strongly with increasing pressure. For many subsea oil and gas pipelines, the operational flow regimes are highly turbulent. For leaks from pressurized subsea gas pipelines, it can be safely assumed the leak will act as a sound source. However, for export oil lines, it is possible that the leak will not act as a sound source [5].

The acoustic detectors can be operated in a continuous mode to detect these waves and consequently the leaks [3]. It can determine the location of the leak, and the size of leak can be estimated. This method can be used on new or retrofitted to existing pipelines and is more sensitive than software-based methods and responds in essentially real time. However, the acoustic sensors detect acoustic signals in the pipeline and discriminate leak sounds from other sounds generated by normal operational changes. The noise conditions due to high production flow may mask the leak signal. Due to the limitation of the detection range, many sensors may be needed to monitor along the pipelines, which means extremely high cost.

3. KEY ATTRIBUTES OF DIFFERENT METHODS

The design of the leak detection system should be integrated in the overall subsea system design. The subsea structures where leak detectors have been installed to date are mainly the terminus of the pipelines on the topsides facilities and subsea at Xmas trees, templates and manifolds. The feedback from subsea system integrators is that integrating the sensors to subsea structures mechanically, and to the control system, in most cases, is solvable, but it is important that this requirement be identified early in the design process [2].

The leak detection system should therefore be included as a primary design requirement and not considered as an add-on late in the design process. However, each leak detection method has its advantages and disadvantages. To evaluate the performance of different methods, the following key attributes of a leak detection system are designated:

- **Leak sensitivity (minimum leak detection threshold):** Are small chronic leaks are detected with relatively false alarm free operations? Is there a supplementary detection system or surveillance program for observing evidence of small chronic leaks?

- **Location estimate capability:** Is location estimate provided or are there tools for postleak alarm to determine the location of the leak?
- **Operational change flexibility:** Can the method work if the pipeline experiences operational changes, such as pigging? Is it important for the project, or are such changes relatively infrequent?
- **Availability:** Can the method monitor a pipeline without interruption, that is, 24 hours a day?
- **Maintenance requirement:** What level of technical expertise is required to maintain the system?
- **Cost:** What capital expenditure (CAPEX) and operating costs (OPEX) are needed.

Table 6.1 summarizes the attributes of different leak detection methods. The method is chosen based on the requirements of the pipeline. Table 6.2 shows the detailed monitoring techniques for different leak detection methods for a pipeline.

4. PRINCIPLES OF LEAK DETECTION

Gradient Intersection Method

The gradient intersection method is based on the fact that the pressure profile along the pipeline with its length, L, changes significantly if a leak occurs. Figure 6.3 shows variations in pressure and flow rate along the flowline when there is a leak occurring at the pipeline [10].

A pressure drop in a leak-free pipeline is a linear real line, as shown in the figure. If a leak occurs, the pressure profile develops a kink at the leak point, as shown by the dotted line in the figure. The leak location can be determined by calculating the intersection point of the pressure profiles upstream and downstream of the leak. The classic gradient intersection approach calculates the gradient of both lines using two pressure readings near the inlet and two pressure readings the outlet. The model-based gradient intersection method calculates the two gradients with the help of the real-time transient model, computed by flow and pressure measurements at the inlet and outlet.

Figure 6.3 shows the pressure profile before and after a leak in a pipeline, then the Bernoulli equation can be used to resolve the location:

$$\frac{P_i}{\rho g} - x \times \beta \frac{Q_i^{2-m} \upsilon^m}{d^{5-m}} = \frac{P_o}{\rho g} + (L - x) \times \beta \frac{Q_o^{2-m} \nu^m}{d^{5-m}} + \Delta h \qquad [6.1]$$

Table 6.1 Key Attributes of Different Methods

Methods	Leak Sensitivity	Location Estimate	Operational Change	Availability	Maintenance Requirement	Cost
Biological	Yes	Yes	Yes	No	Low	High
Visual	Yes	Yes	Yes	No	Low	High
Acoustic	No	Yes	No	Yes	Medium	Medium
Sampling	Yes	Yes	Yes	No	Medium	High
Negative pressure	No	Yes	No	Yes	Low	Low
Flow trend monitoring	No	No	No	Yes	Low	Low
Mass balance with line pack compensation	See Table 6.2	No	No	Yes	Low	Low
RTTM	See Table 6.2	Yes	Yes	Yes	Medium to high	Medium
Pressure trend monitoring	See Table 6.2	No	No	Yes	Low	Low

Note: The attributes are rated as follows: Yes = good; No = no good; Low = good; Medium = average; High = not good.
Source: Eisler [8].

Table 6.2 Monitoring Techniques of Different Leak Detection

Leak Detection Method	Leak Size	Time
Mass balance with line pack compensation	0.15% to 1% for single-phase lines with LACT units; 5% to 30% for multiphase lines depending on metering	Minutes to hours for medium to large leaks;, 24 hours to weeks for chronic leaks, depending on the length of the pipeline
Pressure trend monitoring	>1%	Minutes to hours for medium to large leaks, depending on length of the pipeline
Acoustic pressure wave	—	Minutes to hours for medium to large leaks, depending on length of the pipeline
Real-time transient model	As good or better than mass balance with line pack compensation	Depends on the size of the leak and the length of the pipeline
Statistical analysis	>1%	Depends on the size of the leak and the length of the pipeline

Source: BP [9].

$$x = \frac{(P_i - P_o)d^{5-m} - \rho g \Delta h d^{5-m} - \rho g L \beta Q_o^{2-m} \nu^m}{\rho g \beta \left(Q_i^{2-m} - Q_o^{2-m}\right) \nu^m}$$

$$x = \frac{\overline{P}_i - \overline{P}_o - KL\overline{Q}_o^2}{K\left(\overline{Q}_i^2 - \overline{Q}_o^2\right)} \qquad [6.2]$$

where

$$K = \frac{\rho g \beta \nu^m}{d^{5-m}}$$

The value K is determined by the least squares method based on the measurements, it may be calculated based on fluid mechanics.

Mass Balance Method

The mass balance method is based on the equation of conservation of mass. In the steady state, the mass entering a leak-free pipeline (M_i) balances the

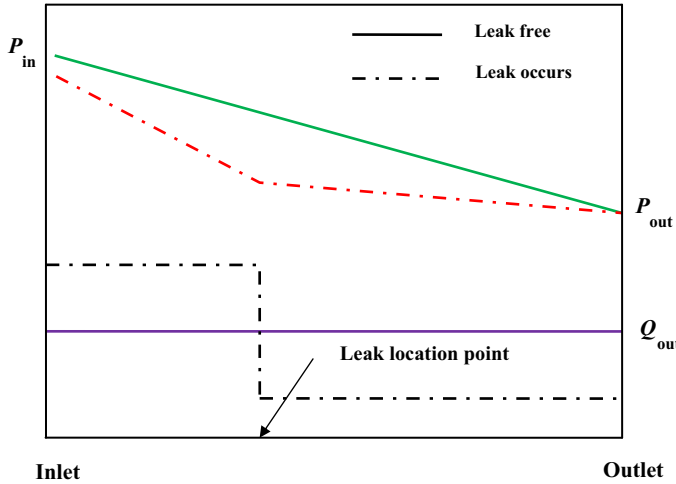

FIGURE 6.3 ***Leak Location Identification Method.*** (For color version of this figure, the reader is referred to the online version of this book.)

mass leaving (M_o). In the more general case, the difference in mass at the two ends must be balanced against the change of mass inventory of the pipeline (ΔM_{pipe}):

$$\Delta M_i - \Delta M_o = \Delta M_{pipe} \quad [6.3]$$

The mass in the pipe depends on the density of the product multiplied by the volume of the pipeline. Both are functions of temperature and pressure, and the density is also a function of the composition of the product. None of these values is necessarily constant along the pipeline.

Any addition mass imbalance indicates a leak. This can be quantified by rearranging the equation and adding a term for leak mass (ΔM_{leak}):

$$\Delta M_{leak} = \Delta M_i - \Delta M_o - \Delta M_{pipe} \quad [6.4]$$

Statistical Leak Detection Systems

Introduction

Statistical leak detection systems use statistical methods to detect a leak, which offers the opportunity to optimize the decision if a leak exists in the sense of chosen statistical parameters. However, great demands are placed on measurements. ATMOS Pipe™ from ATMOS International is an example [11, 12].

ATMOS Pipe applies advanced statistical techniques to flow, pressure, and temperature measurements of a pipeline. Variations generated by operational changes are registered, and thus, reliable system performance

can be achieved through tuning statistical parameters. It does not solve partial differential equations to calculate flow or pressure in a pipeline, but it detects changes in the relationship between flow and pressure using the measurement data available.

Leak Detection Algorithm

ATMOS PIPE applies statistical techniques to detect changes in the overall behavior of flow and pressure at the ingress and egress points. The relationship between the pipeline pressure and flow always changes after a leak develops in a pipeline. For example, a leak could cause the pipeline pressure to decrease and introduce a discrepancy between the ingress and egress flow rate. The leak detection system is designed to detect such changes, that is, pattern recognition.

Leak determination is based on probability calculations at regular sample intervals. The basic principle used for the probability calculations is mass conservation and hypothesis testing: leak against no leak. Although the flow and pressure in a pipeline fluctuate due to operational changes, statistically, the total mass entering and leaving a network must be balanced by the inventory variation inside the network. Such a balance cannot be maintained if a leak occurs in a network. The deviation from the established balance is detected by an optimal statistical test method: the sequential probability ratio test (SPRT)[13].

The combination of the probability calculations and pattern recognition provides ATMOS with a very high level of system reliability, that is, a minimum of spurious alarm rate. Under leak-free operations, the mass balance principle determines that the difference between the ingress and egress flow rates should be equal to the inventory variation in a pipeline. Therefore, the following term is calculated [3]:

$$\tau(t) = \sum_{1}^{M} Q_{\mathrm{i}}(t) - \sum_{1}^{N} Q_{\mathrm{o}}(t) - \sum_{1}^{L} \Delta Q_{\mathrm{p}}(t) \qquad [6.5]$$

where

$\tau(t)$ = corrected flow difference term at time t; in practice, $\tau(t)$ usually fluctuates around a nonzero value due both to the inherent differences in the instruments and fluid compressibility

$Q_{\mathrm{i}}(t)$ = the flow measurement at the ingress points and $Q_{\mathrm{o}}(t)$ at the egress points

M = number of ingress points

N = number of egress points

L = number of pipeline sections

ΔQ_p = correction term for the inventory variation over the sample period of $t - 1$ to t

ΔQ_p is a function of pressure and temperature in the pipeline. Different product types in the network introduce changes in the inventory calculations. The mean value of this process remains unchanged unless a leak develops in a pipeline or an instrument error occurs. The distinction between these two failure modes has to be made by further analysis, such as instrument change pattern identification. ATMOS Pipe can identify typical instrument faults, thus informing operators of possible faulty instruments.

Sequential Probability Ratio Test

The cores engine of ATMOS Pipe is the sequential probability ratio test sample analysis methodology, which was originally developed as a very effective statistical quality control application. Zhang [3] developed algorithms to apply SPRT to measurement data from the pipeline SCADA system and installed the application on a many pipelines with excellent results.

ATMOS Pipe compares two statistical hypotheses: the pipeline measurement data that contain evidence of a leak (H_1) versus the pipeline data that contain no evidence of a leak (H_0). Figure 6.4 shows the probability density functions for leak-free and leak tests. In the figure, m represents the mean value of $\tau(t)$ under normal (leak-free) operations and Δm is a

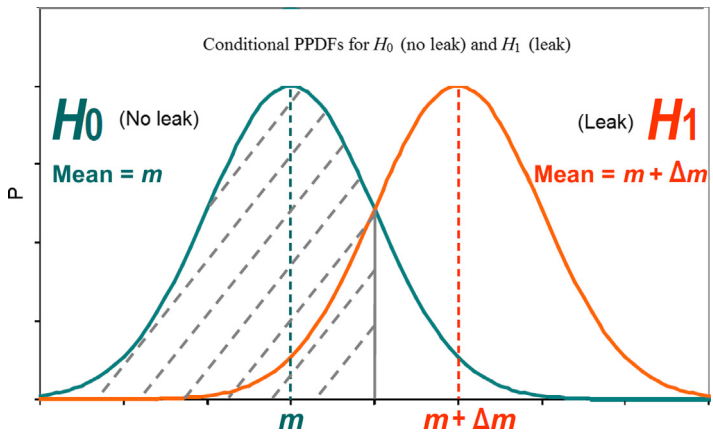

FIGURE 6.4 ***Conditional Probability Density Functions for Leak-free and Leak Tests.*** (For color version of this figure, the reader is referred to the online version of this book.)

parameter determined by the leak size to be detected. Once this comparison yields a confidence level of 99%, a leak alarm is signaled. This methodology reduces false alarms to a couple per year on liquids systems with reasonable measurement data.

To take into account instrument drifts over time, m is tuned slowly using measurements available during a no-leak alarm period. The value σ^2 depends on the fluctuations of the flow and pressure signals in a pipeline. For changing operating conditions in the pipeline, different values of σ^2 are used. Usually, three operating modes are identified automatically in a pipeline:

- Steady state operation, operating status = 0.
- Medium operational change, operating status = 1.
- Large operational change, operating status = 2.

After a large operational change, it takes longer for the SPLD system to detect a leak than during steady state operations. The choice of the different values of σ^2 is determined to achieve maximum system reliability, without loss of leak detection functionality.

The SPRT for testing hypothesis H_1 against H_0 is transformed to the calculation of the following cumulative sum:

$$\lambda(t) = \lambda(t-1) + \frac{\Delta m}{\sigma^2} \cdot \left[\tau(t) - m - \frac{\Delta m}{2} \right] \qquad [6.6]$$

By comparing the online calculated value $\lambda(t)$ with a preset threshold value, a leak alarm can be generated.

After a leak is detected, the leak rate is estimated by subtracting the online updated value m from the average value of $\lambda(t)$ shown in the equation.

Negative Pressure Wave Method

When a leak occurs, a rarefaction wave is produced in the pipeline contents. The wave propagates both upstream and downstream from the leak site. The wave travels with a speed equal to the speed of sound in the pipeline contents. Pressure transducers can be used to measure pressure gradient with respect to time. Usually, two sensors are used for each pipeline segment to help discriminate between noise and externally caused pressure drops.

The pressure drop fluctuations and volatility is quite different with the normal operation and with an almost vertical front; when the fluctuations and volatility exceed the predefined value, the leak occurs.

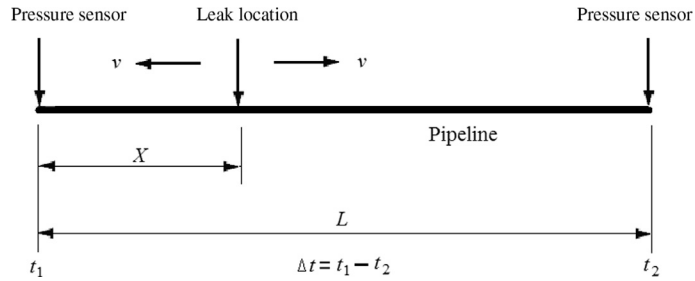

FIGURE 6.5 *Leak Location lidentification Method.*

The negative pressure wave method is able to detect leaks in steady state conditions, and small variations in pressure can easily lead to undetected leaks. It is most useful in liquid pipelines, as pressure waves are quickly attenuated in gas pipelines.

Key factors of the negative pressure method include

1. Pressure signal processing (wavelet transform method).
2. Wave travel speed determination in pipeline.
3. Pressure drop fluctuations critical value determination.

As shown in Figure 6.5, the leak location can be identified based on the following equations:

$$\Delta t = \frac{X}{\alpha - v} - \frac{L - X}{\alpha + v} \qquad [6.7]$$

$$X = \frac{1}{2a}\left[L(\alpha - v) + \Delta t\left(\alpha^2 - v^2\right)\right] \qquad [6.8]$$

and the propagation speed of liquid is calculated by

$$\alpha = \sqrt{\frac{K/\rho}{1 + [(K/E)(D/t)]C_1}}$$

where

α = propagation speed of the pressure wave
v = speed of fluid
ρ = density of the fluid
K = fluid bulk modulus
D = inside diameter of pipe
t = pipe wall thickness
E = pipe material modulus of elasticity, kg/m^2
C_1 = parameter for pipe and liquid properties

This technique works without malfunction if pressure and flow stay constant in daily operation, which is true for some liquid pipelines but never for gas pipelines. Statistical methods to prevent false alarms normally are not used. The only way to avoid false alarms is to set wide alarm limits. This causes a short time to detect a leak within liquid pipelines. In gas pipelines, pressure changes are rather slow, so leak detection is also slow. This method detects only sudden leaks of adequate size.

REFERENCES

[1] API 1130. Computational pipeline monitoring for liquid pipelines. Washington, DC: American Petroleum Institute; 2002.

[2] DNV-RP-F302. Selection and use of subsea leak detection systems. Bærum, Norway: Det Norske Veritas; April 2010.

[3] Zhang J. Designing a cost effective and reliable pipeline leak detection system. Manchester, UK: REL Instrumentation Limited; 1996.

[4] Eisler B, Lanan GA. Fiber optic leak detection systems for subsea pipelines; 2012. OTC 23070, Offshore Technology Conference, Houston.

[5] HSE. Pipeline leak detection study; 1996. OTH 94 431, London.

[6] Djeziri MA, Bouamama BO. Reliability analysis of fluid leak detection and isolation system. J Energy Power Eng May 2010;4(5).

[7] Geiger G. Fundamentals of leak detection. Breda: the Netherlands: KROHNE Oil and Gas; 2008.

[8] Eisler B. Leak detection systems and challenges for arctic subsea pipelines; 2011. OTC 22134, Offshore Technology Conference, Houston.

[9] BP. The Baku-Tbilisi-Ceyhan (BTC) pipeline project ESIA. Oil Spill Prev Mitigations 2003. Appendix 6.

[10] Gajbhiye RN, Kam SI. Leak detection in subsea pipeline: A mechanistic modeling approach with fixed pressure boundaries. SPE Projects Facilities Construction 2008;3(4).

[11] Zhang J, Mauro ED. Implementing a reliable leak detection system on a crude oil pipeline. Dubai: United Arab Emirates: Advances in Pipeline Technology; 1998.

[12] Beushausen R, Tornow S, Borchers H, Murphy K, Zhang J. Transient leak detection in crude oil pipelines. Proceedings of IPC 2004 International Pipeline Conference. Calgary: Alberta, Canada; October 2004.

[13] Baptista RM, Maricato ALG, Masiero PA. A pipeline LDS trial: Comparing compensated volume balance against SPRT statistical based LDS in a Brazilian pipeline. In: Proceedings of IPC 2004 International Pipeline Conference. Calgary: Alberta, Canada; 2004.

CHAPTER 7

Fiber Optic Monitoring System

Contents

1. Introduction 145
2. Fiber Optic Sensor Techniques 147
   Fiber Bragg Grating Sensor 147
   Distributed Fiber Optic Sensors 148
      Rayleigh Scattering *149*
      Raman Scattering *151*
      Brillouin Scattering *152*
3. Types of Sensing Fiber Optics 158
   Telecommunication Optical Fiber 158
   Photonic Crystal Fiber 158
   Polymer Optical Fiber 159
4. Application of Fiber Optic Monitoring on Subsea Pipelines 159
   Objectives 160
   Choice of Optical Fiber 160
   Geometric Structure of Optical Cable 161
   Solutions to Pipe Joint Crossing 162
   Fiber Optic Layout in RTP 162
   Fiber Survival Issue 163

References 164

1. INTRODUCTION

Optical fibers were first envisioned as optical elements in the early 1960s. Charles Kao [1] first suggested the possibility that low-loss optical fibers could be competitive with coaxial cable and metal waveguides for telecommunications applications. However, not until 1970, when Corning Glass Works announced an optical fiber loss less than the benchmark level of 10 dB/km [2, 3], did commercial applications begin to be realized.

Optical fiber is designed for total internal reflection, no light is transmitted through the core to the cladding. In optical fiber, as shown in Figure 7.1, n_1 is the core index of refraction, and n_2 is the cladding index of refraction. The third fundamental law of geometrical optics, also known as *Snell's law*, is shown in Eq. [7.1]. The critical angle θ_I can be obtained from Eq. [7.1], when the angle θ_T is 90° for the total internal reflection. The numerical aperture

Subsea Pipeline Integrity and Risk Management
ISBN 978-0-12-394432-0
http://dx.doi.org/10.1016/B978-0-12-394432-0.00007-X

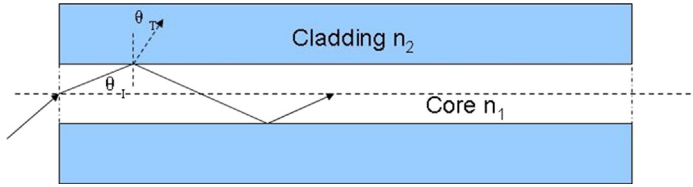

FIGURE 7.1 ***Light Propagation in Optical Fiber.*** (For color version of this figure, the reader is referred to the online version of this book.)

(N.A.) of optical fiber in Eq. [7.3] is a measure of the light acceptance capability of the optical fiber.

$$\frac{\sin\theta_T}{\sin\theta_I} = \frac{n_1}{n_2} \qquad [7.1]$$

Given $\theta_T = 90°$, the critical angle θ_I is shown as follows:

$$\sin\theta_I = \frac{n_2}{n_1} \qquad [7.2]$$

$$\text{N.A.} = n_1\sqrt{1-\left(\frac{n_2}{n_1}\right)^2} = \sqrt{n_1^2 - n_2^2} \qquad [7.3]$$

Optical fiber science and technology relies heavily on materials science, integrated and guided-wave optics, quantum mechanics and physics optics, communications engineering, and other disciplines. Within the fiber optic communication applications, many efforts were exploited to decrease the impact of external environmental factors on the optical fibers. On the other hand, optical fibers can be used as fiber optic sensors utilizing the same physical principle to measure strain, temperature, acoustic field, pressure, and other quantities by modifying the fiber so that the quantity to be measured modulates the intensity, phase, polarization, and wavelength or transit time of light in the fiber. Fiber optic sensors are widely used and, over the past 20 years, built a track record in the oil and gas industry in applications including pipeline condition and leakage monitoring, optimization of oil well productivity, and liquefied natural gas (LNG) plant leakage detection and cooldown process monitoring [4]. A particularly useful feature of intrinsic fiber optic sensors is that, if required, they can provide distributed sensing over ultralong distance, which is suitable for the pipeline applications. Fiber optic sensing and monitoring have already been practical in subsea flexible reinforced thermoplastic pipe (RTP) developed by Offshore Pipelines and Risers (OPR) Inc. The RTP is a smooth and

continuous pipeline. The application of fiber optic sensor technology in subsea RTP and underlying mechanisms is addressed in this chapter.

2. FIBER OPTIC SENSOR TECHNIQUES

In the past decades, the fiber optic sensor techniques developed from the experimental stage to practical applications. For instance, distributed fiber optic sensors were installed in dams and bridges to monitor the internal deformation parameters of these facilities. With the rapid development of optical networks, the cost of fiber optic sensors substantially dropped, due to the decreasing price of commercially optical key components in fiber optic communications, such as laser light sources and photo detectors. The fiber optic sensors have wide applications in sensing technology, with better results than some conventional sensors. Fiber optic sensors, possessing a number of advantages in a variety of sensing applications because of their small size, light weight, electromagnetic interference immunity, and extremely optical low-loss, have a capacity to make multiple measurements distributed along the length of the fiber and can easily be interfaced with data communication systems.

Fiber Bragg Grating Sensor

The Fiber Bragg Grating (FBG) sensor consists of distributed Bragg reflectors in a short segment of optical fiber that reflects particular wavelength light and transmits all others, as shown in Figure 7.2. This function can be achieved by creating permanent periodic refractive index variation along the propagation axis of the fiber core using ultraviolet light, which generates a wavelength-specific dielectric mirror.

For FBG sensors, the Bragg wavelength is sensitive to strain and temperature simultaneously. The relative shift in Bragg wavelength is given as follows:

$$\frac{\Delta\lambda_B}{\lambda_B} = (1 - p_e)\varepsilon + (\alpha_\Lambda + \alpha_n)\Delta T \qquad [7.4]$$

where p_e is strain optic coefficient, α_Λ is the thermal expansion coefficient of optical fiber, α_n is the thermo-optic coefficient, ε is applied strain, and ΔT is the change of temperature.

FBG is one kind of popular commercial technology and widely used in many applications, such as civil health monitoring, pressure sensors for extremely harsh environments, strain and temperature sensors in composite materials for aircraft structures [5, 6]. FBG sensors are very sensitive to

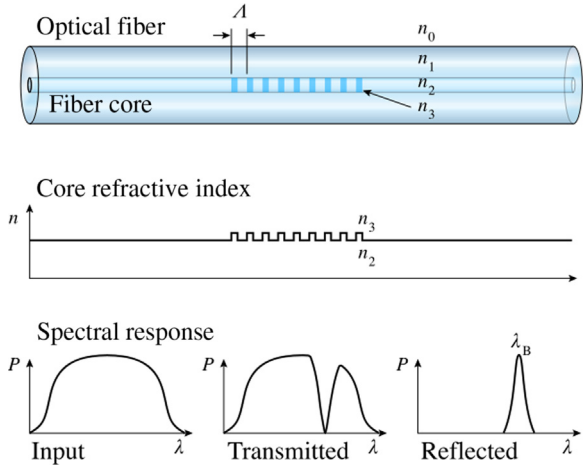

FIGURE 7.2 ***Fiber Bragg Grating Structure, with Refractive Index Profile and Spectral Response.*** (For color version of this figure, the reader is referred to the online version of this book.)

nonuniform strain distribution along the entire length of the grating, which changes the reflection spectrum from the FBG sensors. Therefore, microscopic deformations cause nonuniform strain and can be detected with typical high sensitivity of 1με strain and 0.1°C temperature. Although the time-based and frequency-based methods can be used to separate signals from different gratings, FBG sensors cannot offer the whole strain-temperature condition of point sensor technology, and the scale range of FBG sensors cannot meet the large strain requirements during the installation and maintenance of RTP.

Distributed Fiber Optic Sensors

Early work on the fiber optic sensor concentrated on measuring at a particular point. However, it is also possible to measure the external parameter field as a function of position along the fiber. Figure 7.3 illustrates the different types of fiber optic sensors. Optical reflectometry is a critical diagnostic tool for light wave systems and components. three reflectometric techniques are commonly used in fiber-based measurements: optical time-domain reflectometry (OTDR), optical low-coherence reflectometry (OLCR), and optical frequency-domain reflectometry (OFDR). These techniques differ in the basic physics and consequently have trade-offs in resolution, speed, sensitivity, and accuracy. OTDR is generally used for long-range (km), low-resolution (≈ 1 m) applications; OLCR achieves

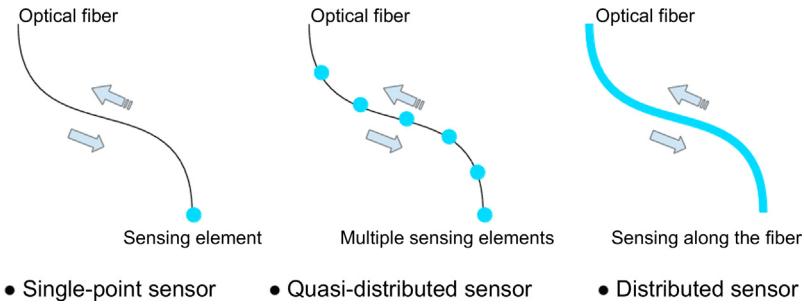

FIGURE 7.3 ***Different Types of Fiber-Optic Sensors.*** (For color version of this figure, the reader is referred to the online version of this book.)

submillimeter resolution over short ranges ($\leq$ 5 m); and OFDR operates in the middle, with a range of tens to hundreds meter and resolution on the millimeter to centimeter scale [7].

The distributed measurement over distances up to several tens of kilometers is unique to the fiber optic sensor based on the OTDR technique. The OTDR was first demonstrated in 1976 to measure the attenuation properties of optical fibers [8]. Because of their utility for measuring the properties of optical fibers, OTDRs are widely used in various applications, such as fiber production, network testing, and fiber optic sensors [9]. An OTDR launches a short pulse of light into the end of a fiber and measures the intensity of Rayleigh-, Brillouin-, and Raman-scattering light as a function of time. The time can be easily converted to distance by considering the velocity of light within the optical fiber. The spatial resolution of the fiber optic sensor system is determined by the pulse length of the light. Based on frequency filters and spectrum analyzers, the frequency and amplitude of a scattering signal can be analyzed with function of acoustic vibration (Rayleigh), temperature (Raman), and temperature-strain (Brillouin), respectively.

Some scattering effects in standard optical fibers of laser light can be influenced by the ambient conditions (strain ε, and temperature, ΔT), as shown in Figure 7.4. The three main scattering processes in optical fibers are Rayleigh, Raman, and Brillouin scattering.

Rayleigh Scattering

Rayleigh scattering is the high-intensity elastic scattering of light based on density and compositional random fluctuations of fiber materials. This elastic scattering is not sensitive to the ambient condition but used for fiber integrity sensing and interferometric sensing. Rayleigh scattering along the length of a fiber can be used as a "signature," since it is a permanent feature of the fiber [11].

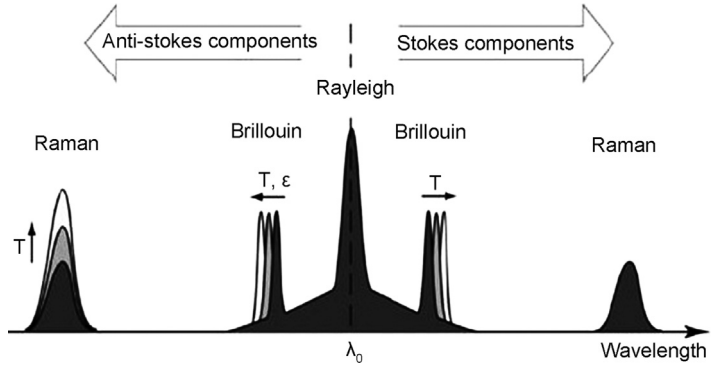

FIGURE 7.4 ***Scattering Effects in Fiber Optic Sensors Caused by Temperature or Strain.*** *Source: Inaudi et al. [10].*

A Rayleigh scattering distributed disturbance sensor (DDS) is based on OTDR with a coherent laser pulse along the optical fiber. The changes of Rayleigh backscattering amplitude represent a disturbance or a vibration along the fiber. Therefore, DDS is used mainly for event detection and does not provide quantitative measurements, such as the amplitude, frequency, and phase of the disturbance.

Using coherent optical time-domain reflectometry (COTDR) techniques, Rayleigh scattering based distributed acoustic sensing (DAS) has the advantages of providing very low noise levels, wide dynamics range, and excellent resolution. By suitable optical component configuration, the coherent length of a pulsed source is increased, and the coherence length larger than instrumental spatial resolution. This phenomenon results in extremely sensitivity of fiber propagation conditions caused by external vibrations, such as third-party intervention. Therefore, the DAS can provide third-party interference monitoring for pipelines.

The rapidly evolving DAS fiber optic sensor can be used for downhole monitoring and geophysical surveillance with advantages in acoustic sensing and imaging applications [12]–[15]. DAS can perform highly sensitive and fast quantitative measurements of acoustic perturbation (phase, frequency, and amplitude over wide dynamics range) of an optical field scattered along the optical fiber with fine spatial resolution. Some novel particular apparatuses and methods of DAS have addressed utilization under harsh conditions. Typically, the maximum measuring range of DAS is around 40–50 km, considering the attenuation of optical fiber and input coherent pulse power. There is a trade-off between spatial resolution and maximum measuring range. For a long measuring range, such as a pipeline, DAS can give 10 m resolution as a typical

value. While for many kilometers of fiber optic cable deployed in the oil and gas wells, there is a spatial resolution of 1 m. Compared with other distributed fiber optic sensors, the DAS has the advantage that acoustic fields digitally record up to tens of kilohertz for kilometers of measurement range, which is a benefit for fast respond sensor with high frequency.

Raman Scattering

Ramen scattering is the inelastic scattering of light and molecular vibration within fiber materials. This scattering process is commonly described as the scattering interaction between incident light and the optical phonon. The magnitude of molecular vibration and the scattering signal are influenced by ambient temperature. The fiber optic distributed temperature sensing (DTS) method using the Raman effect, as shown in Figure 7.5 was developed at the beginning of the 1980s.

Most temperature sensors that use Raman scattering compare the Stokes to anti-Stokes waves. The higher the temperature, the more anti-Stokes scattering there will be, which is expressed in the following equation:

$$\frac{P_{AS}}{P_S} = \left(\frac{\lambda_S}{\lambda_{AS}}\right)^4 e^{\frac{-h\Delta\nu}{KT}} \qquad [7.5]$$

where P_{AS} is the measured anti-Stokes power, P_S is the measured Stokes power, λ_S is the wavelength of the Stokes scattered light, and λ_{AS} is the wavelength of the anti-Stokes scattered light.

The temperature of distance along the optical fiber can be determined by following equation [16]:

$$T(z,t) = \frac{\gamma}{\ln\left(\frac{P_S(z,t)}{P_{AS}(z,t)}\right) + C(t) - \int_0^z \Delta\alpha(z')dz'} \qquad [7.6]$$

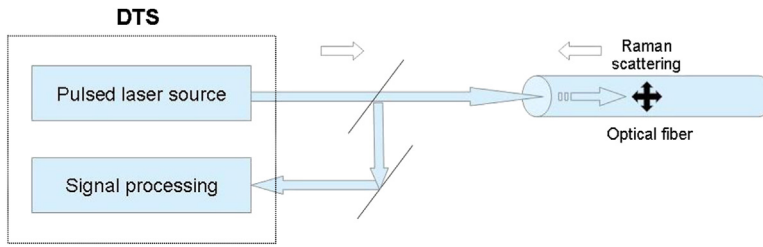

FIGURE 7.5 ***Raman-Based Distributed Temperature Sensing.*** (For color version of this figure, the reader is referred to the online version of this book.)

where T is the temperature; z is the distance, with $z = 0$ at the DTS instrument end; γ depends on the distribution of quantum states. In practice, γ is treated as constant for a given DTS instrument, although there are minor changes in γ as function of instrument temperature and power supply. $C(t)$ accounts for the differences in effective detector sensitivities for Raman signals. The term $\Delta\alpha(z)$ represents the differential attenuation of the Stokes and anti-Stokes scattering along the optical fiber. This parameter needs to be compensated for to obtain the correct temperature.

The principle of leak detection using DTS is that the thermal properties of product being carried in the pipeline (oil, gas, water) are significantly different from the environment surrounding the pipeline. The distributed optical fiber should be carefully designed based on the thermal properties of carried product.

A single DTS is capable of measurement up to 30 km of pipeline with spatial resolution of 1 m over the whole range. The limited distance is the reason that Raman scattering is the weakest of the three kinds of scattering lights. The temperature resolution of 0.1°C can be achieved. The detection range can be extended with help of a multiplexer, allowing measurement range up to 60 km. This kind of facility would be easy for onshore pipelines but may be trouble for long-distance subsea pipelines. An onshore LNG pipeline with a 57-km ethylene gas pipeline leak detection applications used DTS [17].

Today, commercial DTS is the most popular option for thousands downhole applications with typically 10-km sensing. However, the response time of DTS is typically on the order of several minutes, to build up enough signals, because of the weak intensity of Raman scattering. Therefore, DTS is suitable for measuring slowly varying temperatures.

Brillouin Scattering

As shown in Figure 7.6, this scattering is due to the interaction between light propagating in a fiber optic and acoustic phonon. Acoustic phonon is bulk vibration in glass at a speed of 6 km/s. These traveling waves change the local glass densities and index of refraction as they move down in the fiber, which act like a moving Bragg grating that backscatters Doppler-shifted light. If energy is lost by the acoustic photon to the glass, the Brillouin shifted light is lower in frequency than the input light and is called *Stokes light*. If the acoustic photon gains energy from the glass, its frequency is increased and the light is called *anti-Stokes light*. Brillouin inelastic scattering of light occurs as a result of refractive index fluctuations caused by acoustic waves resulting from thermally generated sound waves, and such thermal agitation is capable of scattering incident light

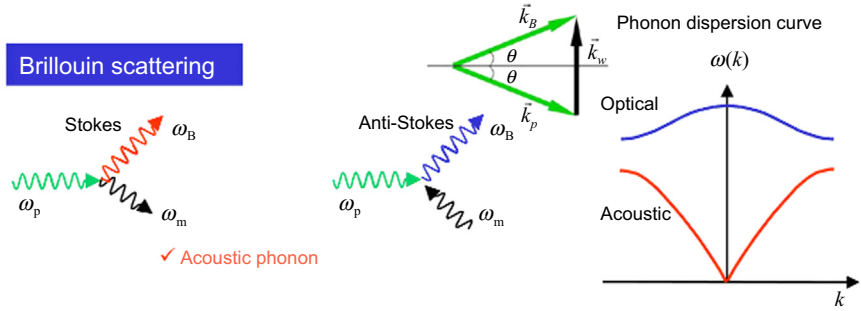

FIGURE 7.6 ***Brillouin Scattering and Phonon Dispersion.*** (For color version of this figure, the reader is referred to the online version of this book.)

with shifted frequencies. Similar to Raman scattering coming from light scattering off optical phonons, Brillouin scattering is scattering off acoustic phonon [10]. Normally, the scattering light is quite low, but light can propagate long distances without significant attenuation in optical fibers. This makes high Brillouin gain a noticeable and often undesirable effect in optical fibers communications. On the other hand, making use of the frequency shifts of Brillouin spectrum in optical fiber on strain or temperature, the fully distributed fiber optic sensor was developed. This kind of long-distance distributed strain sensor has been found applications in civil structures, environmental monitoring, the aerospace industry, and geotechnical engineering.

Figure 7.7 shows the spontaneous Brillouin backscattering in a fiber optic sensor. Brillouin scattering in optical fiber is the interaction of an electromagnetic field (photon) with density variation of the optical fiber. With high input laser intensity, the beating between the pump and Stokes waves creates a modified density change via the electrostriction effect, resulting in so-called the stimulated Brillouin scattering.

1. In spontaneous Brillouin scattering,
   - Scattering is from environmental (strain, thermal) induced acoustic wave.
   - Stokes and anti-Stokes components have comparable intensities.
2. In stimulated Brillouin scattering,
   - A strong pump wave can generate, via electrostriction, an acoustic wave.
   - Positive feedback-gain enhances the scattering intensity.
   - A strong scattering signal can build up from thermal noise.

As for frequency shift, in the acoustic mode, the direction of vibration of the two neighboring atoms is the same; that is, atoms oscillate with a small relative phase shift.

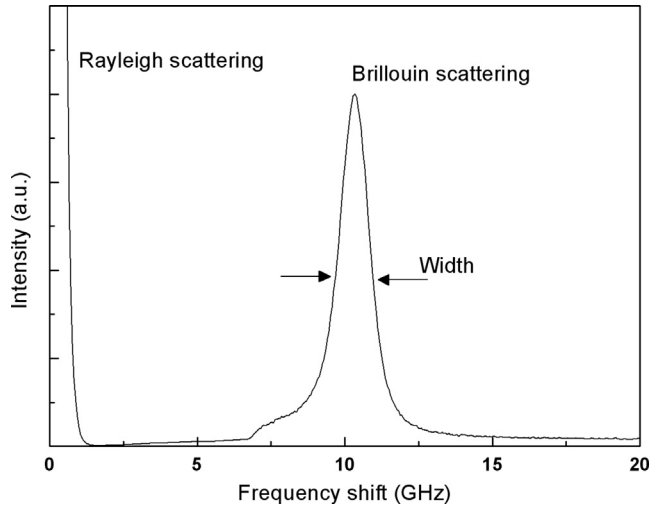

FIGURE 7.7 ***Brillouin Back-Scattering (Intensity, Frequency Shift, and Width) in a Fiber Optic Sensor.***

Energy conservation is expressed as follows:

$$\hbar\omega_{\mathrm{B}} = \hbar\omega_{\mathrm{p}} \pm \hbar\omega_{\mathrm{m}} \tag{7.7}$$

Momentum conservation is expressed as follows:

$$\overrightarrow{k}_{\mathrm{B}} = \overrightarrow{k}_{\mathrm{p}} \pm \overrightarrow{k}_{\mathrm{m}} \tag{7.8}$$

$$\omega_{\mathrm{m}} \ll \omega_{\mathrm{p}},\ \omega_{\mathrm{B}} \simeq \omega_{\mathrm{p}},\ \left|\overrightarrow{k}_{\mathrm{B}}\right| \simeq \left|\overrightarrow{k}_{\mathrm{p}}\right| \tag{7.9}$$

$$\begin{aligned} \overrightarrow{k}^{2}_{\mathrm{m}} &= \overrightarrow{k}^{2}_{\mathrm{p}} + \overrightarrow{k}^{2}_{\mathrm{B}} - 2\left|\overrightarrow{k}_{\mathrm{p}}\right|\left|\overrightarrow{k}_{\mathrm{B}}\right|\cos 2\,\theta \approx 2\,\overrightarrow{k}^{2}_{\mathrm{p}}(1 - \cos 2\,\theta) \\ &= 4k_{\mathrm{p}}^{2}\sin^{2}\theta \end{aligned} \tag{7.10}$$

$$\omega_{\mathrm{m}} = k_{\mathrm{m}}v_{\mathrm{sound}} = 2\omega_{\mathrm{p}}n_{\mathrm{p}}\frac{v_{\mathrm{sound}}}{c}\sin\theta \tag{7.11}$$

$$\frac{\omega_{\mathrm{m}}}{\omega_{\mathrm{p}}} \propto \frac{v_{\mathrm{sound}}}{c} \approx 10^{-5} \tag{7.12}$$

The type of dispersion relation of the acoustic mode determines several key features of the scattering light, such as a small relative frequency shift 10^{-5}. Here, n_{p} is the index of refraction, V_{sound} is the acoustic velocity. The

frequency shift for Brillouin scattering light (GHz) is much smaller than the frequency shift for Raman scattering (THz), as shown in Figure 7.4. The frequency shift of Brillouin scattering ω depends on the angle θ, it is at its highest scattering efficiency in the backward direction ($\theta = \pi$).

The intensity of the Brillouin scattering light can be shown as

$$I_{\mathrm{HH}} = I_0 V_{\mathrm{s}} \pi^2 kT \frac{\varepsilon^4}{\lambda_0^4} \frac{1}{\rho \nu_{\mathrm{L}}^2} \left| p_{44} + (p_{12} + p_{44}) \cos\theta \right|^2 \qquad [7.13]$$

where H refers to horizontal relative to a horizontal scattering plane. The incident light intensity is I_0, the scattering volume is V_{s}, kT is the thermal phonon energy, ρ is the mass density, ν_{L} is longitudinal sound velocity, and p_{ij} are the elastic-optic coefficients. Since the scattering arises from the fluctuations in the dielectric constant ε, this ultimately comes from strains produced by sound waves.

The line width of Brillouin scattering light is

$$\delta\omega = 4n2\Gamma \frac{\omega^2}{c^2} \sin^2\left(\frac{\theta}{2}\right) \qquad [7.14]$$

$$\Gamma = \frac{1}{\rho}\left[\frac{4}{3}\eta_{\mathrm{s}} + \eta_{\mathrm{b}} + \frac{\kappa}{C_{\mathrm{p}}}(\gamma - 1)\right] \qquad [7.15]$$

where Γ is the damping parameter, η_{s} is the shear viscosity coefficient, η_{b} is the bulk viscosity coefficient, and κ is the thermal conductivity.

There are two kinds of Brillouin-based fiber optic sensosr [18]. Brillouin optical time-domain analysis (BOTDA) is attributed to the pump and probe wave interaction induced Brillouin amplification over the entire sensing length; while for Brillouin optical time-domain reflectometry (BOTDR), as shown in Figure 7.8, only one pump pulse is used and BOTDR works in the spontaneous Brillouin scattering regime. Stimulated Brillouin systems are not as commonly used as the spontaneous systems. However, stimulated Brillouin scattering (SBS) enhances the Brillouin scattering in BOTDA with an intense signal and better spatial resolution (which means longer sensor length) compared with a spontaneous scattering BOTDR. Fiber optic sensors based on Brillouin scattering have proven to be a powerful tool for distributed measurements of strain and temperature. Typical temperature resolution is in the area of 0.1 to 3°C, and strain resolution in the range of 20 με, both with local resolution of 1 to 3 m; however, the absolute ranges largely depend on the

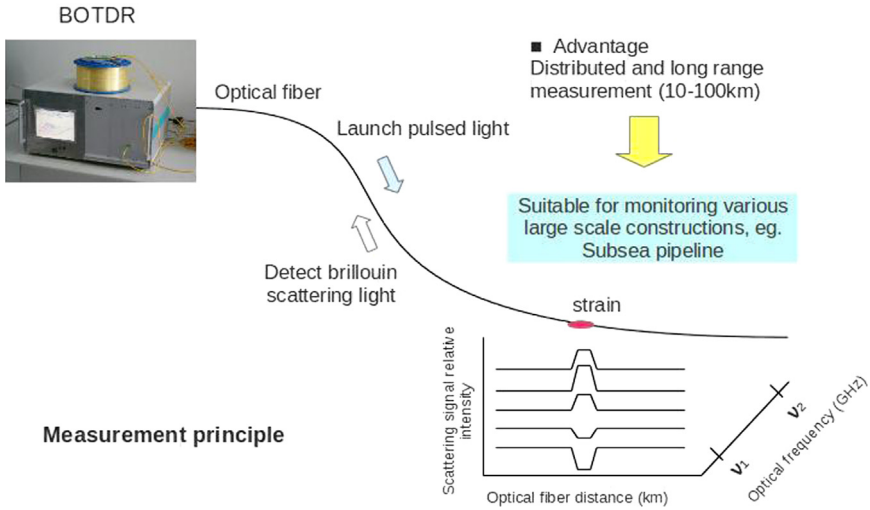

FIGURE 7.8 ***Fibre Optic using Brillouin Optical Time-Domain Reflectometry.*** (For color version of this figure, the reader is referred to the online version of this book.)

optical cable construction and monitoring length. Maximum sensor length for single-mode fiber based on Brillouin backscattering is typically in the range of 30–100 km, depending on the optical power loss (i.e., splices and fiber construction). The spatial resolution and temperature (strain) resolution are compromised for long sensing length. The 100-km sensing range is made possible without need of inline amplifiers inside the sensing length; for longer distances (>100 km), erbium-doped fiber amplifiers (EDFAs) can be utilized to improve frequency-division multiplexing based BOTDA, achieving spatial resolutions of 2 m and temperature resolutions of 1°C [19]. The typical measurement scale of strain and temperature is -3%-~+4% and –200–~+800°C, respectively, depending on optical cable materials. However, the reliable breaking strain of the fibers is on the order of 1%.

The basis of Brillouin scattering diagnostic systems lies in three parameters of the scattering light: the frequency shift, the intensity, and the line width. In many practical cases, the frequency shift would be considered as the principle measuring parameter, due to its relative higher resolution. The Brillouin frequency varies as a function of strain and temperature, where ν_{B0} is the Brillouin frequency at zero degrees Celsius and zero strain, as shown in Eq. [7.16]. For strain measurement, temperature is treated as a constant. Such an assumption may not be applicable during field operation; hence, different approaches of simultaneous

temperature and strain measurement have been developed using the intensity, line width, and multi-Brillouin peak features in addition to the Brillouin peak frequency shift.

$$\nu_{\mathrm{B}} = \nu_{\mathrm{B0}} + \frac{\partial \nu}{\partial T} T + \frac{\partial \nu}{\partial \varepsilon} \varepsilon \qquad [7.16]$$

Three measurable quantities can be used to simultaneously measure the temperature and strain using BOTDR or BOTDA:

- Brillouin scattering intensity and frequency shift.
- Brillouin scattering intensity and line width.
- Brillouin scattering line width and frequency shift.

Brillouin scattering has been used in many different systems to measure temperature and strain, including systems that use Raman scattering as well. Since Raman scattering does not depend on strain, by measuring the Brillouin scattering's temperature- and strain-dependent signal, then subtracting out the temperature calculated by the Raman scattering signal, both the temperature and strain can be calculated. Alternatively, optical cable has tight and loose optical fiber for Brillouin scattering, which can be used for strain and temperature measurements, respectively.

The distributed fiber optic system basically consists of two components: host controller and fiber optic sensing cable. To detect the acoustic vibration, temperature, and strain change, the fiber optic sensing cable should be clamped appropriately to the pipeline with regard to different work conditions. Physical contact between the leaking fluid and strain matrix is essential.

For subsea pipeline monitor applications, FBG sensors can be embedded in metal joints for monitoring the key components. DTS and BOTDR or BOTDA can be used for the leak detection, since loss of transported medium may result in a temperature change at the optical cable location on the outside of the pipeline. BOTDR or BOTDA can be used for strain measurements during the subsea pipeline installation and operation, while BOTDA is considered in the longer-distance pipeline applications. However, BOTDR could be a better choice for the inspection of RTP in the installation and operating conditions, since one of the major benefits of spontaneous Brillouin scattering over stimulated Brillouin scattering is that access to only one end of the fiber is needed for the laser signal and data acquisition. Access to both ends of the sensing fiber allows the sensing fiber to sense the entire pipeline, even if it breaks somewhere along the path.

3. TYPES OF SENSING FIBER OPTICS

Telecommunication Optical Fiber

There are four main types of normal fiber optic cables: multimode, single mode, polarization maintaining, and graded index. The major differences are in the density of the fibers in the cross sections, leading to different propagation properties of those fibers. Figure 7.9 shows these four types of fibers, along with their cross sections as a function of their index of refraction. Both the multimode and single-mode fibers are step index fibers, where there is an abrupt change from the core to the cladding. However, the multimode fiber's core is larger than that of the single-mode fiber. This configuration allows the propagation of more light modes with more wavelengths. Polarization maintaining fiber is a single-mode, step index fiber. It has stress rods in the fiber, which separate the propagation paths in the core into "fast" and "slow" axes. Each axis propagates only linearly polarized light and can be viewed as two separate paths in the same optical fiber.

Photonic Crystal Fiber

Photonic crystal fiber (PCF) is a three-dimensional FBG, a new class of optical fiber consisting of small air holes in fiber glass, as shown in Figure 7.10. This allows it to confine light in hollow cores or with confinement characteristics not possible in conventional optical fiber, especially in nonlinear optics, high-power delivery. The simultaneous measurement of temperature

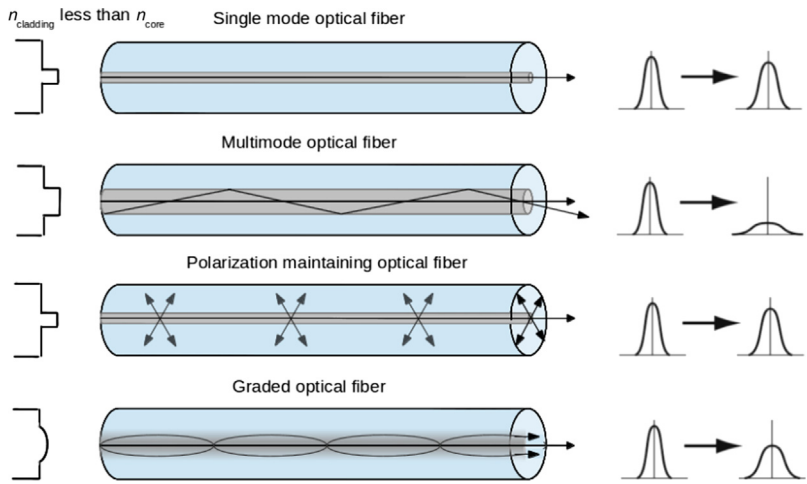

FIGURE 7.9 ***Profiles of Four Types of Fibers and Dispersions of Input Signal.*** (For color version of this figure, the reader is referred to the online version of this book.)

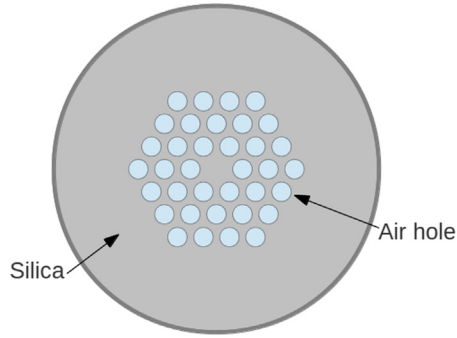

FIGURE 7.10 ***Optical Microscopy Image of Photonic Crystal Fiber.*** (For color version of this figure, the reader is referred to the online version of this book.)

and strain using of PCF in Brillouin scattering sensing can be realized by the frequency shift on different scattering signals [20]. The disadvantage of PCF is its extremely high cost.

Polymer Optical Fiber

Polymer optical fiber (POF) is a special optical fiber made out of polymer. A variety of optical polymers are used in the fabrication of POFs, including polymethyl-methacrylate (PMMA), amorphous fluorinated polymer (CYTOP), polystyrene (PS), and polycarbonate (PC). POF has significant advantages for some sensing applications, including high elastic strain limits, high fracture toughness, high flexibility in bending, and high sensitivity to strain. It is noted that the high elastic strain limits (10–15%) could be a primary advantage in RTP monitoring, compared to 6% for traditional small-diameter silica optical fiber [21]. The actual reliability is lower than this value due to the presence of surface flaws on silica optical fiber. POF sensor applications were found in harsh civil environments, using its unique mechanical properties [22]. However, the high attenuation ($\sim$200 dB/km) of POF limits its application for long-distance sensing.

4. APPLICATION OF FIBER OPTIC MONITORING ON SUBSEA PIPELINES

Resistance to corrosive agents such as wet carbon dioxide and sodium chloride is one of the primary benefits of RTP to reduce operating cost. However, the mechanical construction and installation damage of RTP is a common and reoccurring stated failure cause, compared to rigid steel pipeline. Installation-related deficiencies for RTP include poor underground

pipe support, inappropriate anchoring, pipeline impacts, and improper backfilling practices. Those conditions should be detected and identified in preliminary inspection; otherwise, the damage of RTP during operation may continue much longer to develop and cause a failure. Meanwhile, the operating condition of the RTP and the third party activities are crucial monitoring issues during the over 20 years lifetime of the whole pipe system. Therefore, RTP integrity management necessarily is developed to meet the requirements. For the continuous, long subsea pipelines, the distributed sensor using fiber optics is a powerful and better tool for the pipeline structural and installation process than the traditional point sensor.

Objectives

The objectives of fiber optic monitoring in RTP technique include

- Development of fiber optic cable hardware for installation and operation.
- Development of monitoring software.
- Structural design, construction processing, calibration, environment simulation performance test of fiber optic sensor cable.
- Layout of integrated fiber optic cable and related construction processing.
- Design and construction processing of fiber optic cable pipe connector.
- Repair or construction of underwater damaged fiber optic cable.

Special requirements for the design and construction of fiber optic monitoring used in subsea engineering are critical for success. State-of-the-art and reliable fiber optic sensor technology should be under discussion to generate an optimum inspection solution. The primary technical challenges include fiber optic layout processing and high strain measurement of flexible pipe during the installation. The potentially most difficult engineering issue is the fiber optic survival during construction (passing over rollers on the laying barge).

Choice of Optical Fiber

Standard cheap silica optical fiber (such as ITU-T G.652 single-mode fiber) can provide an economic and effective solution for long distance monitoring. G.652 is optimized in the 1310-nm range. Low water peak fiber has been specifically processed to reduce the water peak at 1400 nm to allow use in that range. The attenuation parameter of G.652 fiber typically is 0.2 dB/km at 1550 nm, and the polarization mode dispersion parameter is less than 0.1 ps/km.

Geometric Structure of Optical Cable

Figure 7.11 shows an optical cable designed for fiber optic monitoring in pipeline applications. The armored cable contains loose and tight fiber optic tubes for temperature and strain sensing, respectively. The tubes are filled with a water-resistant filling compound. A steel wire located in the center of core as a metallic strength member is covered with polyethylene (PE) when the fiber number is high. An aluminum polyethylene laminate (APL) is applied around the cable core, which is filled with the filling compound to protect it from water ingress. After corrugated and braided steel tape armor and Kevlar are applied, the cable can be completed with a PE outer sheath. This kind of optical cable has good mechanical performance and the flexibility to suffer high strain during RTP installation; it also has good resistance to harsh environments and good compatibility with the outer PE materials of RTP during integration. Additionally, copper conductor concentrically outside of the optical cable can be used as to deliver power for amplifying long–distance optical signal.

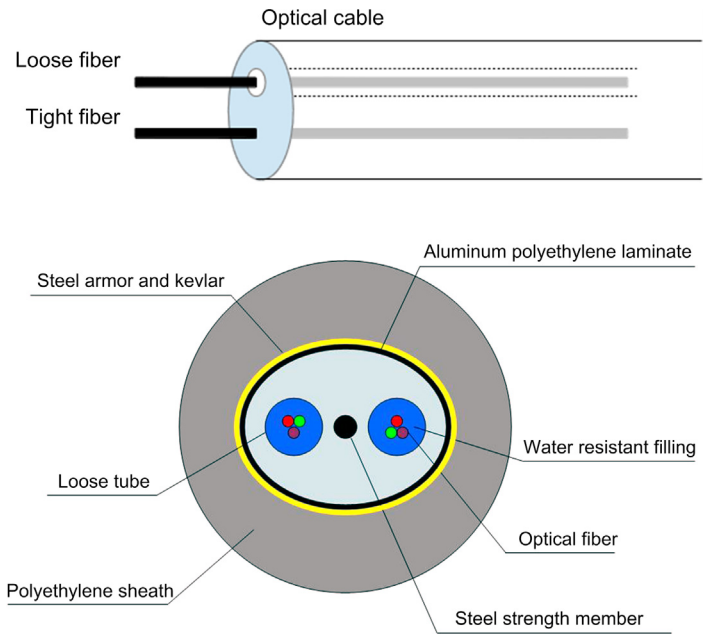

FIGURE 7.11 ***Loose and Tight Fiber Optic Sensors.*** (For color version of this figure, the reader is referred to the online version of this book.)

Solutions to Pipe Joint Crossing

Two possible solutions for fiber optic assembling in the pipe joint crossing are fiber optic connectors and fiber optic fusion. The typical insertion loss of fiber optic connectors is 0.2 dB, and the splice loss of fiber optic fusion is 0.02 dB. The fiber optic connector is easy handled and of low cost but should be covered with water-blocking materials in field applications. The fiber optic fusion splice is another option, with lower optical loss. However, optical loss per splice and connectors are all higher than the optical cable's loss per length and splices, and connectors should be limited as much as possible to long-distance pipeline monitoring.

Fiber Optic Layout in RTP

A good fiber optic layout can help to get three-dimensional temperature-strain pipe monitoring information. There are two possible ways of integrating a fiber optic system. One is optical cable binding or bonding on the outer PE surface of the RTP, as shown in Figure 7.12. This fiber optic layout can be used for DTS temperature monitoring for gas and oil leaks but is limited in strain or DAS acoustic sensing.

Another possible way is put the fiber optic integration inside the outer PE of the RTP. This method does not deteriorate the mechanical performance of the RTP for protecting the optical cable and monitoring the well's real strain variation and acoustic field for fluid dynamics flow. Figure 7.13 illustrates the two kinds of fiber optic distribution.

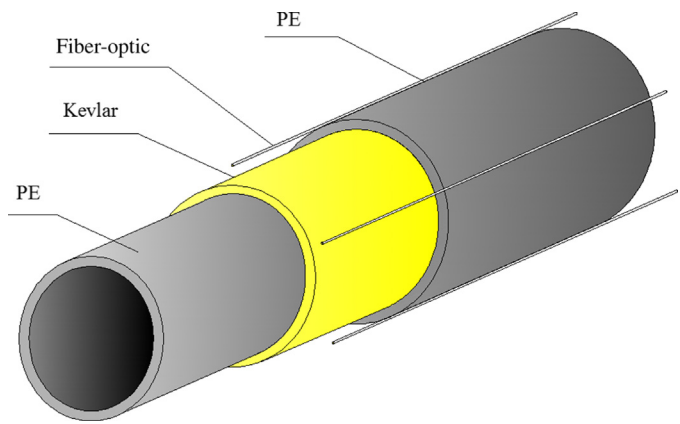

FIGURE 7.12 ***Fiber Optic Integration on the Surface of RTP.*** (For color version of this figure, the reader is referred to the online version of this book.)

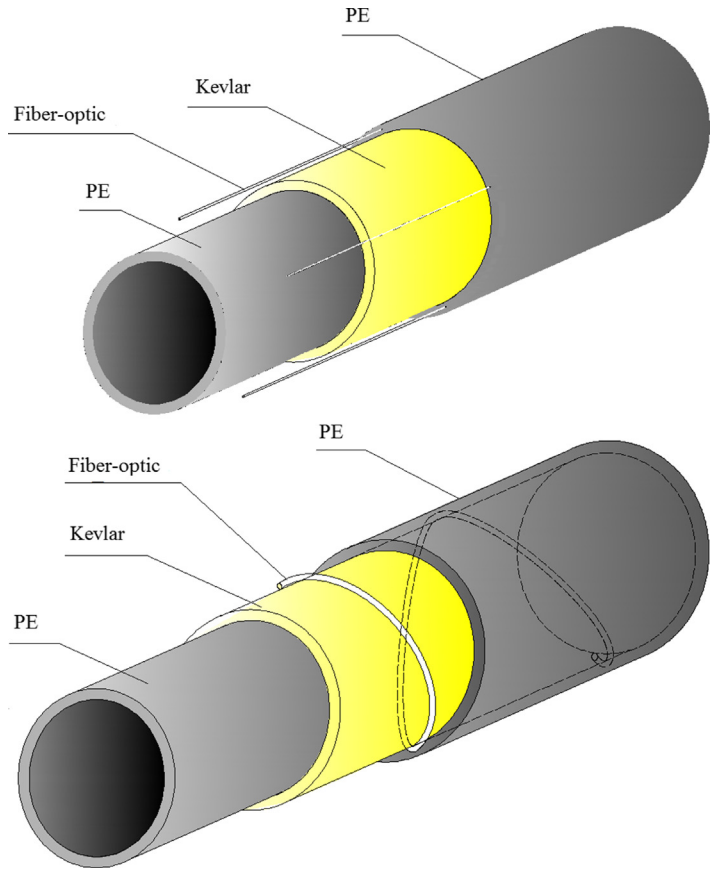

FIGURE 7.13 ***Fiber Optic Integration Inside RTP.*** (For color version of this figure, the reader is referred to the online version of this book.)

Fiber Survival Issue

Since the fiber optic monitoring system in RTP is based on the signal from the optical fiber, the most important component of the system is the optical fiber. Problems due to other optical components can be solved outside the pipeline. Once the optical fiber is set into the pipeline, it cannot be changed; fiber optic survival during the operation of the pipeline is also a big issue. During pipeline operation, the optical fiber has to survive both thermal extension and strain without modification of the scattering parameters. Many of the fiber survival issues can be solved by placing the sensing fiber in a steel capillary tube; however, this introduces new issues associated with strain insensitivity.

Table 7.1 Survivable Temperature Ranges of Different Coatings

	Temperature limit [°C]	Cost [US $/m]
Standard SMF	200	0.45
Polyimide coated SMF	300	5.50
Aluminum coated SMF	400	22.0
Copper alloy coated SMF	700	22.0
Gold coated SMF	700	35.0

The coating of the fiber also has to be chosen carefully, since the optical fiber must survive several thermal cycles in the operation or integration process. Different coatings can be applied to the fiber, in which the fibers are grouped into two categories: standard acrylate-coated fibers and specially coated fibers. Normal fibers could encounter problems at high temperatures. Table 7.1 summarizes the survivable temperature ranges of different coatings. The acrylate coating is vaporized in 200°C, leaving a bare fiber. A bare fiber is much riskier than a coated fiber; if the fiber breaks, the sensor is rendered useless.

Table 7.1 demonstrates that the integrity of standard single-mode fiber should be considered, since it is the cheapest one for the pipelines with lengths usually over several tens of kilometers. In the operating condition of a flexible RTP, the normal operating strains are up to around 2–3%. A normal fiber at room temperature can take up to 2% strain without breaking, although up to 6% strain in theory. The obvious trade-off between fiber safety and accuracy of the strain measurement has to be considered in the whole system design.

As shown in Section 4, the optical cable can be placed in a capillary tube, which straightens before the fiber experiences strain. The capillary tube can be spiraled in the flexible RTP pipe, as shown in Figure 7.13. The fiber can also be spiraled in the capillary tube, adding up to 2% of the length for the fiber compared to the length of the capillary tube. Using both spiraling techniques, the fiber can actually be 5% longer than the length of the flexible RTP pipe. However, if the fiber is loose in the flexible RTP, the strain measurements are limited.

REFERENCES

[1] Kao KC, Hockham GA. Dielectric fibre surface waveguides for optical frequencies. Proc IEE 1966;113:1151–8.
[2] Keck DB, Schultz PC, Zimar FW. Method of forming optical waveguids fibers. U.S. patent 3737292.
[3] Kapron FP, Keck DB, Maurer RD. Radiation losses in glass optical waveguides. Appl Phys Lett 1970;17:423.

[4] Strong A, Sanderson N, Lees G, Hartog A, Twohig R, Kader K, Hilton G, Mullens S, Khlybov A. An integrated system for pipeline condition monitoring and pig tracking. Pipeline Pigging and Integrity Management Conference; February 2009.
[5] Varasi M, Vannucci A, Singorazzi M, Ferraro P, Imparato S, Voto C, et al. Integrated optical instrumentation for the diagnostics of parts by embedded or surface attached optical sensors. U.S. patent 5493390.
[6] Bunphy J, Meltz G, Varasi M, Vannucci A, Singorazzi M, Ferraro P, et al. Embedded optical sensor capable of strain and temperature measurement using a single diffraction grating. U.S. patent 5399854.
[7] Soller B. High resolution optical frequency domain reflectometry for characterization of components and assemblies. Opt Exp 2005;13:666–74.
[8] Barnoski MK, Jensen SM. Fiber waveguides: A novel technique for investigating attenuation characteristics. Appl Opt 1976;15:2112–5.
[9] Culshaw B, Kersey A. Fiber-optic sensing: A historical perspective. J Lightwave Technol 2008;26(9):1064–78.
[10] Inaudi D, Glisic B, Figini A, Walder R. Pipeline leakage detection and localization using distributed fiber optic sensing. RIO Pipeline Conference; October 2007.
[11] Maier RJ, et al. Distributed sensing using rayleigh scatter in polarization-maintaining fibres for transverse load sensing. Measures Sci Technol 2010;21:094019.
[12] Farhadiroushan M, Parker T, Shatalin S. Method and apparatus for optical sensing; Patent No. PCT/GB2010/050889.
[13] Molenaar MM, Hill DJ, Webster P, Fidan E, Birch B. First downhole application of distributed acoustic sensing (DAS) for hydraulic fracture monitoring and diagnostics. SPE 140561 SPE Drilling & Completion, Society of Petroleum Engineers 2012; 27(1):32–8.
[14] Mestayer J, Cox B, Wills P, Kiyashchenko D, Lopez J, Costello M, et al. Field trials of distributed acoustic sensing for geophysical monitoring; 2011. SEG 2011-4253 SEG Annual Meeting, September 18 - 23, 2011, San Antonio, Texas.
[15] Shahril SSB, Rahim PA, Ishak MF, Kasim MH, Ayob A. Offshore first fiber optic enable coil tubing application for complex milling, cementing and perforation operation—Malay Basin historical milestone; 2012. SPE 159454 Abu Dhabi International Petroleum Conference and Exhibition, 11-14 November 2012, Abu Dhabi, UAE.
[16] Van de Giesen N, Steele-Dunne SC, Jansen J, Hoes O, Hausner MB, Tyler S, et al. Double-ended calibration of fiber-optic raman spectra distributed temperature sensing data. Sensors 2012;12:5471–85.
[17] Tanimola F, Hill D. Distributed fibre optic sensors for pipeline protection. J Nat Gas Sci Eng 2009;1:134–43.
[18] Bao X, Chen L. Recent progress in Brillouin scattering based fiber sensors. Sensors 2011;11:4152–87.
[19] Bao X, Zou L, Yu Q, Chen L. Development and application of the distributed temperature and strain sensors based on Brillouin scattering, sensors. Proc IEEE 2004;3:1210–3.
[20] Zou L, Bao X, Afshar S VI Chen. Dependence of the Brillouin frequency shift on strain and temperature in a photonic crystal fiber. Opt Lett 2004;29(13):1485–7.
[21] Kurkjian CR, Matthewson MJ. Mechanical strength and reliability of glass fibers. In: Mendez A, Morse TF, editors. Specialty optical fibers handbook. Burlington, MA: Elsevier Academic Press; 2007. pp. 735–81.
[22] Peters K. Polymer optical fiber sensors—A review. Smart Mater Structures 2011;20. 013002.

CHAPTER 8

Risk Analysis for Subsea Pipelines

Contents

1. Introduction 171
   - General 171
   - Risk Analysis Objectives 171
   - Risk Analysis Concepts 171
   - Risk-Based Inspection and Integrity Management 172
2. Acceptance Criteria 173
   - General 173
   - Risk to Individuals 174
   - Societal Risk 174
   - Environmental Risk 174
   - Financial Risks 175
3. Identification of Initiating Events 176
4. Cause Analysis 176
   - General 176
   - Fault Tree Analysis 177
   - Event Tree Analysis 177
5. Probability of Initiating Events 178
   - General 178
   - HOE Frequency 178
6. Causes of Risk 180
   - General 180
   - First Party Individual Risk 180
   - Societal, Environmental, and Material Loss Risk 181
7. Failure Probability Estimation Based on Qualitative Review and Databases 182
   - Generic Hazard and Pipeline Damage List 182
   - Example of Risk Review 183
8. Failure Probability Estimation Based on Structural Reliability Methods 185
   - General 185
   - Simplified Calculations of Reliability Index and Failure Probability 186
   - Strength and Resistance Model 187
   - Evaluation of Strength Uncertainties 187
9. Consequence Analysis 188
   - Consequence Modeling 188
     - *Discharge* *189*
     - *Dispersion of Gas* *189*
     - *Dispersion of Liquid* *189*
     - *Ignition* *189*
     - *Combustion* *190*

Subsea Pipeline Integrity and Risk Management
ISBN 978-0-12-394432-0
http://dx.doi.org/10.1016/B978-0-12-394432-0.00008-1

Damage and Loss 190
Uncertainty 191
Estimation of Failure Consequence 191
10. Example 1. Risk Analysis for a Subsea Gas Pipeline 193
General 193
Gas Releases 193
Representative Hole Sizes 193
Discharge 194
Subsea Plume 194
Airborne Dispersion 194
Effect of Water Depth 195
Stability 195
Wind Speeds 195
Hazard Ranges 195
Individual Risk 196
Acceptance Criteria 196
Cause Analysis 196
Assumptions 196
Consequence Analysis 197
Risk Estimation 197
Societal Risk 197
Acceptance Criteria 197
Initiating Incidents 197
Merchant Vessels 197
Construction Vessels 198
Random Failures 198
Cause and Consequence Analysis 198
Risk Estimation 199
Environmental Risk 199
Risk of Material Loss 199
Initiating Incidents 199
Consequence Analysis 199
Risk Estimation 200
11. Example 2. Dropped Object Risk Analysis 200
General 200
Acceptable Risk Levels 200
Quantitative Cause Analysis 201
Probability Cones 201
Probability of Pipeline or Spool Hit 202
Energy Absorbed by Steel Pipe 202
Basic Data and Assumptions for Risk Analysis 203
Results 204
Probabilities 204
Energy Absorbed by Steel Pipe 205
Consequence Analysis 205

12. Example 3. Use of RBIM to Reduce Operation Costs 206
General 206
Inspection Frequency for Corroded Pipelines 207
Examples of Prioritizing Tasks 210
References 211

1. INTRODUCTION

General

In recent years, risk analysis has become increasingly recognized as an effective tool for the management of safety, environmental pollution, and financial risks in the pipeline industry. The purpose of this chapter is to apply risk-based inspection planning methodologies to pipeline systems, to develop a set of methods and tools for the estimation of risk using a structural reliability approach and incidental databases, and to illustrate our risk-based inspection and management approach through a few examples.

After outlining the constituent steps of a complete risk analysis methodology, this chapter gives detailed information about each step of the methodology, so that a complete risk analysis can be achieved [1]. Willcocks and Bai [2] give detailed guidance on evaluation of failure frequency, consequence, risk, and risk-based inspection and integrity management of pipeline systems.

Risk Analysis Objectives

The objectives of risk analysis are

- To identify and assess, in terms of likelihood and consequence, all reasonably expected hazards to health, safety, and the environment in the design, construction, and installation of a pipeline.
- To ensure adherence to the appropriate international, national, and organizational acceptance criteria.

Risk Analysis Concepts

Cause analysis follows completion of an investigation of initiating events; the final stage is an analysis of consequences. An outline of the methodology is given in Figure 8.1.

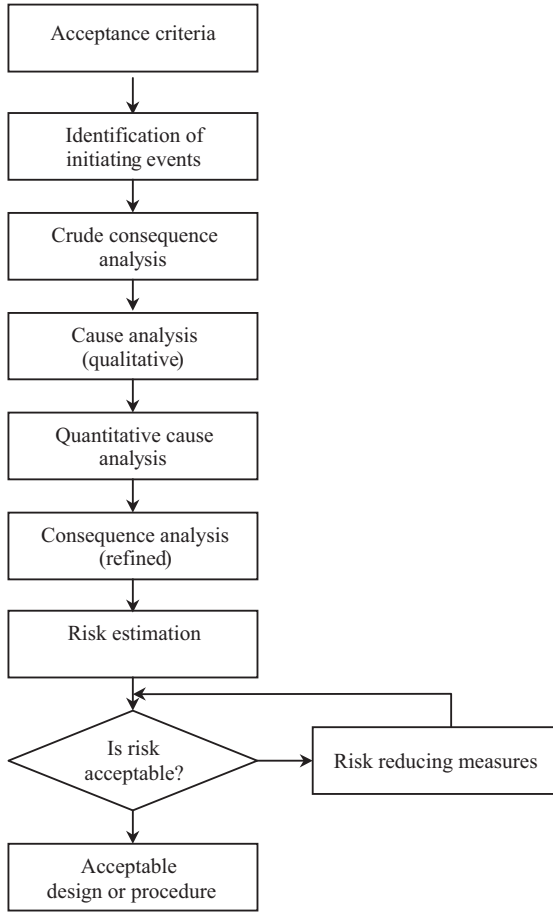

FIGURE 8.1 ***Risk Analysis Methodology.***

Risk-Based Inspection and Integrity Management

Risk-based inspection and integrity management (RBIM) is a means of focusing and optimizing the use of resources to "high-risk" areas to minimize costs and ensure effective and efficient asset management by ensuring the required confidence in the assets' integrity and availability. It is employed in pipeline systems due to the high costs for a pipeline modeling, inspection, and maintenance but credible risks of failure.

RBIM is essentially the determination of required structural reliability analysis (SRA), inspections (type, frequency, time, and extent), maintenance tasks (e.g., repair to pipeline intervention, coatings, corrosion inhibitors) to resttain the risk of failure in credible or potentially high-risk modes to an

"acceptable level." This is accomplished through the establishment of failure patterns and failure rates, which also identifies failure warnings.

These factors define the failure risks. Depending on the level of risk of failure for each mode and pattern of failure, the required analysis, inspections, maintenance, and repair tasks are selected. For example, a review of historical failure databases, such as PARLOC2001, indicates that the major failure modes are internal corrosion and external impact. Therefore, the main efforts (in terms of design, structural modeling, inspections, etc.) should focus on these failure modes [3, 4].

2. ACCEPTANCE CRITERIA

General

The acceptance criteria are distinctive, normative formulations against which the risk estimation can be compared. Most regulatory bodies give acceptance criteria either qualitatively or quantitatively. The NPD (The Norwegian Petroleum Directorate) regulation states the following:

- To avoid or withstand accidental events, the operator shall define safety objectives to manage the activities.
- The operator shall define acceptance criteria before risk analysis is carried out.
- Risk analysis shall be carried out to identify the accidental events that may occur in the activities and the consequences of such accidental events for people, for the environment, and for assets and financial interest.
- Probability reducing measures shall, to the extent possible, be given priority over consequence reducing measures.
- Subsea pipeline systems shall be, to a reasonable extent, protected to prevent mechanical damage to the pipeline due to other activities along the route, including fishing and shipping activities.

Individual corporations may choose to implement internal acceptance criteria. These acceptance criteria may be based on the relative cost between implementing a risk-reducing measure and the potential loss. Also, many projects specify a pipeline availability requirement. Thus, total losses must be such to ensure required availability.

If the risk estimation arrived at is not within the acceptable risk, then it is necessary to implement alterations. This new system should be analyzed and compared with the risk acceptance to ensure adequate risk levels. This is an iterative process, which eventually leads to a system or design that is acceptable.

Risk to Individuals

The FAR (fatal accident rate) associated with postcommissioning activities (the installation and retrieval of pigging equipment) has been evaluated. The FAR acceptance criteria are defined to be 10 fatalities per 10^8 working hours. The maximum FAR (number of fatal accidents per 10^8 hours worked) for the operational phase should be ≤ 10. The maximum FAR for the installation phase should be ≤ 20.

Societal Risk

The society risk is third party (societal) risks posed to passing fishing vessels and merchant shipping. Acceptance of third party risks posed by the pipeline should be on the basis of the F-N curves shown in Figure 8.2.

Environmental Risk

All incidents considered to initiate, in the assessment, individual and societal risks during the operational phase are considered to initiate possible

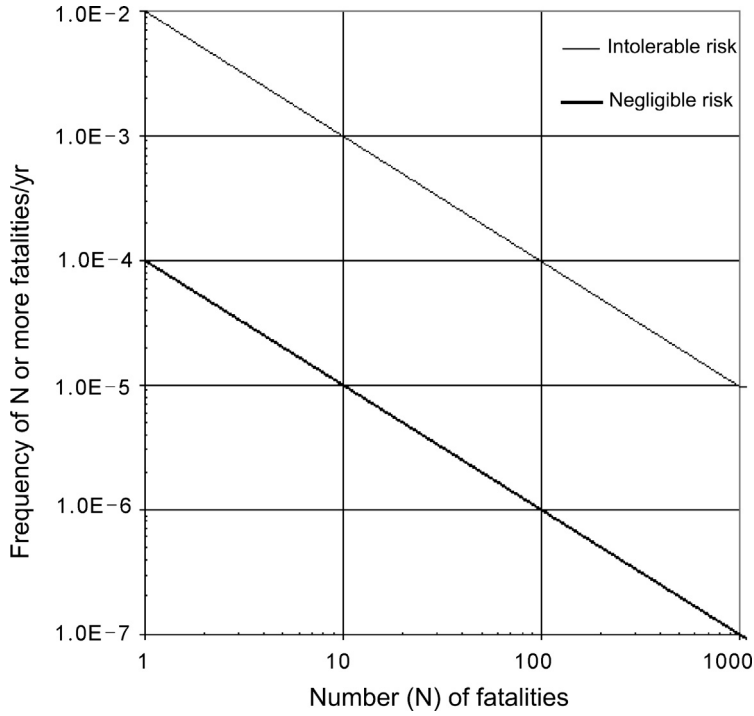

FIGURE 8.2 *Societal Risk Acceptance Criteria.*

Table 8.1 Acceptance Criteria for Environmental Risk

Category	Recovery Period	Operational Phase Probability Per Year	Installation Phase Probability Per Operation
1	<1 year	$<1 \times 10^{-2}$	$<1 \times 10^{-3}$
2	<3 years	$<2.5 \times 10^{-3}$	$<2.5 \times 10^{-4}$
3	<10 years	$< \times 10^{-3}$	$<1 \times 10^{-4}$
4	>10 years	$< \times 10^{-4}$	$<5 \times 10^{-5}$

environmental risks. Loss of containment incidents during operation of pipeline have minor local environmental effects. As shown in Table 8.1, the environmental consequences of loss of containment incidents are classified as being Category 1; that is, the recovery period will be less than 1 year.

In addition, any incidents having the potential to result in the release of corrosion inhibitors during commissioning of the pipeline are considered to initiate possible environmental risks. Acceptance of the environmental risks associated with construction and operation is normally based on the operator's criteria, which is established based on economic and political considerations.

Causes of loss of containment incidents considered during the operational phase are

- External impact (sinking vessels, dropped objects, trawl impact).
- Corrosion (external and internal).
- Material defect.

Financial Risks

All incidents considered as initiating in the assessment of individual and societal risks are considered to be initiating for the purposes of determining the risks of material loss. In addition, any incidents occurring during construction and installation and having the potential to result in damage to or delay in the construction of the pipeline are considered to initiatie risks of material loss. The costs of incidents have been considered as being made up from

- Notional cost of fatalities.
- Cost of repair.
- Cost of deferred production.

The expected (average) numbers of loss of containment incidents and associated fatalities have been used to derive an expected annual cost incorporating each of the quantities just given. The acceptability of risks of material loss are determined using cost-benefit analysis. Risk reduction

measures should be implemented if the cost-benefit analysis shows a net benefit over the full life cycle.

To summarize, the acceptance criteria is based on a cost-benefit evaluation, where the expected benefits must be much greater than the costs of implementing and operating with the risk reducing measure; that is,

$$C_{IMPL} + C_{OP} \ll C_{RED} \quad [8.1]$$

where

C_{IMPL} = cost of implementing the risk reducing measure
C_{OP} = net present value of operational cost related to the measure
C_{RED} = net present value of expected benefits as a result of the risk reducing measure

3. IDENTIFICATION OF INITIATING EVENTS

Identification of initial events is regularly referred to as *hazard identification* in the offshore industry. The main techniques that exist are

- **Checklists:** Review of possible accidents using lists developed by experts.
- **Accident and failure statistics:** Similar to checklists but derived from failure events.
- **Hazard and operability study:** Used to detect sequences of failures and conditions that may exist to cause an initiating event.
- **Comparison with detailed studies:** Use of studies that broadly match the situation being studied.

After the completion of this investigation, it is necessary to examine the hazards and identify the significant hazards, which need to be analyzed further.

4. CAUSE ANALYSIS

General

There are two purposes of cause analysis: First, it is necessary for the identification of the combinations of events that may initiate risky events. Second, the probability of the initiating event occurring must be assessed. The first purpose requires a qualitative assessment of the system and the latter requires a quantitative one.

The qualitative analyses aim to; detect all causes and conditions that could result in an initiating event and develop the foundation for possible

quantitative analysis. The aim of the quantitative analyses is to determine the probability value for the occurrence of an initiating event. The analysis tools available are stated next. This chapter discusses only the first two approaches.

- Fault tree analysis.
- Event tree analysis.
- Synthesis models.
- Monte Carlo simulations.
- Equipment failure rate databases.

Fault Tree Analysis

The fault tree is a graphical diagram of logical connections between events and conditions that must be present if an initiating event should occur. A fault tree for a system can be regarded as a model showing how the system may fail or a model showing the system in an unwanted situation. The qualitative analysis maps systematically all possible combinations of causes for a defined unwanted event in the system. If available data can be supplied for the frequencies of the different failure causes, quantitative analysis may be performed. The quantitative analysis may give numerical estimates of the time between the occurrence of each unwanted event, the probability of the event, and the like.

The fault tree analysis (FTA) has three major phases:

1. **Construction of the fault tree:** This is the identification of combinations of failures and circumstances that may cause failures or accidents to occur.
2. **Evaluation of the fault tree:** This is the identification of particular sets of causes that separately causes system failure or accident.
3. **Quantification of the fault tree:** This is overall failure probability assessment from the sets of causes as just defined.

Event Tree Analysis

An event tree is a visual model for description of possible event chains that may develop from a hazardous situation. Top events are defined and associated probabilities of occurrence are estimated. Possible outcomes from the event are determined by a list of questions, where each question is answered yes or no. The questions often correspond to safety barriers in a system, such as "Isolation failed?" and the method reflects the designers' way of thinking. The events are partitioned for each question, and a probability is given for each branching point. The end events (terminal events) can be gathered in groups according to their consequence to give a risk picture.

5. PROBABILITY OF INITIATING EVENTS

General

The methods just stated gives a methodology, which can be applied to any scenario such that it is possible to determine the conditions that will result in an initiating event. However, it is necessary to determine how the probability value is to be assigned, when using fault tree analysis and event tree analysis (ETA).

Reliability analysis is used as the main method of determining the probability of failure caused by the physical aspects of a pipeline: corrosion, trawling impact, vortex-induced vibrations, and so forth.

Failure events that are not caused by physical failure of the pipeline may not be compatible with the reliability method of analysis; an example of this is the probability of human error. This type of failure requires deeper analysis, using techniques such as historical data analysis or comparable circumstances from other industries.

HOE Frequency

Human or organization error (HOE) probability is an area of pipeline risk analysis rarely quantified with reasonable accuracy; this is primarily due to physical and mental distance placed between individuals designing, constructing, and operating the pipeline. A justifiable basis for a risk evaluation can be established by implementing an assessment of HOE. The purpose of a HOE evaluation is not to predict failure events, rather it is to identify the potentially critical flaws. The limitation of this is that one cannot analyze what one cannot predict.

Little definitive information is available on the rates and effects of human errors and their interactions with organizations, environments, hardware, and software. Even less definitive information is available on how contributing factors influence the rates of human errors.

The lack of dependable quantitative data currently available on HOE in design and construction of pipeline structures can be compensated for using the following four primary sources of information, presented in work by Bea [5]:

1. Use of judgment based on expert evaluations.
2. Simulations of conditions in a laboratory, office, or on site.
3. Sampling general conditions that exist on site, in the laboratory, and office.
4. Process reviews, accident, and near miss databases.

Table 8.2 Influence on Bias

Type of Bias	Influence on Judgment
Availability	Probability that easily recalled events are distorted
Selective perception	Expectations distort observations of variables relevant to strategy
Illusory correlation	Encourages the belief that unrelated variables are correlated
Conservatism	Failure to sufficiently revise forecasts based on new information
Small samples	Overestimation of the degree to which small samples represent a population
Wishful thinking	Probability of desired outcomes judged to be inappropriately high
Illusions of control	Overestimation of the personal control over outcomes
Logical construction	Logical construction of events that cannot be accurately controlled
Hindsight	Overestimation of the predictability of past events

Source: Bea [5].

Considering the quantity of conclusive data available, the principle mode by which to quantify assessments is the judgment method. As investigations into pipeline failures should eventually lead to comprehensive and reliable databases of HOE, these databases complement judgments and allow a more justifiable quantification to be arrived at.

It is necessary that any results deemed to be meaningful are qualified and unbiased. Investigations by Bea [5] gives a number of biases that can distort the actual causes of HOE, these are listed in Table 8.2. It is important for the evaluator to try to minimize these biases, as it is impossible for them to be eliminated entirely.

Following research by Williams [6], Swain and Guttman [7], and Edmondson [8], quantified data for HOE has been developed. This is based on experience gained in the nuclear power industry in the United States. Experiments and simulations led to information regarding human task reliability.

Work undertaken by Swain and Guttman [7] presents general error rates depending on the familiarity of the task being undertaken by the individual, including a range of limitations or circumstances that the individual may be experiencing, this is shown in Figure 8.3. By assessing the intensity of these limitations or circumstances, the value assigned to certain tasks can be adjusted. Other investigations [6] appear to correlate with this information. However, a multitude of influences affect these values and have potentially

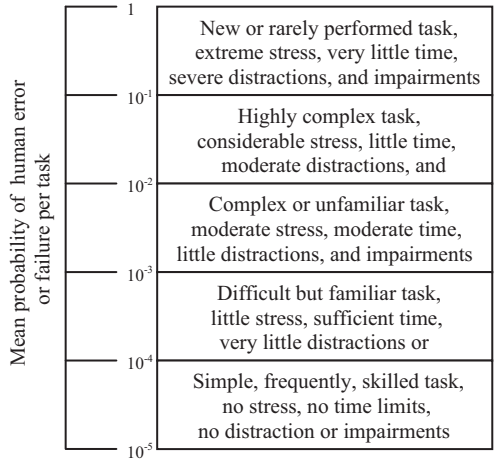

FIGURE 8.3 ***Human Error Rates.***

dramatic effects on the normal rates of errors (i.e., factors of 1E-3 or more). These influences include organizations, procedures, environments, hardware, and interfaces. Information regarding these influences can be found in Bea and others. [5, 6, 9]

It is important to establish the significance of any error that may occur, as this is not established in the information developed. An error can be either major and significant or minor and not significant. Studies performed by Swain and Guttman [7] and Dougherty and Frangola [10] indicate that minor or not significant errors are often noticed and rectified, thus reducing their importance in human reliability. Further quantification of human reliability has been corroborated for a number of tasks relating specifically to structural design; the necessary information is investigated by Bea [5].

6. CAUSES OF RISK

General

This section outlines some common causes for the four different risk scenarios outlined in the introduction.

First Party Individual Risk

The scope of this type of risk is limited to a consideration of the potential for ignited releases as a result of dropped object impact associated with maintenance

and work activities taking place after commissioning or random failure of the pipeline (discussed in next section).

The sources of the potential dropped objects are assumed to be the vessels employed for maintenance or work. The assumptions made to determine the probability of loss of containment is as follows:

- Objects are assumed to fall in a 30° cone centered at a point directly above the pipeline.
- Objects are assumed to fall with equal probability at any point within the circle on the seabed defined by the drop cone. It is assumed that all dropped objects enter the sea, rather than landing on part of the vessel.
- The probability that the hazard zone resulting from a loss of containment coincides with the dropping vessel and is assumed to be 0.5.

Details of such operations are unlikely to be known during design, thus judgment is often required (based on previous experience) and the analysis updated later. During design, this analysis is necessary, since decisions about protective requirements need to be considered.

Societal, Environmental, and Material Loss Risk

Risks associated with the construction, installation, and commissioning of the pipeline do not affect members of the general public. Only incidents that occur during the operation of the pipeline are therefore considered to be initiating with respect to societal risk.

The hazards giving rise to societal risk also contribute to the environmental and material loss risks. These hazards include the following:

1. **Fishing interaction:** Movement of fishing vessels around the location of subsea pipelines pose a risk. The frequency of such an event can be derived from existing databases (PARLOC) [4].
2. **Merchant vessels:** Incidents caused by passing merchant ships include emergency anchoring, dropped containers, and sinking ships. Databases can again be used to determine the density of merchant vessels and the probability of these incidents occurring.
3. **Construction vessels:** Loss of containment incident frequencies as a result of construction vessel activities may be estimated based on databases. However, while it is accepted that construction activities contribute to the overall loss of containment frequency for pipelines, it is not considered to be appropriate to treat such incidents as initiating for societal risk calculations. This is because the presence of construction vessels, in itself, excludes the presence of merchant shipping.

4. **Random failures:** This may be due to any material failure of the pipeline and can usually be determined using reliability analysis.

7. FAILURE PROBABILITY ESTIMATION BASED ON QUALITATIVE REVIEW AND DATABASES

A risk review "largely at a qualitative level" of the pipeline segments to generic failure and degradation modes is performed to establish the failure modes that may pose a threat at various locations along the pipeline. The risk review is based on

- Generic and historical failure rates from relevant pipeline databases.
- Pipeline design and history of operating conditions.
- Known condition and incidents affecting pipelines and basic or high-level structural damage and probability predictions.

The review is incorporated within a spreadsheet, in which as much design and operational data as possible regarding the pipeline is first input. Where relevant, the pipeline is divided into suitable segments, for example, where other components in the line exist, such as tees, risers, riser bases, spools, crossing of shipping lanes, trawling areas, and inshore areas. In this way, the specific failure modes relevant to a particular location, item, or component can be established.

A high-level (basic) structural reliability assessment considering the specific failure mode is made, mainly considering the normal and accepted uncertainties. Failure predictions based on generic or historical failure data are also made. These represent the accidental cases, where the pipeline will have been subject to conditions outside its design conditions or required design conditions were not achieved. The occurrence of accidental events are generally random, often result in failure immediately or within a very short time period, such that inspecting the pipeline for accidental conditions and damage generally provides no benefit. The main means in dealing with accidental, unplanned conditions is to eliminate or reduce their likelihood to acceptable levels. Thus, the identification of potential accidental events and their elimination is critical to the effective risk management of pipeline systems.

Generic Hazard and Pipeline Damage List

Extreme environmental loads:

- Earthquakes.
- Severe wave and current loading.

- Seabed movement and instability.

Process deviations:

- Overpressure
- Underpressure
- Over- and undertemperature
- Process upset, offspec product into line.

Excessive internal corrosion.
Excessive internal erosion.
Excessive external corrosion.
External interference.
Commercial marine traffic:

- Dropped anchors.
- Dragged anchors.
- Sinking vessels.
- Grounding vessels.

Fishing and trawling:

- Impact loading.
- Pullover loads.
- Hooking.
- Trawl pullover combined with thermal buckling.

Munitions.
Falling and rolling boulders.

Example of Risk Review

A sample of such a review is presented here, considering internal corrosion of a new pipeline transporting normally dry gas but containing CO_2. The gas is dried to a high quality prior to export by a glycol drier. Thus, the potential for internal corrosion (and hence failure) from CO_2 in wet service exists, it cannot be readily discounted, and further assessment is required.

The general issues are what are the required reliabilities of the gas drier, gas monitoring and process upset detection requirements, drying of the line after an upset, extent of corrosion allowance, and if any and how often the line should be cleaned and inspected.

Part of the input data to the workbook is the product mass balance: The user is to ensure that all potential corrosive products are entered. For the case in question, the cause of internal corrosion is CO_2 in wet service as a result of (a) minute water content during normal production, (b) process upset, and (c) accidental operation (e.g., accidental water ingress into line during subsea pigging operations).

In this case, the corrosion rates for each condition are calculated based on de Waard and Lotz 1993 [11] (which is included in the workbook) and the expected duration of wet service. For the process upset and accidental cases, estimates of the duration of wet service need to be established. These are based on [11]

- Probability or frequency of process upsets (based on driers reliability).
- Probability of detection (are there alarms, process trips on drier, monitoring of gas quality, etc.).
- Probability of drying line within a certain period after an incident.
- Probability of accidental ingress (based on historical failure probability of gas pipelines from internal corrosion, PARLOC2001 [4]).

The uncertainties (potential variation) in these estimates are also entered, high estimates are generally used. A basic conservative estimate of the pipelines structural reliability over time is then made based on the predicted safe operating pressure (accounting for corrosion damage) according to Bai et al., 1997 [12], design pressure and uncertainties in these estimates.

With respect to the estimates of accidental corrosive or wet service, the frequency of such an occurrence is based on the historical corrosion failure rate from PARLOC2001. Accidental internal corrosion conditions can result in very significant corrosion rates but should rarely occur. Therefore, accidental corrosive service is not included in the "normal or accepted" estimate of yearly corrosion rates over the life of the pipeline.

The causes of potential accidental events and resulting extreme conditions to the line are to be identified and estimated as far as reasonably practical, such as undetected water ingress during subsea pigging or other activities in which water or other or increased corrosive products may be introduced (undetected). Eliminating or reducing the likelihood of these events is the main means of managing this risk. The potential time to failure in the event of such accidental operation is also predicted. For the case in question, it was considered that water ingress from subsea pigging was the only potential accidental condition. If it occurred, the service limit state acceptance criteria would be exceeded relatively quickly (within the year), although actual pipeline failure would be expected to take a few years. Thus, normal cleaning pigging on a yearly base should protect against failure from such an accidental event, although if it occurs, significant corrosion damage is inevitable.

It was found that the corrosion depended greatly on the upset frequency and incidental duration, such that reliable means of detection and limitation of incidental duration is required. With such means in place, the assessment

predicts negligible corrosion, so that neither corrosion allowance is recommended nor intelligent pigging operations. However, it is considered that an inspection should be made on a medium-term basis (e.g., every 3–5 years), particularly in the early phase of operation, to verify the corrosion prediction models and ensure no damage during RFO (ready for operations). Only if it is 100% certain that no significant upsets and accidental operations have occurred should such an inspection be omitted. With such means in place, the assessment predicts negligible corrosion, so neither corrosion allowance is recommended nor intelligent pigging operations.

8. FAILURE PROBABILITY ESTIMATION BASED ON STRUCTURAL RELIABILITY METHODS

General

Where the failure mode is identified as being significant or more specific details of the structural damage (defect data) to the pipeline are known (i.e., for pipelines that have been in operation for a number of years), a more detailed SRA is possible and justified. Such analyses are performed using simple SRA spreadsheet-based tools, based on simplistic bootstrap probabilistic methods (API 2A-LRFD [13]), that do not require propriety software. For such analysis, the following base data are required:

(1) **Measured defect data from a survey:** If such data are available, then this needs to be formed into useful input data, such as the nature of the defects (type of corrosion or pitting, grove, girth welds), mean defect depth, length, and area, along with the variance and standard deviation of such parameters. Otherwise, nominal defects are assumed, based (where possible) on experience from similar lines.

(2) **Pipeline material/ and strength properties:** The pipeline SMYS, SMTS, and flow stress are required. The variance in these mean values need to be established and generally are obtainable from published and manufactures data.

(3) **Pipeline geometric properties:** The following geometric properties in terms of mean value and variance need to be developed for each relevant section of the pipeline:
- Nominal diameter, not expected to vary along pipeline.
- Wall thickness, the design and mean wall thickness, and variations along the pipeline length.
- Ovality, again may vary along the pipeline length, although a design limit will be specified.

(4) Pipeline loading characteristics: Pressure loading at relevant segments along the pipeline is to be defined in terms of mean operating pressure, standard deviation, and variance. Extremely high pressures should be accounted for, based on the reliabilities of pressure regulating and protection systems. The temperature profile is not a strict loading but affects the corrosion rates and axial force in pipeline. Over the operating life, the temperature profile may vary and may need to be accounted for.

Simplified Calculations of Reliability Index and Failure Probability

The probability of failure depends on the likelihood of the loading exceeding the pipelines strength or resistance, as illustrated in Figure 8.4.

The safety index (β) is defined as (API 2A-LRFD [13])

$$\beta = \frac{\text{Mean Safety Margin}}{\text{Uncertainty}} = \frac{R_m - S_m}{\sigma_{RS}} = \frac{P_{safe,mean} - P_{op,mean}}{\sigma_{P_{safe,mean}P_{op,mean}}} \qquad [8.2]$$

and the probability of failure P_f is calculated from

$$P_f = 1 - \Phi(\beta)$$

by establishing and accounting for the main uncertainties in the

- Pipelines nominal strength (load resistance against specific loading) dependent on the type of damage or degradation to the pipeline.
- Pipelines nominal operating loads.

The reliability (safety) index (β) and probability of failure ares calculated for a single defect as presented in the following text and illustration. These

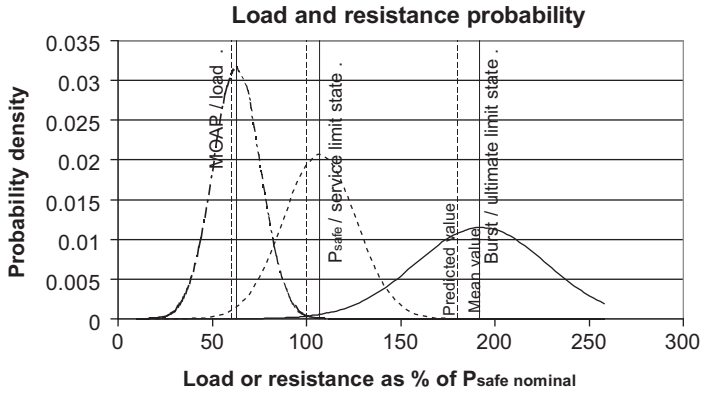

FIGURE 8.4 *Load and Resistance Probability Densities.*

probabilities for all defects are then combined to give the safety index and failure probability of a pipeline segment and pipeline as a whole.

Strength and Resistance Model

An example model for the pipeline mean resistance (strength) against structural damage is presented here for damage from internal corrosion. The model was developed by Bai et al. [12], although many other models are available, such as Shell model [14].

Evaluation of Strength Uncertainties

The uncertainty of pipeline strength depends on

- Material strength uncertainty.
- Defect measurement, detection, and prediction uncertainty.
- Pipeline parameter and geometry uncertainty.
- Strength model uncertainty.

The uncertainties are measured in terms of standard deviations and variance from mean values and combine to give an uncertainty in the predicted pipeline safe operating pressure. The mean bias (B) and covariance of the burst prediction model is (Bai et al., 1997 [12]), for model bias, B_M,

$$B_M = \frac{P_{\text{burst,actual}}}{P_{\text{burst,predicted}}} = 1.07, \text{ with a COV (coefficient of variation) of } 0.18$$

and the mean bias and variances of the equation parameters for pipeline strength are

$$\text{Bias for normalized area: } B_{XA} = \frac{X_{A,\text{actual}}}{X_{A,\text{predicted}}} = 0.8, \text{ with a COV of } 0.08$$

$$\text{Bias for normalized flow stress: } B_{Xf} = \frac{\sigma_{f,\text{actual}}}{\sigma_{f,\text{predicted}}} = 1.14, \text{ with a COV of } 0.06$$

$$\text{Bias for normalized length: } B_{XfL} = \frac{X_{L,\text{actual}}}{X_{L,\text{predicted}}} = 0.9, \text{ with a COV of } 0.05$$

Multiplying the mean bias by the "predicted value" gives the mean "actual value": $B_{\text{mean}} \cdot X_{\text{predicted}} = X_{\text{mean.actual}}$.

Thus, the nominal or design $P_{safe.design}$ value is calculated using the predicted values. The mean P_{safe} value is calculated by substituting the measured or assumed $X_{mean.actual}$ values into the preceding equation and multiplying by the model bias B_M giving $P_{safe.mean}$:

$$P_{\text{mean burst value}} = P_{\text{mean safe value}} \cdot \gamma$$

Criterion P_{safe} is determined by applying a safety factor to the predicted burst pressure (ultimate limit state), this is about 1.8 to give the desired or required reliability. P_{safe} is the service limit state.

The term P_{safe} is thus a factored value of P_{burst} to account for the P_{burst} bias and variance. The mean value and variance of P_{safe} is dependent on only the corrosion parameter predictions (length and depth) and not the model bias and variance, as the latter are accounted for by the safety factor.

9. CONSEQUENCE ANALYSIS

Consequence Modeling

The consequence model attempts to model the sequence of events that occur after a failure event. The sequence for consequence modeling is shown in Figure 8.5. Note that this method of consequence modeling is suitable only for failures relating to the pipeline releasing some type of fluid or gas. The following steps for the modeling of a release event gives only a

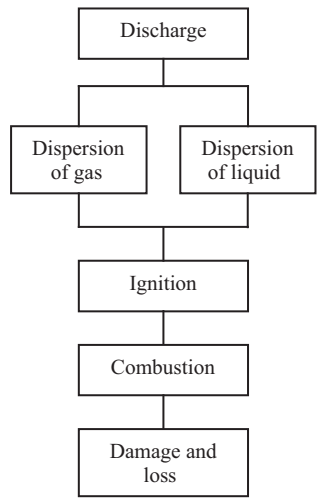

FIGURE 8.5 ***Modeling of Consequences.***

general outline of the sequence of events that ultimately leads to a calculation of the various losses. Many models exist for modeling these release characteristics (from simple to sophisticated). However, no extensive research or experimentation studied the modeling of subsea releases, so generally there is a high degree of uncertainty in this modeling and conservatism is often used. One specific suite of computer modeling programs available is the HGSystem written by Thornton Research Center [15].

Discharge

To determine dispersion, information is required for the discharge, this includes hole size, duration, rate, and quantity.

Dispersion of Gas

Leakage of a gas pipeline under water results in a plume, which rises and exits from the surface of the water in the shape of a circle.

Dispersion of Liquid

The dispersion depends on the fluid released. Unstable condensate tends to be modeled as gas release (although a sound qualitative discussion about hydrate formation in water is required). Stable condensates eventually rises to form a liquid pool at the surface. However, much of the dispersion is very complex and difficult to model.

Ignition

A leakage that does not ignite (i.e., not toxic, H_2S) presents no risk to humans. A risk of ignition is developed using the following equation:

$$f_{\text{fire}} = f_{\text{leakage}} \times p_{\text{ignition}} (\text{per year}) \qquad [8.3]$$

where p_{ignition} is the probability of ignition occurring, given a leak of a flammable substance. This can be determined using an ignition model, which considers all possible methods by which ignition could take place.

Subsea releases can usually be considered to be delayed; hence, ignition results in an explosion or flash fire (few unconfined flammable gas clouds develop into an explosion) for gas leakage. A fire pool could arise from an oil leak. However, in the case of a shallow water release, a low momentum jet

fire may develop, if ignition occurs before a significant cloud can develop. Such an ignition results in a jet flame.

Combustion

- **Jet fire**: There are a number models establishing jetfire characteristics. A jet fire is characterized by flame length and radiated heat flux.
- **Pool fire**: The height of the flame depends highly on the depth of the slick, the rate of combustion of the liquid, and the wind speed.
- **Explosion:** Clouds of flammable gas can explode when ignited. This is termed an *unconfined vapor cloud explosion* (UVCE). This type of explosion is relatively mild and has two effects: heat and force. The force effects can be modeled using the multienergy method. For humans exposed to an explosion, heat is the critical factor in determining bodily harm. Force can also act indirectly on persons exposed to the explosion, injury or death can result from flying debris or glass splinters. For structures, the effect of force is critical.

Damage and Loss

It is also necessary to model the potential damage and loss that can occur to the following [13]:

1. Humans:
   - Heat from explosions or fires.
     The injury depends on the dose, which is $D = \text{time} \times (\text{kW/m}^2)^{4/3}$. 50% death rate is likely when exposed to $D_{50} = 2000\ \text{sec} \times (\text{kW/m}^2)$.
   - Force and missiles from explosions:
     There is a 50% chance of lung injury at 1.4 barg.
     There is a 50% chance of perforated eardrum at 0.5 barg.
   - Toxic effects:
     For a majority of substances the D_{50} dose is known, that is a product of the time exposed and the $(\text{concentration})^n$ which results in a 50% likelihood of death.
2. Material loss:
   - Repair of pipeline.
   - Loss of production:
     This is cost of lost income due to incapacity to provide a product to sell, which is a function of the time it takes to restore the pipeline to a functioning state.
3. Environmental damage.

Uncertainty

All of the models in the sequence of analysis contain a significant degree of uncertainty. If taking a pessimistic approach and use factors of safety in the magnitude of 1.5 for each stage of calculation, this results in a total factor of safety of (1.5^4=) 5. This might be an unrealistic overestimate of the total value, so it is necessary to adjust this figure to suit the situation.

Another difficulty with the consequence modeling technique is that it is necessary to assume an initial discharge condition (i.e., the size of hole). This has a large influence over the models used; for a more comprehensive analysis, a sample of likely release conditions could be evaluated. However, generalizations can be made regarding hole size based on failure rate data and type of failure; for example, corrosion is likely to lead to small pin pricks, whereas third party interference tends to cause large diameter holes.

Estimation of Failure Consequence

The consequences of failure are

- Consequential production losses.
- Contract penalties (these can be extremely severe).
- Cost of repairing the pipeline.
- Cost of repairing any damage to adjacent installations and environment.
- Potential fatalities.
- Cost of negative publicity.

The potential consequences depend greatly on the operating pressure, pipeline length, diameter, and content and size of the failure or release. The last has been based on historical failure rates, for subsea North Sea pipelines presented in PARLOC [4].

Potential fatalities and damage to adjacent installations and environment are assessed using standard consequence assessment methods incorporated within a spreadsheet suite of tools based on numerous published methods. The potential development of loss of containment is illustrated in the event tree, Figure 8.6. Consequence analysis techniques are generally well established within the oil and gas industry, although in certain areas better models are still required. The specific consequence models used for a subsea gas release are pipeline time-dependent gas release primarily based on Fanneløp and Lryhming [16], although other models are also used for comparison; subsea plume modeling primarily based the methods for dispersion of subsea release reviewed by Rew et al. [17]; and hydrodynamics of underwater blowouts (Fanneløp and Sjøon [18]). The potential surface

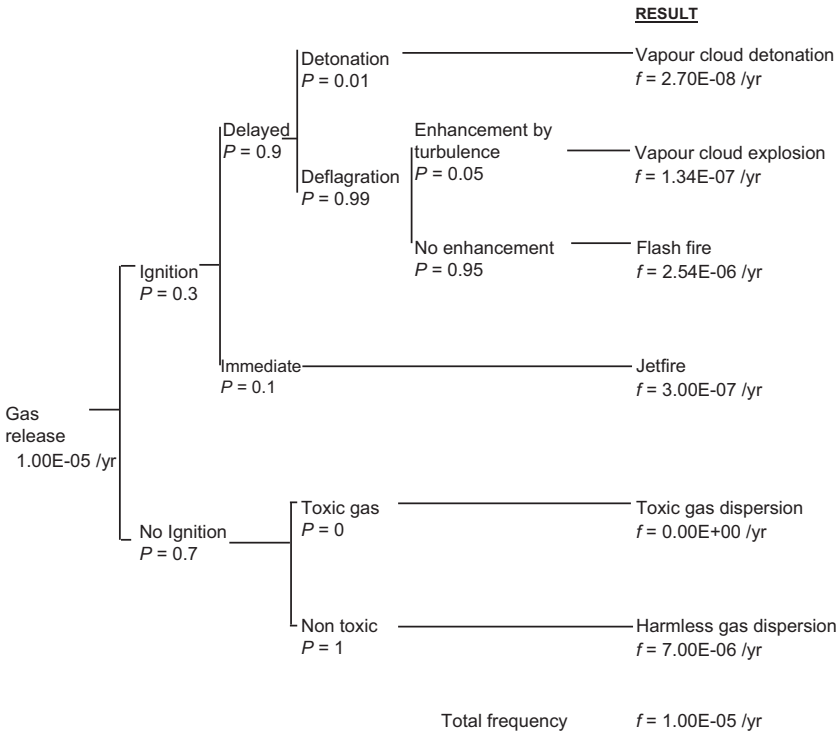

FIGURE 8.6 ***Event Tree for a Gas Release.***

gas cloud size and dispersion extent is modeled based on the methods reviewed by Rew et al. and using HGSystem suite [15]. The potential explosion, flash fire extent, and effects at the sea surface are calculated based on methods presented by AIChemE [19].

The calculated risks are compared against acceptance criteria. Where these are not met, further design or operational measures must be introduced to reduce the risks to within acceptable limits. The risk cost can calculated by adding all of the preceding consequence cost elements and multiplying them by the predicted frequency of pipeline failure and accident probabilities as presented by Bai et al., 1999 [20] and Goldsmith et al. [21]. As the probability of failure increases with time (i.e., due to the time-dependent structural degradation), the risk cost from the last inspection can be plotted against the inspection and maintenance costs for increasing intervals, as illustrated in Figure 8.7. In this way the optimum value inspection interval can be selected [21].

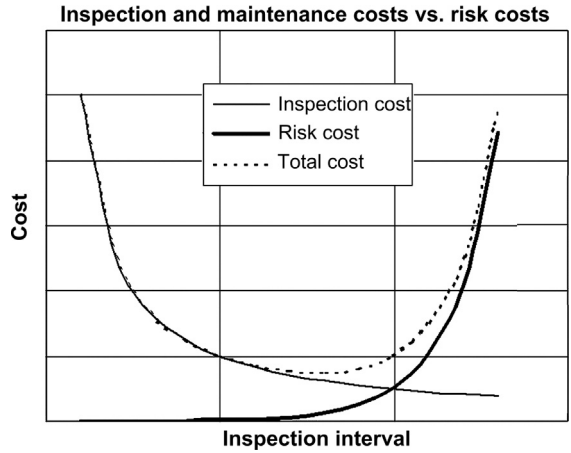

FIGURE 8.7 ***Maintenance Costs Versus Risk Costs.***

10. EXAMPLE 1. RISK ANALYSIS FOR A SUBSEA GAS PIPELINE

General

This risk analysis example evaluates the risk acceptance and risk estimation of a North Sea pipeline transporting dry gas. This example covers all aspects of the risk methodology developed in the chapter. By first determining the gas release for different hole sizes, it is then possible to determine the potential effects on each type of risk.

Gas Releases

To provide an analysis that can be considered representative for the entire pipeline, the release rates have been estimated (conservatively) on the assumption that the water depth is 300 m. This leads to a differential pressure at the site of loss of containment of ≈ 250 bar.

Representative Hole Sizes

Potential hole sizes are modeled through the use of three representative hole sizes with diameters of 20 mm, 80 mm, and 200 mm. The 20-mm and 80-mm hole sizes have been selected to provide ease of comparison with the hole sizes considered in the PARLOC database. The largest hole size considered is 200 mm. This is considered to be a conservative upper bound to the equivalent hole size caused by major structural damage to the pipeline.

Table 8.3 Hole Sizes for Example 1

Diameter of Hole (mm)	Mass Release Rates (kg/s)	Time (Hours)
20	14.6	6000
80	233.2	375
200	1457.1	60

Discharge

Release rates have been estimated using SPILL. This is part of the HGSystem suite of programs [15]. The rates predicted for these hole sizes are given in Table 8.3. Indicative duration's for these releases are also shown below. These durations are based on the time required to blow down the pipeline through the hole and it is assumed that the mass release rates decrease linearly with time.

The durations given in the table do not take into account emergency response actions initiated following the detection of a loss of containment. Hazard durations therefore are assumed to be based on the time expected for the existence of a release to be detected. These durations are assumed to be 168, 48, and 6 hours, respectively. Note that these times represent hazard durations rather than leak durations; that is, they are estimates of the time required for the detection and location of a leak and the imposition of measures to exclude shipping traffic from the affected locality. Also note that the risk analysis results are not sensitive to the value assumed for the hazard duration for 20-mm holes, since these do not result in flammable releases.

Subsea Plume

The effect of a subsea gas release may be modeled as an inverted conical plume with a half cone angle of between 11° and 14° in a zero current velocity situation. Assuming the most conservative case, this results for a 150 m diameter release zone at the sea surface for the assumed 300 m water depth.

Airborne Dispersion

Airborne dispersion is modeled using the program HEGADAS-S, part of the HGSystem suite [15]. This program assumes that the gas evolves as a momentumless release from a rectangular pool. The pool has been taken to be 150 m × 150 m, to reflect the release into the atmosphere of the subsea plume.

Effect of Water Depth

Releases from greater depths result in somewhat reduced mass flow rates. This is due to the increased seawater pressure at the site of loss of containment. Subsea dispersion over a greater depth results in a larger gas evolution zone at the surface. These effects mean that the surface concentrations, and hence the dispersion distances and hazard zone dimensions, reduce with increasing release depth. The assumption of a 300-m release depth for all loss of containment incidents is therefore conservative.

Stability

Pasquill stability classes define meteorological conditions from very unstable, A, to moderately stable conditions, F. These parameters are used in the modeling of airborne dispersion. Two values of the Pasquill stability class are used: Class D (neutral stability) and Class F (moderately stable conditions). Class D is appropriate for nighttime and overcast daytime and is therefore assumed to be representative of 75% of the time, with Class F being representative of the remaining 25%.

Wind Speeds

Since no fixed installations are at hazard as a result of subsea releases from the pipeline, wind direction is not required as an input to the risk assessments. Wind speeds are required, however, since they determine the extent of the flammable gas clouds that may be generated by a release. The wind speeds and relative frequencies used to determine the hazard ranges associated with various releases are summarized in Table 8.4.

Hazard Ranges

Hazard ranges are calculated in terms of the extent of the lower flammability limit (LFL) for different release rates, wind speeds, and water depths. A concentration of 5% by volume has been used to represent the LFL.

Table 8.4 Relative Frequency of Representative Wind Speeds

Wind Speed Range (m/s)	Representative Wind Speed (m/s)	Relative Frequency
0 to 5	2	0.26
5 to 11	8	0.49
11 to 17	14	0.21
over 17	20	0.05

Table 8.5 Average Hazard Areas for Different Hole Sizes

Hole Size	Hazard Area (m^2)
20 mm	0
80 mm	4900
200 mm	18650

A total of 18 gas dispersion analyses have been undertaken. These results are combined, using the data for relative frequency of Pasquill class and wind speed, to provide an estimate of the hazard area associated with each of the three hole sizes. These are shown in Table 8.5.

Individual Risk

Acceptance Criteria

The risks to which workers are exposed are compared with the maximum operational FAR of 10 fatalities per 10^8 hours worked.

Cause Analysis

Statistics of dropped object frequencies have been obtained from the 1992 *Offshore Reliability Data Book*, OREDA-92 [22]. This data source records a total of seven dropped objects against a total calendar time of 648,200 hours or an operational time of 22,800 hours. Assuming an average lift duration of 5 minutes this is equivalent to 0.42 lifts per hour with a probability of a dropped object of 2.56×10^{-5} per lift [22, 23].

Two lifting operations have been assumed at each work location, corresponding to one lift for installation of structures and one lift for pigging operations.

Assumptions

The following assumptions are made in addition to those stated earlier in the chapter:

1. Water depth has been assumed to be 300 m.
2. The probability that the hazard zone resulting from a loss of containment coincides with the dropping vessel is assumed to be 0.5.
3. The probability of ignition has been taken as 0.3.
4. It is assumed that 50% of the persons on the vessel are working at any one time.

Consequence Analysis

It is assumed that all persons on the vessel are at risk, the FAR is then a function of the proportion of persons on the vessel who are working, not of the total number of persons on the vessel.

Risk Estimation

The number of ignited releases per working location is given by

$$f_{\text{lift}} \times p_{\text{drop}} \times p_{\text{imp}} \times p_{\text{haz}} \times p_{\text{ign}} = 2 \times \left(2.56 \cdot 10^{-5}\right) \times 0.016 \times 0.5 \times 0.3 = 1.23 \cdot 10^{-7}$$

If the vessel remains on location for 48 hours and has n persons on board, then this results in x fatalities, as a result of $24n$ hours worked. The FAR is therefore equal to 0.51×10^{-8} (1.23×10^{-7} divided by 24). This is far less than the acceptance criteria established.

Societal Risk

Acceptance Criteria

The acceptance criterion is 10^{-3} deaths per year.

Initiating Incidents

Damage frequencies due to trawling gear interaction have been extracted from the PARLOC database. These are considered to be conservative, since the failure frequencies given in the PARLOC report are where no failures have been experienced. This is based on a theoretical analysis that does not take into account the robustness of the pipeline.

Merchant Vessels

Because the minimum water depth for the pipeline is approximately 275 m, emergency anchoring has not been considered. Incidents initiated by passing merchant vessels have therefore been restricted to dropped containers and sinking vessels. The initiating incident frequency data adopted is given in Table 8.6.

Table 8.6 Initiating Incident Frequencies

Incident	Frequency	Hazard Distance
Dropped container	5.15×10^{-6} per hour	15 m
Sinking vessel	2.11×10^{-7} per hour	150 m

Construction Vessels

Loss of containment incident frequencies, as a result of construction vessel activities, is given in PARLOC. However, while it is accepted that construction activities contribute to the overall loss of containment frequency for pipelines, it is not considered to be appropriate to treat such incidents as initiating for societal risk calculations. This is because the presence of construction vessels, in itself, excludes the presence of merchant shipping.

Random Failures

Material and corrosion defect failure rates have been taken from PARLOC. Once again, these data are considered to be conservative, particularly with respect to corrosion failure rates for export gas pipelines with a diameter >10 in. It should, however, be understood that the corrosion defect failure rates used here can be considered to be conservative only provided that the pipeline is operated under the design conditions (i.e., dry). If the pipeline is to be frequently or continuously operated under wet conditions, then the corrosion-related failure rates are significantly higher. The failure rates obtained from PARLOC are appropriate for the localized spot corrosion, which may be experienced (often in association with a pre-existing defect) in a normally dry gas line in which corrosion is actively controlled and monitored on an ongoing basis.

Cause and Consequence Analysis

The total number of trawler crossings of the pipeline per year has been determined. It has been assumed that 50% of the trawlers have a crew of 5 persons and 50% will have crews of 10 persons. It has been assumed that 15 people, on average, are at risk per merchant vessel. This value is based on a population at risk of 10 people for 95% of vessels and 100 people for 5% of vessels.

In the absence of knowledge concerning the intensity of future third party construction activity, it is not possible to predict the societal risks associated with those activities. These risks are subject to control by the third party concerned and contribute to the individual risks (the FAR) for those specific activities. In the absence of detailed information concerning the density of merchant vessel shipping, it has been assumed to be high. A merchant vessel crossing frequency of 29 per km year has been assumed.

The assumptions made with respect to the relative frequency of holes of different sizes are shown in Table 8.7.

Table 8.7 Calculated Trawling Impact Frequencies

Trawling Impact Frequency	Total Area	Pipeline
f_{imp}/(year × km)	2.63	0.42

Risk Estimation

The expected number of third party fatalities per year is 9.75×10^{-6} for the various scenarios considered. In view of the conservative nature of the calculations undertaken, it is considered that the societal risks associated with the pipeline are acceptable.

Environmental Risk

No risk is posed, since the material being transported is dry gas.

Risk of Material Loss

Initiating Incidents

All incidents considered as initiating in the assessment of individual and societal risks are considered to be initiating for the purposes of determining the risks of material loss posed by the pipeline.

In addition, any incidents occurring during construction and installation and having the potential to result in damage to or delay in the construction of the pipeline are considered to be initiating with respect to risks of material loss.

Consequence Analysis

Both repair cost and lost production cost have been assumed to be linearly related to the time taken for repair. Material costs for repairs have been neglected. Costs assumed are as follows:

- Lost production 20 MNOK (million Norwegian Krone) per day.
- Cost of repair spread 1 MNOK per day.
- Cost per fatality 100 MNOK.

The time required for the repair of small or medium damage is assumed to be 16 days (clamp repair), the time required for repair of large damage (new spool piece installed using mechanical connectors) is assumed to be 30 days. Three-days vessel mobilization has been assumed in each case. The costs (based on these assumptions) incurred as the result of different sizes of damage are shown in Table 8.8. A discount factor of 7% is used to determine net present values (1998 NOK) of future costs. The frequencies of incidents resulting in loss of containment are summarized in Table 8.9.

Table 8.8 Costs of Repairs

Hole Size	Small	Medium	Large
Cost of repair (MNOK)	19	19	33
Cost of lost production (MNOK)	380	380	660

Table 8.9 Contributions to Overall Loss of Containment Rate

	Small	Medium	Large	Total
Trawlers (sinking)	0	0	5.7×10^{-10}	5.7×10^{-10}
Merchant (sinking)	1.3×10^{-8}	3.7×10^{-9}	4.51×10^{-8}	6.18×10^{-8}
Material defect	4.92×10^{-7}	4.92×10^{-7}	4.92×10^{-7}	1.48×10^{-6}
Corrosion	3.14×10^{-6}	0	0	3.14×10^{-6}
Trawl impact	1.16×10^{-6}	2.91×10^{-7}	0	1.45×10^{-6}
Subtotal (per km year)	4.80×10^{-6}	7.86×10^{-7}	5.60×10^{-7}	6.13×10^{-6}
Maintenance and work (per year)	5.37×10^{-7}	5.37×10^{-7}	5.37×10^{-7}	1.61×10^{-6}
Total	6×10^{-4}	9.9×10^{-5}	7.1×10^{-5}	7.7×10^{-4}

Risk Estimation

The expected discounted lifetime cost of incidents is deemed acceptable, as it is only a small percentage of the steel cost of the pipeline.

11. EXAMPLE 2. DROPPED OBJECT RISK ANALYSIS

General

This calculation is used to present an assessment of the risk posed by dropped objects hitting spools, umbilicals, and pipeline sections around a template. The example concentrates on the determination of the probability of dropped objects hitting subsea installations.

Acceptable Risk Levels

There is a need to distinguish between an SLS (serviceability limit state) and the ULS (ultimate limit state). For this example, an SLS is assumed to be a dent damage larger than 3.5% of the pipe diameter, while the ULS corresponds to bursting due to internal overpressure and combined dent and crack defects. The pipeline does not burst unless a large dent and a certain depth of cracks exist simultaneously.

The principle used in establishing the acceptance criteria is that the recovery time (for the most sensitive population) following environmental damage should be insignificant relative to the frequency of occurrence of environmental damage. For this example, marine (pelagic) birds have been identified as the most sensitive resources during all seasons.

The damage category has been defined as minor for the field. The acceptance criterion is therefore a frequency $<2.0 \times 10^{-2}$ for the field as a whole. This can broadly be grouped into three main risk areas: pipelines, templates and topside, and risers.

The acceptance criterion for pipelines alone is therefore assumed to be one third of the field specific criterion, namely, a frequency $<7.0 \times 10^{-3}$.

Quantitative Cause Analysis

Probability Cones

An object dropped at the sea surface is assumed to land within an area on the seabed that is swept out by a cone starting at the drop point. This area is determined by a cone with angle ϕ.

It is further assumed that the probability of an object hitting a point within the cone follows a normal distribution and can be described as a function of distance x from the cone centerline:

$$p(x) = \frac{1}{\sigma \cdot \sqrt{2\pi}} \cdot \exp\left[-\frac{1}{2} \cdot \left(\frac{x - \mu}{\sigma} \right)^2 \right] \qquad [8.4]$$

where

$p(x)$ = probability of hitting a point a distance x from the cone centerline
σ = standard deviation
x = distance from the cone centerline
μ = mean value of x (here = 0)

The cone sweeps out an area with 99% cumulative probability of a hit from a dropped object when

$$X = d \cdot \tan\phi \qquad [8.5]$$

where

X = distance from the cone centerline giving 99% cumulative probability of hit
d = water depth
ϕ = cone angle

The value of σ in Eq. [8.4] can thus be determined by solving

$$\int_{-a}^{a} p(X)dX = 0.99 \qquad [8.6]$$

where $a = X/\sigma$

Probability of Pipeline or Spool Hit

The probability of hitting parts of the pipeline or spool consists of three parts:

- Probability of dropping an object.
- Probability of the object landing within a cone area containing the pipeline or spool.
- Probability of object hitting the spool or pipeline (inside the cone area).

This is expressed in Eq. [8.7]:

$$P(\text{hit}) = P(\text{drop}) \cdot P(A_c) \cdot \frac{A_f}{A_c} \qquad [8.7]$$

where

P(hit) = probability of a dropped object hitting a pipeline, spool, or umbilical

P(drop) = probability of an object being dropped

$P(A_c)$ = probability of a dropped object hitting the cone area A_c

A_f = area of pipeline, spool, or umbilical within A_c, assumed = length x 1 m

Energy Absorbed by Steel Pipe

The energy required for a knife edge indentor to produce a dent in a pipeline may be calculated as follows:

$$E_d = 25 \cdot \text{SMYS} \cdot t^2 \cdot \sqrt{\frac{\Delta^3}{\text{OD}}} \qquad [8.8]$$

where

t = wall thickness

SMYS = specified minimum yield strength

Δ = dent depth, assumed a maximum 3.5% of OD based on serviceability

OD = outside diameter

Table 8.10 Basic Data and Assumptions

Item	Unit	Value
Water depth	m	300
Cone angle	°	30
P(drop)	—	3.0×10^{-5}
Rig activity:	Rig days/template/20 years	500
	Number of lifts/rig day	20
Design life	Years	20
Pipeline outside diameter	mm	259.8
Pipeline wall thickness	mm	15.6

The effect of coatings and surface area of the falling object is conservatively neglected in Eq. [8.8].

Basic Data and Assumptions for Risk Analysis

This example considers the hit probabilities for a generalized L-spool. Table 8.10 presents the basic data for these calculations.

A 100-m section of dumped rock is assumed to follow directly after each spool. The hit probabilities are calculated for two areas:

- Probability of hitting the spool between the template and the start of the rock.
- Probability of hitting the pipeline outside the rock but inside the 99% cone area.

The probability of the line being hit outside the 99% cone is considered negligible. Two pipelines and one umbilical are assumed for each template. The probability calculated considers a hit on any of these three items; for simplicity, it is modeled as a total hit area of 3 × (one generalized spool length) × (a 1-m corridor around each item).

The assessment is based on objects being dropped through the moon pool of the drill rig. Although objects may be dropped from the cranes, drops through the moon pool are assumed to be the worst case, as these normally happen closest to the spools. A drill rig is present on the field for the whole lifetime of the field (20 years). A total of 17 templates has been assumed. This means that the time spent on one template is 20 years/17 ≈ 425 days. Also, 75 days is added to this to account for increased drilling activities in the pre- and early production phase, after the lines are installed, giving a total of 500 days of drilling operations. There is an average of 20 lifts/day during these 500 days, giving a total of 10,000 lifts/20 years.

Results

Probabilities

Cone radii are found using simple geometric principles:

$$\text{Cone radius, end spools}: \left(30^2 + 30^2\right)^{1/2} = 42$$

$$\text{Cone radius, end of dumped rock}: \left(130^2 + 30^2\right)^{1/2} = 133$$

$$X = 300\ \text{m} \cdot \tan 30 = 173.2\ \text{m}$$

From Eq.[8.5] and a table of the standard normal distribution:

$$\sigma = X/2.575$$
$$= 67.2\ \text{m};\ \text{in a normal distribution},\ P(-2.575 < x < 2.575) = 0.99$$

The cone area of the cone section encompassing the spools is

$$A_c = \pi \cdot (42)^2 = 5542\text{m}^2$$

The spool area within this cone area is

$$A_f = 60\ \text{m} \cdot 3 \cdot 1\text{m}$$
$$= 180\ \text{m}^2\ \text{(length of pipe and umbilical within } A_c \text{ with a 1 m corridor)}$$

The probability of a hit within A_c is

$$42\ \text{m}/67.2\ \text{m} = 0.625 \Rightarrow P(-0.625 < x < 0.625) = 0.468$$
$$\text{P(hit)} = 3 \times 10^5 \cdot 180/5542 \cdot 0.468$$
$$= 4.6 \times 10^7/\text{lift}$$
$$= 4.6 \times 10^7/\text{lift} \cdot 20\ \text{lifts/rig day} \cdot 500\ \text{rig days}$$
$$/20\ \text{years/template}$$
$$= 4.6 \times 10^3/20\ \text{year/template}$$
$$= 2.3 \times 10^4/\text{year/template} \cdot 17\ \text{templates}$$
$$= 3.9 \times 10^3/\text{year}$$

To calculate the probability of a dropped object hitting the pipelines outside the dumped rock area, this procedure is repeated considering the

cone section between the end of the dumped rock and the end of the 99% cone area, giving

$$A'_c = \pi \cdot \left(173.2^2 - 133^2\right)^{1/2} = 38,670 \text{ m}^2$$

$$A'_f = 3 \cdot (173.2 - 133) \cdot 1 \text{ m}$$
$$= 120.6 \text{ m}^2 (\text{length of pipe and umbilical within } A_c \text{ with a 1 - m corridor})$$

The probability of a hit within A'_c is

$$133 \text{ m}/67.2 \text{ m} = 1.979 \Rightarrow P(-1.979 < x < 1.979) = 0.952$$

$$P(\text{hit within } A_c) = 0.99 - 0.952 = 0.038$$

$$P'(\text{hit per lift}) = 3 \times 10^{-5} \cdot 120.6/38670 \cdot 0.038 = 3.6 \times 10^{-9}/\text{lift}$$

$$P'(\text{hit per template}) = 3.6 \times 10^{-9}/\text{lift} \cdot 20 \text{ lifts/rig day} \cdot 500 \text{ rig days/20 years/template}$$
$$= 3.6 \times 10^{-5}/20 \text{ years/template}$$

$$P'(\text{hit per year for all templates}) = 1.8 \times 10^{-6}/\text{year/template} \cdot 17 \text{ templates}$$
$$= 3.0 \times 10^{-5}/\text{year}$$

Energy Absorbed by Steel Pipe

The energy required to produce a dent of 3.5% of OD is found to be 5.2 kJ. Only items of approximately 1 tonne have impact energy less than 5.2 kJ. It is assumed that most dropped objects are heavier than this and, consequently, also assumed that all dropped objects damage the spool or pipeline enough for repair to be required.

This assumption is conservative, because the falling object area (the object will not necessarily indent the pipe in a "knife edge" fashion) and the protection offered by the pipeline coating is neglected.

Consequence Analysis

As stated earlier, this example analysis pays little attention to the consequence of pipeline failure. The only consequence considered is the environmental damage that could be suffered. The category of damage that the environment is likely to suffer is "minor."

12. EXAMPLE 3. USE OF RBIM TO REDUCE OPERATION COSTS

General

The risk-based integrity management approach can be used to achieve the following:

1. **To optimize the intervals between planned shutdowns and the amount of inspections:** The optimization can be conducted through a cost-benefit analysis or structural target reliability levels, particularly where all costs cannot be accounted for.
2. **To select inspection methods:** An inspection method that yields most of the return for the dollars spent for safety and business is to be selected.
3. **To give priority to the areas where risks are highest**: For safety- or business-critical elements, it is necessary to accept additional inspection costs.
4. **To prevent unplanned shutdowns:** The cost associated with loss of production and transportation as a result of an unplanned shutdown can be reduced by focusing inspection effort on safety- and business-critical elements.
5. **To maintain the capacity of oil and gas transportation**: Most of business risk is due to the reduced value of maximum allowable operating pressure.

These targets are achieved through the establishment of inspection programs in which basic questions like what to inspect, when to inspect, and how to inspect are answered.

The cost saving through the use of RBIM needs to be balanced with the costs of applying the RBIM. Much of the inspection expenditure is to satisfy prescriptive legislative requirements and many operators are concerned as to the value derived from such frequent inspection regimes. Risk-based inspection (RBI) is increasingly becoming an interesting and profitable alternative to traditional, frequently performed inspections, which may bring little added value. An optimum interval of inspection may be obtained by minimizing the total costs. The selected interval of inspection, however, should be less than that determined by the requirements of regulatory and company's safety and business criteria.

The use of RBI also allows operating expenditure to be focused on a few "critical elements" that give the greatest return on expenditure.

Inspection Frequency for Corroded Pipelines

The spreadsheet tool receives processed defect data similar to the following format. The safe operating pressure, safety index, and failure probability are calculated for each defect over the remaining life of the line and in Table 8.11. The future corrosion damage in this case is predicted based on de Waard and Lotz [11] and considers process operating conditions. The individual defect failure probabilities are combined to give the failure probability for each segment and the pipeline as a whole.

The nominal P_{safe} is calculated from the equation that follows, using nominal calculated and measured values of X_A and X_L:

$$P_{safe} \equiv \frac{1}{\gamma} \cdot 2 \cdot \sigma_f \cdot \frac{t}{D} \cdot \frac{1 - X_A}{1 - \left(1 + 0.6275 \cdot X_L + 0.003275 X_L^2\right)^{-0.5}} = 137.6 \text{ barg}$$

where

$$X_A \equiv \frac{0.66 L \cdot d}{L \cdot t} \equiv 0.33, \quad X_L \equiv \frac{L^2}{Dt} \equiv 0.4$$

Table 8.11 Input Data

Pipeline Section Properties	Parameter	Unit	Value
Section diameter	D	(m)	1
Section nominal wall thickness	t	(m)	2.50E-02
	δ_t	(m)	0.0005
Factor of safety (new criteria)	γ		2
Usage factor	F		0.72
	SMYS	(MN/m^2)	445
Ultimate tensile strength	UTS	(MN/m^2)	553
MAOP	P	(MN/m^2)	16.02
	P_{yield}	Bar	222.5

Corrosion Damage Parameters	Parameter	Unit	Value
Type (spiral, pit, groove, circum weld)			Groove
Measured max defect depth	d_o	(m)	5.E-03
Stand deviation	σ_{do}	(m)	5.E-04
Average corrosion rate	r	(m/yr)	4.00E-04
Stand deviation	σ_r	(m/yr)	4.0E-05
Measured width		(m)	0.05
Spiral angle		(degree)	90.00
Measured corrosion length	L_m	(m)	0.05

and P_{safe} is the operating pressure that gives an acceptable/desirable safety index (γ), that is, the probability of burst for the individual defect considered ($P_{burst} = \gamma \cdot P_{safe}$).

The mean P_{burst} is calculated by substituting it into the nominal P_{burst} equation, the mean X_A and X_L values are obtained by multiplying the measured value by its bias; that is, $X_{A\ mean} = X_{A\ nominal} \cdot B_{XA}$. The bias is obtained from analysis of experimental data and, for this case, given previously. The equation is further multiplied by the P_{burst} model bias X_M and normalized by dividing through by the SMYS. Thus, the normalized mean P_{burst} (R_m) is given by

$$P_{safe} \equiv 2 \cdot \sigma_f \cdot \frac{t}{D} \cdot \frac{1 - X_A}{1 - \left(1 + 0.6275 \cdot X_L + 0.003275 X_L^2\right)^{-0.5}} \cdot B_{X_F} \cdot B_{X_M}$$

$$= 336 \text{ barg}$$

The mean load is taken to be 137 barg multiplied by the load bias 1.05 giving a mean load of 144.5 barg.

The variance of the mean resistance R_m is estimated from the variances of X_A, X_L, X_F, X_M, the values of which are given previously; thus $V_{Rm} \sim S(V_A^2 + V_L^2 + V_F^2 + V_M^2)^{0.5} \sim 0.212$. The variance for the load (S_m) is taken from Bai et al., 1999 [20] as 0.02. The safety index β is calculated as $[\ln(R_m/S_m)/\sigma_{\ln RS}]$, where

$$\sigma_{\ln RS} = \left\{(\ln[(R_m + V_{Rm}.R_m)/R_m])\right\}^2 + \left\{(\ln[(S_m - V_{Sm}.S_m)/S_m])\right\}^2\}^{0.5}$$

$$= 0.19$$

Thus, $\beta = \ln [336.0/(137.6 \times 1.05)]/(0.19) = 4.56$ and the probability of failure $P_f = 1 - \Phi[\beta] = 2.33 \times 10^{-6}$. This is well below the ultimate limit state acceptance criteria of 1×10^{-4}. Thus, if only this defect exists, the safety factor of 2 can be reduced. For year 0, Table 8.12 calculates the following safety levels for lower safety factors [24].

Table 8.12 Safety Levels

Safety Factor	P_{safe}	Safety Index	P_f
1.8	152.2	4	3.1×10^{-5}
1.6	171.2	3.75	8.61×10^{-5}

Note: For $\gamma = 1.6$, $P_{operating} = 160$ barg.

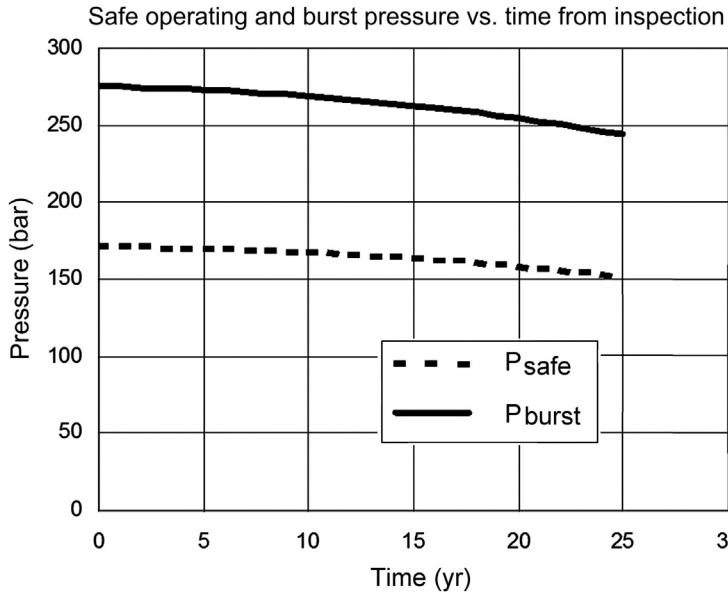

FIGURE 8.8 ***Operating and Burst Pressure Versus Time from Inspection.***

Thus, P_{burst}, P_{safe}, and the safety index are predicted for the service life of the pipeline as illustrated in Figures 8.8 and 8.9. This analysis is repeated for every defect considered and an overall failure probability is established.

If a safety factor greater than 1.6 is required, then the cost of repairing the defect(s) verses reducing the operating pressure needs to be evaluated. However, the defect(s) may be located near the export end of the pipeline, so that the local operating pressure is much less than P_{safe}. Thus, depending on the relative costs, pressure protection systems may be put in place to prevent the local pressure exceeding P_{safe}, without reducing the inlet pressure and transport rates. If a safety factor of 1.6 is adequate (e.g., few significant defects), then initially no pressure derating is required. After approximately 5 years the ULS acceptance criteria is exceeded; at that point, either an intelligent inspection is performed to verify the predicted corrosion damage or the pressure is reduced (to a level that accounts for the uncertainty in predicted corrosion damage), depending on the relative costs. If many defects exist, the particular defects and segments can be ranked in terms of contribution to failure probability. Alternatively, the line could be inspected when the predicted failure probability falls below 1×10^{-4} to establish whether the predicted corrosion rates are correct.

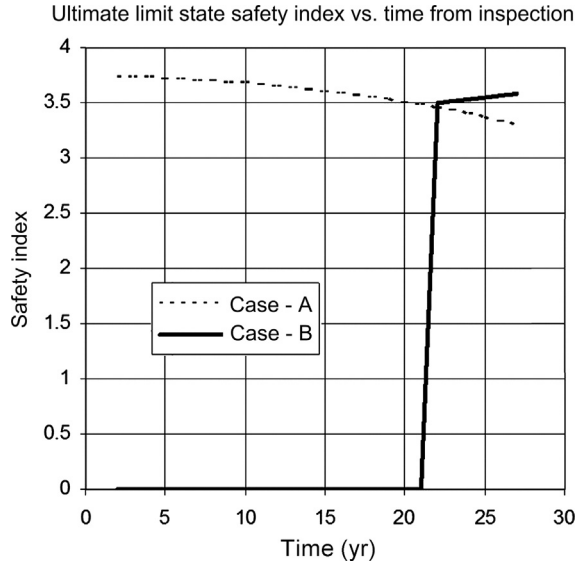

FIGURE 8.9 ***ULS Safety Index Versus Time From Inspection.***

Case B represents the situation where the operating pressure is reduced to P_{safe}.

Examples of Prioritizing Tasks

The RBIM tools can also be used to prioritize which areas to inspect and repair or take other corrective actions. For a pipeline system, all pressure-containing parts that cannot be readily isolated (so that their failure does not affect the overall system) are generally equally critical and cannot be prioritized by this means. However, supporting structures and equipment, such as rock supports, protection structures, and riser support, have varying criticality levels, which can also be used to rank their inspection and maintenance requirements.

From the previous example, the failure predictions for each defect location are plotted versus location and time and compared to required reliability targets, see Figure 8.10.

Due to the high safety risks within the platform safety zone, the target ULS reliability is 1×10^{-5}/yr compared to 1×10^{-4}/yr for the midline. Thus, it can be seen that the defects at KP 0.2 need to be repaired soon and the export pressure needs to be reduced until the repair has been carried out. The defect or segment at KP 20, also within a safety zone, needs to be repaired shortly unless the local operating pressure can be kept below P_{safe}.

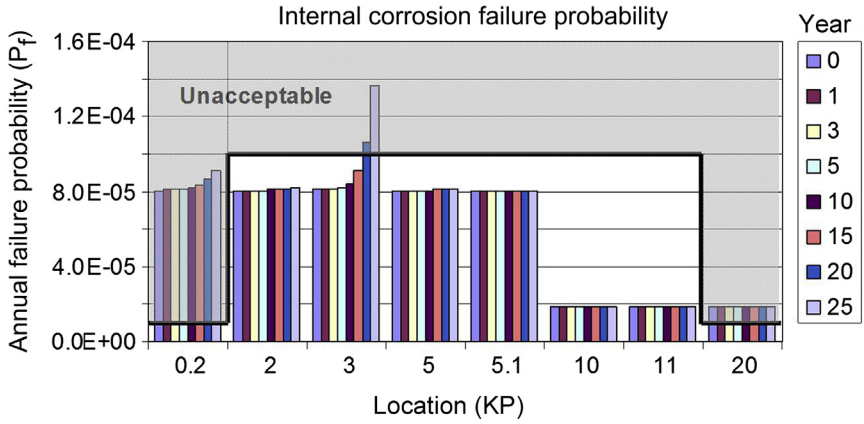

FIGURE 8.10 ***Specific Defect or Location Failure Probability With Time.*** (For color version of this figure, the reader is referred to the online version of this book.)

For the midline section, all defects are within the acceptance criteria, although the one at KP 3 could develop into a concern. Also, overall, these defects exceed the acceptance criteria, so those that pose the greatest likelihood of failure can be repaired first, such as, KP 2.0–5.1.

The local failure predictions can also be converted into local fatality, material loss, and environmental damage risks and compared against risk acceptance criteria. This chapter presents a number of examples and approaches of applying a pipeline risk-based inspection and integrity management.

REFERENCES

[1] Sørheim M, Bai Y. Risk analysis applied to subsea pipeline engineering. St. John's, Canada: Proc. of OMAE'99; 1999.
[2] Willcocks J, Bai Y. Risk based inspection and integrity management of pipeline systems. Seattle, USA: Proc. of ISOPE'2000; 2000.
[3] Total maintenance takes hold on Forties field. Offshore Engineer; November 1993.
[4] PARLOC2001. The update of loss of containment data for offshore pipelines. Prepared by Mott MacDonald Ltd for HSE. 5th Edition. UK: HSE Books; July 2003.
[5] Bea R. The role of human error in the design, construction and reliability of marine structures. SSC-378. Washington, D.C: Ship Structure Committee; 1994.
[6] Williams JC. A data-based method for assessing and reducing human error to improve operational experience. California: Proc. of IEEE, Fourth Conference on Human Factors in Power Plants; 1988.
[7] Swain AD, Guttman HE. Handbook of human reliability analysis with emphasis on nuclear power plant applications. NUREG/CR-1278. Washington, DC: U.S. Nuclear Regulatory Commission; 1981.
[8] Edmondson JN. Human reliability estimates within offshore safety cases. In: Proc. of Symposium on Human Factors in Offshore Design Cases. Scotland: Aberdeen; 1993.
[9] Bea R. Human and organization factors: engineering operating safety into offshore structures. Reliability Eng Sys Saf 1998;61:109–26.

[10] Dougherty EM, Fragola JR. Human reliability analysis. New York: John Wiley and Sons; 1986.
[11] De Waard C, Lotz U. Prediction of CO_2 corrosion of carbon steel; 1993. Paper no. 69. CORROSION/93.
[12] Bai Y, Xu T, Bea R. Reliability-based design and re-qualification criteria for longitudinally corroded pipes. Honolulu, Hawaii: ISOPE'97; 1997.
[13] API 2A-LRFD. Planning, designing and construction of fixed offshore platforms – Load and resistance factor design. Washington, DC: American Petroleum Institute.
[14] Ritchie D, Voermans C, Larsen MH, Vrankx WR. Planning repair and inspection of ageing corroded lines using probabilistic methods. Risk based and limit state design and operations of pipelines. Aberdeen: IBC UK Conferences Ltd; 1998.
[15] HGSystem 3.0, edited by Post, l. Chester, UK: Shell Research Limited.
[16] Fanneløp TE, Lryhming I. Massive release of gas from long pipelines Jan.'81. J Energy 1981.
[17] Rew PJ, Gallagher P, Deaves DM. Dispersion of subsea release, review of prediction methodologies, prepared for the Health and Safety Executive. OTH 95 465. UK: HSE Books; 1995.
[18] Fanneløp TK, Sjøen K. Hydrodynamics of underwater blowouts. The Ship Research Institute of Norway; January 1980.
[19] IChemE A. Guidelines for Evaluating the Characteristics of Vapour Cloud Explosions. Flash Fires, and BLEVEs. New York: American Institute of Chemical Engineers; 1994.
[20] Bai Y, Sørheim M, Nødland S, Damsleth P. LCC modeling as a decision making tool in pipeline design. St. John's, Canada: Proc. of OMAE '99; 1999.
[21] R. Goldsmith R. Lifetime risk-adjusted cost comparison for deepwater well riser systems. OTC 10976. Houston: Offshore Technology Conference; 1999.
[22] OREDA. Offshore reliability data book. Veritec; 1992.
[23] Norwegian Petroleum Directorate. Regulations Concerning Implementation and use of Risk Analysis in the Petroleum Industry, YA-049. Stavanger: Norwegian Petroleum Directorate; 1992.
[24] Sotberg T, et al. The SUPERB Project: Recommended target safety levels for limit based design of offshore pipelines. Yokohama, Japan: Proc. of OMAE'97; 1997.

CHAPTER 9

Risk-Based Inspection

Contents

1. Introduction 213
2. Modeling the Risk 216
   - General 216
   - Causes of Failure 217
   - Probability of Failure 217
   - Consequence of Failure 218
     - *Safety Consequence* *219*
     - *Economic Consequence* *219*
     - *Environmental Consequence* *219*
   - Estimation of Risk 220
3. Acceptance Criteria 221
4. RBI Process 222
   - General 222
   - Screening Assessment 222
   - Initial Assessment 223
     - *PoF Assessment* *224*
     - *CoF Assessment* *224*
     - *Risk Level and Presentation of Risk Results* *225*
   - Detailed Assessment 226
     - *Data Collection* *228*
     - *Identification of Failure Modes* *229*
     - *Segmentation of Pipeline* *229*
     - *Risk Assessment* *229*
     - *Acceptance Criteria* *230*
   - Risk Evaluation and Optimized Inspection Plan 231

References 232

1. INTRODUCTION

The integrity of the pipeline system is an indispensable condition for the continuity of producing oil and gas production. The inspection of subsea pipeline plays a significant role in preventing failures during its in-service operation. In general, inspection and maintenance expense is a large portion of the pipelines' operating costs. Therefore, optimized strategies

Subsea Pipeline Integrity and Risk Management
ISBN 978-0-12-394432-0
http://dx.doi.org/10.1016/B978-0-12-394432-0.00009-3

should be taken to balance the contradiction between direct cost saving from inspection and maintenance activities and basic confidence in integrity of the pipeline system. The methods, frequency, and acceptance criteria used in the inspections can affect the likelihood of failure of the system. The inspection frequencies for the pipelines have traditionally been driven by prescriptive industry practices, usually at time-based intervals. However, these inspection practices do not consider the possibility of failure of a component under its operating and loading conditions, nor the consequences of the failure. It is difficult to recognize whether the service reliability can be achieved by varying inspection methods, locations, or frequencies; therefore, not easily to identify if an inspection activity is excessive and provides no measure of increased assurance for the integrity of the pipeline system.

Risk-based inspection (RBI) is a means to design and optimize an inspection scheme based on the performance of a risk assessment progress using historical database, analytical methods, and experience and engineering judgment. RBI planning is a method for establishing inspection strategy based on the probabilistic risk analysis, where the inspection effort is focused on those elements with a potential to reduce the risk. Inspection planning based on the RBI approach uses safety, economic, and environmental risk of failure as a rational and cost-efficient decision framework for determining: when, what, where, and how to inspect.

The probabilistic risk analysis techniques started in the nuclear industry in 1970s, American Society of Mechanical Engineers (ASME) published first RBI principles overview document in 1991 [1]. American Petroleum Institute (API), Det Norske Veritas (DNV), and American Bureau of Shipping (ABS) developed RBI methodology and software in the middle of 1990s and after [2–6]. RBI provides an excellent tool to evaluate the consequences and likelihood of component failure from specific degradation mechanisms and develop inspection approaches that will effectively reduce the associated risk of failure. However, RBI is still a developing technology. Various RBI methodologies are available in the marketplace, each of them has its own merits and weaknesses. The objective of RBI is to aid the development of optimized inspection, monitoring, and testing plans for meeting specified system acceptance criteria. A commonly used three-step RBI process can be described as follow:

- Define a risk and establish its acceptance criteria. Such as how to define a risk, how frequent is this damage-caused failure going to occur, what

consequences may this damage-caused failure result in, how to judge whether this risk is acceptable or not.
- Assess the risk. Such as what method to be used to assess the risk, how to assess the risk, what level will the risk be categorized, is the risk level acceptable or not.
- Establish inspection plan. Such as when to perform the next inspection based on the risk assessment result, how to perform, and where to look for.

In actual case, defect assessment may be performed in prior to the RBI process, which provides input data, such as what damage may cause a risk, where to look for the damage, how to identify the damage, and etc., to the entire RBI process. In the RBI process, "high risk" areas and major failure modes are identified and analyzed. These data lead us to target inspection and maintenance resources at these areas of the structure or system where they can have the greatest effect in reducing risk, the occurrence probability and consequences of unplanned failures, and to reduce the cost of unproductive inspections.

The RBI progress should be considered as a complement of risk-based integrity management progress. The final object of inspection is to assist pipeline's rectification and integrity maintenance. Once the risk level of the pipeline is identified as unacceptable an inspection or risk reduction activity is initiated, and then the update of the database for risk analysis and the optimized inspection scheme as shown in Figure 9.1.

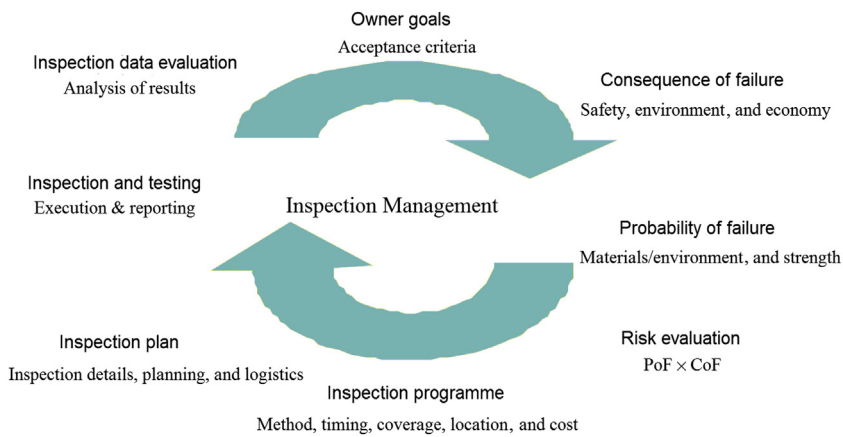

Figure 9.1 RBI Management Processes. *Source: Marley et al. [7].*

2. MODELING THE RISK

General

The implementation of an RBI procedure starts with the determination of the relevant failure modes that should be regarded. After identification of the relevant failure modes, the risk of failure can be assessed by estimating the corresponding probability and consequence in relation to a level that is acceptable, and then the inspection and repair used to ensure the level of risk remains below that acceptance limit. The risk is the combination of the probability of some event occurring during a time period of interest and the consequences associated with the event. In the RBI analysis process, risk matrices are used to calculate the risk of associated component, in which the risk is defined as the product of the probability of failure (PoF) and the consequence of failure (CoF):

$$\text{Risk} = \text{PoF} \times \text{CoF} \qquad [9.1]$$

The risk can be represented in a matrix with the columns and rows as probability and consequence respectively. Three different risk assessment methods are commonly used in RBI process, which are qualitative, quantitative, and semiquantitative methods.

Qualitative methods are based on few essential data and lead to a rough estimation of the failure probability. The qualitative rankings (PoF and CoF rankings) are usually the result of using an engineering judgment-based approach to the assessment, in which a numerical value is not calculated, but a descriptive ranking is given, such as low, medium, or high. The advantages of using a qualitative approach are finishing the assessment quickly at a low initial cost, little requirements for detailed information, and the results easily presented and understood.

Quantitative methods are model-based approaches in which quantitative values are expressed and displayed in qualitative terms by assigning bands for PoF and CoF, and assigning risk values to risk ranks to compare with the risk criteria. A much more wide database is supposed to be well prepared for the quantitative analysis, and the PoF value may be evaluated by using structural reliability method and CoF by well published consequence modeling all in numerical precise.

Semiquantitative methods use more information and calculations, which results in a more accurate failure probability. The quantitative methods consider fully probabilistic approaches and lead to an accurate determination of the existing failure probability. However, in engineering practices, the

data required for the fully quantitative approach is typically not available. Therefore, the semiquantitative approaches are widely used in RBI. Several qualitative and quantitative risk assessments exist [2, 4, 8]. A key to any successful risk analysis is choosing the right method or combination of methods for the problem.

Causes of Failure

Causes of failure for subsea pipelines are commonly divided into two types: time-based damage causes and event-based damage causes.

Time-based damage causes are predictable damages, such as internal corrosion, external corrosion, and erosion etc., which are amenable to inspection. Over time the PoF and hence risk of subsea pipelines increase and the time for inspection of pipeline is determined as the time when the risk exceeds the acceptance limit.

Event-based damage causes are often unpredictable damages, such as dents from dropped objects, fish bombing, free spanning, and changing seabed stability etc., about which the PoF is mainly constant hence the risk is also constant with time. In this case, the inspection interval of pipeline is depended on risk level. When the risk is tolerable, it will not generate a date for inspection. When the risk exceeds the risk limit, however, inspection should be performed at a regular interval.

Probability of Failure

PoF is estimated as failure frequencies of different types of degradation mechanisms operating in the pipeline system. Failure probabilities can be estimated both qualitatively and quantitatively. As shown in Table 9.1, in a qualitative RBI analysis, the exampled failure frequencies are expressed as ranking categories from 1 (very low) to 5 (very high). In a quantitative RBI analysis, however, PoF is usually expressed as the frequencies of an event per unit time numerically, e.g. annual probability.

Table 9.1 Exampled Qualitative & Quantitative Expression of PoF

	PoF				
Qualitative	Very low	Low	Medium	High	Very high
rankings	1	2	3	4	5
Quantitative	$<10^{-5}$	10^{-4}–10^{-5}	10^{-3}–10^{-4}	10^{-2}–10^{-3}	$>10^{-2}$

PoF, probability of failure.

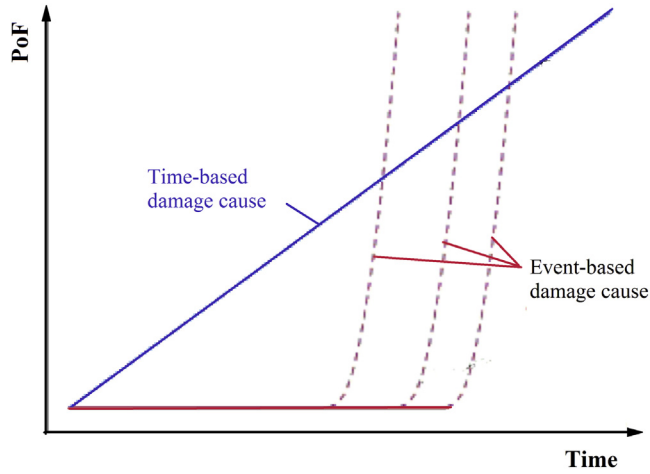

Figure 9.2 Schematic of Damage Progression. (For color version of this figure, the reader is referred to the online version of this book.)

In a qualitative RBI progress, the PoF categories are decided using historical database, analytical methods, and experience and engineering judgment. In a quantitative risk assessment, however, PoF value may be calculated with structural reliability analysis (SRA) method based on soundly built database.

The changing manner of failure probability with time is calculated using degradation models based upon the damage modes and the damage incurred by the pipeline system. Figure 9.2 illustrates the variations of failure probability with time for the two different types of failure causes. For the time-based damage causes, such as corrosion and erosion, PoF of pipeline accumulates over time based on continuous degradation models. This model is usually amenable to inspection as the damage rate allowances for a number of inspections before failure. For the event-based damage causes, such as dropped objects, PoF remains constant during the incubation period, but increase quickly once the events accrued. This model is unpredictable, as inspection does not measure the triggering event.

Consequence of Failure

CoF is defined for all consequences that are of importance to the pipeline owner, such as number of people affected (injured or killed), property damage, amount of a spill, area affected, outage time, mission delay, money lost, or any other measure of negative impact for the quantification of risk. Consequence is usually divided into three categories of safety, economic,

and environmental consequence to be analyzed respectively by qualitatively or quantitatively way.

Safety Consequence

Safety consequence concerns the potential personal injure or life lose usually caused by ignition, explosion, pollution, or toxic release, but failure of pipeline components containing high-pressure nonhazardous fluids alike. And the location of personnel at different phases of operation will influence the severity of safety consequence.

Economic Consequence

Economic consequence concerns both the business loss of production interruption and the cost of repairs due to the failure of pipeline component. Leak and rupture are two typical failure modes to initiate repair activities and the location of the failure (e.g. above water, splash zone, etc.) will influence the repair consequence.

Economic consequences due to business interruption or deferred production relate to the costs due to the shutdown of the pipeline and contract penalties (these can be extremely severe). The use of redundant by-pass lines in the pipeline system is an important way used to maintain the production.

A detailed quantitative methodology by which to evaluate the cost of consequence has been developed by Bai [9, 10] and can also be used to minimize these potential costs to the owner of the pipeline.

Environmental Consequence

The environmental consequence is defined as the damage to the ecosystem and it can be short-term (clean-up) and long-term affects both locally and globally. Generally, the consequence is directly associated with the product leakage due to the damage of pipelines. The combination of clean-up costs, regulatory fines, and loss of public relations should be evaluated as a factor within the RBI consequence evaluation, as well as the long-term impact on the environment for each release scenario. Relevant information that is needed to determine consequence includes fluid type, phase, release rate, inventory release, toxicity, and flammability.

The environmental consequence can be determined in terms of the following factors.

- The category of fluid. A detrimental consequence will usually only arise from fluid releases (i.e. oil).
- The location of release. A pollution impact assessment will provide an understanding of the sensitivity and balance of the surrounding

Table 9.2 Exampled Qualitative & Quantitative expression of CoF

	A	B	C	D	E
CoF Rankings	**Very low**	**Low**	**Medium**	**High**	**Very high**
Safety (deaths)	0	0.1	1	10	100
Environmental (recovery period)	0	<1 year	<3 years	<10 years	>10 years
Economic (MNOK)	<250	250	500	750	>750

CoF, consequence of failure. MNOK, Million Norwegian Krone.

ecosystem, such that an assessment can be made of the damage incurred by contamination of the fluid being transported.

- The volume and dispersion of release. The volume of release is dependent on both the rate and the duration of the release. The dispersion of the release will be different for subsea and atmospheric releases. This analysis can be undertaken using an appropriate program.

All the factors referred above influence the recovery period of the environment significantly. The release of production, which boasts no polluting properties at all causes the minimum defect to the ecosystem with zero recovery periods. If there is a polluting production release, the severity of pollution depends on the magnitude of dispersion area and location of release. The data in Table 9.2 is only a sample of measuring environmental consequences by recovery periods [10]. Table 9.2 shows exampled qualitative and quantitative expresses of CoF for a pipeline system. For a qualitative evaluation in RBI analysis of pipeline system, failure consequence is expressed as ranking categories from A (very low) to E (very high). For every ranking of CoF from A (very low) to E (very high), there will be a quantitative consequence interval correspondingly.

Estimation of Risk

The risk associated with a failure from a given degradation mechanism is estimated as the combination of the PoF and the CoF. The risk can be presented as a matrix of CoF and PoF categories. To achieve adequate resolution of detail, a 5 × 5 risk matrix shown in Table 9.3 is recommended. The matrix has PoF on the vertical axis and CoF on the horizontal.

In the table, the risk matrix shows three risk levels: low risk, medium risk, and high risk, and the risk increases from low level at the left-bottom corner to high level at the right-top corner. Normally, low risk is acceptable, and action such as general visual inspection needs to be taken to ensure

Table 9.3 Example of Risk Matrix [11]

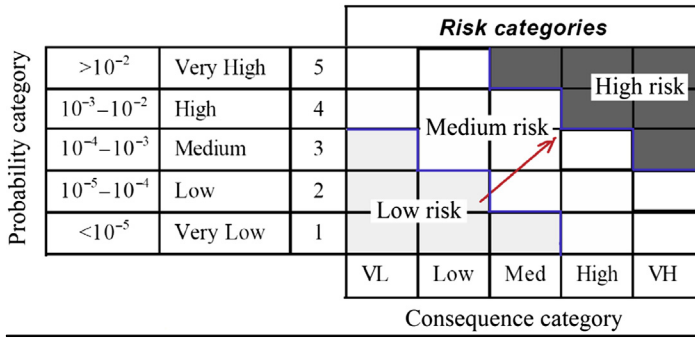

that risk remains within this region. Medium risk is also acceptable and action, such as Nondestructive testing, functional tests, and other condition monitoring activities should be taken to measure extent of degradation and ensure risks do not rise into the high-risk region. High risk is unacceptable and action must be taken to reduce probability, consequence, or both to ensure that risk lies within the acceptable region.

3. ACCEPTANCE CRITERIA

In RBI process, risk acceptance criteria need to be established previously to compare with the result of risk analysis to assist decision. The acceptance criteria are targets of risks reduction and help maintain the confidence in pipeline integrity. The acceptance criteria are developed by various regulatory bodies, design codes, and operators based on previous experience, design code requirements, national legislation, or risk analysis. Thus the acceptance criteria adopted is often dependent on the relevant authority and owner of the pipeline.

In qualitative RBI progress, risk is commonly presented in a 5×5 matrix with PoF on the vertical axis and CoF on the horizontal axis as showed in Table 9.3. Risk matrices can graphically illustrate the progress of how the risk is evaluated and how the inspection priorities in the strategy are developed. The risk's reduction is also shown when effective measures have been taken to reduce the ranks of PoF or CoF. The risk matrix can be further broken down into individual matrices for safety, economic, and environmental risk, respectively as shown in Table 9.4. The acceptance criteria are generally expressed in terms of safety risk, economic risk, and

Table 9.4 Risk Ranking Matrix (For color version of this table, the reader is referred to the online version of this book.)

5	$>10^{-2}$	Unacceptable area				
4	10^{-2}–10^{-3}					
3	10^{-3}–10^{-4}					
2	10^{-4}–10^{-5}	Acceptable area				
1	0–10^{-5}					
		A	B	C	D	E
Safety (deaths)		0	0.1	1	10	100
Enviromental (recovery period)		0	< 1 year	< 3 years	< 10 years	> 10 years
Economic (MNOK)		<250	250	500	750	>750

environmental damage with respect safety. While in quantitative RBI process, all the chosen traditional criteria should be transformed to risk matrices and the most important thing is to design the risk limit of unacceptable risk area.

4. RBI PROCESS

General

The basic RBI process may be divided into the following four steps:

- Screening assessment.
- Initial assessment.
- Detailed assessment.
- Risk evaluation and optimized inspection plan.

The RBI assessment starts from the collections of information for screening, and other steps of the process. The first step of RBI assessment process is the screening assessment. It is performed to focus the risk assessment on the critical failure causes identified from a wide range of possible failure causes for the various components of a pipeline system.

Screening Assessment

In the screening step, each pipeline is addressed for all damage causes. In this step, both PoF and CoF values are identified as "insignificant" or "potential". The initial assessment is initiated based on the screening results only when the both PoF and CoF values for the respective failure causes are

Table 9.5 Example of Screening Matrix

	CoF Insignificant	CoF Potential
PoF potential	Corrective maintenance	Initial assessment initiated
PoF insignificant	Minimum surveillance	Preventive maintenance and/or monitoring

PoF, probability of failure; CoF, consequence of failure.

evaluated as "potential". Some general advices of further actions on the results of screening assessment are given in Table 9.5 as an example of screening matrix.

- When the PoF is "insignificant", the inspection has no effect on further reducing the risk; if the CoF is also "insignificant", then the recommended action is minimal surveillance.
- If the PoF is "insignificant", but the CoF is "potential", then preventive maintenance and/or monitoring should be considered to address the risk.
- When the PoF is "potential", but the CoF is "insignificant", then the inspection can be used to reduce risk, but is unlikely to be cost-effective. A likely cost-effective solution is often to carry out corrective maintenance in case of failure.
- Where both the PoF and CoF are "potential", the inspection can be effective in reducing the risk level. The introduction of measurer for reducing the CoF should further be evaluated.

Damage causes may be grouped into three categories:

- Event-based. For example, dropped object, dragging trawl gear, landslide, anchor drop, and etc.
- Condition-based. For example, change in pH, in operating parameters, or in CP (cathodic protection) system, and etc.
- Time-based. For example, corrosion, erosion, fatigue, and etc.

The screening process should be carried out in workshop environment by the RBI team as part of a working session.

Initial Assessment

In most cases, initial assessment is a semiquantitative assessment of the criticality of the pipeline systems considered to identify an inspection-planning program based on the limited information provided.

Table 9.6 PoF Categories

PoF	Identification	Description
1	Very low	So low frequency that event considered negligible.
2	Low	Event rarely expected to occur.
3	Medium	Event not expected to happen on individual components, but integrated over a large number of comp. has the probability of happening once a year.
4	High	Event individually may be expected to occur during the lifetime of the pipeline. (Typically a 100-year storm)
5	Very high	An event expected to happen more than once over the service life.

PoF, probability of failure.

In this step, the PoF and CoF rankings are expressed in a risk matrix. For example, a 5×5 risk matrix used consists of a vertical axis of PoF and a horizontal axis of CoF. Both the PoF and CoF are ranking in five categories with PoF from 1 (Very low) to 5 (Very high) and CoF from A (Very low) to E (Very high).

PoF Assessment

The PoF can vary from very low to very high or numerically express from 1 to 5 correspondingly, as described in Table 9.6. These ranks may be divided in terms of typical annual failure probability based on engineering judgments as defined in DNV-RP-F107 [12].

CoF Assessment

There are a large numbers of expression rules from available engineering experiences to assist for judging the CoF rankings: safety, economy, and environmental. Sample indications of the ranking for safety, economy, and environmental are given in Tables 9.7, 9.8, and 9.9.

For the three consequence-categories considered, the following aspects are accounted for:

Safety Consequence

- Product transported.
- Manning on installations.

Environmental Consequence

- Product transported.
- Pipeline size/Gross flow rate.

Table 9.7 Safety CoF Ranking [12]

CoF	Identification	Description
A	Very low	No person(s) are injured.
B	Low	(not used)
C	Medium	Serious injury, one fatality (working accident)
D	High	(not used).
E	Very high	More than one fatality (gas cloud ignition)

CoF, consequence of failure.

Economy Consequence

- Product transported.
- Pipeline size/Gross flow rate.

Risk Level and Presentation of Risk Results

As the categories of PoF and CoF for specific failure causes acting on a pipeline system have been obtained from the above analyses, the risk

Table 9.8 Economy CoF Ranking [12]

CoF	Identification	Description
A	Very low	Insignificant effect on operation, small or insignificant cost of repair
B	Low	Repair can be deferred until scheduled shutdown, some repair costs will occur.
C	Medium	Failure causes extended unscheduled loss of facility or system and significant repair costs. Rectification requires unscheduled underwater operation with prequalified repair system before further production.
D	High	Failure causes indefinite shutdown and significant facility or system failure costs. Rectification requires unscheduled underwater operation without prequalified repair system before further production. Or Failures resulting in shorter periods of shut down of major parts of the hydrocarbon production for the field.
E	Very high	Total loss of pipeline and also possible loss of other structural parts of the platform. Large cost of repair including long time of shut down of production. Or Failures resulting in shutdown of the total hydrocarbon production for a longer period.

CoF, consequence of failure.

Table 9.9 Environmental CoF Ranking [12]

CoF Identification		Description
A	Very low	None, small, or insignificant on the environment. Either due to no release of internal medium or only insignificant release.
B	Low	Minor release of polluting media. The released media will decompose or be neutralized rapidly by air or seawater.
C	Medium	Moderate release of polluting medium. The released media will use some time to decompose or neutralize by air or seawater, or can easily be removed.
D	High	Large release of polluting medium, which can be removed, or will after some time decompose or be neutralized by air or seawater.
E	Very high	Large release of high polluting medium, which cannot be removed and will use long time to decompose or be neutralized by air or seawater.

CoF, consequence of failure

categories for the pipeline are established by combining both of them in a 5 × 5 matrices. Table 9.10 shows an example of risk ranking matrix. Table 9.11 describes the different responding for each risk in the categories. An As-low-as-reasonably-practicable (ALARP) region has been indicated and represented by the "M" risk level in Table 9.10. It identifies an area where the risk is acceptable, however further reduction of the risk should be pursued with cost-benefit evaluation.

Detailed Assessment

Figure 9.3 shows a flowchart of RBI procedure for a pipeline system. In the detailed assessment, the PoF and CoF are more thoroughly analyzed than those in the initial assessment. The PoF and CoF rankings are numerically depicted. Much more wide database is requested to be well prepared for the

Table 9.10 Example of Risk Ranking Matrix for All Consequence Categories (For color version of this table, the reader is referred to the online version of this book.)

5	Very high	M	H	H	VH	VH
4	High	L	M	H	H	VH
3	Medium	L	L	M	H	H
2	Low	VL	L	L	M	H
1	Very low	VL	VL	L	L	M
POF / COF		A	B	C	D	E

Table 9.11 Risk Categories Rankings

Risk Factor	Risk Identification	Description
VL	Very low	Risk considered to be none, small, or insignificant. Further action is not required.
L	Low	Risk considered to be minor. Initiation of further action should be evaluated.
M	Medium	Risk considered to be medium. At next inspection in the plan, action should be implemented.
H	High	Risk considered to be high. Inspection reports should be reviewed. In an advisable time, action should be implemented to reduce risk.
VH	Very high	Risk considered to be severe. Inspection reports should be reviewed immediately. If no more information is obtained, initiation of action should be implemented immediately to reduce risk.

quantitative analysis, and the PoF value may be evaluated by using structural reliability method and the CoF by well published consequence modeling in numerical precise.

The detailed assessment is performed on a component level, defining the different sections of the pipeline. This is in contrast to the initial assessment,

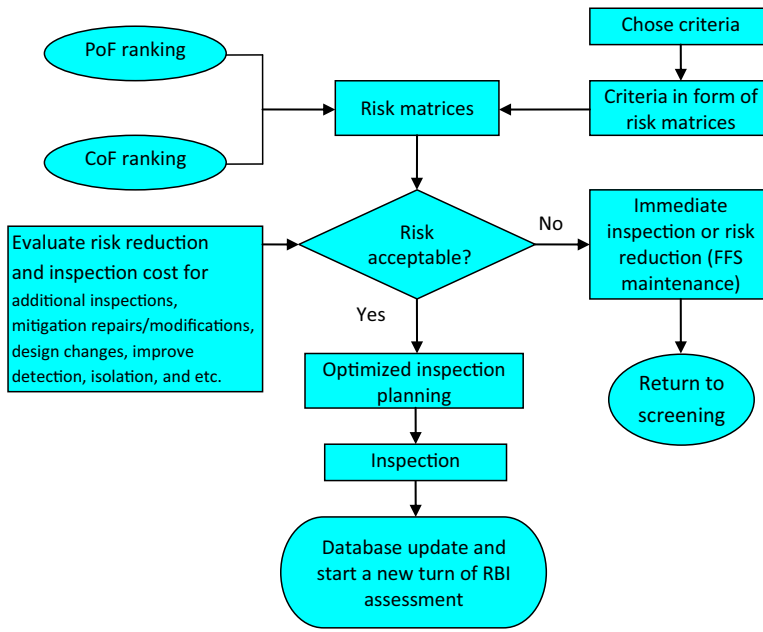

Figure 9.3 Flowchart of RBI Procedure (FFS, Fitness-for-Service).

which considers the whole pipeline system as one component. Furthermore, the detailed assessment considers individual degradation mechanisms resulting in damage, in contrast to the overall damage cause used in the initial assessment [13].

The detailed assessment may involve the following steps:

- Segmenting the target pipeline.
- Identifying the component damage causes and degradation mechanisms.
- Assessing PoF for each degradation mechanisms.
- Assessing CoF with consideration of safety, economy, and environmental effects.
- Determining risk level for each pipeline segment and degradation mechanisms.
- Ranking pipeline segments according to critical risk level or acceptance criteria.
- Developing inspection plan/alternative remedial actions.

Results from inspections and monitoring are vital information in the RBI process, and the full benefits of RBI are seen when the method is utilizing historical inspection results. Before having any inspection results, it is necessary to use a conservative approach incorporating predication uncertainties in the modeling of potential degradation rates. These uncertainties can be reduced based on inspection results.

The damage causes considered in the initial assessment are also the basis for the detailed assessment, but each damage cause can cover several degradation mechanisms. For instance there are several degradation mechanisms that can result in the damage cause "internal corrosion", as for instance CO_2 corrosion, H_2O corrosion, bacteria etc.

The detailed assessment considers the degradation mechanisms, in contrast to the initial assessment that addresses the damage causes. Detailed assessment therefore requires more detailed information regarding, for example for internal corrosion, information about the product and operation. Following is an example of detailed RBI assessment of subsea pipelines.

Data Collection

Before the RBI assessment, data gathering is performed for the operating pipelines first. The data are available in electronic or paper format. For some pipelines only basic data were available, such as pipe outer diameter, wall thickness, operating pressure, and transported medium.

Identification of Failure Modes

An identification of the failure modes is carried out by evaluating the historical data provided by the operator and an RBI team workshop with the operator's staff. The following major threats are identified for aged pipelines:

- Corrosion.
- Impact.
- Fatigue.

Segmentation of Pipeline

As the risk is not constant along a pipeline route, it is beneficial to divide the pipeline into segments, in which each pipeline segment has an approximately constant PoF and a constant CoF. Based on the collected data and the identified failure modes the pipeline may be divided into segments as shown in Figure 9.4. Along the pipeline route the PoF and CoF may change due to different wall thickness, environmental conditions, water depth, crossing locations, and etc. For each segment, the PoF and CoF are nearly constant and have to be assessed separately.

Risk Assessment

For the risk assessment, the PoF and CoF are evaluated for each pipe segments. The quantitative level of PoF evaluation may performed based on the SRA method. The PoF is dependent on the likelihood of the loading exceeding the pipelines strength/resistance. The SRA approach has been

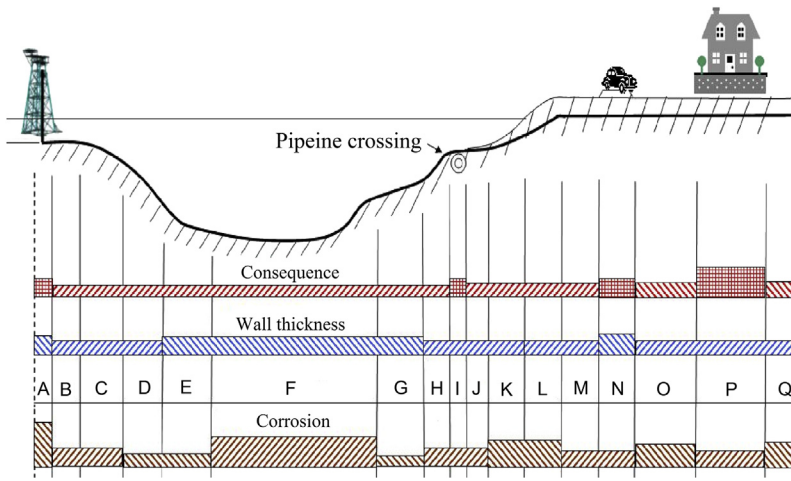

Figure 9.4 Segmentation of Pipeline *Source: Stadie-Frohbös et al. [14].* (For color version of this figure, the reader is referred to the online version of this book.)

detailed in Chapter 8 and the PoF is calculated for each pipe segments. The probabilities for all segments are then combined to give the safety index and failure probability of the whole pipeline. In addition to the PoF, the CoF assessment is also found in Chapter 8 of this book and other documents [10,15]. The financial, environmental, and safety aspects are considered in the risk analysis.

Acceptance Criteria

The safety principles adopted in DNV OS-F101 [16] utilize risk principles, where the target annual failure probability is dependent on the consequence of a failure. The different pipe segments are divided into different safety classes depending on the pipe content and location of each segments.

The safety classes include: high, normal, and low. The safety classes detailed in DNV-OS-F101 are dependent on category of fluid transported and location of pipeline. The default target safety level is a total annual failure probability of 10^{-5} for failure modes that cause a threat to personnel. For nonhazardous fluids, a failure probability of 10^{-4} is defined as acceptable, as shown in Table 9.12.

The above failure probabilities apply for so-called "Ultimate Limit State". The failure of pipeline means that the pipeline is subject to a loss of containment incident and no longer able to operate. A maximum acceptable risk level can be defined for an operating pipeline, and when this acceptable limit is exceeded, an inspection or other remedial actions have to be taken. The maximum level can be considered in different ways, such as risk cost, safety risk, risk of large hydrocarbon release to environment, and etc. The risk cost is defined as the consequence cost multiplied by the annual probability for this cost.

The acceptable or tolerable risk level for the pipeline should be defined for a detailed assessment. The risk level that operators accept or tolerate is a balance between the cost to reduce the risk and the consequence in case of a failure. The acceptable risk level within a risk category, such as economy and environment, may not be defined by only one risk value, but a combination of probability and consequence.

Table 9.12 Acceptable Annual Failure Probability per Pipeline [17]

Safety Class		
Low	**Normal**	**High**
10^{-3}	10^{-4}	10^{-5}

Risk Evaluation and Optimized Inspection Plan

The risk analysis results from above are the present risk level, and its increasing rate and then the future risk level are also predictable for time-based damages of a pipeline. Figure 9.5 illustrates the variation of risk with time, and the next inspection is figured out by comparing with the acceptance criteria. For time-based damage causes, the risk level increases continuously with time. Once the acceptable risk limit defined according to given criteria prior is exceeded, an inspection will be initiated. The increase velocity of risk depends on the increase rate of PoF. For each damage type, for example, corrosion, the time increments for development of the PoF are determined depending on the corrosivity of the fluid, level of monitoring, operation temperature, protection system, and etc. In the figure, the system is assigned the PoF based on inspection, and the PoF increases by 1 unit by the determined time increments. Thus an inspection interval and the next time for inspection can be predicted.

Event-based damage causes are often unpredictable damages, for example, pipe dents from dropped objects, fish bombing, free spanning, and changing sea-bed stability, and etc. The PoF is mainly constant in a long unknown incubation period, but the failure risk develops quickly after that period. In this case, the inspection interval is depended on risk level. When the risk is tolerable, it will not generate a date for inspection. However, inspection should be performed at a regular interval. Table 9.13 shows the inspection intervals for event-based damage cause. The higher the risk rank is, the more frequently the inspection is performed.

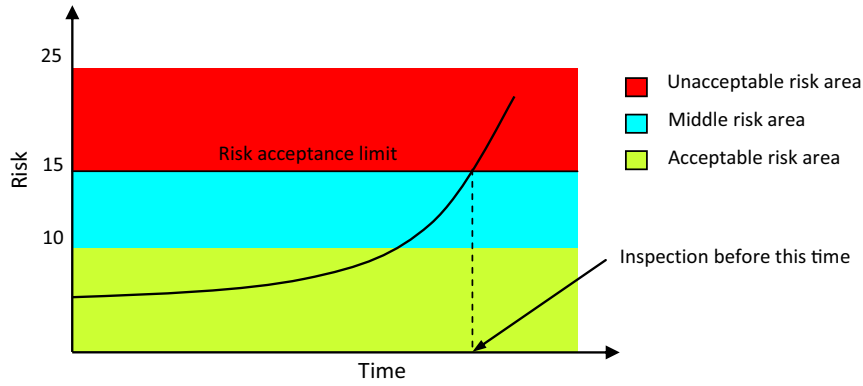

Figure 9.5 Setting of Inspection Intervals. (For color version of this figure, the reader is referred to the online version of this book.)

Table 9.13 Event-based Damage Cause Inspection Criterion

PoF:	Inspection Intervals, Event-based (example)				
5	NO	4	2	1	1
4	NO	6	4	2	1
3	NO	10	6	4	2
2	NO	10	10	6	4
1	NO	NO	NO	NO	NO
CoF:	A	B	C	D	E

PoF, probability of failure; CoF, consequence of failure

REFERENCES

[1] ASME. Risk-based inspection-development of guidelines: general document. New York: American Society of Mechanical Engineers; 1991.
[2] ABS. Guidance notes on risk assessment applications for the marine and offshore oil and gas industries. Houston: American Bureau of Shipping; 2000.
[3] ABS. Guide for surveys using risk-based inspection for the offshore industry. Houston: American Bureau of Shipping; 2003.
[4] API. Risk-based inspection. API-RP-580. 2nd ed. Washington, DC: American Petroleum Institute; 2009.
[5] DNV. Integrity management of submarine pipeline systems. DNV-RP-F116. Oslo, Norway: Det Norske Veritas; 2009.
[6] DNV. Risk based inspection of offshore topsides static mechanical equipment. DNV-RP-G101. Oslo, (Norway): Det Norske Veritas; 2010.
[7] Marley MJ, Jahre-Nilsen C, Bjørnøy OH. RBI planning for pipelines. Stavanger (Norway): Proc. of ISOPE; 2001.
[8] Muhlbauer W. Pipeline risk management manual. 3rd ed. Houston: Elsevier; 2004.
[9] Sørheim M, Bai Y. Risk analysis applied to subsea pipeline engineering. St. John's (Canada): Proc. of OMAE; 1999.
[10] Bai Y, Bai Q. Subsea pipelines and risers. Oxford (UK): Elsevier Science; 2005.
[11] Bjørnøy OH, Jahre-Nilsen C, Marley MJ, Williamson R. RBI planning for pipelines, principles and benefits. Rio de Janeiro (Brazil): Proc. of OMAE; 2001.
[12] DNV. Risk assessment of pipeline protection. DNV-RP-F107. Oslo (Norway): Det Norske Veritas; 2010.
[13] Bjørnøy OH, Jahre-Nilsen C, Eriksen Ø, Mørk K. RBI planning for pipelines description of approach. Rio de Janeiro (Brazil): Proc. of OMAE; 2001.
[14] Stadie-Frohbös G, Lampe J. Risk based inspection for aged offshore pipelines. Nantes (France): Proc. of OMAE; 2013.
[15] Willcocks J, Bai Y. Risk based inspection and integrity management of pipeline systems. Seattle (USA): Proc. of ISOPE; 2000.
[16] DNV. Submarine pipeline systems. DNV-OS-F101. Oslo (Norway): Det Norske Veritas; 2007.
[17] DNV. Corroded pipelines. DNV-RP-F101. Oslo (Norway): Det Norske Veritas; 2010.

CHAPTER 10

Reliability-Based Strength Design of Pipelines

Contents

1. Introduction 233
2. Failure Probability 234
3. Uncertainty Measures 234
   Selection of Distribution Functions 234
   Determination of Statistical Values 235
4. Calibration of Safety Factors 235
   General 235
   Target Reliability Levels 235
5. Reliability-Based Determination of Corrosion Allowance 236
   General 236
   Reliability Model 237
      Determination of Corrosion Rate *238*
      Determination of Maximum Allowable Defect Depth *239*
   Design Examples 239
      Dry Gas Line *239*
      Wet Liquid Line *241*
   Discussion 243
   Recommendations 244
References 245

1. INTRODUCTION

One of the major contributions to the oil and gas field development costs is the wall thickness of subsea pipeline systems for the transport of oil and gas. The wall thickness is determined from the loads that the pipeline must sustain in both installation and operating conditions. For shallow waters, the internal pressure usually dictates the pipeline design, but for deeper waters, the external hydrostatic pressure exerts an increasing influence. In addition to external loads such as waves and currents, uneven seabed, trawl boards, pullovers and expansion needs to be considered. However, uncertainties exist in the design parameters and wall thickness, which should be considered in the design. The reliability of the pipeline should be subjectively evaluated to save costs without unnecessary conservatism.

Subsea Pipeline Integrity and Risk Management
ISBN 978-0-12-394432-0
http://dx.doi.org/10.1016/B978-0-12-394432-0.00010-X

In principle, reliability-based design of subsea pipelines involves the following aspects:

- Identification of failure modes for specified design cases.
- Definition of design formats and limit state functions (LSFs).
- Uncertainty measurements of all random variables.
- Calculation of failure probability.
- Determination of target reliability levels.
- Calibration of safety factors for design.
- Evaluation of design results.

2. FAILURE PROBABILITY

Generally, limit state function is introduced and denoted by $g(Z)$, where Z is a vector of all uncertainty variables. Failure occurs when $g(Z) \leq 0$. For a given LSF with g(Z), the probability of failure P_f is defined as

$$P_f(t) = P[g(Z) \leq 0] \tag{10.1}$$

The results of failure probability can also be expressed in terms of a reliability (safety) index, β, which is uniquely related to the failure probability by

$$\beta(t) = -\Phi^{-1}\left[P_f(t)\right] = \Phi^{-1}\left[-P_f(t)\right] \tag{10.2}$$

where $\Phi(\cdot)$ is a standard normal distribution function.

Two general approaches are available to solve Eq. [10.1]: analytical and simulation methods, respectively, which were discussed in last two chapters and in *Marine Structure Design* [1].

3. UNCERTAINTY MEASURES

Considering the uncertainties involved in the design format, each random variable, X_i, can be specified as [2]

$$X_i = B_x \cdot X_C \tag{10.3}$$

where X_C is the characteristic value of X_i, and B_x is a normalized variable reflecting the uncertainty in X_i.

Selection of Distribution Functions

Usually, the determination of a distribution function is strongly influenced by the physical nature of the random variables. Also, it may be related to a

well-known description and stochastic experiment. Experience from similar problems is also very useful. If several distributions are available, it is necessary to identify by plotting the data on a probability paper, by comparing the statistical tests, and so forth. Normal or lognormal distributions are normally applied when no detailed information is available. For instance, resistance variables are usually modeled by a normal distribution, and a lognormal distribution is used for load variables. The occurrence frequency of a damage (e.g., an initial crack) is described by a Poisson distribution. An exponential distribution is used to model the capacity of detecting certain damage [3].

Determination of Statistical Values

Statistical values used to describe a random variable are mean value and coefficient of variation (CoV). These statistical values shall normally be obtained from recognized data sources. Regression analysis may be applied based on methods of moment, least-square fit methods, maximum likelihood estimation techniques, and the like.

4. CALIBRATION OF SAFETY FACTORS

General

One of the important applications of structural reliability methods is to calibrate safety factors in design format to achieve a consistent safety level. The safety factors are determined so that the calibrated failure probability, $P_{\mathrm{f,i}}$, for various conditions is as close to the target reliability level P_{f}^{T} as possible:

$$\sum f_{\mathrm{i}}\left(P_{\mathrm{f,i}}(\gamma) - P_{\mathrm{f}}^{T}\right)^{2} = \text{minimum} \qquad [10.4]$$

where f_{i} is the relative frequency of the design case number i.

Target Reliability Levels

When conducting structural reliability analysis, target reliability levels in a given reference time period and reference length of pipeline should be selected. The selection is based on consequence of failure, location and content of pipelines, relevant rules, access to inspection and repair, and so on. The target reliability levels have to be met in design to ensure that certain safety levels are maintained [4].

Target reliability levels may be specified by the operator, guided by authority requirements, design philosophy, and risk attitude in terms of

Table 10.1 Target Reliability Levels

	Safety Classes		
Limit States	**Low**	**Normal**	**High**
SLS	10^{-1}–10^{-2}	10^{-2}–10^{-3}	10^{-2}–10^{-3}
ULS	10^{-2}–10^{-3}	10^{-3}–10^{-4}	10^{-4}–10^{-5}
FLS	10^{-3}	10^{-4}	10^{-5}
ALS	10^{-4}	10^{-5}	10^{-6}

Source: Sotberg et al. [5].

economics. The target reliability level for damaged pipelines should be defined in the same level as intact pipeline. The target reliability level needs to be evaluated, considering the implied safety level in the existing rules and codes. The following safety classes are proposed for evaluating the target reliability levels:

- **Low safety class:** Here, failure implies no risk of human injury, minor environmental damage, and economic consequences.
- **Normal safety class:** This is a classification for temporary conditions where failure implies risk of human injury, significant environmental, and economic consequences.
- **High safety class:** This is a classification for operating conditions where failure implies risk of human injury, significant environmental, and economic consequences.

Sotberg et al. proposed target reliability levels, shown in Table 10.1, for the limit state based design of subsea pipelines [5].

5. RELIABILITY-BASED DETERMINATION OF CORROSION ALLOWANCE

General

This subsection is based on the papers by Nødland et al. [6, 7].

To calculate the pipeline reliability accurately, sufficient statistical data must be available as a basis for describing key input parameters in the form of probability distribution functions. In addition, an element of engineering judgment must be included. The reason for this is that experiences from a particular pipeline or from the laboratory are never directly transferable to a new pipeline, because differences always exist, such as amount and chemical composition of water, flow regimes, and condensation rates. Furthermore, the methods available to calculate corrosion rates are

empirical or semi-empirical and, as such, valid only for a narrow band of operating parameters (i.e., flow rate, temperature, pH, and pressure). The picture can be further complicated by possible formation of scales or deposits on the pipe wall. In addition, the corrosion rate model normally used, that is, the deWaard-Milliams or Shell formula, deWaard et al. [8, 9] is based on laboratory data only and generally recognized to be very conservative when applied to "real life."

At present, statistical data that can be used in a reliability analysis of subsea pipelines are limited. Some data exist to give a reasonable representation of the uncertainty in defect lengths in gas lines and pipe wall thickness. When it comes to the calculation of corrosion rates, very little work has been carried out to provide a statistical basis from which to work. Therefore, the probability functions are estimated primarily from engineering judgment. Hence, the reliability found from the calculated probabilities of failure (or unacceptable corrosion depth) should not be taken as an exact value but rather as a subjective evaluation of pipeline reliability [10].

The calculated reliability can then be used in life cycle cost (LCC) analyses, where the combination of corrosion allowance and operating parameters that give the highest net present value (NPV) represent the optimum corrosion allowance. Following this approach, the relative effect of different design and operating parameters on the pipeline reliability may be evaluated.

The scope of this section is to describe a method to calculate the reliability of a corroded pipeline for different design and operating parameters. Examples are included to illustrate the effect of different parameters on the reliability.

Reliability Model

Corrosion in a pipeline becomes unacceptable when the corrosion depth exceeds the allowable amount This can be described by the limit state function, as by Edwards et al. [11]:

$$g(\overline{X}) = d - \mathrm{CR} \cdot t \qquad [10.5]$$

where

d = maximum allowable corrosion depth
CR = corrosion rate
t = duration of wet service
$\overline{X}$= vector containing all the basic uncertainty variables

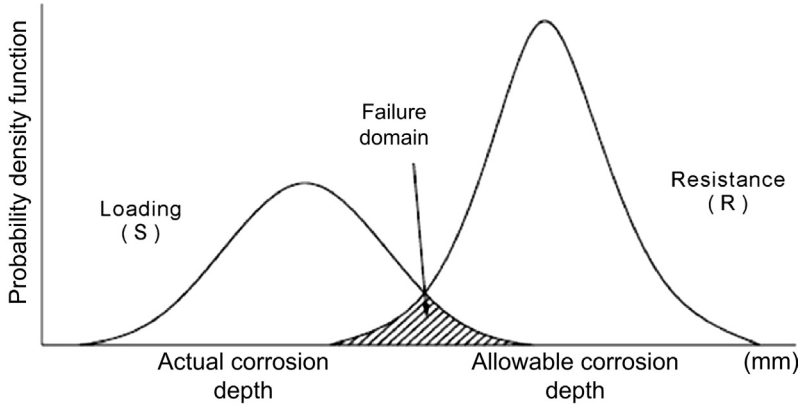

FIGURE 10.1 ***Probabilistic Limit State Function.***

Because the parameters in g cannot be determined precisely, probability distributions are used to describe the parameters, which are shown in Figure 10.1.

The corrosion is unacceptable in the shaded region of the figure, representing a high corrosion rate and a low allowable corrosion depth. This corresponds to $g(\overline{X}) < 0$, which is the criterion for failure. The probability of failure therefore is

$$P[g(\overline{X}) < 0] = \int_V f_{\overline{X}}(\overline{x}) d\overline{x} \qquad [10.6]$$

where

V = failure domain = $\{\overline{x} | g(\overline{X}) < 0\}$

$\int_V f_{\overline{X}}(\overline{x})$ = joint probability density function for $\overline{X}$

$\overline{X}$ = realization of X in the basic variable space

The reliability is expressed as a function of (1.0 – probability of failure). The calculation of the probability of nonacceptance is carried out using the proprietary software STRUREL (RCP, 1996), where the second-order reliability method (SORM) is used [12].

Determination of Corrosion Rate

Corrosion rates (CRs) can be based on empirical equations (e.g., Shell models by deWaard et al [9, 10]) or on experience or measured data. In a pipeline design, a combination of these and sound engineering judgment from a qualified corrosion engineer is necessary. In the examples that follow,

a deterministic corrosion rate (based on deWaard et al., 1995 [9]) is multiplied by a probabilistic variable, x_m, called the *corrosion rate uncertainty factor*. Engineering judgment and operational experience are used to determine x_m.

Determination of Maximum Allowable Defect Depth

Formulas for calculating the maximum allowable defect depth, d, are available from codes or from the literature [13]. In the examples presented next, d is based on ASME B31G. This means that the calculated reliability is not based on a failure probability but rather on a probability of not satisfying the acceptance criteria of ASME B31G.

Design Examples

Two examples are given to show how the reliability of a pipeline may be calculated and how changing the corrosion allowance affects the calculated reliability. In each example, a sensitivity study is done to demonstrate the effect of future operation on the pipeline reliability. The results from the sensitivity study can be used to evaluate the most efficient method to increase reliability: adding wall thickness or changing procedures for operation [14].

The examples are

- A dry gas line that is occasionally wetted due to production upsets. Corrosion occurs for only a limited time following an upset. It is assumed that $L \leq 4.48 \cdot \sqrt{D \cdot t}$. The sensitivity parameter is the number of upsets per year.
- A wet line transports liquids. Corrosion occurs continuously over the whole lifetime. It is assumed that $L > 4.48 \cdot \sqrt{D \cdot t}$. The sensitivity parameter is the inhibitor performance.

Dry Gas Line

The deterministic design data for the line are presented in Table 10.2 and the probabilistic parameters are shown in Table 10.3. Two values of the corrosion allowance are considered:;

- 0 mm.
- 3 mm (commonly used in pipeline design, based on experience).

The conservatism in the corrosion rate model is often explained by the model being based on laboratory experiments which reflect "real life" rather poorly. However, The condensation of water in a gas line may result in "fresh", unsaturated water which is known to give a more corrosive

Table 10.2 Deterministic Design Parameters

Parameter	Unit	Dry Gas Line	Wet Liquid Line
D	mm	1016	508
t_{-c} [1)]	mm	26.6	13.5
Pressure	bar	200	130
Temperature	°C	50	50
CO_2 content	mole %	4.5	0.5
Design life	years	50	20
F_{scale}, F_{pH}	-	1	1

Note: t_{-c} = Total wall thickness − corrosion allowance

Table 10.3 Probabilistic Design Parameters and Uncertainty Factors, Dry Gas Line

Parameter	Distribution	Mean Value	Std. Dev.	Reference
Corrosion rate uncertainty factor[1]	Normal (Gauss)	1.5	0.3	See text
Duration of wet service	Normal (Gauss) (see text)	$3n$[2]	$2\sqrt{n}$	See text
Defect length	Lognormal	30 (mm)	20 (mm)	Emden gas line
Wall thickness uncertainty factor[1]	Normal	1.04	0.04	Engineering judgment

Note:
[1]In the limit state function, corrosion rate and wall thickness values are multiplied by their respective uncertainty factors.
[2]n = Number of upsets/lifetime

environment than water saturated with corrosion products. Also, in a long pipeline it is appropriate to consider extreme value statistics, as the probability of seeing "worst case" corrosion rates increase with length. The mean value of the corrosion rate uncertainty factor is therefore greater than 1. There is also a large scatter in the laboratory data upon which the Shell model is based deWaard et al (1995) [9], which is reflected in the large standard deviation.

It has been assumed that three operational upsets will occur per year in the base case. Sensitivity cases are shown to evaluate the effect of reducing this number to one or two upsets per year. In this context, an upset is defined as water or wet gas ingress into the pipeline. It has further been assumed that the time from the start of the ingress until the upset is detected

and corrected and the line returned to the dryness before the upset can be described by a lognormal probability distribution function with a mean value, m, of 3 days and a standard deviation, s, of 2 days. It has also been assumed that the upsets are independent occurrences and the line is dried after the previous upset before a new upset occurs. The total duration of wet service, t_w, throughout the lifetime of the field can then be described by a normal distribution with the following parameters:

$$m_{t_w} = n \cdot m \quad [10.7]$$

$$s_{t_w} = \sqrt{n} \cdot s \quad [10.8]$$

where

m_{t_w} = mean value for total duration of wet service
s_{t_w} = standard deviation for total duration of wet service
n = total number of upsets during lifetime (should not be less than approximately 20 for the assumption of the normal distribution to be true)
m = mean value for drying time, single upset
s = standard deviation for drying time, single upset

The analysis cases are summarized in Table 10.4. The analysis results are presented in Figure 10.2.

Wet Liquid Line

The deterministic design data for the line are presented in Table 10.2 and the probabilistic parameters are shown in Table 10.5.

Three values for the corrosion allowance are considered;

- 5 mm.
- 6 mm (calculated from conventional, deterministic approach).
- 7 mm.

The rationale behind establishing the corrosion rate uncertainty factor is the same as for the dry gas line. However, because the pipe wall in a liquid or multiphase line is washed with liquids, "fresh" water from condensation is

Table 10.4 Sensitivity Cases, Duration of Wet Service

Case	n	m_{tw}	s_{tw}	Comment
Base case	150	450	24.49	3 single upsets/year
S1	100	300	20	2 single upsets/year
S2	50	150	14.14	1 single upset/year

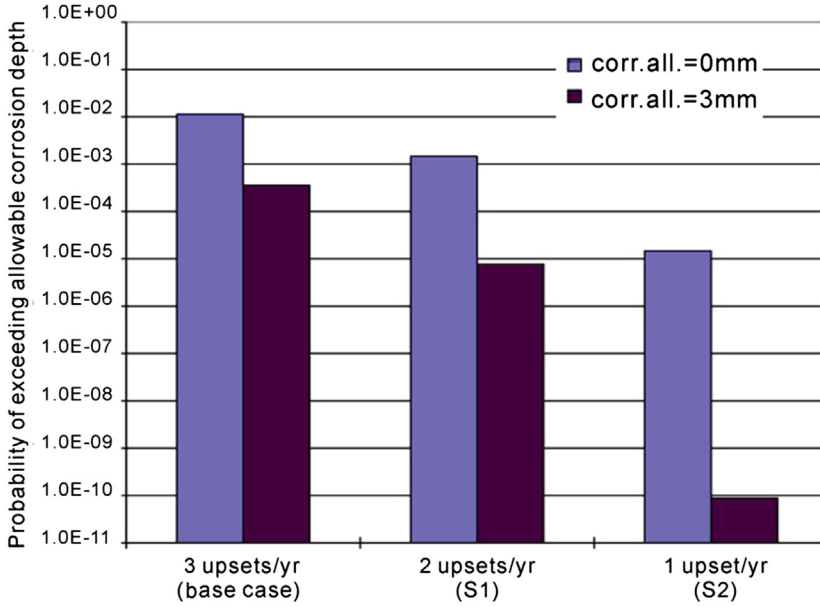

FIGURE 10.2 ***Calculated Probabilities for a Gas Pipeline with Operation Upsets.*** (For color version of this figure, the reader is referred to the online version of this book.)

Table 10.5 Probabilistic Design Parameters and Uncertainty Factors, Wet Liquid Line

Parameter	Distribution	Mean Value	Std. Dev.	Reference
Shell '95 model uncertainty factor[1,2]	Normal (Gauss)	0.04	0.25	See tex
Inhibitor efficiency, *i*	Beta	See text	0.03	See tex
Wall thickness uncertainty factor[2]	Normal	1.04	0.04	[6, 7], and engineering judgment

Notes:
[1]Corrosion rate uncertainty factor, $x_m = 1 +$ Shell '95 model uncertainty factor.
[2]In the limit state function, corrosion rate and wall thickness values are multiplied by their respective uncertainty factors.

assumed not to be present. Also, the corrosivity of the water phase is limited by the presence of hydrocarbons, corrosion products, and inhibitor. The worst case corrosion rate is therefore considered to be less in a liquid line than a gas line. The mean value of x_m is accordingly assumed to be less in a liquid line than a gas line. Based on this, the corrosion rate model uncertainty factor, x_m, is taken to be (1 + Shell '95 model uncertainty factor); that is, it is assumed that the Shell model is a reasonable representation of the extreme corrosion rates.

Table 10.6 Sensitivity Parameters, Inhibitor Performance

Case	Distribution	Mean	Std. Deviation
1	Beta, range 0.7 to 0.99	0.9	0.02
2	Beta, range 0.7 to 0.99	0.9	0.03
3	Beta, range 0.7 to 0.99	0.85	0.035

Three cases are considered for the inhibitor efficiency. These are described in Table 10.6. The cases are meant to represent different levels of commitment to prudent operation of the pipeline. In this context, commitment comprises proper selection of inhibitors, monitoring of inhibitor performance, and ability to execute corrective actions if the inhibitor protection becomes inadequate.

The basis for the suggested inhibitor efficiency distributions is the deterministic value of 85%, as described in NORSOK MD-P-001. The rationales behind the selection of distributions are as follows [15, 16]:

Case 1. Very high level of commitment to operation. Probability of seeing values of inhibitor performance <85% is very low (~1%).

Case 2. High level of commitment to operation. Probability of seeing values of inhibitor performance <85% is low (~10%).

Case 3. Low level of commitment to operation. Probability of seeing values of inhibitor performance <85% is high (~50%).

An upper efficiency limit of 99% and a lower limit of 70% are assumed. It is assumed that measures are taken during operation to keep the efficiency within this band. Note that the inhibitor efficiency is an average value for the whole life of the line, as the limit state function considers the average corrosion over the total life; that is, it does not give a day to day picture of the corrosion in the line. From this, it follows that values well below 85% may still be acceptable for short time periods. The analysis results of probability of exceeding the allowable corrosion depth are shown in Figure 10.3.

Discussion

The examples illustrate how the uncertainties in the design parameters may be addressed and how the reliability of the pipeline can be subjectively evaluated. The results show that the reliability of a pipeline is related to both the future operation of the line and the size of the corrosion allowance.

An important trend can be seen from the results; The effect of the corrosion allowance on increasing the reliability decreases as the corrosivity of the line increases. This means that, if the corrosion rate is relatively high, a

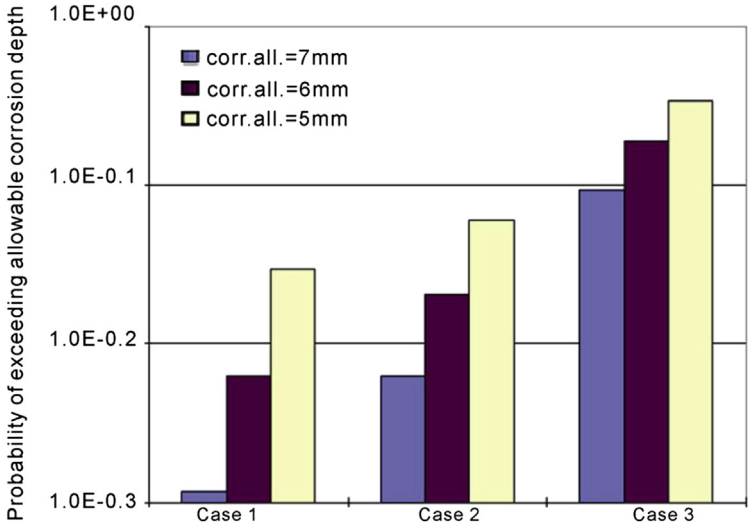

FIGURE 10.3 ***Calculated Reliability of Wet Liquid Pipeline with different Inhibitor Efficiencies.*** (For color version of this figure, the reader is referred to the online version of this book.)

corrosion allowance is a poor way of increasing the reliability compared to reducing the corrosion rate, say, by changing the operating parameters.

The reliability is expressed as (1.0 – probability of exceeding the acceptable corrosion depth). Reaching the maximum acceptable depth does not mean that the line will fail, due to the inherent safety level in the B31G code. Furthermore, the corrosion depth is likely to increase over a long period of time, which means that the defects are likely to be detected by inspections before they reach a critical size. The cost of repair or reducing the capacity of the line is therefore the most likely consequence of exceeding the maximum depth.

The optimum corrosion allowance is selected by minimizing the life cycle cost, where the CAPEX, OPEX, and risk (probability of failure times cost of failure) are considered for each candidate corrosion allowance.

Recommendations

Better statistical presentation of input parameters increases the confidence in the calculated reliability and, consequently, the life cycle cost. Data taken from operational experience are particularly in demand, as this reduces the gap between the existing laboratory models and "real life." Similarly, corrosion rate models are needed that can predict field corrosion rates with better accuracy.

Reliability-based methods are being developed to predict the maximum allowable corrosion depth. By merging these methods with the method presented here, the probability of failure (or bursting) can be calculated instead of the probability of exceeding an allowable depth. This removes unnecessary conservatism, but it also affects the acceptable reliability because factors such as environmental damage and human safety have to be considered in addition to cost.

REFERENCES

[1] Bai Y. Marine structural design. Elsevier Science; 2003.
[2] Soares CG. Quantification of model uncertainty in structural reliability. In: Soares CG, editor. Probabilistic methods for structural design. Norwell, MA: Kluwer Academic Publishers, Springer Netherlands; 1997.
[3] ISO/DIS 13623. Petroleum and natural gas industries; Pipeline transportation systems. Switzerland: International Standard Organization; 1997.
[4] Kiefner JF. Corroded pipe: Strength and repair methods. Fifth Symposium on Line Pipe Research; 1974.
[5] Sotberg T, Moan T, Bruschi R, Jiao G, Mørk KJ. The SUPERB project: Recommended target safety levels for limit state based design of offshore pipelines. Yokohama, Japan: Proc. of OMAE'97; 1997.
[6] Nødland S, Bai Y, Damsleth PA. Reliability approach to optimise corrosion allowance. Risk-Based and Limit State Design and Operation of Pipelines, IBC. Aberdeen: Scotland; May 1997.
[7] Nødland S, Hovdan H, Bai Y. Use of reliability methods to assess the benefit of corrosion allowance. Norway: EUROCORR '97, Trondheim; September 1997.
[8] deWaard C, Lotz U. Prediction of CO_2 corrosion of carbon steel; 1993. Paper no. 69. CORROSION/93.
[9] deWaard C, Lotz U, Dugstad A. Influence of liquid flow velocity on CO_2 corrosion: A semi-empirical model; 1995. Paper no. 128. CORROSION/95.
[10] DNV. Rules for submarine pipelines. Oslo, Norway: Det Norske Veritas; 1996.
[11] Edwards JD JD, Sydberger T T, Mørk KJ. Reliability-based design of CO_2-corrosion control; 1996. Paper no. 29. CORROSION/96.
[12] RCP. SYSREL 9.0. Munich: Germany; 1996. RCP Consulting.
[13] ASME. B31G. Manual for determining the remaining strength of corroded pipelines. New York: American Society of Mechanical Engineers; 1991.
[14] Jiao G, Sotberg T, Bruschi R, Igland RT. The SUPERB project: Linepipe statistical properties and implications in design of offshore pipelines. Yokohama, Japan: Proc. Of OMAE'97; 1997.
[15] NORSOK M001. Materials selection, rev. 1. Lysaker, Norway: NORSOK Standard; December 1994.
[16] NORSOK Y-002. Reliability-based limit-state principles for pipeline design. Lysaker, Norway: NORSOK Standard; 1997.

CHAPTER 11

LCC Modeling for Pipeline Design

Contents

1. Introduction 248
   - General 248
   - Probabilistic versus Deterministic LCC Models 249
   - Economic Value Analysis 249
2. Initial Cost 250
   - General 250
   - Management 251
   - Design and Engineering Services 252
   - Materials and Fabrication 253
   - Marine Operations 253
   - Operation 253
3. Financial Risk 254
   - General 254
   - Probability of Failure 254
   - Consequences of Failure 254
     - *General* *254*
     - *Cost Associated with Averting Fatalities and Injuries* *255*
4. Time Value of Money 256
5. Example of Fabrication Tolerance Using the LCC Model 257
   - General 257
   - Background 257
   - Analysis Procedure Using the LCC Model 258
     - *Step 1. Definition of Structure* *258*
     - *Step 2. Quality Aspect Considered* *258*
     - *Step 3. Failure Modes Considered* *258*
     - *Step 4. Limit State Equations* *258*
     - *Step 5. Definition of Parameters and Variables* *261*
     - *Step 6. Reliability Analysis* *264*
     - *Step 7. Cost of Consequence* *265*
     - *Step 8. Calculation of Expected Costs* *265*
     - *Step 9. Initial Cost* *266*
     - *Step 10. Comparison of Life Cycle Costs* *266*
6. Example of On-Bottom Stability Using the LCC Model 267
   - Introduction 267
   - Analysis Procedure Using the LCC Model 268
     - *Step 1. Definition of System* *268*
     - *Step 2. Quality Aspects Considered* *268*
     - *Step 3. Failure Modes* *268*

Subsea Pipeline Integrity and Risk Management
ISBN 978-0-12-394432-0
http://dx.doi.org/10.1016/B978-0-12-394432-0.00011-1

Step 4. Limit State Equations 268
Step 5. Definition of Variables and Parameters 268
Step 6. Reliability Analysis 269
Step 7. Cost of Consequence 269
Step 8. Expected Cost 269
Step 9. Initial Cost 269
Step 10. Comparison of Life Cycle Costs 269
References 269

1. INTRODUCTION

General

Pipeline engineering projects can be divided into several specific stages, with separate sources of cost. These stages include pre-engineering, conceptual engineering, detailed engineering, fabrication, construction, operation, and abandonment. Although all the different cost aspects are considered, this occurs in a segmented manner. The costs related to all activities such as conceptual engineering, fabrication, and installation are considered isolated, addressed at different points in the pipeline life cycle, and not viewed on an integrated basis.

It is necessary to assess these costs as interdependent entities. Thus, in addressing the economic aspects of pipelines, one must look at the total cost in the context of the overall life cycle, especially in the early stages of conceptual design. Life cycle cost (LCC), when included as a variable in the pipeline development process, provides opportunity to design economically optimized pipelines.

The benefit of the life cycle cost model of decision is that it is very flexible [1]. It is possible to analyze any aspect of the system being designed. In the case of pipeline engineering, this type of analysis can be used at all levels of design and management; it can be used as a management tool in the assessment of which training programs to implement, such that workforce efficiency is increased. Alternatively, it could be used by an engineer to work out the most economic method of preventing failure due to corrosion (i.e., inhibitors, corrosion allowance, or high-quality materials).

This chapter presents a generic model that is used in most industries such that it can be implemented into pipeline engineering, as shown in Bai et al. [2]. The life-cycle cost method is discussed in a step-by-step procedure. Each step is explained in terms of pipeline engineering, so

that it can be used for future reference in the determination of subsea pipeline using the LCC method.

Probabilistic versus Deterministic LCC Models

By using the LCC, it is possible to express the total cost of a design alternative in terms of a mathematical expression, which can be generically described as follows:

$$\text{Total(NPV)} = \text{CAPEX (NPV)} + \text{OPEX (NPV)} + \text{RISKEX(NPV)} \quad [11.1]$$

where

CAPEX = capital expenditure or initial investment
OPEX = operational costs, this includes planned (regular maintenance) and unplanned costs (repair of failures)
RISKEX = risk expenditure
NPV = net present value

A deterministic method of solving this expression involves identifying and estimating any foreseeable costs based on historical data and past events. There are several methods of estimating cost in this way, which include engineering judgment, analogy, and the parametric method [1].

A probabilistic method of solving this expression involves identifying costs and developing a probability distribution that best approximates the cost. Various statistical methods exist for developing a probability distribution based on historical data.

Economic Value Analysis

Cui et al. [3] introduced the idea of economic value analysis (EVA), which is based on the LCC model. It uses the idea of a trade-off between quality and cost. *Quality* is defined as the ability to satisfy requirements. In pipeline engineering, these requirements include serviceability, safety, compatibility, and durability [4]. Good quality in the design and construction of a pipeline can increase the safety and thus reduce the maintenance cost. However, introducing strict quality controls, capital costs increase and may not be recovered from the revenue generated in the operational phase. So economic value analysis develops the LCC model into a method by which it is possible to minimize the total life cycle cost of a structure. This chapter develops a methodology for economic value analysis:

1. Identify the structure or system to be considered.
2. Identify the quality item(s) to be considered for the system.

3. Identify the principal failure modes for the structure or system to be considered. In general, several failure modes (such as buckling, fatigue, on-bottom stability) may be considered for a complex structure, such as a pipeline or a pipe segment.
4. Write the limit state equations for each failure mode for the structure/system. This equation describes failure condition. The main point of this step is that, in limit state equations, the quality item identified in step 2 must be explicitly considered.
5. Collect all of the statistical data for each parameter in the limit state equations. This consists of the limit state equations and can be in terms of probabilistic methods (statistical distributions) or deterministic values.
6. Compute the probability of failure, P_{fs}, as a function of the quality measure.
7. Define the consequences of failure and the related costs of these consequences for the structural system, C_f.
8. Compute the expected cost of failure, $E(C)$, of the system during service life as a function of the quality measure.
9. Define the initial costs of construction (C_o) as a function of the quality measure.
10. Perform the EVA, computing the quality measure or tolerance that minimizes the total expected life cycle costs, $E(C)$.

$$\text{Minimum } E(C) = \text{Minimum } \left(C_o + C_f \cdot P_{fs}\right) \qquad [11.2]$$

It should be noted that Eq. [11.2] can be related to Eq. [11.1]. The term C_o corresponds to either an initial investment or planned costs. The second part, $C_f \cdot P_{fs}$, corresponds to unplanned costs that may occur during the pipeline lifetime.

2. INITIAL COST

General

When making a decision at any level, it is always beneficial to identify the possible alternatives. In business situations, the alternatives nearly always have related initial costs. This initial cost is always a function of some quality aspect of the alternative. *Quality* can be defined as a measurement of the extent to which the alternative covers the requirements of the situation. In

engineering businesses, these requirements include those of serviceability, safety, compatibility, and durability:

- Serviceability is the suitability for the proposed purposes, that is, functionality. Serviceability is intended to guarantee the use of the system for the agreed purpose and under the agreed conditions of use.
- Safety is the freedom from excessive danger to human life, the environment, and property damage. Safety is the state of being free of undesirable and hazardous situations. The capacity of a structure to withstand its loading and other hazards is directly related to and most often associated with safety.
- Compatibility assures that the system has no unnecessary or excessive negative impacts on the environment and society during its life cycle. Compatibility is also the ability to meet economic and time requirements.
- Durability assures that serviceability, safety, and environmental compatibility are maintained during the intended life of the marine system. Durability is freedom from unanticipated maintenance problems and costs.

The alternatives available must fulfill the minimum criteria for each of these requirements, which is set forward by those that own, operate, design, construct, and regulate pipelines. Any additional quality that is attained from an alternative has financial implications over the lifetime of the product, as explained earlier.

This section defines the different types of quality aspects in pipeline engineering. These different types include management, design and engineering services, material and fabrication, marine operations, and operation. It is important to recognize that the quality aspect to be analyzed possibly lead to a failure, and the calculation of risk of failure can be found using the techniques discussed in the risk section of this chapter.

Management

Management can be defined as the coordination and control of individuals and systems. The activity of management is present throughout the entire pipeline development process. By implementing different strategies or plans, it is possible to influence the quality of performance of the individuals and systems. Research carried out by Bea [5, 6] implies that the quality of performance of individuals and systems in the design, construction, and reliability of marine structures is a function of the frequency of human or organizational errors (HOEs).

Factors that contribute to HOEs can be categorized into individual, organizational, and systemic (hardware, software) errors. Individual or human errors are those made by a single person that contribute to an accident.

The sources of organizational errors can be placed into three general categories. The first involves upper level management. The lack of appropriate resources and commitments to achieve reliability and the provision of conflicting goals and incentives (e.g., maintain production when it needs to be decreased to allow maintenance on the system) are examples of upper level management errors. The second involves front line management. Information filtering (make it look better than it really is, tell the boss what he wants to hear—good news) and redirection of resources to achieve production at the expense of safety are examples of front line management errors.

The third category involves the design, construction, or operating team. Teamwork in which there is an inherent and thorough process of checking and verification have proven to be particularly important: "if you find a problem, you own it until it is either solved or you find someone to solve it."

Errors can also be observed with human-system (equipment, structure, software, or instructions manuals) interfacing. These are described as system (hardware) errors and procedure (software) errors. System errors can be attributed to design errors and result in an operator making improper decisions. Similarly, the procedures and guidelines provided to design, construct, or operate a system could be seriously flawed.

The effects of management errors should be included in the risk in a quantitative manner. Very often, the largest risk is that associated with intrinsic human errors. The influence of human errors on LCC should be accounted for through use of quantitative risk analysis in which failure probability and consequence are estimated.

Through these subdivisions of HOE, it is possible to specify quality aspects that can be varied. One example of the numerous ways in which this could be implemented when deciding on the recruitment of new engineers. By recruiting an experienced engineer, the likelihood of design error is low and the salary high; however, if a graduate engineer is hired, the likelihood of design errors taking place is quite high and the salary is low. This can be assessed using life cycle cost analysis and the most economically viable solution may be reached.

Design and Engineering Services

The scope of the quality aspects that this category covers is conceptual engineering and preliminary engineering. The detailed engineering of a pipeline structure allows very little scope for the alteration of quality aspects

of the pipeline and is hence not discussed. The limits of each of these areas are outlined as follows, based on work by Langford and Kelly.[7]

1. Conceptual engineering:
   - To establish technical feasibility and constraints on the system design and construction.
   - To eliminate nonviable options.
   - To identify the required information for the forthcoming design and construction.
   - To identify interfaces with other systems, planned or currently in existence.
2. Preliminary engineering. To engineer the pipeline so that the system concept is fixed, which includes
   - To verify the sizing of the pipeline.
   - To determine the pipeline grade (included in material section) and wall thickness.
   - To verify the pipeline against design and code requirements for installation, commissioning, and operation.

The level of engineering is sometimes specified as being sufficient to detail the design for inclusion into an "engineering, procurement, and construction" (EPC) tender. The EPC contractor should then be able to perform the detailed design with the minimum number of variations as detailed in their design.

Materials and Fabrication

This category of quality aspects is probably the one in which most experience has been gained in terms of financial analysis of the options available. This category covers the quality of all materials used in the pipeline development and the quality of fabrication of these materials.

Marine Operations

This category of quality aspects covers all marine operations required prior to the operation of the pipeline and the extraordinary marine operations required to maintain operation of the pipeline (i.e., repair). An example of the application of LCC would be, when deciding on the type of laying barge to use, analysis of the balance between day rates and days down.

Operation

The operation of a pipeline includes all activities performed after the installation of the pipeline. This primarily involves the inspection of the pipeline, but not, as stated already, the repair of the pipeline.

3. FINANCIAL RISK

General

It is possible to arrive at financial values that represent the financial losses likely to occur in a pipeline using quantitative risk analysis approach.

The risk can be determined by the following generic expression:

$$\text{Risk} = \text{Probability of failure} \times \text{Consequence of failure} \qquad [11.3]$$

The two elements used to calculate the risk can be separated into the probability of failure, which is equivalent to the frequency of failure, and the consequence of failure. In using risk for financial analysis, it is necessary to determine the consequence of failure in monetary terms.

Probability of Failure

In determining the probability of failure, two levels of failure causes can be identified, direct failure and indirect failure. Direct failures are related to physical aspects of the pipeline failing, such as corrosion, fatigue, or on-bottom instability. Indirect failures pertain to system or human errors that may eventually lead to a direct failure. The direct failures can be determined using structural reliability analysis. For reliability analysis to be considered a probability of failure, it is necessary to incorporate a deterministic value for human error (usually a factor between 5 and 10). The indirect failures can be modeled using a number of quantitative risk analysis techniques, including event tree analysis. Both the structural reliability analysis and quantitative risk analysis techniques for subsea pipelines are developed fully in Sørheim and Bai [8].

Consequences of Failure

General

Consequence is the determination of the possible outcome(s) of a failure event. Two methods are available to measure the consequences of a release event, these are consequence modeling and the interval method:

- **Consequence modeling:** This is an analytical method to assess the sequence of events after a failure has occurred. The different stages that occur after a release include discharge, dispersion, ignition, combustion, and damage and loss. This method is discussed further in [8].
- **Interval method:** The interval method is an approximate method. By using engineering judgment and historical data, it is possible to give estimated upper and lower bound consequence scenarios. This allows a scope

of different consequence scenarios to be evaluated, thus a decision can be reached on which scenario best suits the philosophy of the decision maker, (optimist, low consequences; pessimist, high consequences or other).

The different types of consequences that are likely to occur as a result of a release event are

- Cost associated with averting fatalities and injuries.
- Environmental damage.
- Production loss.
- Material repair.

Cost Associated with Averting Fatalities and Injuries

Although any human loss is unacceptable, it is necessary to account for all possible scenarios. Cost associated with averting fatalities and injuries ("human loss") would place a financial burden on the owner. There are currently two main methods used for determining the economic value of a human life. It must be noted that this is a statistical life, not an identifiable individual. Society has always been ready to spend much more to save an individual in a specific situation—trapped coal miner, for instance. The statistical life reflects the amount that society is willing to spend to reduce the statistical risk of accidental death by one individual.

The first method is the human capital approach in which the value is based on the economic loss of future contributions to society by an individual. The second approximation, willingness to pay, identifies how much an organization is willing to pay (in terms of other goods and services given up) to gain a reduction in the probability of accidental death. Each method has drawbacks and benefits.

Injuries frequently cost more than fatalities. This cost should also be included in consequence modeling.

Material Repair

Material repair is a function of the extent of damage that the pipeline has experienced. There are three ways in which a breach of containment is likely to be repaired: hyperbaric weld repair, spool piece installation, and bolted sleeve installation. Information regarding the cost of these repairs are available from most operating companies.

Production Loss

The production loss calculates the financial loss from the time lost due to the damage of the pipeline, which is a function of the time it takes to repair the

pipeline. This can be calculated from the value of the product being transported per unit and the volume of product that could potentially be transported during repair.

The cost that arises from the inconvenience caused to the receivers of the transported goods must also be included. By assessing contractual agreements between operator and purchaser, it is possible to identify potential costs.

Environmental Damage

It is necessary to assess each case on its own merits. The following factors are the most influential in determining any cost:

- Volume and type of product lost.
- Probable currents and exposed coastline.
- Topography and location of "sensitive areas" (nature reserves, farming, recreational areas, potable water sources, etc.).
- Existing emergency response capacity.

A useful source of information for an estimated value of the financial loss suffered is the use of risk matrices available from most operators of offshore installations. A typical risk matrix includes information that could be correlated to the circumstances of a pipeline failure.

4. TIME VALUE OF MONEY

The time value of money in the form of an interest rate is an important element in most decision situations involving the flow of money over time. The reason for this is that money earns interest through its investment over a period of time, a dollar to be received at some future date is not worth as much as a dollar in the hand at present.

Money also has a time value due to the purchasing power of a dollar through time. During periods of inflation the amount of goods that can be bought for a particular amount of money decreases, as the time of purchase occurs further in the future. Therefore, when considering the time value of money it is important to recognize both the earning power and the purchasing power of money.

In analyzing the time value of money for a LCC model, it is necessary to evaluate all costs on a common basis. This is usually when an initial investment is made, therefore, all costs must be evaluated in terms of the initial investment cost. At this stage, it is necessary to assess the types of costs likely to be encountered: single payment, annual payments, or varying annual payments.

When calculating the cost of risk, it is necessary to recognize that different types of probabilities exist: immediate, time independent, and time dependent. Immediate failure is a failure that occurs immediately on installation of the pipeline (e.g., hydrostatic collapse or hoop stress criterion). Since the failure occurs immediately, the cost does not have to be adjusted to account for time value of money principles.

$$\text{Risk} = \text{Consequence cost}\ (t = 0) \times P_f \qquad [11.4]$$

The second type, time independent, is a failure that can occur at any point during the lifetime of the pipeline (e.g., trawling impact or dropped objects). It is therefore necessary calculate the present value of the consequence on the basis of a failure occurring at the midpoint of its life. This gives an equal assessment of the failure occurring at any given point in time:

$$\text{Risk} = \text{NPV}\ [\text{Consequence cost}\ (t = \tfrac{1}{2}\ \text{Total life time})] \times P_f \qquad [11.5]$$

The time dependent failure results in the most complex assessment of the cost assessment. These types of failures include fatigue and corrosion. Failure probability increases per year; hence, it is necessary to adjust the consequence cost for each year and multiply by the failure rate of the same year, this can then be cumulated to give a total risk cost:

$$\text{Total risk cost} = \sum \{\text{NPV}\ [\text{Consequence cost}\ (t)] \times P_f\ (t)\} \qquad [11.6]$$

5. EXAMPLE OF FABRICATION TOLERANCE USING THE LCC MODEL

General

The purpose of this calculation example is to demonstrate the validity of life cycle cost modeling as a method by which to justify choices among design alternatives. This example [9] looks at the practicalities of assessing the failure probability, the cost of consequence, the implementation of economic theory, and the utilization of interval method, following the steps outlined in the introduction.

Background

Pipeline fabrication quality is one particular aspect of pipeline design that could give potential cost savings over the life cycle. Good quality in the fabrication of a pipeline can increase the safety and thus reduce the cost of unplanned maintenance and the cost of consequences. However, too

stringent quality requirements can drive up fabrication costs, and this increase of initial cost may not compare favorably to lesser-quality options. This design example compares the LCC of two fabrication qualities, in terms of the probability of failure due to corrosion, and thus arrives at a judgment as to which fabricator is more economically viable.

Analysis Procedure Using the LCC Model

Step 1. Definition of Structure

The structure to be considered is a subsea pipeline.

Step 2. Quality Aspect Considered

The quality aspect to be considered in this example is the fabrication tolerance to be used. This calculation example considers two fabricators, each of which produce a different quality of pipe. The different qualities of pipeline are implemented into the problem through a random variable, modeling the uncertainty in wall thickness. The exact nature of this variable is described fully in "Step 5. Definition of Parameters and Variables."

Step 3. Failure Modes Considered

To simplify the scope of the example, the only design aspect to be considered is the design criteria for corrosion allowance. From this, only two failure modes are likely, hoop stress and hydrostatic collapse.

Step 4. Limit State Equations

By considering corrosion depth as the load and wall thickness as the resistance, it is possible to apply load-resistance factored design (LRFD) methodology to pipeline corrosion allowance design. This introduces a welcome opportunity to take into account the range of uncertainties inherent in corrosion rate calculations and residual strength of corroded pipelines in the design.

Corrosion Rate and Defect Length

The corrosion rate (CR) is based on De Waard and Lotz's 1993 formula [10], which gives corrosion rate as a function of temperature, pressure and CO_2 content. In addition, effects due to pH, saturation of corrosion products, glycol content, and scale formation may be accounted for.

The following assumptions are made:

- The corrosion rate during normal operation is negligible.

- Corrosion occurs only following an upset where water or wet gas is introduced into the line. The time during which corrosion can occur is labeled t_w (= total duration of wet service). The determination of t_w is described in Step 5.
- Glycol is present in the line as a continuous film on the pipe wall because of carryover from the glycol drying unit. The water ingress in the line thus results in an increased water content in the glycol film. The water content in the glycol film is assumed to increase to a maximum of 50% following an upset.

The depth of an attack is modeled as shown in Eq. [11.7]:

$$d = \mathrm{CR} \cdot t_w \tag{11.7}$$

where

CR = corrosion rate

t_w = total duration of wet service

Allowable Corrosion Depth Based on Hoop Stress

ASME B31G [11] defines a safe operating pressure, P', for a corroded pipe with a short defect (i.e., $A \leq 4$, see Equation [11.9]) [1]:

$$\Delta P' = 1.1 \cdot \Delta P \cdot \left[\frac{1 - \frac{2}{3} \cdot \frac{d}{t}}{1 - \frac{2}{3} \cdot \left(\frac{d}{t\sqrt{A^2+1}} \right)} \right] \tag{11.8}$$

where

ΔP = design pressure (internal – external)

D = maximum allowable depth of corroded area

t = nominal wall thickness of pipe

$$A = \text{Constant} = 0.893 \cdot \frac{L}{\sqrt{D \cdot t}} \tag{11.9}$$

L = axial extent of the defect

D = nominal outside diameter of pipe

Pressure is related to the wall thickness, as shown in Eq. [11.10]:

$$\Delta P = \mathrm{SMYS} \cdot \frac{2 \cdot t}{D - t} \cdot \eta \tag{11.10}$$

where

η = usage factor

Equations [11.8]–[11.10] are combined to give Eq. [11.11] for short corrosion defects ($L \leq 4.48 \cdot \sqrt{D \cdot t}$) [9]. The increased strength of the pipe wall in uncorroded sections of the pipe (due to the remaining corrosion allowance) thus is taken into account. These calculations allow for no reduction in design pressure during the lifetime.

$$d_h = \frac{1.5 \cdot t \cdot \left(\frac{1.1 \cdot t}{t_{-c}} \cdot \frac{D - t_{-c}}{D - t} - 1 \right)}{\frac{1.1 \cdot t}{t_{-c}} \cdot \frac{D - t_{-c}}{D - t} - \frac{1}{\sqrt{1 + \frac{0.8 \cdot L^2}{D \cdot t}}}} \qquad [11.11]$$

where

d_h = allowable corrosion depth based on hoop stress
t = wall thickness including corrosion allowance
t_{-c} = wall thickness excluding corrosion allowance

Allowable Corrosion Depth Based on Collapse

A corrosion defect may reduce the hoop buckling capacity of a pipe. The allowable corrosion depth based on collapse may easily be derived based on the formulation in Chapter 3 of Bai and Bai [12].

Limit State Function

The limit state function, $g(\overline{X})$, forms the basis for the reliability calculations. This function expresses Resistance – Load as a function of $\overline{X}$, where $\overline{X}$ is a vector containing all the basic uncertainty variables describing the loads and resistances. Deterministic values may also be included in g. The criterion for nonacceptance (or failure) is consequently defined as $g(\overline{X})) < 0$, with the corresponding probability

$$P[g(\overline{X}) < 0] = \int_V f_{\overline{X}}(\overline{x}) d\overline{x} \qquad [11.12]$$

where

V = failure domain = $\{\overline{x} \| g(\overline{X}) < 0\}$
$f_{\overline{X}}(\overline{x})$ = joint density function for $\overline{X}$
$\overline{x}$ = realization of $\overline{X}$ in the basic variable space

Since two failure modes are investigated (i.e., hoop stress and local collapse for load and displacement control), two limit state functions are needed to describe the system. The system probability of failure may therefore be approximated by

$$P_{system} = [g_1(\overline{X}) < 0] + P[g_2(\overline{X}) < 0] \qquad [11.13]$$

The calculation of the probability of failure is done by the proprietary software SYSREL [13]. The limit state functions used for the corrosion allowance calculations are shown in Eqs. [11.14] and [11.15]:

$$g_1(\overline{X}) = \frac{1.5 \cdot x_t \cdot t \cdot \left(\frac{1.1 \cdot x_t \cdot t}{x_t \cdot t_{-c}} \cdot \frac{D - x_t \cdot t_{-c}}{D - x_t \cdot t} - 1 \right)}{\frac{1.1 \cdot x_t \cdot t}{x_t \cdot t_{-c}} \cdot \frac{D - x_t \cdot t_{-c}}{D - x_t \cdot t} - \frac{1}{\sqrt{1 + \frac{0.8 \cdot L^2}{D \cdot x_t \cdot t}}}} - \mathrm{CR} \cdot x_m \cdot \frac{t_w}{365} \qquad [11.14]$$

where

x_m = corrosion rate model uncertainty factor

x_t = wall thickness uncertainty factor (from manufacturing process)

$$g_2(\overline{X}) = p_c - \frac{\gamma_R \cdot p_e}{\sqrt{1 - \left[\frac{M_{F,c} \cdot \gamma_R \cdot \gamma_F \cdot \gamma_c}{M_c} \right]^2}} \qquad [11.15]$$

where p_c is calculated from Eq. [4.15] of Chapter 4 of Bai and Bai [12]. Note that the expression for g_2 is somewhat simplified for clarity. In the analysis, the Eq. [2.20] of Chapter 2 of Bai and Bai [12] is solved for p_c with h given in Eq. [11.16]:

$$h = t - \mathrm{CR} \cdot x_m \cdot \frac{t_w}{365} \qquad [11.16]$$

In addition, the expression for wall thickness, t, in the limit state function, is always multiplied by its uncertainty factor, x_t, and M_c is calculated from Eq. [3.27] in Chapter 3 of Bai and Bai [12].

Step 5. Definition of Parameters and Variables

Pipeline, Operational and Environmental Data

The pipeline data presented in Table 11.1 are used for the analysis. The required wall thickness for hoop stress is 13.0 mm. However, a wall thickness of 15.9 mm is chosen because high moments and strains are expected in the line due to the uneven seabed. The expected functional strains and moments are shown in Table 11.2. The benefit from the higher wall thickness is increased local buckling capacity and, hence, reduced need for seabed intervention. The calculation of the allowable collapse pressure is based on the parameters given in Table 11.2.

The operational data used are presented in Table 11.3. The temperature drop in the bundle is estimated based on the calculated temperature profiles, an inlet temperature of 70°C, and a bundle length of 400 m.

Table 11.1 Pipeline and Environmental Data

Parameters	Unit	Value
Internal diameter	mm	425.2
Wall thickness	mm	15.9
Wall thickness, required for hoop stress only	mm	13.0
Ovality	—	1.5%
External pressure	MPa	3.65

Table 11.2 Functional Moments and Force

Parameter	Value	Reference
M_F	0.6 MPa	Preliminary in-place analysis
F	250 kN	Preliminary in-place analysis

Table 11.3 Operational Data

Parameters	Unit	Value
Design pressure	Bar	225.0
Temperature at end bundle or start pipeline	°C	45.0
CO_2 content	Mole %	3.0

Defect Length

Intelligent pig inspections from the Emden gas pipeline show defect sizes after approximately 20 years of service, which can be illustrated by the lognormal distribution function shown in Figure 11.1 with (mean = 30, std. dev. = 20) [2]. This function has been used to describe the expected defect length in the line.

Note that the defects in the Emden line have occurred following a history of operational difficulties. After these have been sorted out, the defect growth and occurrences of new defects have decreased significantly.

Wall Thickness Uncertainty

In this calculation example, the parameter being investigated is the fabrication quality of the pipeline. As additional complexity would be introduced into the limit state equations, it has been chosen to represent this difference in fabrication quality through the wall thickness uncertainty variable. This parameter is represented in the Table 11.4.

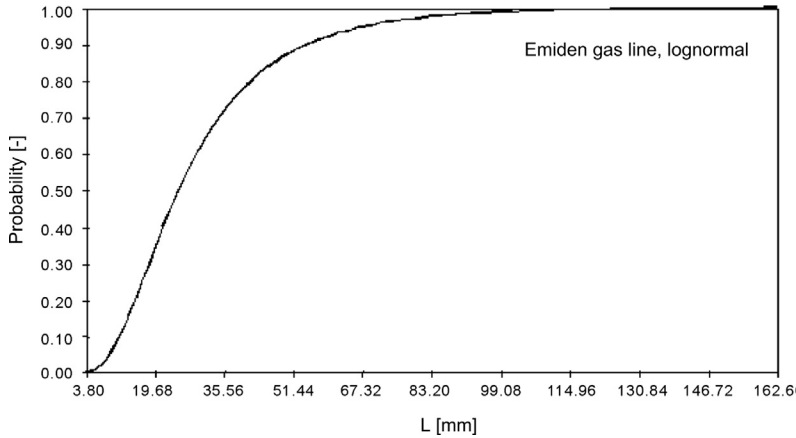

FIGURE 11.1 ***Cumulative Probability Distribution of Defect Lengths.***

Table11.4 Wall Thickness Parameter

Variable	Description	Distribution	Mean	Variance	Upper Bound	Lower Bound
x_t	Wall thickness uncertainty	Beta	1.02	High quality = 0.005 Low quality = 0.035	1.1	0.95

It is important to note that the difference between the qualities of pipeline depends on the variance of the parameter; the greater the variance, the less likely the fabricator is manufacturing to the specified size. The smaller the variation, the more constant the fabricator is in producing the pipe. These values were chosen using engineering judgment, so that reality is simulated to a reasonable extent.

Common Input Parameters

The basic parameters are summarized in Table 11.5.

For the purpose of this example, an upset is defined as water or wet gas ingress into the pipeline. Detection of an upset is assumed to lead to immediate shutdown. It is assumed that the upsets are independent occurrences and the line is dried after the previous upset before a new upset occurs. The total time of wet operation (t_w) is a product of the number of upsets per year, the duration of each upset, and the number of years operated.

Table 11.5 Summary of Common Input Parameters

Parameter	Comment	Distribution	Basic Value
CR	Corrosion rate, mm/yr	Constant	2.0
x_m	Model uncertainty	Gumbel distribution, max	Mean: 1.5 Std. dev.: 0.5
U	Number of upsets per year	Normal	Mean: 3 Std. dev.: 2
t (single upset)	Duration of wet line operation, single upset, days	Lognormal	Mean: 3 Std. dev.: 2
L	Length of defect, mm	Lognormal	Mean: 30 Std. dev.: 20
W_t	Wall thickness, mm	Constant	15.9
ID	Internal diameter, mm	Constant	425.2

Step 6. Reliability Analysis

Through the use of SYSREL [13], a reliability analysis program, it is possible to determine the cumulative failure probability of each year of operation. The annual failure probability was found using the equation that follows:

$$P_f(n) = \mathrm{CP}_f(n) - \mathrm{CP}_f(n-1) \qquad [11.17]$$

where

P_f = annual probability of failure
CP_f = cumulative probability of failure
n = year.

Figure 11.2 gives the distribution of annual failure probabilities.

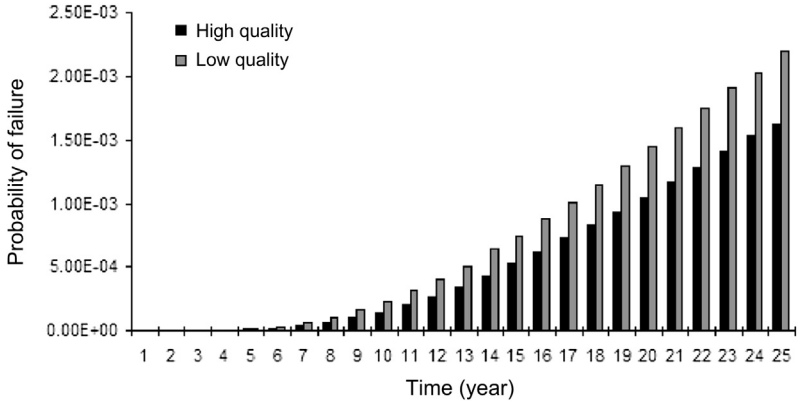

FIGURE 11.2 *Annual Failure Probabilities.*

Step 7. Cost of Consequence

In evaluating the cost of consequences of failure of pipeline, it is necessary to consider the mode of failure and the potential outcomes of those modes of failure. In developing the consequence costs, four separate costs can be considered: unplanned maintenance, environmental damage and cleanup, loss of production, and loss of human life, as shown in Table 11.6.

To calculate these costs accurately, it is necessary to carry out a thorough analysis of the possible consequences of pipeline failure. This can be simplified to the extreme boundaries of these consequences. As in our case, the consequences discussed in step 8 can be envisaged.

Step 8. Calculation of Expected Costs

In this calculation example, the development of corrosion increases with time, this has already been accounted for in the calculation of the probability of failure and is shown in Figure 11.2. To calculate the expected cost of these failure probabilities, it is necessary to consider the time value of money, such that the cost of consequences are projected to reflect the year in which the failure occurs. By multiplying this future expected value by the probability of failure for that year, it is possible to calculate the expected cost. Finally, this value must then be represented in present value form, so that it is possible to evaluate all costs equally. Summation over all of the years being evaluated gives an expected cost in terms of present value [13]:

$$\mathrm{EC} = \sum \mathrm{NPV}\{\mathrm{rate}, n, [\mathrm{FV}(\mathrm{inflation}, n, C)] \times P_{\mathrm{fn}}\} \qquad [11.18]$$

Table 11.6 Cost of Consequences

Cost	Variable	Boundary	Description	Cost (NOK)
Unplanned maintenance	C_{UM}^{U}	Upper	Spool replacement	20,000,000
	C_{UM}^{L}	Lower	Sleeve clamp	9,000,000
Environmental cost	C_{E}^{U}	Upper	>2500 m^3	5,000,000
	C_{E}^{L}	Lower	<100 m^3	250,000
Loss of production	C_{LP}^{U}	Upper	See note 1	0
	C_{LP}^{L}	Lower	See note 1	0
Human loss	C_{HL}^{U}	Upper	See note 2	0
	C_{HL}^{L}	Lower	See note 2	0

[1]Loss of production is a function of the time to repair; it is assumed that the time to repair in both cases is approximately equal.
[2]It is assumed that no human life is lost as a result of failure.

where

EC = expected cost

NPV (·)= economic expression for deriving a present value based on a future value

rate = economic return that can be expected from an alternative investment

n = year

FV(·)= economic expression for deriving a future value based on a present value

inflation = the amount by which the relevant is expected to rise by each year

C = cost being evaluated

P_{fn} = probability of failure in year n

In this calculation example, the inflation rate used is 2% and the "interest rate" used is 6%. The expected costs are given in Table 11.7.

Step 9. Initial Cost

The initial cost of the low-quality pipeline is assumed to be NOK (Norwegian Krone) 6500 per tonne. From this, a total cost for the pipeline can be calculated; it is assumed that the high-quality pipeline costs 5% over the cost of the low-quality pipeline. The initial costs are outlined in Table 11.8.

Step 10. Comparison of Life Cycle Costs

In this final step, it is possible to compare the two life cycle costs generated. To do this, it is necessary to consider all the combinations of the expected costs, thus giving the decision maker a full set of information being used to

Table 11.7 Expected Costs

Cost Type	Variable	Low Quality, Expected Cost	High Quality, Expected Cost
Maintenance, unplanned	C_{UM}^{U}	NOK 517,451	NOK 374,392
	C_{UM}^{L}	NOK 232,853	NOK 168,477
Environmental	C_{E}^{U}	NOK 129,363	NOK 94,490
	C_{E}^{L}	NOK 6,468	NOK 4,680

Table 11.8 Initial Costs

	Low Quality	High Quality
Initial cost (C_{I})	NOK 21,859,125	NOK 22,952,081

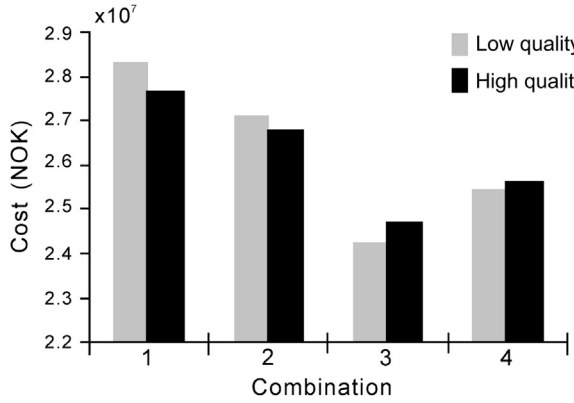

FIGURE 11.3 ***Comparison of LCC for Alternative Combinations.***

justify the final decision. Using the following equation, the final life cycle costs were found:

$$\mathrm{LCC} = C_{\mathrm{I}} + C_{\mathrm{F}} \qquad [11.19]$$

where

C_{I} = initial cost

C_{F} = sum of all costs associated with the failure or loss of performance of the pipeline

In this case, this involves the following:

C_{UM} = interval cost of unplanned maintenance, $[C^{U}_{\mathrm{UM}}, C^{L}_{\mathrm{UM}}]$

C_{E} = interval cost of environmental damage, $[C^{U}_{\mathrm{E}}, C^{L}_{\mathrm{E}}]$

The graphical representation in Figure 11.3 shows that, for the different combinations of consequences used, the optimal pipeline fabrication varies between high and low quality. This provides a basis from which a decision about the fabrication tolerance can be selected.

6. EXAMPLE OF ON-BOTTOM STABILITY USING THE LCC MODEL

Introduction

This example outlines the use of LCC modeling when deciding the method by which to stabilize a pipeline. This problem is discussed only in general terms, from which it would be possible to complete a more detailed assessment.

Analysis Procedure Using the LCC Model

Step 1. Definition of System

The system to be considered is a pipeline.

Step 2. Quality Aspects Considered

The quality aspect to be considered is on-bottom stability. From this, it is possible to identify different mechanisms by which the pipeline may be stabilized. These include

- Concrete coating.
- Dumping rocks.
- Dynamic stability.

Step 3. Failure Modes

The failure modes for on-bottom stability design criteria are

- Sliding lateral stability.
- Uplift vertical stability.

Given the high degree of correlation between the uplift and sliding modes of failure, the probability of stability failure is equal to the maximum of either the probability of sliding failure or the probability of uplift failure.

Step 4. Limit State Equations

Two limit state equations, one for each of the failure modes, these can be expressed as follows. For uplift failure,

$$g_1(X) = W - F_{\mathrm{L}} \qquad [11.20]$$

For lateral failure,

$$g_2(X) = Ru - F_{\mathrm{D}} \qquad [11.21]$$

where

W = submerged weight of pipe
F_{L} = hydrostatic uplift force
Ru = resistance of soil (friction)
F_{D} = hydrostatic drag force

Step 5. Definition of Variables and Parameters

As can be noticed from the Eqs. [11.20] and [11.21], there are few variables to be considered. However, a greater amount of complexity can be added to the model by introducing probabilistic variables.

Step 6. Reliability Analysis

The reliability analysis could be performed using SYSREL (as in the previous example). It is important to note the type of probability of failure that is determined in this procedure. For this example, the failure is a time independent failure, since the forces causing failure (currents and wave action) are random in nature.

Step 7. Cost of Consequence

Movement of the pipeline could result in buckling, which could result in similar consequence scenarios as those presented in the previous example. Alternatively, the consequence may be to stabilize the pipeline further. This is a very case-specific matter, which requires further details.

In determining the cost consequence, it is necessary to use the time value of money to determine the NPV of cost of consequences.

Step 8. Expected Cost

By multiplying the cost of consequences and the risk found, it is possible to determine the expected cost of failure.

Step 9. Initial Cost

The initial cost of the method by which the pipeline is stabilized can be found universally among pipeline design consultants and operators.

Step 10. Comparison of Life Cycle Costs

The final product of this analysis renders a range of on-bottom stability methods along with their potential life-cycle costs, allowing an informed decision to be reached.

REFERENCES

[1] Fabrycky WJ, Blanchard BS. Life-cycle cost and economic analysis. Englewood Cliffs, NJ: Prentice-Hall; 1991.

[2] Bai Y, Sørheim M, Nødland S, Damsleth PA. LCC modeling as a decision making tool in pipeline design. OMAE'99 1999.

[3] Cui W, Mansour AE, Elsayed T, Wirsching W. Reliability based quality and cost optimisation of unstiffened plates in ship structures. In: Oosterveld MWC, Tan SG, editors. Proceedings of PRADS '98. Amsterdam: Elsevier Science BV; 1998.

[4] Bea R. Human and organization factors in the safety of offshore structures. In: Soares CG, editor. Risk and reliability in marine technology. Rotterdam, The Netherlands: A. A. Balkema; 1998.

[5] Bea R. The role of human error in the design, construction and reliability of marine structures. SSC-378, U. S. Coastguard, Washington, DC: Ship Structure Committee; 1994.
[6] Bea R, et al. Life-cycle reliability characteristic of minimum structures. Florence, Italy: OMAE'96; 1996.
[7] Langford G, Kelly PG. Design, installation and tie-in of flowlines. JPK Report No. 4680.1; Stavanger, Norway; 1990.
[8] Sørheim M, Bai Y. Risk analysis applied to subsea pipeline engineering. St. John's, Canada: OMAE'99; 1999.
[9] Nødland S, Bai Y, Damsleth P. Reliability approach to optimise corrosion allowance. IBC Conference on Risk Based and Limit State Design and Operation of Pipelines 1997.
[10] DeWaard C, Lotz U. Prediction of CO_2 corrosion of carbon steel. Paper no. 69., CORROSION '93; 1993.
[11] ASME B31G. Manual for determining the remaining strength of corroded pipes. New York: American Society of Mechanical Engineers; 1993.
[12] Bai Q, Bai Y. Subsea pipeline design, analysis, and installation. Houston, TX: Gulf Publishing; 2014.
[13] SYSREL. A structural system reliability program, rev. 9.10. Munich, Germany: RCP Consulting; 1996.

CHAPTER 12

Quantitative Risk Analysis Based RBI

Contents

1. Introduction 271
   Definitions 272
   Motivation and Objective 272
2. Methodology and Basic Principle 273
   Probability of Failure 274
   Consequence of Failure 275
   Risk Determination and Inspection Plan 276
3. Quantitative Risk Analysis Based RBI Process 276
   Collection of Information 276
   Risk Acceptance Criteria 277
   Pipeline Segmentation 277
   Quantitative Risk Assessment 278
      PoF Determination 278
      CoF Determination 280
   High-Risk Locations and Major Failure Mechanisms 281
   Inspection Plan 282
4. Case Study 282
   Pipeline Segmentation 282
   PoF Calculation 283
   PoF Modification 283
   PoF Analysis 284
   CoF Identification 285
   Risk Determination 285
   High-Risk Location and Major Degradation Mechanisms 286
   Inspection Plan 287
   Summary 287
References 288

1. INTRODUCTION

With increasing public awareness and concern for the pipeline operating conditions, risk-based inspection has been becoming a hot topic. Software has already been developed to do the risk-based inspection (RBI) analysis, for example, the DNV ORBIT software [1]. However, traditional RBI can do risk assessment for pipelines only based on inspection records or simply

Subsea Pipeline Integrity and Risk Management
ISBN 978-0-12-394432-0
http://dx.doi.org/10.1016/B978-0-12-394432-0.00012-3

qualitative assessments for a new pipeline, which may not reflect the risk condition clearly.

This chapter describes a new approach of quantitative risk assessment (QRA) based RBI (QRBI) to do risk assessment for a new pipeline or a pipeline without inspection records on which to establish an optimized inspection plan and ensure that the level of risk remains below the acceptance limit in the infant mortality phase.

QRBI is a semi-quantitative analysis both in probability of failure (PoF) and consequence of failure (CoF) for different pipeline sections. Major degradation mechanisms and high risk locations are identified. The PARLOC Database 2001 is used to calculate the PoF, while CoF is determined mainly by the software POSVCM form MMS and HGSYSTEM from Shell.

Definitions

QRBI planning is a method for establishing optimized inspection strategy based on the QRA for a new pipeline or a pipeline without inspection records, where the inspection efforts focus on the major degradation mechanisms and high-risk locations to ensure the pipeline system's integrity in the infant mortality phase.

Inspection planning based on the QRBI approach uses safety, economic, and environmental risk of failure as a rational and cost efficient decision framework for determining high-risk pipeline sections and major degradation mechanisms.

QRBI includes initial assessment and detailed assessment. The initial assessment focuses on the use of PARLOC database to determine the risk, and the detailed assessment focuses mainly on the evaluation and modification of the PARLOC risk database on the basis of internal and external corrosion and external impact according to the actual data to identify the risk ranking.

Motivation and Objective

Figure 12.1 illustrates the well-known bathtub curve shape of failure rate changes over time. In the initial period, some equipment or installations have a high initial rate of failure, the portion of the curve is called the *burn-in phase* or *infant mortality phase*, in which, the defects developed during initial manufacture of a component cause failures. After these defects are eliminated, the curve levels into the second zone, which is called the *constant*

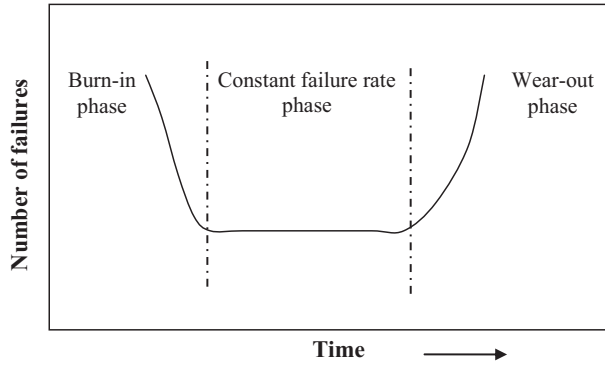

FIGURE 12.1 ***Common Failure Rate Curve (Bathtub Curve).*** *Source: Bai and Bai [2].*

failure zone and reflects the phase where random accidents maintain a fairly constant failure rate.

In the initial in-service years for a pipeline, the failure frequency is high; it is necessary and meaningful to perform a quantitative and precise assessment to identify the major degradation mechanisms and high-risk locations in this infant mortality phase, which can be evaluated by QRBI. An inspection plan based on QRBI is a rational and cost-effective decision framework for developing an inspection strategy that can be used to ensure system integrity.

QRBI is a means of focusing on and optimizing the use of resources to "high-risk" areas in the infant mortality phase. The objectives of QRBI are

- To assess in terms of likelihood and consequence all reasonably expected hazards to health, safety, and the environment in the infant mortality phase for a new pipeline.
- To identify the major failure mechanisms and high-risk locations for a pipeline that is new or without inspection records in the infant mortality phase.
- Establish an optimized and cost-effective inspection plan to ensure the pipeline system integrity in the infant mortality phase.

2. METHODOLOGY AND BASIC PRINCIPLE

In QRBI study, the risk associated with a component is the product of the probability of component failure (PoF) and the consequence of failure (CoF). Both PoF and CoF are determined in terms of detailed figures.

The following tools can be used in QRBI analyses:

- PARLOC Database 2001.
- DNV RP F101.
- DNV RP F107.
- DNV RP F111.
- Software of POSVCM, HGSYSTEM, Adios, and the like.

Probability of Failure

The data contained in PARLOC Database 2001 can be considered as a starting point in the identification of potential hazards and provide initial indications of the likely levels of loss of containment frequency for an individual pipeline. They also provide indications of the level of reliability achieved in the operation of North Sea pipelines, which can be used in the context of quantified risk assessment.

The PARLOC database is used to predict pipeline failure rates based on the following two assumptions:

- The development of failure rates is coherent with the historical statistic results in the PARLOC database.
- The PARLOC database from the North Sea is applicable to pipeline maritime space analysis.

The main PoF calculation processes based on the PARLOC database are as follows;

- Identify the pipeline length and transporting product, which can be used to find relative information in the Tables 5.4 to 5.8 of the PARLOC database.
- Determine the relativity of failure mechanisms in different sections to use Table 2.2 of the PARLOC database.
- Use Tables 5.4 to 5.8 to determine the PoF, which equals relativity multiplied by the frequency per year.
- Then, according to the histories, properties, characteristics, and functions of individual pipelines, identify which bound to take: lower bound, best estimated, or upper bound.
- Use Tables 4.6 to 4.8 of the PARLOC database to calculate the relativity of different hole sizes.
- Determine the PoF in different hole sizes, then add the PoF of each different hole size.

Consequence of Failure

The consequence of failure is defined for all consequences of importance to the company, such as safety, economy, and environment. the CoF is evaluated as the outcome of a failure based on the assumption that such a failure will occur. Estimation of the consequence of failure is a vital part of the QRBI process and is important for prioritization in the assessment.

Consequence is normally divided into the categories of safety, economic, and environmental consequences. Normally, the severest problem to gas leakage is safety and to oil spill is environmental.

The consequences of failure are

- Consequential production losses.
- Contract penalties.
- Cost of repairing the pipeline.
- Potential fatalities.
- Cost of negative publicity.

The safety consequences include individual and social consequences. Individual consequences are concerned with the fatalities. Social consequences are the third party (society) risks posed to the passing fishing vessels and merchant shipping. Acceptance of the third party risks posed by pipeline should be on the basis of the F-N curves (N is the number harmed, and F is the frequency attributed to each event). The economic consequences are quantified using money loss, including the direct product loss due to the spill or rupture, repair costs, and product loss duo to the downtime. The environmental consequences are mainly quantified in terms of the product dispersed in the water, recovery years of the environment, and so forth.

The potential consequences depend greatly on the operating pressure, pipeline length, diameter, and content and size of the failure or release. The leakage volume of oil and gas can be determined by the POSVCM from MMS and HGSYSTEM software from Shell, respectively. Representative hole sizes with diameters of 20 mm, 80 mm, and 200 mm can be modeled in these software. The product dispersed in water can be simulated using the software of Adios, and the recovery years of the environment can be determined by the dispersed volume of product, the local ecosystem, and treatment by local government. In general, the qualitative consequence of failure introduced in the "Quantitative Risk Assessment" subsection of Section 3 can be used in QRBI.

Risk Determination and Inspection Plan

The major failure mechanisms and high-risk locations are determined, combined with the PoF and CoF. The risk prediction and inspection plan should focus on these items and areas.

3. QUANTITATIVE RISK ANALYSIS BASED RBI PROCESS

As shown in Figure 12.2, the following steps are carried out for a quantitative risk analysis based RBI analysis [3]:

- Develop risk acceptance criteria.
- Collection of information.
- Determine pipeline segmentation.
- Quantitative risk assessment for all sections.
- Identify major degradation mechanisms and high-risk locations in the infant mortality phase.
- Generating an inspection plan.
- Use these as input into the inspection management system.

Collection of Information

The information mainly includes pipeline design data, operation data, pipeline alignments, and a corrosion study report. These data are used to

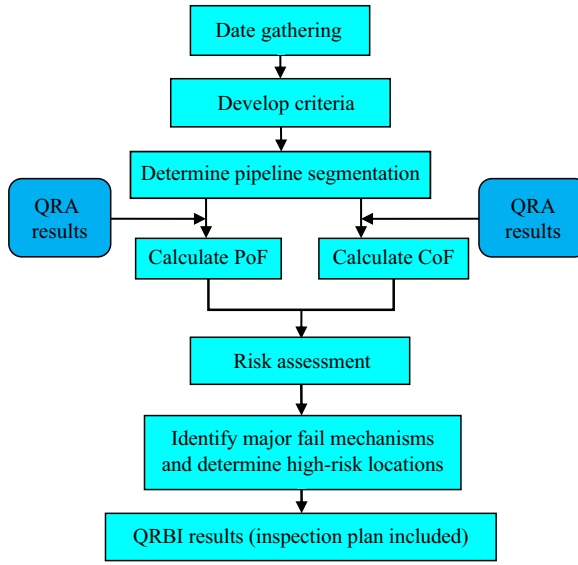

FIGURE 12.2 ***QRBI Process.*** (For color version of this figure, the reader is referred to the online version of this book.)

5	$>10^{-2}$					
4	10^{-2} - 10^{-3}			Unacceptable area		
3	10^{-3} - 10^{-4}					
2	10^{-4} - 10^{-5}	Acceptable area				
1	0 - 10^{-5}					
		A	B	C	D	E
Safety (deaths)		0	0.1	1	10	100
Environmental (recovery period)		0	< 1 year	< 3 year	< 10 year	> 10 year
Economic (MNOK)		<250	250	500	750	>750

FIGURE 12.3 ***Quantitative Risk Acceptance Criteria.*** (For color version of this figure, the reader is referred to the online version of this book.)

determine the PoF and CoF, also to predicate the risk and establish an optimized inspection plan.

Risk Acceptance Criteria

Similar to the traditional RBI, the QRBI risk quantifies from the aspects of individuals, environment, and economy. The safety class depends on the product, personnel, and location class. If the product is toxic or the location is a sensitivity area, then the safety class should be taken as high. Figure 12.3 shows a quantitative risk acceptance, because the failure consequence is quantitative. Figure 12.4 shows a qualitative risk acceptance.

Pipeline Segmentation

Pipeline segmentation is determined to save effort in analyzing inapplicable damage causes in some parts. A pipeline usually does not have a constant hazard potential over its entire length; as conditions along the line route

PoF category	Annual probability of failure					
5	Expected failure	M	H	H	VH	VH
4	High	M	M	H	H	VH
3	Medium	L	M	M	H	H
2	Low	VL	L	M	M	H
1	Virtually nil	VL	VL	L	M	M
CoF of failure category		A	B	C	D	E

FIGURE 12.4 ***Qualitative Risk Acceptance Criteria.*** (For color version of this figure, the reader is referred to the online version of this book.)

change, so does the risk ranking, Thus, damage causes may be applicable for only some sections or components of a pipeline system.

In QRBI assessment, each pipeline system should be divided into several components, as the following components address different damage causes and degradation mechanisms being encountered:

- Riser above water.
- Riser in splash zone;
- Riser below water and pipeline in location class 2 (within 500 m of installation).
- Pipeline in location class 1 (beyond 500 m of installation).
- Pipeline approach the sensitive location, for example, park and city.
- Pipeline passes the trawling zone.
- Onshore part of pipeline.

The detailed segmentation apply to the condition of individual pipeline.

Quantitative Risk Assessment

In the QRBI assessment, PoF and CoF are determined for different failure mechanisms in different sections of the pipeline system. The following degradation mechanisms are considered:

- Internal corrosion.
- External corrosion.
- External impact(anchor, wreck, and trawler).
- Material defect(material-weld defect and material-steel defect).

PoF Determination

Failure Rates from PARLOC Database 2001

The PARLOC Database 2001 is considered the starting point in calculation of the PoF. In the PARLOC database, the failure rate is divided into three categories: lower bound, best estimated, and upper bound. Which category should be taken depends on the condition of the individual pipeline and the experience of engineer; for example if one section is not buried and is in the trawling zone, the upper bound of trawling PoF should be taken. Also the equivalent hole size for incidents to operating pipelines is divided into three categories: small (0–20 mm), medium (20–80 mm), and large (larger than 80 mm). So the failure rates should consider the equivalent hole to further reflect the probability of failure.

Similarly, the failure rates of a pipeline in the riser, pipeline, and shore zone or sensitivity zone can be determined according to the PARLOC Database 2001.

PoF Modification

The preceding failure rates are statistic results deduced from the PARLOC database. However, note that individual pipelines may have quite different histories, properties, characteristics, and functions. Therefore, these values require further modification based on the special conditions of the oil export pipeline and the experience of the engineer. For example, in a concrete coating section where no impact comes from the external environment to the pipeline, the external impact can be neglected.

In the PoF modification of degradation mechanisms, the details are as follows.

Damage from external impact may arise from several causes, such as dropped objects, anchor impact, anchor dragging, trawling, boat impact to risers, or fish bombing.

External impact is an event-based damage cause, the failure rate tends to vary with a changing environment, and the underlying mechanism is usually random and should exhibit a constant failure rate as long as the environment stays constant. So, to predicate the risk is very difficult. However, the following items can be calculated and used to predict the risk from the external impact:

- Impact frequency from a dropped anchor (DNV GL 13).
- Impact frequency from trawling (DNV GL 13).
- Probability of a direct dropped anchor impact calculation.
- Dropped anchor impact assessment (DNV-RP-F107).
- Trawler impact dent assessment (concrete coating and non-concrete).
- Trawler impact frequency calculation.
- Trawler pullover force calculation.

In the PoF modification of internal corrosion, the following items should be considered:

- Internal corrosion rate prediction.
- Prevention strategies, water removal, and corrosion inhibition.

Generally, in the infant mortality years for a pipeline, external corrosion is not a problem due to the cathodic protection and external coating. However, in the splash zone, the external corrosion is high, so this zone should be inspect frequently.

In the PoF modification of external corrosion, the following items should be considered:

- Coating system.
- CP system.
- External corrosion rate prediction.

CoF Determination

In the QRBI assessment, the CoF is measured in terms of safety, environmental pollution, and business for gas pipelines and oil pipelines, respectively [4].

Safety Consequences

Safety consequences include individual and social consequences (Table 12.1).

It is assumed that individual consequences are applicable to just riser and safety zone segments when considering the likelihood of people in the vicinity. Safety consequences for risers and safety zones may be considered to be similar to the topside failure consequences; however, their inventories may be much larger. These components are in close proximity to both human activity and potential ignition sources. Safety consequences are usually presented in terms of potential loss of life (PLL).

The spill volume of oil and gas can be determined by the software of POSVCM and HGSYSTEM, respectively.

Environmental Consequences

Environmental consequences are concerned with the impact of various types of product release to the environment. The volume of oil spill dispersed in water can be modeled using the software Adios.

Table 12.1 The Safety Consequence Model

	Safety		
Product	**With Personnel**	**Occasional Personnel**	**No Personnel**
Gas, well fluid	E	D	B
Gas, semi-processed	E	C	A
Gas, dry	E	C	A
Oil, well fluid	D	C	B
Oil, semi-processed	C	B	A
Oil, dry	C	B	A
Condensate, well fluid	E	D	B
Condensate, semi-processed	E	C	A
Condensate, dry	E	C	A
Treated seawater	B	A	A
Raw seawater	B	A	A
Product water	B	A	A

Table 12.2 The Environment Consequence Model

Product	Environment			
Pipe size	$D < 8$-in.	$D > 8$-in.	$D > 16$-in.	$D > 32$-in.
Gas, well fluid	B	B	B	C
Gas, semi-processed	A	A	A	B
Gas, dry	A	A	A	B
Oil, well fluid	B	C	D	E
Oil, semi-processed	B	C	D	E
Oil, dry	B	C	D	E
Condensate, well fluid	B	B	C	D
Condensate, semi-processed	B	B	C	D
Condensate, dry	B	B	C	D
Treated seawater	A	A	A	A
Raw seawater	A	A	A	A
Product water	B	B	B	C

Environmental pollution severity is determined by the oil spill volume dispersed in water and the local conditions, for example, the fishing resources. The environmental pollution ranking is determined by the recovery years of natural resources, which are decided by the recovery of local resource and local government effort. How to determine the pollution severity is illustrated in the "Quantitative Risk Assessment" subsection. Table 12.2 gives a qualitative environment consequence model.

Economic Consequences

Economic consequences are concerned with repair costs and business loss due to interruption in production. The repair can be divided into two parts, consequence for leak and consequence for rupture. The repair consequences also depend on the location of the failure (e.g., above water, splash zone area, or underwater). Economic consequences due to business interruption or deferred production relate to the costs due to the shutdown of pipeline. An important factor to be considered is redundancy in the system, whereby production is maintained by using bypass lines. Table 12.3 gives a qualitative economy consequence model.

High-Risk Locations and Major Failure Mechanisms

Risk is the product of PoF and CoF. In QRBI risk assessment, every section and every degradation mechanism of the pipeline system is determined to identify the major failure mechanisms and high-risk locations.

Table 12.3 Economy Consequence Model

Product	Economy			
Pipe size	$D < 8$-in.	$D > 8$-in.	$D > 16$-in.	$D > 32$-in.
Gas, well fluid	B	C	D	E
Gas, semi-processed	B	C	D	E
Gas, dry	B	C	D	E
Oil, well fluid	B	C	D	E
Oil, semi-processed	B	C	D	E
Oil, dry	B	C	D	E
Condensate, well fluid	C	D	E	E
Condensate, semi-processed	C	D	E	E
Condensate, dry	C	D	E	E
Treated seawater	A	B	C	D
Raw seawater	A	B	C	D
Product water	A	B	C	D

Inspection Plan

The result from the QRBI assessment defines a proposed inspection plan for pipelines that are new or without inspection records.

For the QRBI assessment, the major objective is to identify the main degradation of every pipeline section, so the inspection plan of QRBI gives recommendation for inspection scheduling, describing [5]

- Which pipeline section is the high-risk location in infant years.
- Which failure mechanism is major for different sections.
- Which degradation mechanisms should be inspected first.

4. CASE STUDY

In this example, the initial assessment is illustrated based on the UK PARLOC, and the detailed QRBI process is assessed by the tools, including the DNV-RP-F107 [6] and DNV-GL-13 [7]. Table 12.4 lists the pipeline parameters.

Pipeline Segmentation

In this example, the pipeline is simply segmented into the following four parts:

- Riser.
- Safety zone.

Table 12.4 Example Pipeline Parameters

Parameter	Unit	Value
Pipe length	km	6.0
Outside diameter	mm	460.0
Wall thickness	mm	17.5
Grade (API Spec 5L)	—	X65
Operating pressure	bar	19.1
Product temperature	K	339.5
Product density	kg/m^3	806.0
Personnel condition	—	Staffed
Product type	—	Oil, well fluid

- Midline without concrete coating.
- Midline with concrete coating.

PoF Calculation

The data contained in the PARLOC database is used as a starting point in the identification of potential hazards and provides initial indications of the likely levels of the loss of containment frequency for an individual pipeline. For different leak causes, the lower bound, best estimated, and upper bound failure frequencies of the 150 km long oil export pipeline derived from PARLOC 2001 (Table 5-7 and Table 5-8) are list in Table 12.5.

PoF Modification

The failure rates in Tables 12.6 and 12.7 are exactly the statistical results from the PARLOC database. However, note that individual pipelines may have very different histories, properties, characteristics, and functions; and these values need further modification based on the special conditions of pipeline.

Table 12.5 Relative Failure Frequencies for Riser

	Frequency per km-yr		
Cause	Lower Bound	Best Estimate	Upper Bound
Anchor	0.00E+00	0.00E+00	0.00E+00
Trawler	0.00E+00	0.00E+00	0.00E+00
Dropped object	0.00E+00	0.00E+00	0.00E+00
Wreck	0.00E+00	0.00E+00	0.00E+00
Internal corrosion	0.00E+00	0.00E+00	0.00E+00
External corrosion	3.95E-02	9.11E-02	1.79E-01
Material defect	1.98E-02	4.55E-02	8.96E-02

Table 12.6 Relative Failure Frequencies for Safety Zone

	Frequency per Year		
Cause	**Lower Bound**	**Best Estimate**	**Upper Bound**
Anchor	1.29E-04	2.73E-02	1.17E-01
Trawler	0.00E+00	0.00E+00	0.00E+00
Dropped object	0.00E+00	0.00E+00	0.00E+00
Wreck	0.00E+00	0.00E+00	0.00E+00
Internal corrosion	4.62E-03	8.00E-03	1.29E-02
External corrosion	1.55E-03	2.67E-03	4.32E-03
Material defect	6.15E-03	1.07E-02	1.73E-02

Table 12.7 Relative Failure Frequencies for Midline

	Frequency per Year		
Cause	**Lower Bound**	**Best Estimate**	**Upper Bound**
Anchor	2.64E-05	5.28E-04	2.51E-03
Trawler	7.94E-05	1.59E-03	7.53E-03
Dropped object	0.00E+00	0.00E+00	0.00E+00
Wreck	1.32E-04	2.64E-03	1.25E-02
Internal corrosion	7.46E-03	1.29E-02	2.09E-02
External corrosion	2.13E-03	3.69E-03	5.97E-03
Material defect	2.13E-03	3.69E-03	5.97E-03

In this case study, it is assumed that the following items are valid:

- Internal corrosion rate is high.
- External corrosion for riser and safety zone is serious.
- Trawler impact frequency is high.
- Trawler impact dent depth assessment is very significant for the section with a concrete coating and unacceptable for pipelines without a concrete coating.
- Drop frequency from anchors is low.

Table 12.8 lists the results of failure probability according to the individual pipeline properties.

PoF Analysis

The analyses of failure probability include the proportion of degradation mechanisms in sections and proportion of section in degradation mechanisms. The analysis results are displayed in Tables 12.9 and 12.10.

Table 12.9 reflects the major degradation mechanisms in each section. For example, in the riser section, the main failure results from external corrosion

Table 12.8 Modified Failure Probability

Cause, Pipeline	Riser	Safety Zone	Midline, No Coating	Midline, Coating
Anchor	0.00E+00	2.73E-02	5.28E-04	2.64E-05
Trawler	0.00E+00	0.00E+00	1.59E-03	7.94E-05
Dropped object	0.00E+00	0.00E+00	0.00E+00	0.00E+00
Wreck	0.00E+00	0.00E+00	2.64E-03	1.32E-04
Internal	0.00E+00	8.00E-03	1.29E-02	7.46E-03
External	3.95E-02	2.67E-03	3.69E-03	2.13E-03
Material	1.98E-02	1.07E-02	3.69E-03	2.13E-03

Table 12.9 Proportion of Degradation Mechanisms in Sections

Cause, Pipeline	Riser	Safety Zone	Midline, No Coating	Midline, Coating
Anchor	0.00%	56.17%	1.70%	0.12%
Trawler	0.00%	0.00%	24.25%	7.41%
Dropped object	0.00%	0.00%	0.00%	0.00%
Wreck	0.00%	0.00%	8.50%	12.31%
Internal	0.00%	16.45%	41.64%	60.28%
External	79.87%	5.49%	11.88%	9.93%
Material	20.34%	21.94%	11.88%	9.93%

Table 12.10 Proportion of Section in Degradation Mechanisms

Cause, Pipeline	Riser	Safety Zone	Midline, No Coating	Midline, Coating
Anchor	0.00%	90.10%	8.27%	1.74%
Trawler	0.00%	0.00%	82.57%	17.43%
Dropped object	0.00%	0.00%	0.00%	0.00%
Wreck	0.00%	0.00%	50.00%	50.00%
Internal	0.00%	23.58%	38.14%	38.14%
External	95.20%	1.42%	1.97%	1.14%
Material	73.37%	17.22%	5.96%	3.44%

and material defect. Table 12.10 reflects the failure mechanism mainly acting on each section, for example, the anchor focus on the safety zone.

CoF Identification

According to the "Quantitative Risk Assessment" subsection, the safety, environment, and economy consequence can be identified, respectively, as in Table 12.11.

Risk Determination

Table 12.12 shows the risk determined by the PoF and CoF.

High-Risk Location and Major Degradation Mechanisms

The high-risk locations can be determined as shown in Table 12.13.

According to Tables 12.9 and Table 12.13, the major degradations of the riser zone are xternal corrosion and material defect loss; the major

Table 12.11 Consequence Results

Consequence Type	Consequence Level
Safety consequence	D
Environmental consequence	D
Economy consequence	D

Table 12.12 Pipeline Segmentation Risk Display

Segmentation, Risk	Cause	Safety	Environmental	Economy
Riser	Anchor	M	M	M
	Trawler	M	M	M
	Dropped object	M	M	M
	Wreck	M	M	M
	Internal	M	M	M
	External corrosion	VH	VH	VH
	Material defect	VH	VH	VH
Safety zone	Anchor	VH	VH	VH
	Trawler	M	M	M
	Dropped object	M	M	M
	Wreck	M	M	M
	Internal	H	H	H
	External	H	H	H
	Material defect	VH	VH	VH
Midline, no concrete coating	Anchor	M	M	M
	Trawler	H	H	H
	Dropped object	M	M	M
	Wreck	H	H	H
	Internal	H	H	H
	External	H	H	H
	Material defect	H	H	H
Midline, concrete coating	Anchor	M	M	M
	Trawler	M	M	M
	Dropped object	M	M	M
	Wreck	M	M	M
	Internal	H	H	H
	External	H	H	H
	Material defect	H	H	H

Table 12.13 High-Risk Location of Different Sections

Segmentation	Cause	Safety	Environmental	Economy
Riser	External corrosion	VH	VH	VH
	Material defect	VH	VH	VH
Safety zone	Anchor	VH	VH	VH
	Internal	H	H	H
	External	H	H	H
	Material defect	VH	VH	VH
Midline, no concrete coating	Trawler	H	H	H
	Wreck	H	H	H
	Internal	H	H	H
	External	H	H	H
	Material defect	H	H	H
Midline, concrete coating	Internal	H	H	H
	External	H	H	H
	Material defect	H	H	H

degradations of the safety zone are anchor impact and material defect; the major degradations of the midline with no coating are internal corrosion and trawler impact; the major degradations of the midline with coating are wreck and internal corrosion.

According to Table 12.10, material defects and external corrosion occur mainly in the riser zone; the anchor impact occurs mainly in the safety zone;, the trawler impact occurs mainly in the midline with no coating; wrecks occur mainly in the midline; internal corrosion occurs mainly in the midline.

Inspection Plan

Inspection planning based on the RBI approach provides a rational and cost-efficient decision framework for determining the following key points [8]:

- Where to inspect.
- What to inspect.

The inspection plan should be made according to the risk analysis results; for example, the external corrosion of the riser zone should be given more attention and be inspected frequently.

Summary

QRBI can identify major degradation mechanisms and high-risk locations for a new pipeline and establish an optimized inspection plan for new

pipeline in the burn-in phase. QRBI assessment is necessary and meaningful for a new pipeline to ensure the pipeline does not fail in the infant mortality phase.

REFERENCES

[1] DNV. Rules for submarine pipelines. Oslo, Norway: Det Norske Veritas; 1981.
[2] Y. Bai Y, Bai Q. Subsea pipelines and risers. Oxford, UK: Elsevier; 2005.
[3] Badaruddin MF, Zhang FY, Bai Y. Quantitative risk assessment (QRA) based leak detection criteria (LDC) design for a subsea oil export pipeline. Honolulu, USA: OMAE2009–79250; 2009.
[4] Mott MacDonald Ltd. PARLOC 2001. The update loss of containment data for offshore pipelines. Liverpool, Merseyside, England: HSE, The UK Offshore Operators Association and The Institute of Petroleum; 2001.
[5] Muhlbauer WK, WK. Pipeline risk management manual. 3rd ed. Houston, TX: Gulf Professional Publishing; 2004.
[6] DNV-RP-F101. Corroded pipelines. Oslo, Norway: Det Norske Veritas; 2004.
[7] DNV Guideline No.13. Interference between trawl gear and pipelines. Oslo, Norway: Det Norske Veritas; September 1997.
[8] DNV-OS-F101. Submarine pipeline systems. Oslo, Norway: Det Norske Veritas; 2000.

CHAPTER 13

Risk- and Reliability-Based Fitness for Service

Contents

1. Introduction 289
   Target Reliability 290
   Data Collection 292
2. Quantitative-Risk Assessment and Target Reliability 292
   Pipeline Segmentation 293
   Probability of Failure 293
   Consequences of Failure 294
   Target Reliability 295
3. SRA and Retaining Pressure Capacity 295
   General 295
   Structure Reliability Assessment Method 296
   Evaluation of Strength Uncertainties 298
   Pipeline Retaining Pressure Capacity 298
4. Corrosion Rate 300
5. Example of Risk- and Reliability-Based FFS 300
   Pipeline Data 300
   Analysis Results 300
   Summary 304
References 305

1. INTRODUCTION

The risk- and reliability-based fitness for service (FFS) discussed in this chapter is focused on pipeline corrosion defects only. First of all, QRA is performed to derive the pipeline target reliability. Then, by using the structural reliability analysis (SRA) method, whether the pipeline is fit for service or not is evaluated by a comparison of pipeline retaining pressure capacity with a given MAOP. The main objectives of QRA and reliability-based FFS study include the following items:

- To portray a pipeline's present risk picture and define the target reliability of every pipeline segment.
- To determine the pressure containment capacity of the pipeline at the time it was last inspected.

Subsea Pipeline Integrity and Risk Management
ISBN 978-0-12-394432-0
http://dx.doi.org/10.1016/B978-0-12-394432-0.00013-5

- To conduct a corrosion assessment to estimate the internal corrosion rates.
- To determine the remaining years for which the pipeline can be safely operated, dated from the last inspection.
- To recommend suitable actions to be taken based on the assessment findings.

The internal CO_2 corrosion is considered the only damage mechanism in this discussion. Mitigation actions are proposed if the pipeline is considered unfit for service. The assessment begins with a review of various data of the pipeline, including pipeline design data and actual pipeline inspection data. The process of QRA and reliability-based FFS study are illustrated in Figure 13.1.

Target Reliability

To ensure certain safety levels of pipeline or pipeline segments, target reliability need to be settled and has to be met at pipeline design phase.

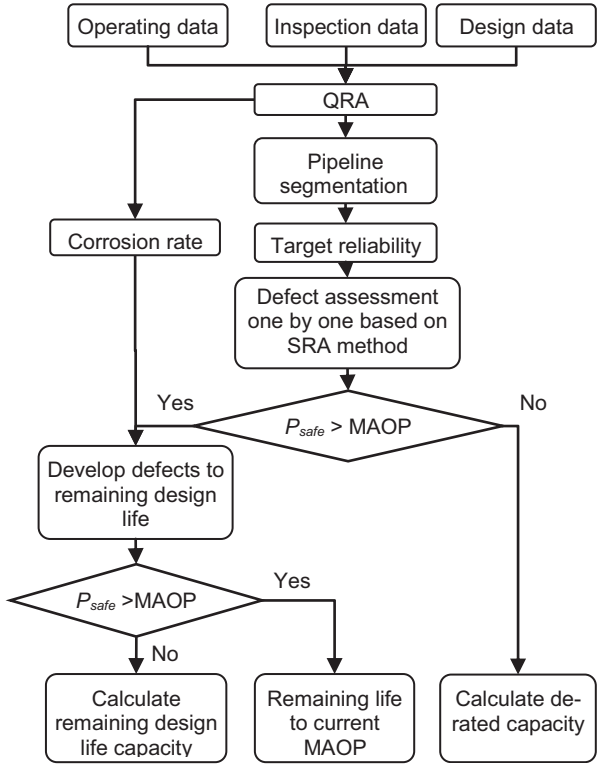

FIGURE 13.1 *Flowchart of SRA Method.*

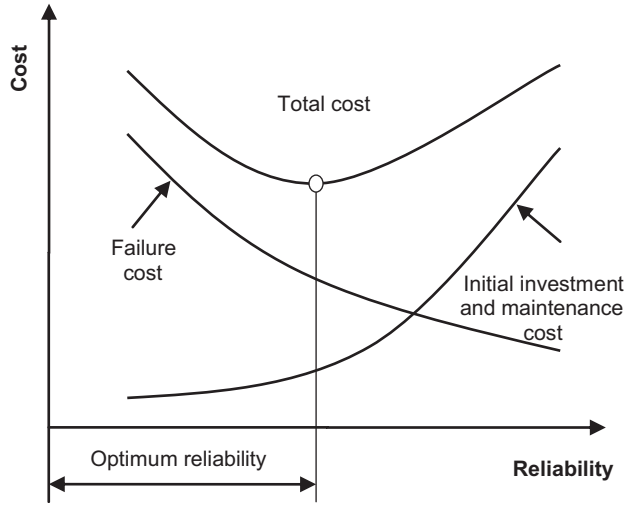

FIGURE 13.2 ***Target Reliability and Minimization of Life Cycle Cost.*** *Source: Jaio et al. [3].*

Theoretically, the life cycle cost-benefit assessment described in Chapter 11 should be the perfect method for determining the optimum target reliability, as shown in Figure 13.2. However, this method is impracticable because of the great uncertainty and complexity at the life cycle cost calculation.

Table 13.1 shows the target reliabilities applied in the subsea pipeline engineering for different limit states.

The selection of target reliability is based on the consequences of failure, location and the contents of pipelines, relevant rules, access to inspection and repair, and the like. Traditionally, the DNV-RP-F101-based FFS assessment method chooses the target reliability merely considering the location and contents of pipeline qualitatively. This chapter, however, introduces a pipeline quantitative risk assessment (QRA) method, which

Table 13.1 Target Reliabilities Versus Safety Classes

	Safety Class		
Limit State	**Low**	**Normal**	**High**
SLS	$10^{-1} \sim 10^{-2}$	$10^{-2} \sim 10^{-3}$	$10^{-3} \sim 10^{-4}$
ULS	$10^{-2} \sim 10^{-3}$	$10^{-3} \sim 10^{-4}$	$10^{-4} \sim 10^{-5}$
FLS	$10^{-2} \sim 10^{-3}$	$10^{-3} \sim 10^{-4}$	$10^{-4} \sim 10^{-5}$
ALS	$10^{-3} \sim 10^{-4}$	$10^{-4} \sim 10^{-5}$	$10^{-5} \sim 10^{-6}$

makes full use of all the data available. The QRA process brings the following benefits to the FFS analysis [2]:

- Much more precise pipeline segmentation.
- Much more precise pipeline failure consequences calculation.
- Much more detailed calculation of corrosion rates.
- Much more beneficial choice of pipeline target reliabilities.

Data Collection

Abundant data are needed for performing the QRA and reliability FFS study for subsea pipelines. The general requirements follow [3]:

1. Pipeline design and operational data:
   - Geometric dimensions.
   - Material data.
   - Coating.
   - CP design data.
   - Fluid compositions.
   - Design and operational pressures and temperatures data.
2. Environmental data:
   - Water depth profile.
   - Wind, wave, and current data.
   - Environmental temperature profile.
   - Geotechnical data.
   - Pipeline alignment maps.
3. Pipeline inspection data.
4. Pipeline accident records, if any.
5. Pipeline technical study reports, if any (such as QRA, EIA (Environmental impact assessment), and corrosion study reports).

It is not necessarily to prepare all the preceding data, and the assessments can be performed at different levels.

2. QUANTITATIVE-RISK ASSESSMENT AND TARGET RELIABILITY

This section intends to perform quantitative risk assessment to establish the pipeline structure target reliability, taking into account pipeline safety, environmental, and economic consequences. Risk assessment involves pipeline segmentation, failure probabilities, and consequence (leakage, dispersion, fire and explosion, etc.) modeling.

Pipeline Segmentation

Since the risk along pipelines is not a constant, it is efficient to divide a long pipeline into shorter sections. The risk evaluator must decide on a strategy for creating these shorter sections to obtain an accurate risk picture. Each section has its own risk assessment results.

The most appropriate method for sectioning the pipeline is to insert a break point wherever significant risk changes occur. A significant condition change must be determined by the evaluator with consideration given to data costs and desired accuracy. The idea is for each pipeline section to be unique, from a risk perspective, from its neighbors. As we know that the neighboring sections can differ in at least one risk condition. An example of a short list of prioritized conditions is as follows:

- Pipeline specification (such as wall thickness or diameter).
- Soil conditions (such as pH or moisture).
- Population density.
- Coating condition.
- Age of pipeline.
- Environmental sensitivity (marine park, nature reserve).

Section length is not important as long as characteristics remain constant. Each pipeline segment has its own risk as the production of failure probability and failure consequence, the assessments of which are addressed in the following sections.

Probability of Failure

Pipeline failure usually takes the form of leakage, which is the initiating event resulting in serious consequences. Probability of failure (PoF) is estimated as failure frequencies of different types of degradation mechanisms operating in the pipeline component. The failure frequency is calculated based on different damage causes. The main damage causes identified for subsea pipelines follow:

- Internal corrosion.
- External corrosion.
- Erosion.
- External impact.
- Free span.
- On-bottom instability.

Two categories of PoF analysis methods are available:

- Direct methods, using available historical databases.
- Indirect methods, using risk models.

The most obvious advantage of the direct database based method is its convenience, because it is based on real historical data. It may not be pipeline specific and difficult to account for effect of pipeline maintenance actions, but its reliability is acceptable in the industry. Although the indirect risk models based method can be used for a specific pipeline, the required data can be very abundant and the calculation is complex, which may lead to obvious uncertainty in the results. Both the acquisition of data and risk calculation are moneyeaters, which are not necessary in some situations.

Which approach is the best choice for pipeline PoF analysis? This decision should be made based on the understanding of the following conditions:

- The purpose of the risk assessment.
- Data available for the risk assessment.
- Benefits and costs.

In this risk and reliability FFS assessment, the main purpose of QRA study is to provide precise target reliability. It is not necessary to perform too complex PoF calculations because of financial consideration. The consequences of Failure (CoF) assessment should be the concern. Thus, the famous UK PARLOC 2001 database is proposed to be used for pipeline PoF assessment. Of course, if a pipeline QRA study report is available, the results should be referred to [4].

Consequences of Failure

The consequences of failure can be expressed as number of people affected (injured or killed), property damage, amount of a spill area affected, outage time, mission delay, money lost, or any other measure of negative impact for the quantification of risk. It is usually divided into the three categories of safety, economic, and environmental consequences to be analyzed, respectively, by qualitatively or quantitatively way.

The consequence analysis is an extensive effort covering a series of steps, including

- Accident scenario, analysis of possible event sequences (event tree analysis, for instance).
- Analysis of accidental loads, related to fire, explosion, impact.
- Analysis of the response of systems and equipment to accidental loads.
- Analysis of final consequences to personnel, the environment, and assets.

Each of these steps may include extensive studies and modeling. Consequence analysis techniques are generally well established within

the oil and gas industry, although in certain areas better models are still required.

Some more well-known QRA tools for consequence analysis are

- **AutoReaGas:** An integrated computational fluid dynamics (CFD) software tool for analyzing combustion in flammable gas mixtures and subsequent blast effects.
- **FIREX:** Prediction of main fire characteristics and responses to fire scenarios based on empirical correlations.
- **MONA:** Advanced and general tool for simulation of single-component multiphase systems.
- **OLGA:** Transient multiphase flow simulator for systems comprising flow lines, risers and process equipment.
- **PHAST:** Windows-based toolkit for determination of consequences of accidental releases of hazardous material.

Target Reliability

When conducting reliability-based FFS analysis, target reliability levels in a given reference time period and reference length of pipeline should be selected. The selection is based on the consequences of failure, location, and contents of pipelines; relevant rules; access to inspection and repair; and so on. Thus, QRA results should supply the most valuable reference information.

3. SRA AND RETAINING PRESSURE CAPACITY

General

The objective of FFS assessment is to identify the current and future conditions of each pipeline with respect to integrity, with an emphasis placed on pressure containment capacity. In this section, the assessment focuses on internal CO_2 corrosion. The capacity of each defect is assessed based on the structure reliability assessment method and the target reliability.

The target reliability is used as the maximum allowable failure rate to deduce the maximum value of pipeline safe operating pressure P_{safe}, which indicates the pipeline retaining pressure capacity (service limit state).

According to ASME B31.4/8, MAOP is the maximum pressure at which a pipeline is allowed to be operated under steady state process conditions. Hence, the maximum value of pipeline safe operating pressure P_{safe} is not allowed to be less than the given MAOP [5]–[7].

Structure Reliability Assessment Method

The safety index β (API 2A-LRFD) is the most popular measure of reliability in industry. The safety index is related to the corresponding failure rate by the formula [8]

$$P_f = \Phi(-\beta) = 1 - \Phi(\beta) \qquad [13.1]$$

where $\Phi(\cdot)$ is the standard normal distribution function.

The structure reliability assessment method is used to calculate the pipeline failure rate and the reliability $R = 1 - P_f$. The SRA model for the pipeline failure rate calculation is presented here for damage due to internal corrosion. The main steps of the SRA method are illustrated in Figure 13.3.

For normalized defect length $X_L = L^2/Dt \leq 50$, the normalized mean, $P_{burst}(R_m)$, is given by

$$R_m = 2 \cdot \sigma_f \cdot \frac{t}{D} \cdot \frac{1 - X_A \cdot B_{X_A}}{1 - \left[1 + 0.6275 \cdot X_L \cdot B_{X_L} - 0.003375(X_L \cdot B_{X_L})^2\right]^{-0.5} \cdot X_A \cdot B_{X_A}} \cdot B_{X_M} \cdot B_{X_F} \qquad [13.2]$$

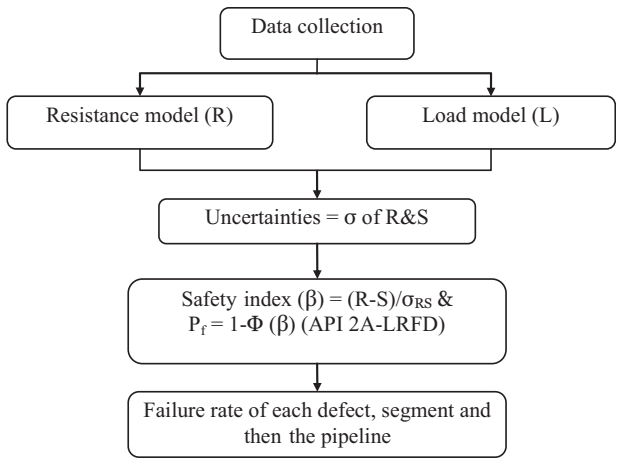

FIGURE 13.3 ***Flowchart of SRA Method to calculate the Pipeline Failure Rate and the Reliability.***

Table 13.2 Bias of Burst Pressure Model

Name	Formula	Bias	COV
Model bias	$B_{X_M} = \frac{P_{\text{burst actual}}}{P_{\text{burst predicted}}}$	1.07	0.18
Normalized area bias	$B_{X_A} = \frac{X_{A\ \text{actual}}}{X_{A\ \text{predicted}}}$	0.8	0.08
Normalized flow stress bias	$B_{X_F} = \frac{\sigma_{f\ \text{actual}}}{\sigma_{f\ \text{predicted}}}$	1.14	0.06
Normalized length bias	$B_{X_L} = \frac{X_{L\ \text{actual}}}{X_{L\ \text{predicted}}}$	0.9	0.05

where B_{X_M}, B_{X_A}, B_{X_F}, and B_{X_L} are model bias and the biases for normalized area, normalized flow stress, and normalized length, respectively (see Table 13.2).

σ_f = flow stress (σ_f = SMTS in ASME B31G)
D = nominal outside diameter
t = wall thickness;
X_A = normalized defect area
X_L = normalized defect length

For the normalized defect length $X_L = L^2/Dt > 50$, the normalized mean, $P_{burst}(R_m)$, is given by

$$R_m = 2 \cdot \sigma_f \cdot \frac{t}{D} \cdot \frac{1 - X_A \cdot B_{X_A}}{1 - (0.032 \cdot X_L \cdot B_{X_L} + 3.3)^{-1} \cdot X_A \cdot B_{X_A}} \cdot B_{X_M} \cdot B_{X_F} \quad [13.3]$$

The COV (coefficient of variation) of the mean resistance, R_m, is estimated from the COV of X_A, X_L, X_F, and X_M (see Table 13.2):

$$V_{Rm} = \left(V_A^2 + V_L^2 + V_F^2 + V_M^2\right)^{0.5} \quad [13.4]$$

The mean load, S_m, is given by

$$S_m = P_{op} \cdot B_{Sm} \quad [13.5]$$

where

P_{op} = operating pressure
B_{Sm} = bias of load (S_m)

Therefore, the safety index can be obtained from this equation:

$$\beta = \ln(R_m/S_m)/\sigma_{\ln RS} \quad [13.6]$$

where

β = safety index

R_m = mean value of strength

S_m = mean value of load

$$\sigma_{lnRS} = \sqrt{\ln\left[\left(1 + V_{Rm}^2\right) \cdot \left(1 + V_{Sm}^2\right)\right]} \qquad [13.7]$$

Evaluation of Strength Uncertainties

The preceding SRA method is based on a limit strength model derived from ASME B31G. The uncertainty of pipeline strength depends on

- Material strength uncertainty.
- Defect measurement, detection, and prediction uncertainty.
- Pipeline parameter and geometry uncertainty.
- Strength model uncertainty.

The uncertainties are measured in terms of standard deviation and variance from mean values and combine to give an uncertainty in the predicted pipeline safe operating pressure. The mean bias (B) and COV of the burst prediction model (Bai et al., 1997) are shown in Table 13.2.

A bias factor, X, is introduced to reflect the confidence in the criterion in the prediction of burst strength:

$$X = \frac{\text{burst true strength}}{\text{burst predicted strength}} \qquad [13.8]$$

Normalized Random Variables in the Design Equation are Listed in Table 13.3.

Two levels of AREA assessment are recommended here. In level 1, AREA is estimated as

$$L^2/(Dt) \leq 30 \text{ AREA} = 2/3L \cdot d$$

$$L^2/(Dt) > 30 \text{ AREA} = 0.85L \cdot d \qquad [13.9]$$

In level 2, the exact area (AREA) of the corrosion profile is estimated by the Simpson integration method.

Pipeline Retaining Pressure Capacity

The calculation of the present pressure retaining capacity for each pipeline segments can be performed with respect to the most significant defects. The target reliability is a structural safety requirement, which means the pipeline failure probability is not allowed to be greater than it. Thus, if one assigns target reliability to failure rate, P_f, in Eq. [13.1] and deduces the value of

Table 13.3 Normalized Random Variables

Name	Formula	Remarks
Normalized area	$X_A = \frac{AREA}{AREA_0}$	AREA = Metal loss area (Ld) $AREA_0$ = Original area (Lt)
Normalized flow stress	$X_F = \frac{\sigma_{flow}}{SMYS}$	σ_{flow} = Flow stress = $SMTS$ in ASME B31G
Normalized length	$X_L = \frac{L^2}{Dt}$	L = Detect length D = Nominal outside diameter t = Wall thickness
Normalized depth	$X_d = \frac{d}{t}$	d = Detect depth

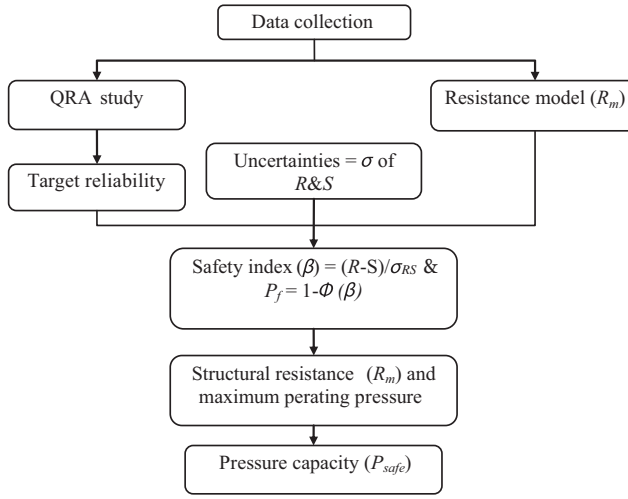

FIGURE 13.4 ***Flowchart of Pressure Capacity Assessment.***

pipeline safe operating pressure, P_{safe}, using the SRA method, this maximum value of P_{safe} indicates the pipeline retaining pressure capacity (service limit state). If this maximum safe operating pressure, P_{safe}, is identified to be less than MAOP, the defect is unacceptable and the pipeline is declared unfit for service.

Figure 13.4 describes the process of pipeline retaining pressure capacity calculation. When the pipeline failure rate is assigned the value of target reliability, one can find the value of safety index β from Eq. [13.1]. Then, by incorporating the mean value of strength, safety index β, and the uncertainty, one can derive the maximum mean load, then the pipeline maximum safe operating pressure (P_{safe}) equals the mean load (S_m) divided by its bias:

$$P_{safe} = S_m / B_m \qquad [13.10]$$

4. CORROSION RATE

The purpose of corrosion rate calculation is to predict the development of corrosion defects. The corrosion caused by the incidences of CO_2 represents the risk to the integrity of carbon steel equipment in a production environment and is more common than damage related to fatigue, erosion, or stress corrosion cracking. In OPR Inc. in-house subsea pipeline integrity management software, PaRIS, both NORSOK and De Waard's models for corrosion rate are programmed [10].

5. EXAMPLE OF RISK- AND RELIABILITY-BASED FFS

Pipeline Data

An example of risk- and reliability-based FFS is given for a subsea oil export pipeline installed in 1982, with a design life of 20 years. Table 13.4 lists the general data of the pipeline with inspection results of corrosion defect at 2003.

Analysis Results

To determine the pipeline safety level and target reliability, a complete risk assessment is performed. A sensitivity study at the target reliability is performed to review the benefits of using reliability-based FFS in comparison to the use of other codes, such as ASME B31G and DNV RP F101. The results are listed in Tables 13.5 to 13.7 and illustrated in Figures 13.5 to 13.10.

Table 13.4 Data of Subsea Oil Pipeline

Parameter	Symbol [unit]	Value
Outer diameter	D [mm]	273.05
Wall thickness	t [mm]	8.5
Standard deviation of t	ρ_t [mm]	0.5
Design factor	F [-]	0.72
SMYS	SMYS [MPa]	358.5
MAOP	MAOP [MPa]	9.3
Operating pressure	P_{op} [MPa]	3
Corrosion rate	r [mm/year]	0.17
Standard deviation of r	ρ_r [mm/year]	0.5
Measured maximum defect depth	d_o/t [-]	0.48
Standard deviation of d_o/t	$\sigma_{d_o/t\ [-]}$	0.05
Measured maximum defect length	L_o [mm]	250
Standard deviation of L_o	$\sigma_{L_o\ [mm]}$	5

Table 13.5 Single Defect Assessment for Target Reliability of 10^{-3}

Pressure Capacity (P_{safe})	(MPa)	P_{safe} vs. MAOP	Remaining Life
ASME B31G	5.99	<MAOP	0
DNV-RP-F101 (Part B)	12.22	>MAOP	7
DNV-RP-F101 (Part A)	10.75	>MAOP	2
Risk- and probability-based FFS	10.98	>MAOP	14

Table 13.6 Single Defect Assessment for Target Reliability of 10^{-4}

Pressure Capacity (P_{safe})	(MPa)	P_{safe} vs. MAOP	Remaining Life
ASME B31G	5.99	<MAOP	0
DNV-RP-F101 (Part B)	12.22	>MAOP	7
DNV-RP-F101 (Part A)	9.17	<MAOP	0
Risk- and probability-based FFS	9.62	>MAOP	6

Table 13.7 Single Defect Assessment for Target Reliability of 10^{-5}

Pressure capacity (P_{safe})	(MPa)	P_{safe} vs. MAOP	Remaining Life
ASME B31G	5.99	<MAOP	0
DNV-RP-F101 (Part B)	12.22	>MAOP	7
DNV-RP-F101 (Part A)	8.24	<MAOP	0
Risk and probability based FFS	8.58	<MAOP	0

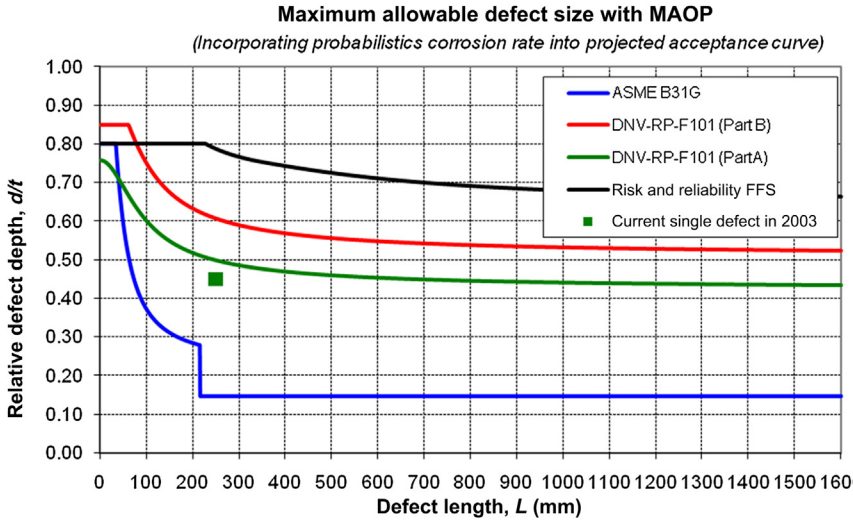

FIGURE 13.5 ***Maximum Allowable Defect per MAOP (Target Reliability = 10^{-3}).*** (For color version of this figure, the reader is referred to the online version of this book.)

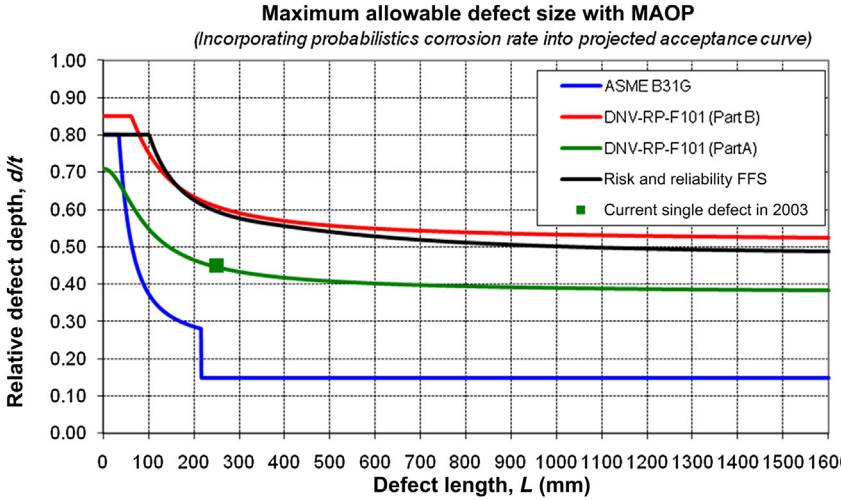

FIGURE 13.6 ***Maximum Allowable Defect per MAOP (Target Reliability*** $= 10^{-4}$***).*** (For color version of this figure, the reader is referred to the online version of this book.)

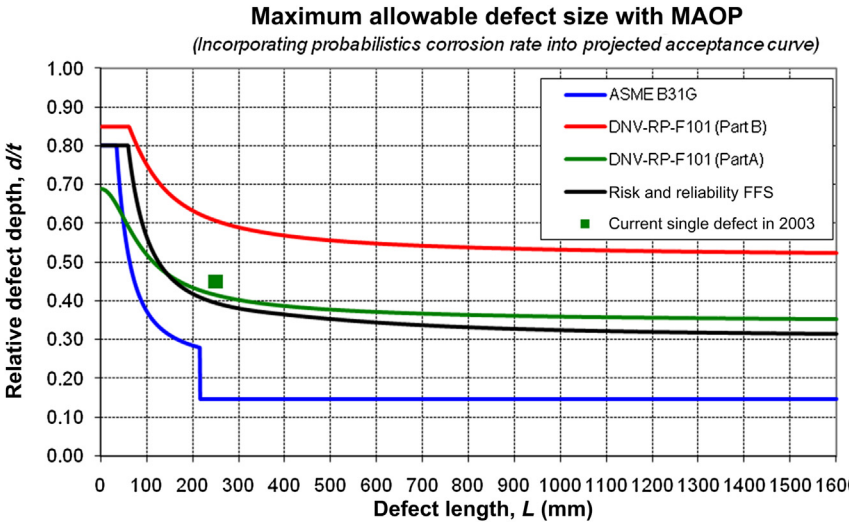

FIGURE 13.7 ***Maximum Allowable Defect per MAOP (Rarget Reliability*** $= 10^{-5}$***).*** (For color version of this figure, the reader is referred to the online version of this book.)

Figures 13.5 and 13.6 reveal that the reliability-based FFS method is much more conservative than the DNV RP F101 (Part A) based method at the maximum allowable defect size, when the target reliability level is lower. This is mainly because the reliability-based FFS method counts the shape effects of corrosion profile, as shown in Eq. [13.9].

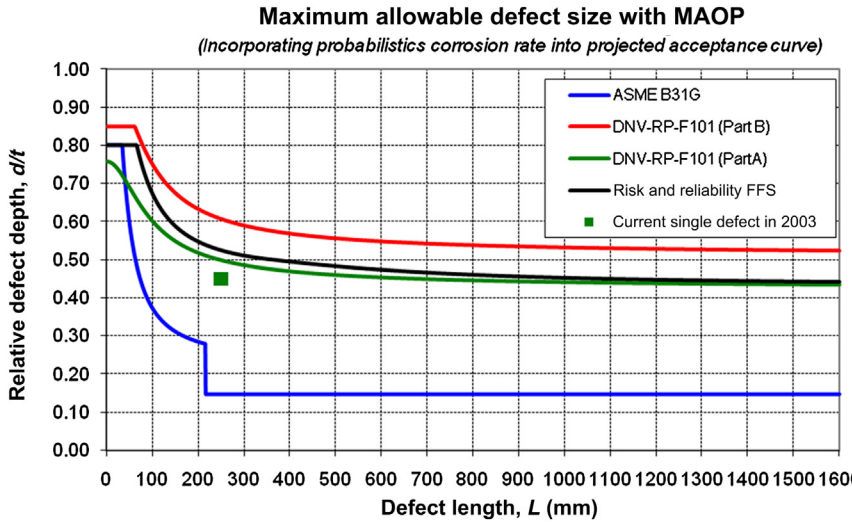

FIGURE 13.8 ***Maximum Allowable Defect per MAOP (Target Reliability*** $= 10^{-3}$***).*** (For color version of this figure, the reader is referred to the online version of this book.)

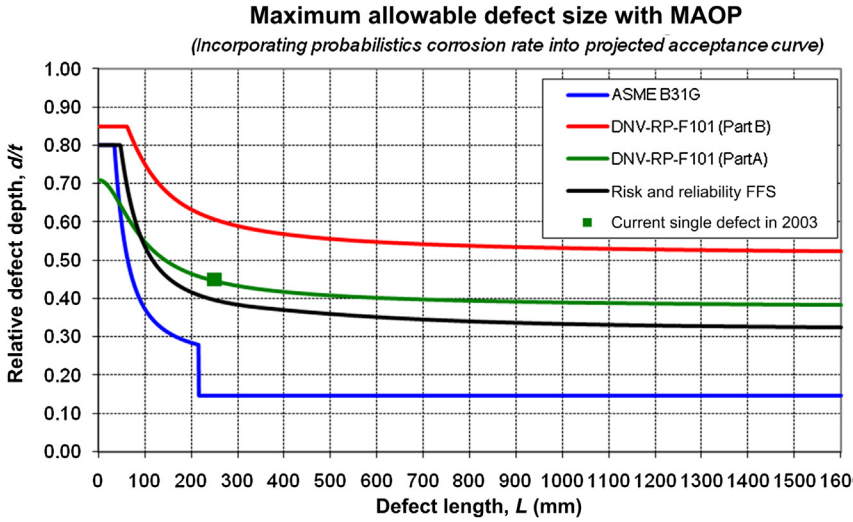

FIGURE 13.9 ***Maximum Allowable Defect per MAOP (Target Reliability*** $= 10^{-4}$***).*** (For color version of this figure, the reader is referred to the online version of this book.)

Figures 13.8 to 13.10 show the maximum allowable defect curves when counting the area of corrosion profile as AREA $= Ld$.

The analysis results can be summarized as follows:

- The risk- and reliability-based method is much more sensitive than the DNV RP F101 (Part A) based method to the target reliability.

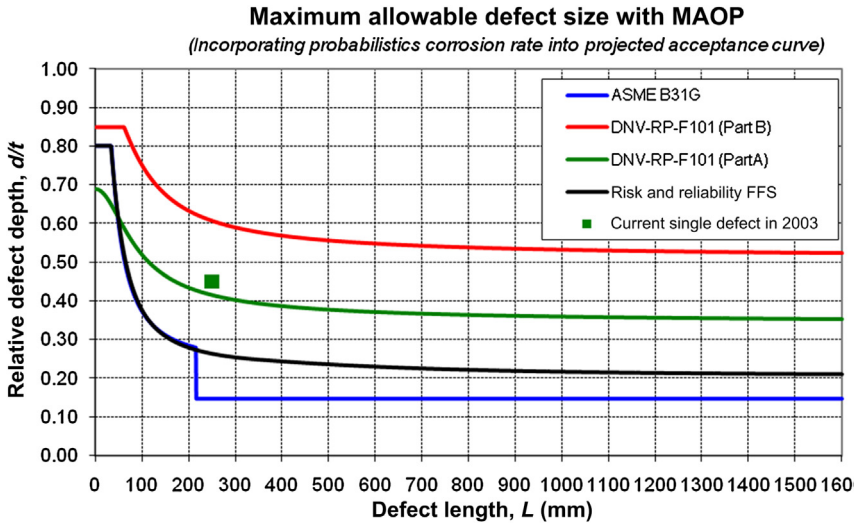

FIGURE 13.10 ***Maximum Allowable Defect per MAOP (Target Reliability*** $= 10^{-5}$***).*** (For color version of this figure, the reader is referred to the online version of this book.)

- At a high target reliability level or safety level, the reliability-based method gives a stricter limit at the maximum allowable defect size than that of the DNV RP F101 (Part A) based method.
- The DNV RP F101 (Part B) and ASME B31G code based method gives only a limit state calculation without counting the effects of target reliability [6].

Summary

The risk- and reliability-based fitness for service assessment addressed in this chapter is a quantitative risk assessment based FFS study process. The main purpose of QRA is to find out target reliabilities for different pipeline segments. With them, a structure reliability analysis is performed to find out the maximum safe operating pressure, which indicates the pipeline retaining pressure capacity. With comparison to the MAOP, a pipeline's fitness for service can be defined. The corrosion rate is also calculated to predict the development of defects. Based on the analysis results, further SRA assessment reveals the pipeline remaining life [11].

In the traditional DNV RP F101 based FFS assessment, the classification of pipeline target reliability is merely a qualitative judgment, just as what has been considered in pipeline design. The advantage of the QRA-based determination of target reliability is that the pipeline is segmented more

scientifically from a risk perspective and every segment has its own target reliability. This assessment also benefits from making good use of available data and reports, which include inspection data, monitoring data, pipeline repair and incident records, corrosion study reports, and QRA report (if any).

There are also many limitations to the risk- and reliability-based FFS assessment and further, deeper studies are needed. Ways forward from this chapter include

1. Only internal CO_2 corrosion is considered in this chapter; external corrosion, erosion, and free span hazards to pipeline fitness should be the further study work.
2. Only longitudinal defects are addressed.
3. Burst model biases and COV considering no uncertainties of inspection tools and defect size.
4. Human errors are not discussed in the assessment.

REFERENCES

[1] Bai Y, Bai Q. Subsea pipelines and risers. Oxford, UK: Elsevier; 2005.
[2] DNV. Corroded pipelines, DNV-RP-F101. Høvik, Norway: Det Norske Veritas; 2004.
[3] Jiao G, Sotberg T, Bruschi R, Igland RT. The SUPERB project: Linepipe statistical properties and implications in design of offshore pipelines. Yokohama, Japan: Proc. of OMAE'97, 1997.
[4] UK PARLOC 2001. The update of the loss of containment data for offshore pipelines, rev. 5. Prepared by Mott MacDonald Ltd for the Health and Safety Executive, the UK Offshore Operators Association and the Institute of Petroleum; Liverpool, Merseyside, England; July 2003.
[5] Norwegian Petroleum Directorate. Regulations concerning implementation and use of risk analysis in the petroleum industry. YA-049, Stavanger, Norway; 1992.
[6] ASME. Code for pressure piping, B31 liquid petroleum transportation piping systems, ASME B31.4–1991 ed. New York: American Society of Mechanical Engineers; 1991.
[7] ASME. Code for pressure piping, B31 gas petroleum transportation piping systems, ASME B31.8–1994. New York: American Society of Mechanical Engineers; 1994.
[8] API 2A-LRFD. Planning, designing and construction of fixed offshore platforms – Load and resistance factor design. Washington, DC: American Petroleum Institute.
[9] Bai Y, Xu T, Bea R. Reliability-based design and re-qualification criteria for longitudinally corroded pipes. Honolulu, Hawaii: ISOPE'97, 1997.
[10] De Waard C, Lotz U, Milliams DE. Predictive model for CO_2 corrosion engineering in wet natural gas pipelines. Corrosion 1991:976.
[11] Bai Y, Mustapha MAB, Zhang FY, Shao VH. Risk and reliability based fitness for service (FFS) assessment for subsea pipelines. OMAE 2010, Shanghai; 2010.

CHAPTER 14

Pipeline Flow Risk Assessment

Contents

1. Introduction 307
2. Risk Assessment Method 308
   General 308
   Risk Acceptance Criteria 308
   Quantitative Risk Assessment 309
3. Blockage Risk Assessment 311
   General 311
   Probability of Failure 312
   Consequences of Failure 313
4. Failure Probability of Gas Pipelines 314
   Hydrate Formation Curve 315
   Hydrate Formation Probability 317
5. Failure Probability of Oil Pipelines 322
   Wax Appearance Temperature Curve 322
   Wax Deposition Probability 323
6. Summary 329
References 329

1. INTRODUCTION

Risk assessment is the process of evaluating the risks and factors influencing the level of safety of a project. It involves researching how hazardous events or states develop and interact to cause an accident. The risk assessment effort should be tailored to the level and source of technical risk involved with the project and the project stage being considered. The assessment of technical risk takes different forms in different stages of the project; for example [1],

- A simple high-level technical review may filter out equipment with technical uncertainty.
- Consequence and severity analyses can be used to identify equipment with the greatest impact on production or safety and the environment.
- Potential failure modes or risk of failure can be identified.
- Technical risk reviews can be used to identify where equipment is being designed beyond current experience.

Subsea Pipeline Integrity and Risk Management
ISBN 978-0-12-394432-0
http://dx.doi.org/10.1016/B978-0-12-394432-0.00014-7

Pipeline flow risk mainly includes fluid leakage and blockage happening in the pipelines. This chapter describes the application of quantitative risk assessment for the blockage in the oil and gas pipelines.

2. RISK ASSESSMENT METHOD

General

When assessing risk, the parameter of probability must be considered to obtain an overall assessment, because not all risks evolves into project certainties. During the assessment, risks are removed to get a global view. This method is based on functional expertise, and a fixed scoring value is used to achieve balance results. For example, if a risk is assessed as having a probability of occurrence between 1% and 20%, then the mean of the range, 10%, is used in the calculation. Table 14.1 illustrates the values utilized for different probabilities at various risk levels in a risk assessment.

A 100% probability does not appear in the table, because a 100% probability is a project certainty. The risk evaluation deals only with scenarios that might happen. Once having identified the probability and established the level of risk, it is necessary to prioritize the actions to be undertaken.

Risk Acceptance Criteria

The risk criteria define the level at which the risk can be considered acceptable or tolerable. During the process of making decisions, the criteria are used to determine if risks are acceptable, unacceptable, or need to be reduced to a reasonably practicable level. Numerical risk criteria are required for a quantitative risk assessment.

As described previously, risk assessment involves uncertainties. It may not be suitable to use the risk criteria in an inflexible way. The application of numerical risk criteria may not always be appropriate because of the

Table 14.1 Probability in Risk Assessment

Risk	Probability	Utilize
Improbable	<20%	10%
Not likely	20–40%	30%
Possible	40–60%	50%
Probable	60–80%	70%
Near certain	>80%	90%

Source: DNV [2].

uncertainties of certain inputs. The risk criteria may be different for different individuals and also vary in different societies and alter with time, accident experience, and changing expectations of life. Therefore, the risk criteria are able to only assist with informed judgment and should be used as guidelines for the decision-making process [3].

In risk analysis, the risk acceptance criteria should be discussed and defined first. Three potential risk categories are proposed in DNV-RP-H101[2]:

- Low.
- Medium.
- High.

The categorization is based on an assessment of both consequence and probability, applying quantitative terms. The categories should be defined for the following aspects:

- Personnel safety.
- Environment.
- Assets.
- Reputation.

A risk matrix is recommended for defining the risk acceptance criteria, a sample of which is presented in Table 14.2.

Quantitative Risk Assessment

Quantitative risk assessment (QRA) (also referred to as probabilistic risk assessment, PRA) is a key tool used in the new approaches. A QRA systemizes the present state of knowledge, including the uncertainties about the processes, activities, phenomena, and systems being analyzed. It identifies possible hazards and threats (such as a gas leakage or flow blockage), analyses their causes and consequences, and describes the risk. A QRA provides a basis to characterize the likely impacts of the activity studied, evaluate whether risk is tolerable or acceptable, and choose the most effective and efficient risk policy. Common practice in probabilistic risk assessment, however, avoids the aggregation of the two components and leaves it to the risk evaluation or management team to draw the necessary conclusions from the juxtaposition of loss and probabilities. In addition, second-order uncertainties are introduced via different types of uncertainty intervals to make the confidence of probability judgments more explicit.

Table 14.2 Sample Risk Matrix

Consequence					Probability (Increasing Probability →)			
Descriptive	**Personnel**	**Environment**	**Assets**	**Reputation**	**Remote (A) Occurred, Unlikely**	**Unlikely (B) Could Occur**	**Likely (C) Easy to Postulate**	**Frequent (D) Occurs Regularly**
1. Extensive	Fatalities	Global or national effect Restoration time > 10 yr	Project prod consequence costs > USD 10 million	International impact neg. exposure	A1 = S	B1 = S	C1 = U	D1 = U
2. Severe	Major injury	Restoration time > 1y. Restoration cost > USD 1 million	Project prod consequence costs > USD 1 million	Extensive national impact	A2 = A	B2 = S	C1 = S	D2 = U
3. Moderate	Minor injury	Restoration time > 1 md. Restoration cost > USD 1K.	Project prod consequence costs > USD 100K	Limited national impact	A3 = A	B3 = A	C3 =	D3 = S
4. Minor	Illness or slight injury	Restoration time < 1 md Restoration cost < USD 1K.	Project prod consequence costs < USD 1K	Local impact	A4 = A	B4 = A	C4 = A	D4 = S

Source: DNV [2].

The QRA of pipeline flow is to check that the pipeline meets the safety requirements (criteria). According to the acceptance criteria and safety classes, the risk related to the pipeline operation is defined as [4]

$$\text{Risk} = \text{Probability of failure} \times \text{Consequence of failure}$$

The probability of failure (PoF) is calculated from the reliability analysis, and the consequence of failure (CoF) intends to focus on safety and environmental criteria. The risk assessment is used to evaluate the integrity of a pipeline system with a view to taking actions to avoid any consequence resulting from pipeline failures.

Some of the basic tools such as statistical estimation theory, fault tree analysis (FTA), and event tree analysis (ETA) are used for analyzing the probabilities and risk. These tools belong to the following main categories of basic analysis methods:

- **Statistical methods:** Data are available to predict the future performance of the activity or system analyzed. These methods can be based on data extrapolation or probabilistic modeling.
- **Systems analysis methods:** These methods (FTA and ETA) are used to analyze systems where there is a lack of data to accurately predict the future performance of the system. Insights are obtained by decomposing the system into subsystems or components for which more information is available. Overall probabilities and risk are a function of the system's architecture and the probabilities on the subsystems or components for which more information is available. Overall probabilities and risk are a function of the system's architecture and the probabilities on the subsystems or component level.

The QRA process is shown in Figure 14.1.

3. BLOCKAGE RISK ASSESSMENT

General

The subsea pipelines lies on the seabed, it is difficult to pig or replace pipes and also increases the construction difficulty and the maintenance cost with many potential safety problems when the subsea pipelines are blocked. This section concerns QRA based on the probability of failure and the consequences of failure estimation for the wax and hydrate blockage. QRA should be introduced to the front end engineering design (FEED) for risk control.

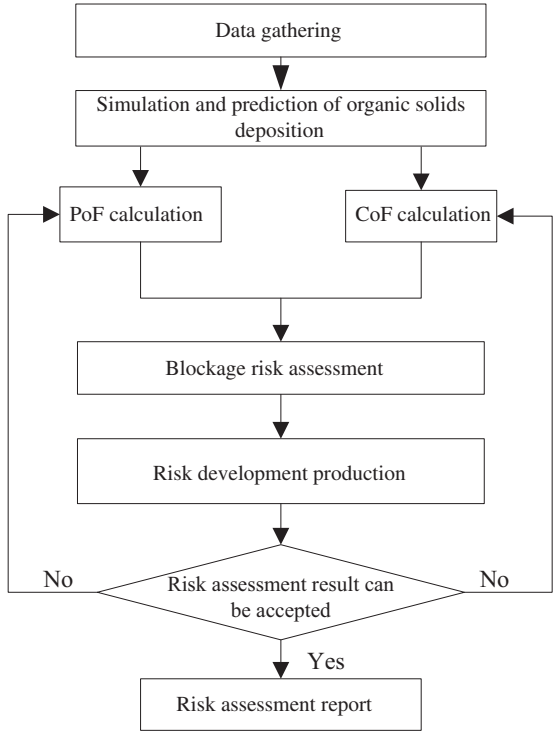

FIGURE 14.1 ***The QRA Process.***

Probability of Failure

The reliability analysis is to calculate the failure probability, and the main reliability calculation methods are the analytic method, embedded method, and Monte Carlo stochastic simulation method [5].

For a subsea pipeline, the probability of failure is calculated by the fast Monte Carlo sampling method based on the Bernoulli law of large numbers in statistics. Supposing the probability of random event (x_i) is the frequency of its happening in N times of independent sampling events; for any given tiny positive $\varepsilon > 0$:

$$\lim_{n \to \infty} \left\{ \left| \frac{m}{N} - p(x_n) \right| < \varepsilon \right\} = 1 \qquad [14.1]$$

Assuming some input parameters are random variables of normal distribution in a period of time, the case that the blockage occurs will happen

Table 14.3 Classification of PoF for an Oil Pipeline

	PoF Class	Description
1	<0.01	Operating safely
2	[0.01, 0.1)	Operating relatively safely; stepping up monitoring
3	[0.1, 0.32)	Operating relatively unsafely; recent parameters need to be changed
4	≥0.32	Operating in danger; recent parameters must be changed

Source: ISO [4].

Table 14.4 Classification of PoF for a Gas Pipeline

	PoF Class	Description
1	<0.0001	Probability is low; the risk can be ignored.
2	[0.0001, 0.001)	Probability is middle; monitor the changes of parameters
3	[0.001, 0.01)	Probability is high; take precautions and change operation condition
4	≥0.01	Probability is very high; safeguard measures must be taken to improve the requirements of gas quality and change operating conditions

Source: ISO [4].

m times in N times of independent sampling, and the failure probability of pipeline blockage is

$$\mathrm{PoF} = m/N \qquad [14.2]$$

Before calculating the failure probability, the blockage mathematic models are built on the relationship with the blockage and the temperature gradient to define the region of the organic solid deposition.

The classification of PoF for an oil pipeline is shown in Table 14.3. The classification of PoF for a gas pipeline is shown in Table 14.4.

Consequences of Failure

The potential consequences of failure are evaluated for the various elements, which are described in Table 14.5. The location where the blockage happens affects these elements directly.

The importance of the considerations depends on the location of the pipelines and is different for onshore pipelines and subsea pipelines. Subsea pipeline consequences should consider the proximity to platforms, nearshore or landfall, environmentally sensitive fields, and cost considerations. such as repair or pigging, loss throughput, production loss. and chemical injection.

Table 14.5 Considerations in Assessing Potential Consequences

Element	Consideration
Public safety	Population density and potential for human exposure, potential for ignition and fire, product toxicity
Environmental impact	Land use, product type, production flow rate, volume of release, topography, beach impact, high-consequence areas, and ultrasensitive areas
Business loss	Cost of repair, loss throughput, production loss, impact to remaining life of asset
Corporate reputation	Compilation of all consequence factors, extent of punitive actions by the regulatory agencies, and media exposure

Source: ISO [4].

Table 14.6 Safety Classification

Safety Class		Description
A	Low	Where failure implies insignificant risk of human injury and minor environmental and economic consequences
B	Normal	Where failure implies low risk of human injury, minor environmental impact, or high economic or political consequences
C	High	Where failure implies risk of human injury, significant environmental impact, or very high economic or political consequences
D	Very high	Where failure implies high risk of human injury

Source: ISO [4].

The safety class definition is based on the fluid categories and pipeline location. Table 14.6 shows the safety classes that can be applied for subsea pipelines.

4. FAILURE PROBABILITY OF GAS PIPELINES

The main components of gas are hydrocarbons. In addition to hydrocarbons, water (H_2O), nitrogen (N_2), carbon dioxide (CO_2), and hydrogen sulfide (H_2S) are often found in the gas pipeline. The hydrocarbons produced from the gas field are composed mainly of methane, ethane, and others. The blockage issue in gas pipelines is caused mainly by the formation of hydrate. The formation of hydrate in subsea gas pipelines was detailed in Chapter 20, "Flow Assurance," of *Subsea Pipelines and Risers* [6]. This chapter studies the formation of hydrate and considers the probability of hydrate formation as the probability of failure.

Hydrate Formation Curve

When natural gas is transported with water in the condition of low temperature and high pressure, icelike crystalline compounds, called *gas hydrates*, may form. The hydrates are composed of nano-scale water cages that enclose gas molecules of appropriate diameters [6]. Hammer-Schmidt first realized that gas hydrates were what was plugging natural gas pipelines [7].

Figure 14.2 shows hydrate formation curves for a gas composition. Above the curve is the hydrate formation region and below the curve is the no hydrate formation region. The higher is the pressure, the lower temperature, the more probability of hydrate formation. For the hydrate formation curves shown in Figure 14.2, the following mathematics fittings are obtained:

$$\Delta = 0.5539 \text{ (Methane)}$$

$$P^* = 3.42 + 5.20 \times 10^{-2} T - 5.31 \times 10^{-5} T^2 + 3.40 \times 10^{-6} T^3 \quad [14.3]$$

$$\Delta = 0.6$$

$$P^* = 3.01 + 5.28 \times 10^{-2} T - 2.25 \times 10^{-4} T^2 + 1.51 \times 10^{-5} T^3 \quad [14.4]$$

$$\Delta = 0.7$$

$$P^* = 2.81 + 5.02 \times 10^{-2} T - 3.72 \times 10^{-4} T^2 + 3.78 \times 10^{-6} T^3 \quad [14.5]$$

$$\Delta = 0.8$$

$$P^* = 2.70 + 5.83 \times 10^{-2} T - 6.64 \times 10^{-4} T^2 + 4.01 \times 10^{-5} T^3 \quad [14.6]$$

$$\Delta = 0.9$$

$$P^* = 2.61 + 5.72 \times 10^{-2} T - 1.87 \times 10^{-4} T^2 + 1.94 \times 10^{-5} T^3 \quad [14.7]$$

$$\Delta = 1.0$$

$$P^* = 2.53 + 6.25 \times 10^{-2} T - 5.78 \times 10^{-4} T^2 + 3.07 \times 10^{-5} T^3 \quad [14.8]$$

$$P = 10^{P^*} \times 10^{-3} \quad [14.9]$$

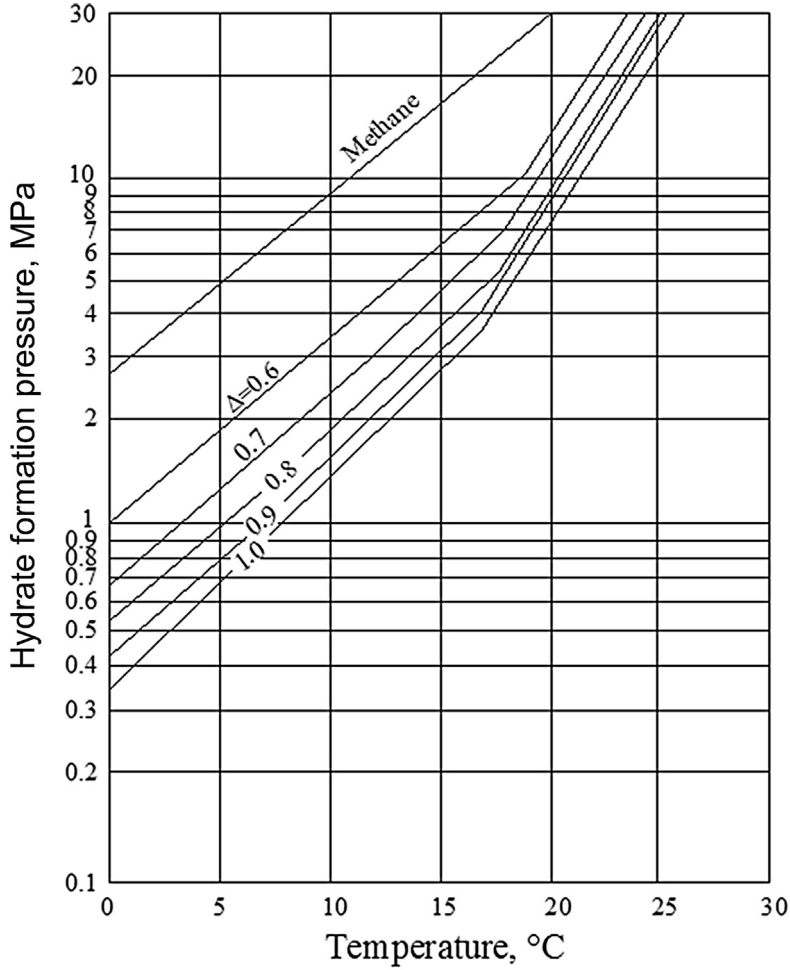

FIGURE 14.2 ***Hydrate Formation Curve.*** *Source: Katz [8].*

where

Δ = the gas relative density

P^* = the parameter of pressure

P = pressure of gas, MPa

T = the temperature of gas, °C

When the relative density and temperature of natural gas are known, the pressure of hydrate formation can be calculated from one of Eqs. [14.3] to [14.9]. An interpolation can be used if the relative density of gas is between two curves in the figure.

Hydrate Formation Probability

In this section, an example is given to explain the calculation process of hydrate formation probability. The main parameters used for the calculation are summarized in Tables 14.7 to 14.9.

The temperature distribution of gas along the pipeline is shown in Figure 14.3. Figure 14.4 shows a comparison between the pressure distribution of gas along the pipeline and the hydrate formation pressures corresponding to the gas temperature shown in Figure 14.3. When the gas pressure is higher than the hydrate formation pressure, hydrates may appear in the pipeline.

The inlet pressure and temperature of gas are set as random variables with normal distribution and the standard deviations of pressure and temperature are 0.1MPa and 1.0°C, respectively; the analyses are carried out

Table 14.7 Material Data of the Pipeline

Parameter	Symbol	Value	Unit
Total length	L	40.0	km
Inner diameter	ID	660.0	mm
Wall thickness	t_1	7.0	mm
Thermal conductivity of pipe	k_1	45.0	W/(m · °C)
Layer thickness of insulation	t_2	20.0	mm
Thermal conductivity of insulation	k_2	0.035	W/(m · °C)

Table 14.8 Environmental Data

Parameter	Symbol	Value	Unit
Buried depth	h	1.0	m
Thermal conductivity of sand	k_3	1.0	W/(m · °C)
Temperature of seawater	T_0	4.0	°C

Table 14.9 Gas Data

Parameter	Symbol	Value	Unit
Flow rate	Q	3.0×10^6	m^3/d
Inlet pressure	P_1	4.0	MPa
Inlet temperature	T_1	8.0	°C
Density of gas	ρ	0.75	kg/m^3

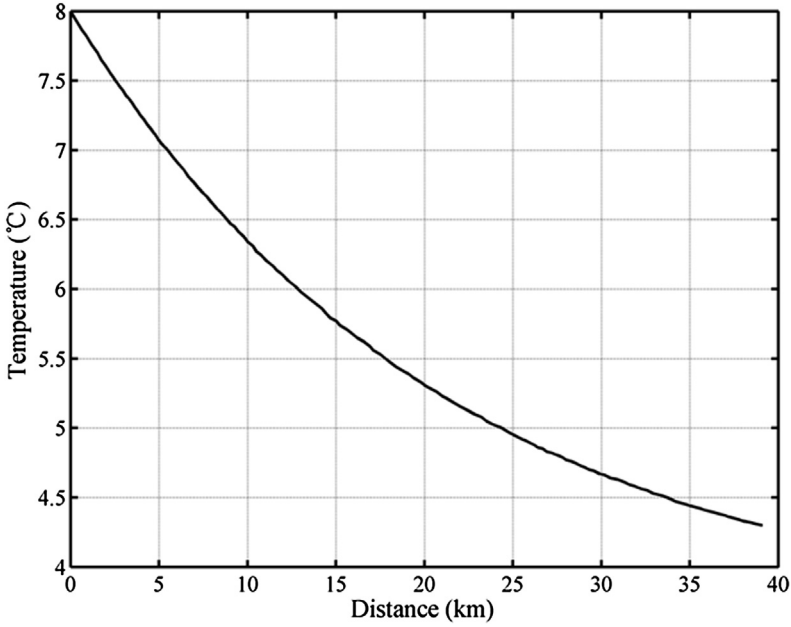

FIGURE 14.3 *Temperature Distribution along the Pipeline.*

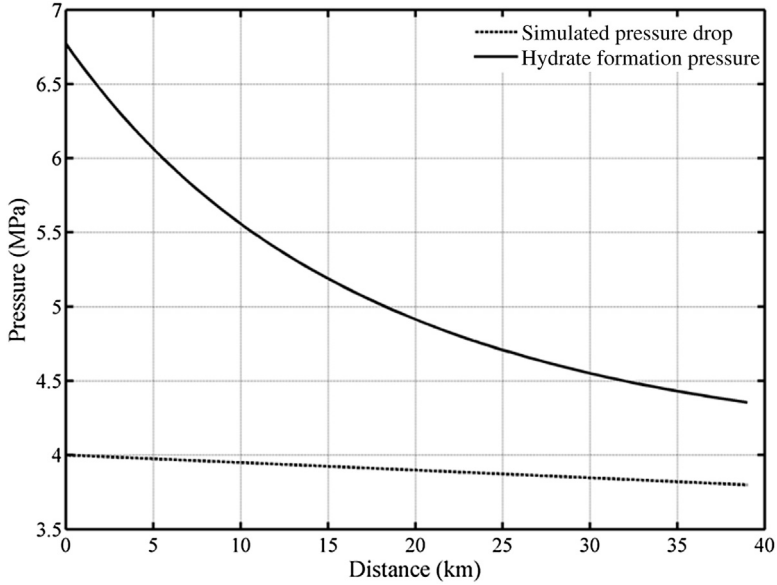

FIGURE 14.4 *Comparison between Gas Pressure and Hydrate Formation Pressure.*

10,000 times by random sampling of inlet pressure and temperature with the standard deviations. The analysis results are shown in Tables 14.10 to 14.13 and Figures 14.5 to 14.8.

Table 14.10 shows the PoFs calculated for different inlet temperatures. The PoF decreases with the increase in inlet gas temperature. Figure 14.5

Table 14.10 Effect of Inlet Temperature on PoF

Inlet Temperature (°C)	Hydrate Formation Probability (%)	PoF Class
8	1.32	4
10	0.19	3
12	0.02	2
14	Close to zero	1

Table 14.11 Effect of Flow Rate on PoF

Min Flow Rate, (m^3/d)	Hydrate Formation Probability (%)	PoF Class
3.0×10^6	1.32	4
3.5×10^6	0.16	3
4.0×10^6	0.01	2
4.5×10^6	Close to zero	1

Table 14.12 Effect of Thermal Insulation Layer Thickness on PoF

Thermal Insulation Layer Thickness (mm)	Hydrate Formation Probability (%)	PoF Class
20.0	1.31	4
30.0	0.26	3
40.0	0.09	2
50.0	0.02	2
60.0	Close to zero	1

Table 14.13 Effect of Input Pressure on PoF

Input Pressure (MPa)	Hydrate Formation Probability (%)	PoF Class
4.0	1.23	4
3.8	0.18	3
3.6	0.03	2
3.4	Close to zero	1

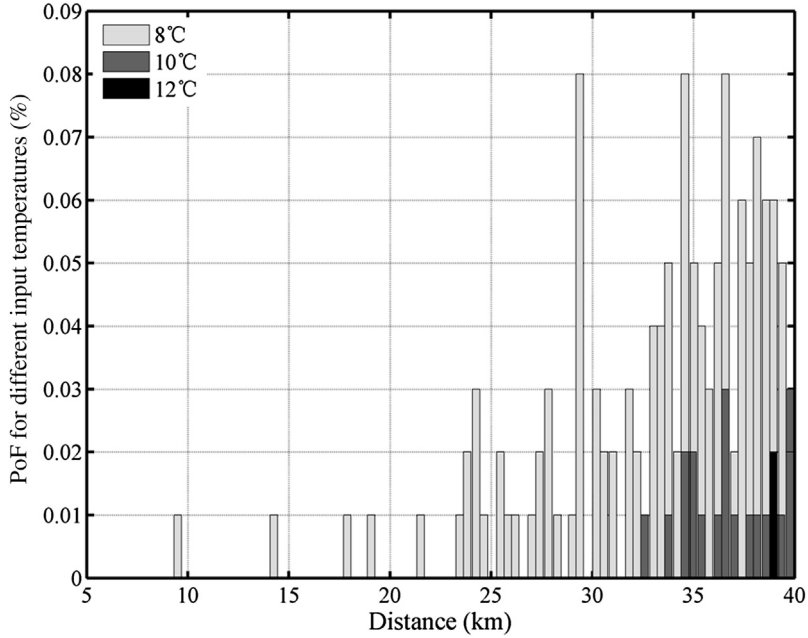

FIGURE 14.5 *Distribution of PoF along the Pipeline for Different Input Temperatures.*

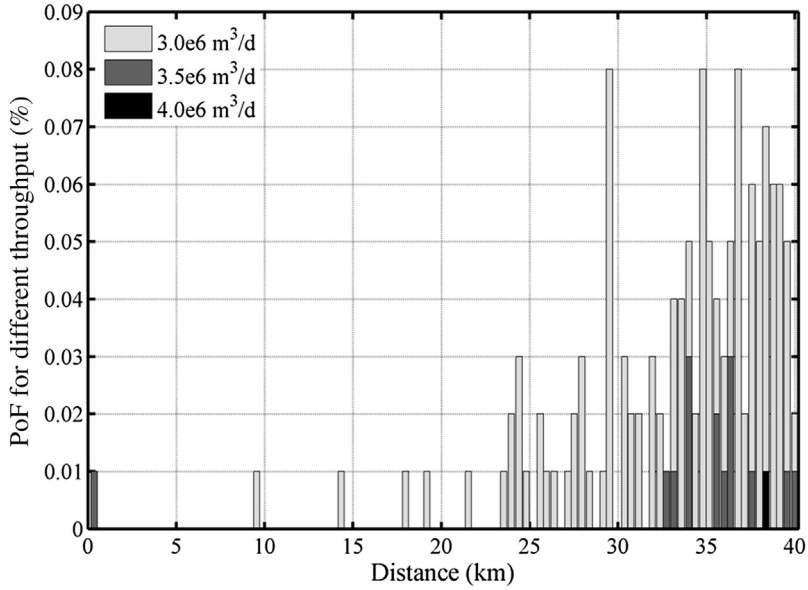

FIGURE 14.6 *Distribution of PoF along the Pipeline for Different Flow Rates.*

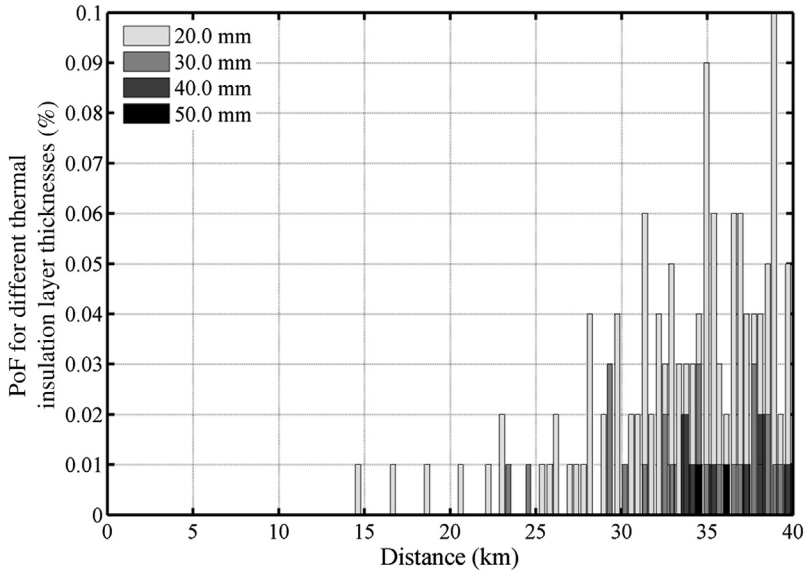

FIGURE 14.7 ***Distribution of PoF along the Pipeline for Different Layer Thicknesses.***

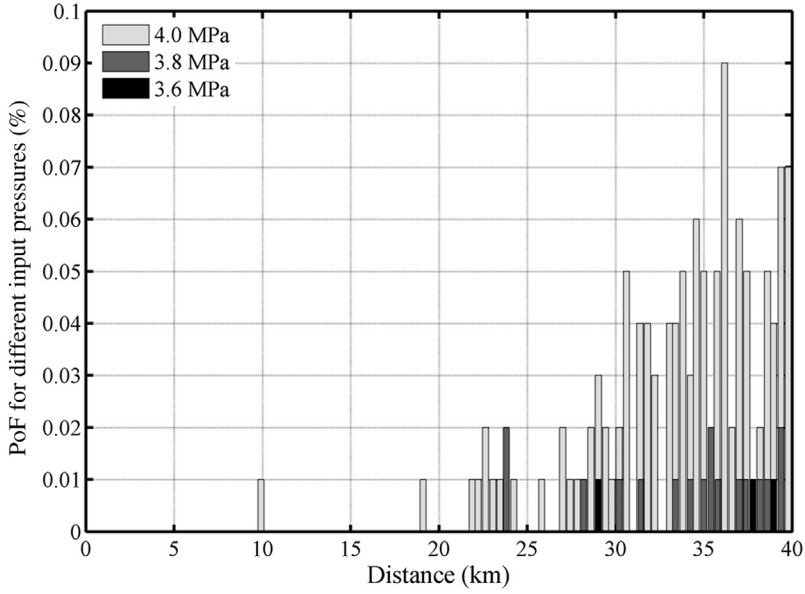

FIGURE 14.8 ***Distribution of PoF along the Pipeline for Different Input Pressures.***

shows the distribution of PoF along the pipeline for different inlet gas temperatures.

Table 14.11 shows the calculated PoFs for different flow rates. The PoF drops with the increase in the flow rate. Figure 14.6 shows the distribution of PoF along the pipeline for different flow rates.

Table 14.12 shows the calculated PoFs for different thicknesses of insulation layer. The PoF drops with the increase in layer thickness. Figure 14.7 shows the distribution of PoF along the pipeline for different layer thicknesses.

Table 14.13 shows the calculated PoFs for different inlet pressures. The PoF drops with the decrease in inlet pressure. Figure 14.8 shows the distribution of PoF along the pipeline for different inlet pressures.

5. FAILURE PROBABILITY OF OIL PIPELINES

Wax deposition is the primary blockage reason for oil pipelines. However, it is difficult to simulate the behaviors of oil in pipelines and predict the actual blockage failure probability. So, this section discusses mainly the wax deposition probability, which is considered the failure probability of oil pipeline.

Wax Appearance Temperature Curve

It is more difficult to understand waxes than pure solids, because they are complex mixtures of hydrocarbons that freeze out of crude oils if the temperature is low enough. Wax deposition can be predicted by the relationship of the temperature and pressure in wax formation. Figure. 14.9 shows a typical curve of the wax appearance temperature (WAT). The wax deposition in an oil pipeline may be judged by comparing the temperature of oil with the wax appearance temperature corresponding to the oil pressure.

The fitting functions of the key curves shown in Figure 14.9 are expressed as follows. At the bubble point curve,

$$P_{bp} = 0.04076 \times T + 6.9829 \quad [14.10]$$

Above the bubble point,

$$P = 2.7826 \times T - 104.1156 \quad [14.11]$$

Below the bubble point,

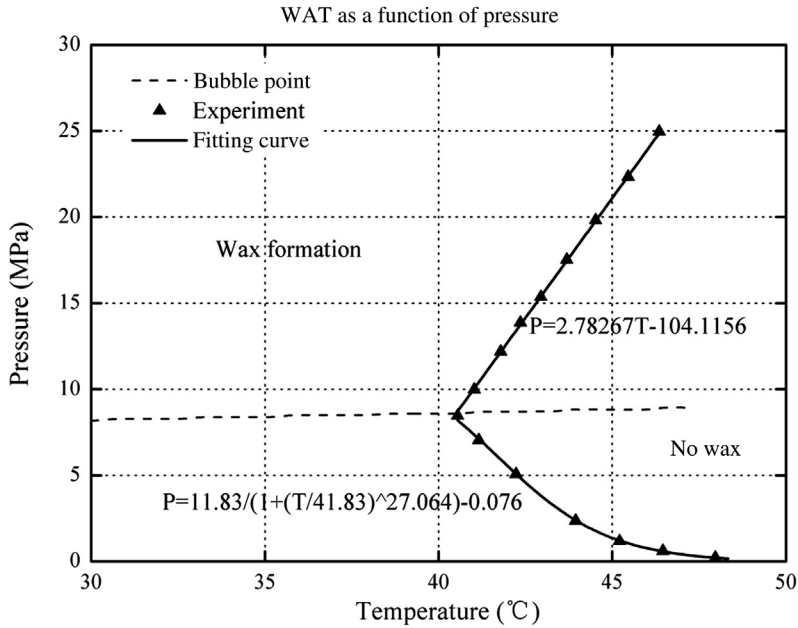

FIGURE 14.9 ***Typical WAT Curve.*** *Source: Edmonds et al. [9].*

$$P = \frac{11.83}{1 + \left(\frac{T}{41.83}\right)^{27.064}} - 0.076 \qquad [14.12]$$

where

P_{bp} = bubble point pressure, MPa
P = wax appearance pressure, MPa
T = wax appearance temperature, °C

Wax Deposition Probability

In this section, an example is given to explain the calculation processes of wax deposition probability. The main parameters used in the calculation are summarized in Tables 14.14 to 14.16.

Figure 14.10 shows the temperature distribution along the oil pipeline. Figure 14.11 shows the comparison between the pressure distribution of oil along the pipeline and the wax appearance pressures corresponding to the oil temperature shown in Figure 14.10. When the oil pressure is in the outside of the bound of wax appearance pressures, wax may deposit in the pipeline.

Table 14.14 Pipeline Material Parameters

Parameter	Symbol	Value	Unit
Total length	L	20.0	km
Inner diameter	ID	205.0	mm
Wall thickness of pipe	t_1	7.0	mm
Thermal conductivity of pipe	k_1	45.0	W/(m · °C)
Thermal insulation layer thickness	t_2	30.0	mm
Thermal conductivity of insulation	k_2	0.07	W/(m · °C)
Concrete thickness	t_3	20.0	mm
Thermal conductivity of concrete	k_3	2.0	W/(m · °C)

Table 14.15 Environmental Data

Parameter	Symbol	Value	Unit
Buried depth	h	1.5	m
Thermal conductivity of sand	k_4	1.22	W/(m · °C)
Temperature of seawater	T_0	4.0	°C
Thermal conductivity of seawater	k_5	0.58	W/(m · °C)

Table 14.16 Oil Data

Parameter	Symbol	Value	Unit
Minimum flow rate	Q	2000.0	m^3/d
Inlet pressure	P_1	7.5	MPa
Inlet temperature	T_1	55.0	°C
Thermal conductivity of oil	k_6	0.14	W/(m · °C)
Density of oil at 20°C	ρ	840.0	kg/m^3

Set the inlet pressure and temperature as random variables of normal distributions, and the standard deviation of pressure and temperature are 0.1MPa and 1.0°C, respectively. The analysis results are shown in Tables 14.17 to 14.20 and Figures 14.12 to 14.15 for 10,000 random samples with different pressures and temperatures.

Table 14.17 lists the PoFs for different inlet temperatures of oil. The PoF drops with an increase in the inlet oil temperature. Figure 14.12 shows the distribution of the PoF along the pipeline for different inlet temperatures.

Table 14.18 shows the PoFs for different minimum flow rates. The PoF drops with an increase in the minimum flow rates. Figure 14.13 shows the distribution of the PoF along the pipeline for different minimum flow rates.

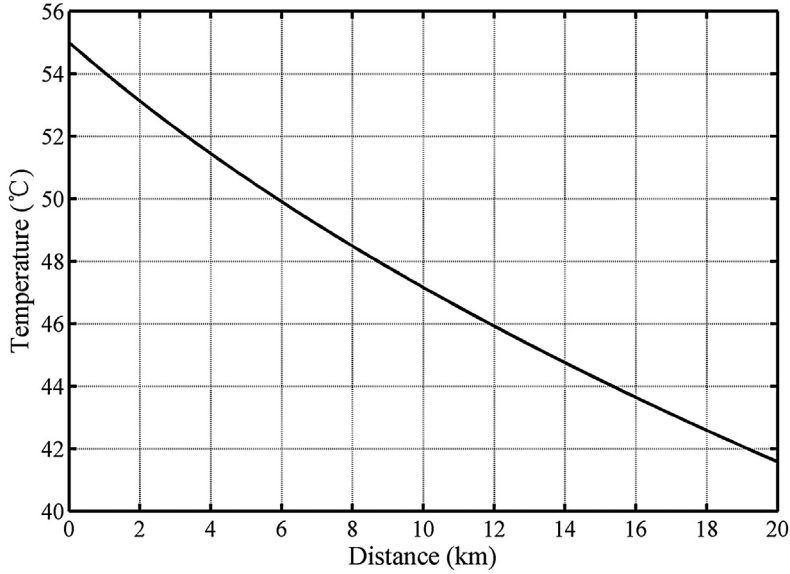

FIGURE 14.10 *Temperature Distribution along Oil Pipeline.*

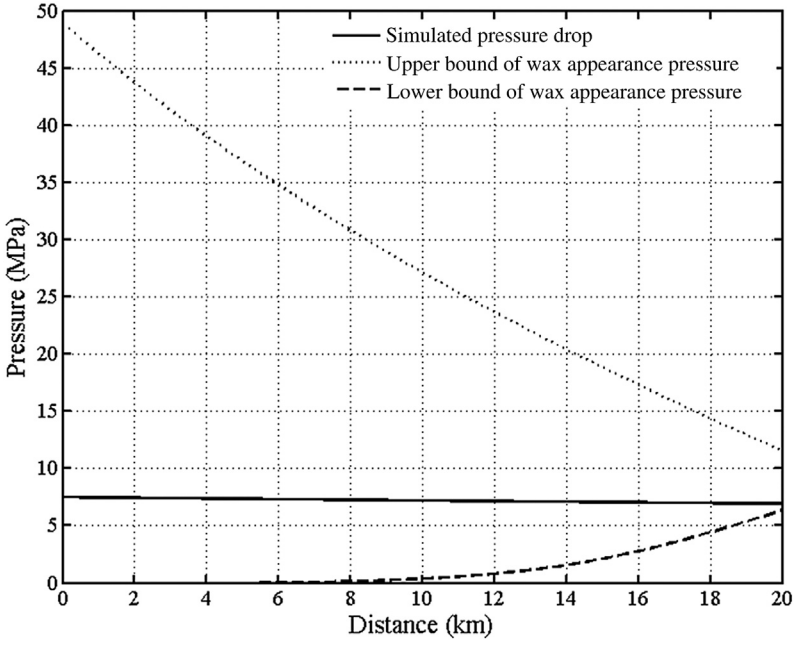

FIGURE 14.11 *Comparison between Oil and Wax Appearance Pressures.*

Table 14.17 Effect of Inlet Temperature on PoF

Inlet Temperature (°C)	Wax Deposition Probability (%)	PoF Class
55	31.84	3
56	8.43	2
57	0.91	2
58	0.05	1
59	Close to zero	1

Table 14.18 Effect of Flow Rate on PoF

Minimum Flow Rate (m^3/d)	Wax Deposition Probability (%)	PoF Class
2000	31.76	3
2300	1.21	2
2600	0.03	1
2900	Close to zero	1

Table 14.19 Effect of Thermal Insulation Layer Thickness on PoF

Thermal Insulation Layer Thickness (mm)	Wax Deposition Probability (%)	PoF Class
30	32.18	4
35	2.53	2
40	0.12	1
45	Close to zero	1

Table 14.20 Effect of Inlet Pressure on PoF

Inlet Pressure (MPa)	Wax Deposition Probability (%)	Pof Class
7.5	31.86	3
9.0	4.54	2
10.5	19.53	3

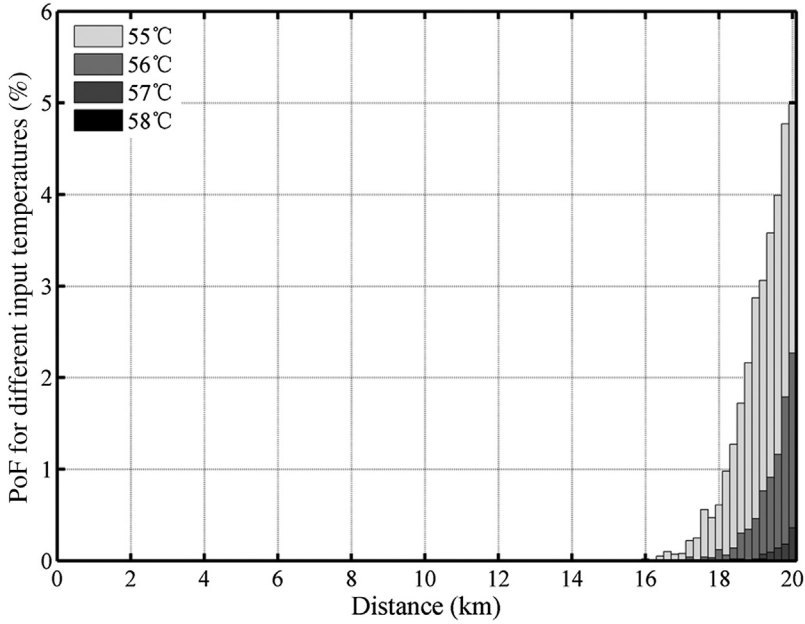

FIGURE 14.12 ***Distributions of PoF along the Pipeline for Different Inlet Temperatures.***

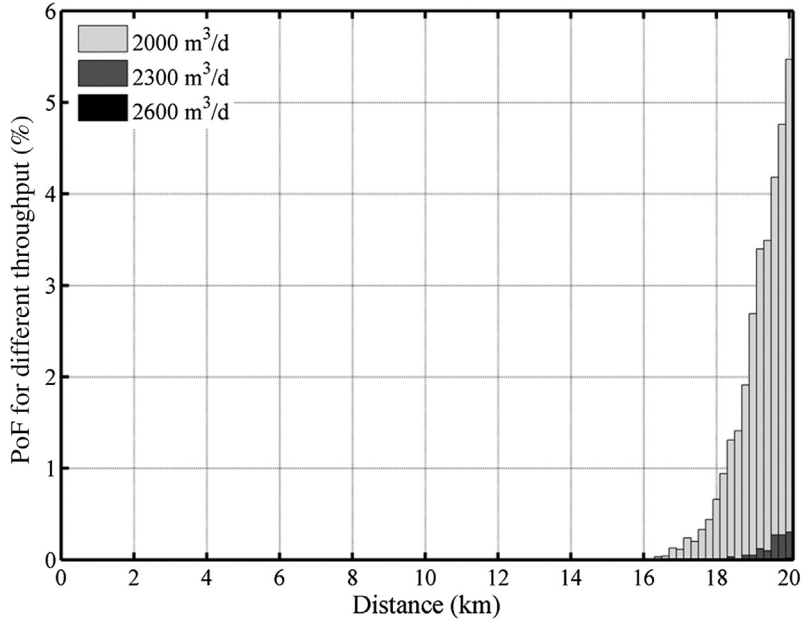

FIGURE 14.13 ***Distributions of PoF along the Pipeline for Different Flow Rates.***

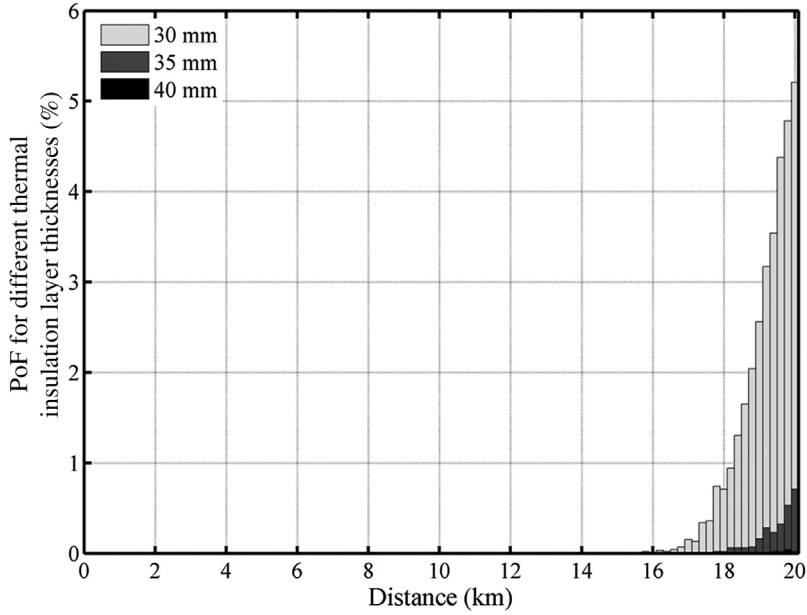

FIGURE 14.14 ***Distributions of PoF along the Pipeline with Different Insulation Thicknesses.***

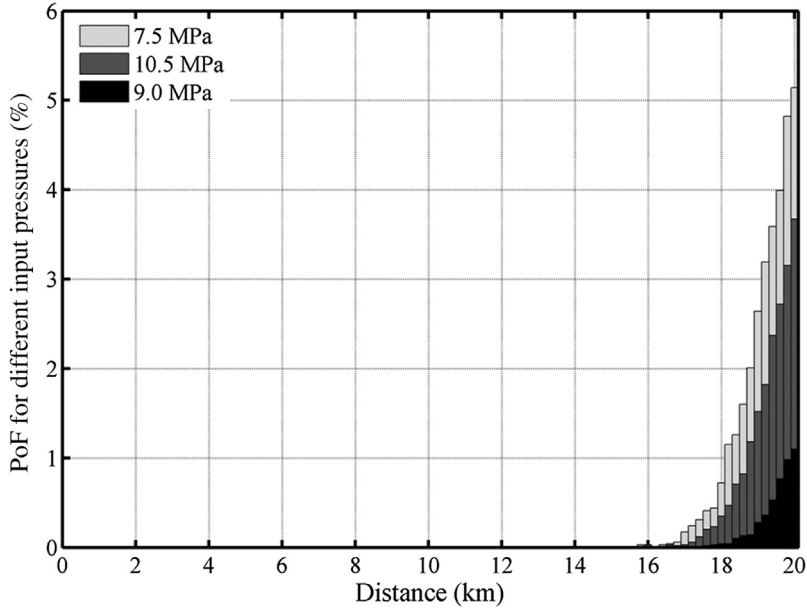

FIGURE 14.15 ***Distribution of PoF along the Pipeline for Different Inlet Pressures.***

Table 14.19 shows the PoFs for different thicknesses of thermal insulation layer. The PoF drops with the increase in thickness insulation. Figure 14.14 shows the distributions of the PoF along the pipeline for different thicknesses of insulation.

Table 14.20 lists PoFs for different inlet pressures. It is unlikely that the PoF is linear with the increase in inlet pressure. Figure 14.15 shows the distributions of the PoF along the pipeline for different inlet pressures.

6. SUMMARY

A risk analysis of the flow blockage due to hydrate formation in gas pipelines and wax deposition in oil pipeline was carried out with QRA. From the analysis results of Figures 14.5 to 14.8 and 14.12 to 14.15, the distributions of the PoF show that the highest probability of blockage is near the end of pipeline, because the temperature has great effect on hydrate formation and wax deposition, and the temperature drops to the lowest value at the end of pipeline.

The following methods may reduce PoF of the flow blockage in gas pipelines due to hydrate formation:

- Increase the inlet temperature of gas or heat up the whole pipeline.
- Increase the minimum flow rate.
- Increase the thickness of thermal insulation layer or use high thermal resistance materials.
- Decrease the inlet pressure of gas, although it reduces flow rate of gas.

The following methods may reduce the PoF of the flow blockage in oil pipelines due to wax deposition:

- Increase the inlet temperature of oil or heat up the whole pipeline.
- Increase the minimum flow rate of oil.
- Increase the thickness of thermal insulation layer or use high thermal resistance materials.

REFERENCES

[1] API. Recommended practice for subsea production system reliability and technical risk management. API RP 17N. Washington, DC: American Petroleum Institute; 2009.
[2] DNV. Risk management in marine and subsea operations. DNV-RP-H101. Høvik, Norway: Det Norske Veritas; 2003.
[3] Wang J. Offshore safety case approach and formal safety assessment of ships. J Safety Research 2002;33:81–115.
[4] ISO. Petroleum and natural gas industries—Pipeline transportation systems—Reliability-based limit state methods. ISO 16708:2006(E). Switzerland: International Standards Organization; 2006.

[5] Rubinstein RY, Kroese DP. Simulation and the Monte Carlo method. New York: Wiley-Interscience; 2008.
[6] Bai Y, Bai Q. Subsea pipelines and risers. Oxford, UK: Elsevier; 2005.
[7] Dendy Sloan Jr E, Koh C. Clathrate hydrates of natural gases. third ed. New York: Taylor and Francis; 2007.
[8] Katz DL. Handbook of natural gas engineering. New York: McGraw-Hill; 1959.
[9] Edmonds B, et al. Latest developments in integrated prediction modelling hydrates. waxes and asphaltenes. Focus on Controlling Hydrates, Waxes and Asphaltenes. IBC, Aberdeen; October 28–29, 1999.

CHAPTER 15

Marine Traffic Risk Assessment

Contents

1. Introduction 332
2. Data Collection 332
   - Vessel Information 332
   - Route, Approach Characteristics, and Navigability Study 333
   - Origin, Destination, and Marine Traffic Volume Study 333
   - Fishery Resources Study 333
   - Offshore Exploration, Development, and Production Activities Study 333
3. Hazards Identification 334
   - General 334
   - Common Marine Traffic Hazards 334
     - *Grounding* *334*
     - *Collision* *335*
     - *Explosion* *335*
     - *Fire* *336*
   - Structural Failure 336
     - *Other Hazards* *336*
   - Statistic Data of Marine Traffic Accidents 336
4. PoF Assessment 336
   - General 336
   - Probability Calculation Methods 337
     - *Statistics Method* *337*
     - *Bayes Method* *337*
     - *Numerical Model Method* *338*
   - Ship Collision Probability 339
   - Ship Grounding Probability 340
5. CoF Assessment 340
   - Assessment Methodology 340
   - The Cost-Efficiency Analysis 341
   - Human Reliability Analysis 342
6. Risk Assessment 342

References 343

Subsea Pipeline Integrity and Risk Management
ISBN 978-0-12-394432-0
http://dx.doi.org/10.1016/B978-0-12-394432-0.00015-9

1. INTRODUCTION

Marine traffic risk assessment (MTRA) forecasts the possible accidents in the concerned region, and the accident results assessed by the possibility of failure (PoF) and the consequence of failure (CoF). Figure 15.1 shows the main procedure of the marine traffic risk assessment [1].

2. DATA COLLECTION

The data relative to risk assessment may come from the timetabled schedules of the port, the vessel arrival and departure records from local marine department, digital capture from the marine department radars, and the visual surveys [2].

Vessel Information

To carry out the MTRA, the vessel is identified first. Generally, the vessel information, such as typical size, typical shape, typical vessel distribution, or the conventional route of the vessel is needed [3]. According to the information, the probability and consequence of accident can be found out or used to forecast the future risk. The following key data should be compiled for the assessment:

- Coastline geometry.
- Traffic routes.
- Traffic volume and type.
- Navigation characteristics.

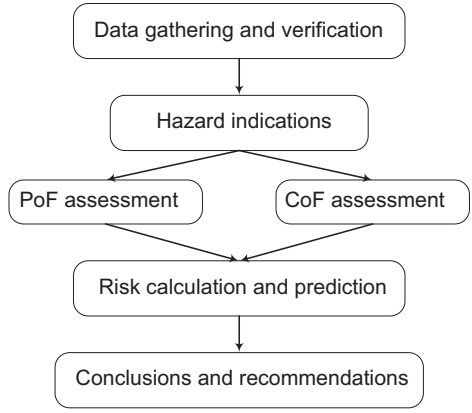

FIGURE 15.1 ***Procedure of Marine Traffic Risk Assessment.***

Route, Approach Characteristics, and Navigability Study

The following information and data have to be sourced or compiled by making appropriate substudies or surveys:

- Conceptual and FEED bases.
- Hydrographic, bathymetric, waves, wind, current, and tidal information.
- Marine environment sensitive areas.
- Navigation route.

Origin, Destination, and Marine Traffic Volume Study

The data of all recreational, commercial offshore operations, fishing, and any other traffic movement that collectively form the regional marine traffic network are available from the relevant government departments and agencies or the consultant has to compile them from the appropriate substudies or surveys.

Fishery Resources Study

The data from the relevant government departments and agencies should be collected or the appropriate substudies or surveys for data compilation should be carried out. The data should cover

- Fish and fish habitats, including any relative marine areas that may be affected by the project.
- Geographical locations and fishing methods employed in regional fishing operations.
- Seasonal variations in fishing activities.
- Customary routes to major fishing grounds from the fish landing sites, used by fishing vessels.

Offshore Exploration, Development, and Production Activities Study

The data from the relevant government departments and agencies should be collected or the appropriate substudies or surveys for the data compiled. The data should include geographical locations and frequency of

- Use of military exercise areas involving ships and aircraft.
- Offshore exploration and exploitation and the routes used by offshore supply and seismic study vessels.

3. HAZARDS IDENTIFICATION

General

The local marine traffic study focuses on the immediate geographical area of the concerned region and approaches to identify

- Types and sizes of ships in the area of the terminal and approaches.
- Local fishing operations.
- Local recreational and other marine activities.
- Routing traffic support services in the terminal area and approaches.

Common Marine Traffic Hazards

The common marine traffic hazards are as follows:

- Grounding.
- Collision.
- Explosion.
- Fire.
- Structural failure.

Grounding

Grounding is a very common hazard, which always happens in the shallow water area near the main waterway [4]. Figure 15.2 illustrates typical grounding forms, which include powered grounding and drifting rounding.

The following factors determine the possibility of grounding:

- Distribution of water depth.
- Density of traffic volume.

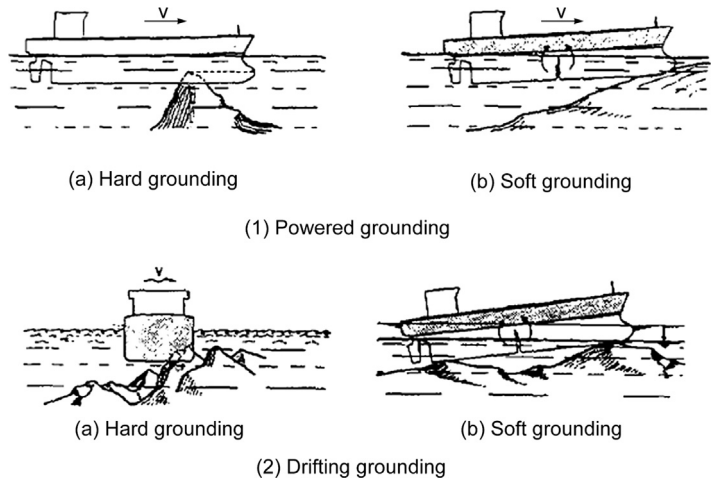

FIGURE 15.2 *Typical Ship Groundings.*

- Speed of the vessel.
- Dimensions of the vessel.
- History grounding accidents.
- Wind and wave data.

Collision

As shown in Figure 15.3, typically, there are four kinds of collisions: ship-ship collision, collision with rigid wall, collision with floating object, and ship-platform collision [5].

A statistical analysis of environmental factors should be conducted to identify if there is any correlation among the collision incidents with poor visibility, high winds, adverse weather, strong currents, or rough seas. The other factors that determine collision accidents are as follows:

- Vessel information (such as vessel type, dimension, speed, adjacent distance, and angle of encounter).
- Waterway distribution.
- Other geographical information.

Explosion

Explosions include explosion accidents and fishery bomb explosions. Explosion accidents may cause the ship to sink or, even worse, the passengers or the sailors do not get help in time or the chemical cargo or crude oil leaks to the environment nearby to bring about pollution.

The fishery bombs generate shock pressure, which decays almost exponentially with distance from the explosive center. For example, a 5-lb bomb generates about 0.5 MPa shock wave pressure at 18 m from the source

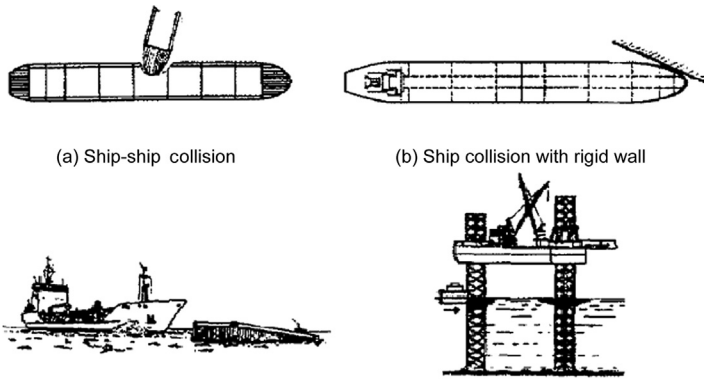

FIGURE 15.3 *Typical Ship Collisions.*

but increases to over 6 MPa if the standoff distance is reduced to 2 m. The fishery bomb explosion may affect the vessels or pipelines nearby.

Fire

Fire is a severe hazard to vessels. Fire may lead to casualties or even explosion when the vessel carry some explosive cargo. Terrible fire accident may lead to marine traffic jam or the smoke results in poor visibility.

Structural Failure

When the structure of vessel fails, the vessel and its passengers are in a highly dangerous condition. If one failure compartment of the vessel carries poisonous liquid, the poisonous liquid may leak into seawater and pollute the environment nearby, which may bring much trouble to local residents.

Other Hazards

In addition to all the hazards juast specified are others that should not be neglected:

- Machinery damage.
- Storm damage.
- Environmental damage.
- Leaking.
- Severe tilting.
- Capsizing.
- Other unknown accident types.

Statistic Data of Marine Traffic Accidents

Figure 15.4 shows the marine traffic accident statistics data by month in the Gulf of Finland [6, 7], in which the grounding and collision are the main accidents. The accident number varies in different months, because the number of the vessels varies due to the production quantity, and the weather condition may be another cause of these accidents.

4. PoF ASSESSMENT

General

The accident probability should be identified first in the marine traffic accident analysis. In this chapter, the grounding and collision of tankers are

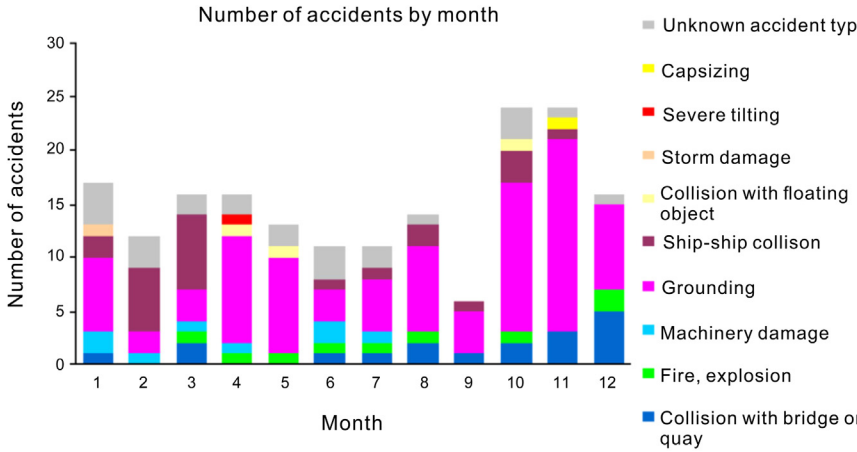

FIGURE 15.4 ***Number of Marine Traffic Accidents in Gulf of Finland.*** *Source: Hanninen [8].* (For color version of this figure, the reader is referred to the online version of this book.)

chosen as the main marine traffic accidents. The following methods can be used to calculate the probability of the tanker grounding and collision [9]:

- Statistics method.
- Bayes method.
- Numerical model method.

Probability Calculation Methods

Statistics Method

The statistics method is based on the existent databases, such as the World Offshore Accident Databank (WOAD) and MSIS (Marine Safety Information System) database, to create a fault tree or event tree model of tanker grounding and collision. The basic events probability of the models depends on the statistics data, and the grounding or collision probability then can be determined. Especially, if the grounding or collision happens when the tanker enters into or departs from the port, the grounding or collision probability depends on the water region and course flux.

Bayes Method

The Bayes model for ship grounding and collision created by Kite-Powell is used to determine the accident probability on a given course. It is supposed that the grounding or collision is caused by series of risk factors. Suppose A is one event that can cause the grounding or collision of the tanker, $X = (X_1, X_2, X_3, \ldots, X_p)$ refers to the explanation factors.

If the probability x of the X_i is given, the probability of A can be determined by the following formula:

$$p(A|x) = l(x|A)p/[l(x|A)p + l(x|S)(1-p)] \quad [15.1]$$

where

$p(A|x)$ = the probability of A if x happens
$l(x|A)$ = the probability of x if A happens
$l(x|S)$ = the probability of x if S happens
p = the nonconditional probability

The contribution of the different factors for ship grounding and collision can be determined using the Bayes method. The corresponding economic loss, the cargo loss, and the environment damage then may be forecasted.

Numerical Model Method

A numerical model for the specific navigation area can determine the probability of ship grounding and collision in this area. The Pedersen model [10] may be used to calculate the probability of ship collision. It estimates the possible number of accidents N_a, the number of accidents when the ships navigate along the design routes. Then, it multiplies the accident number, N_a, with the accident probability, and the actual numbers are found. The term P_c is the cause function for the accidents, and the calculation is based on the statistics data.

To get the value of N_a, the following crossing area is used. Suppose the traffic flux of this water region is known, and the ships have been classified according to type, the maximum displacement, or the length, loaded conditions or ballast conditions, whether they have a bulb bow or not, and so forth. The value of N_a equals the possible number of ship-ship collisions of the overlap region Ω shown in Figure 15.5, assuming the ship navigates along the design routes. The term N_a represents the accident numbers of the j type vessel on the second route and the i type vessel on the first route in the duration of Δt; and all this can be expressed by the following formula [11]:

$$N_a = \sum_i \sum_j \left[\iint_{\Omega(zi,zj)} \frac{Q_i^1 Q_j^2}{V_i^1 V_j^2} f_i^1(z_i) f_j^2(z_j) V_{ij} D_{ij} dA \Delta t \right] \quad [15.2]$$

where

Q_i^a = traffic flux (equals the number of j type ships crossing route a at unit time, $a = 1, 2$)
V_j^2 = velocity of the corresponding ship

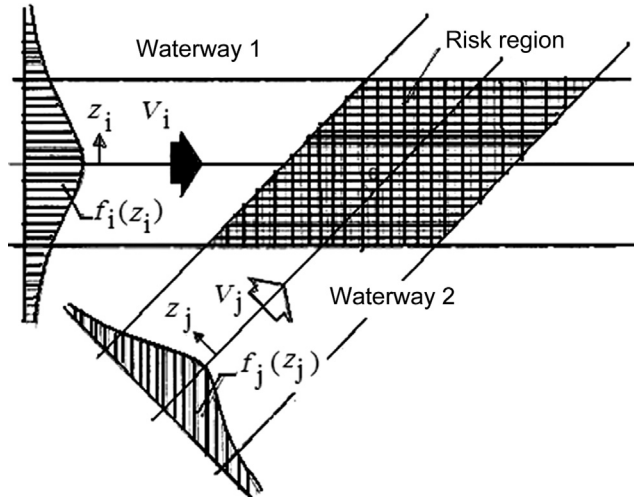

FIGURE 15.5 *Risk Region of Ship-Ship Collision in Crossing Area.*

f_i^a= lateral distribution function of j type ship on the route a, $a = 1, 2$
D_{ij} = geometrical collision diameter

$$V_{ij} = \sqrt{\left(V_i^1\right)^2 + \left(V_j^2\right)^2 + 2\left(V_i^1\right)^2\left(V_j^2\right)^2 \cos\theta}$$

According to the calculation formula, the possible collision numbers equal

$$N_{\text{ship-ship}} = P_c \cdot N_a \qquad [15.3]$$

The term P_c may be evaluated according to the observation results and is in the range of 0.5×10^{-4}–2.0×10^{-4} according to the analysis results. The accident number at various regions is converted to the probability of the interested region.

Ship Collision Probability

The following items may be the most common causes for the ship collision, according to the statistical data:

- Competency defects of crew.
- Observation carelessness.
- Nonuse or improper use of radar.
- Imroper use due to dependency on VHF.
- Wrong judgment of the situation.

- Too few duty crew members to deal with current situation.
- Ship occupies other ships' courses.
- Breaking local or international collision avoidance rules.
- Slow avoidance.
- Operation errors of the pilot.
- Sudden electric cutoff of rudder gear or the main engine.
- Abnormal offcourse environment or natural environment.
- Chaotic traffic condition.

Ship Grounding Probability

As described previously, ship grounding includes two categories:

- **Powered grounding:** It may be caused by navigation errors or mindless crew that induces the ship to collide with the beach.
- **Drift grounding:** It may be caused by ship losing self-navigation ability due to operation errors or propulsion equipment failure and colliding with beach before the help of available towing or maintaining.

The ship grounding probability should be calculated in according with the following formula based on the ship grounding in DNV rules:

$$P(\text{ship grounding}) = P(\text{powered grounding}) + P(\text{drift grounding})$$

Here, the plus sign means "or" If $P(c)$ means the ship grounding probability, $P(a)$ means the powered grounding probability and $P(b)$ means the drift grounding probability; therefore:

$$P(c) = P(a) + P(b) - P(a \cdot b) \qquad [15.4]$$

5. CoF ASSESSMENT

Assessment Methodology

Particularly in the case of tankers, if a grounding or collision happens, the oil spill is one of the most severe consequences. The leaked oil may cause damage to the environment. Especially, the leakage of a VLCC (very large crude carrier) can heavily threaten the environment and the local habitants [12]. Therefore, it is necessary to calculate the probability of the oil outflow from tankers.

The traffic accidents of tankers are stochastic events and so is the damage position of the oil compartment, so the probability method is introduced in this chapter. The International Marine Organization (IMO) established a

series of rules aimed at the newly designed tankers [13]. This can be found in the International Convention for the Prevention of Pollution from Ships (MARPOL) 73/78 13F (5) Appendix I [13]. The rules provide a series of probability methods in calculating the oil spill after grounding and collision. To calculate the oil spill quantities caused by grounding and collision, the hydrostatics and quasi-hydrodynamic methods are used, in which the following three parameters should be determined first:

- Zero outflow probability, P_0.
- Mean outflow parameter, O_M.
- Extreme outflow parameter, O_E.

The probability density functions can be seen in Appendix A of MARPOL [13], it is based on the statistics data from the different classification societies and the figures are fitted by the IMO, assuming that all the various probability density functions are independent.

The Cost-Efficiency Analysis

The cost-efficiency analysis of oil outflow is a key step to any risk assessment, because the oil outflow after grounding and collision may cause environment damage, pollution treating costs, and the loss of the cargo. According to the calculation results of the United States Coast Guard (USCG), the oil outflow volume per year of the tankers may be expressed as

$$O_A = 0.575 \times 0.0042 \times (O_M \times C) \quad [15.5]$$

where

$O_M \times C$ = means outflow of the tanker, m^3

If the capital costs of the tankers is converted into the annual costs, the total cost of the tanker can be determined

$$CT_A = CC \times CRR + OC \quad [15.6]$$

where

CC = capital cost of the tanker

CRR = cost recovery rate

OC = operating costs

Thus, the net benefit of the tanker can be expressed by the following formula:

$$NB = (CT_{A2} - CT_{A1})/(O_{A1} - O_{A2}) \quad [15.7]$$

Human Reliability Analysis

The human and organization error is the main cause of the grounding and collision of tankers. According to the statistical data, 80% of the collision accidents was caused by the human and organization error, and the ratio is as high as 90% for the grounding accidents. Therefore, it is important to do human reliability analysis for the evaluation of grounding and collision accidents. The following methods are commonly used for the human reliability analysis:

- Quality analysis method.
- Quantity analysis method.
- System action management (SAM) method.

Paté-Cornell and Murphy [14] used the SAM method to do human reliability analysis for the explosion of the Piper Alpha Offshore Platform; it may be used as guideline for the human analysis reliability of the tanker grounding and collision too.

6. RISK ASSESSMENT

For tankers, the main risk is the oil outflow after grounding or collision, because the oil spill may cause hazards to the environment, the local habitants, the marine creatures, or the safety of the crew. The following methods may be used for the risk assessment:

- IMO direct calculation method.
- Direct integration method.
- Simplified calculation method.

The most dangerous condition is a fully loaded tanker ready for departure, which should be chosen for the risk assessment of the tankers [15]. The compartments of ship that may cause the oil outflow include the crude oil compartment, fuel compartment, diesel compartment, lubricant compartment, and the sump oil. The risk assessment may be carried out following the following steps:

- Determine the main dimension of the tanker.
- Classify the tanker according to the type, tonnage, and route.
- Calculate the probability of a tanker collision or grounding.
- Evaluate the oil outflow after grounding or collision.
- Complete the risk assessment;

The comparison of the risk assessment results to the risk limits determines whether the risk is accepted or not. If the risk exceeds the

risk limits, some risk mitigation measures should be identified to reduce the risks to allowable levels.

REFERENCES

[1] Fujii Y, Yamanouchi H, Matui T. Survey on vessel traffic management systems and brief introduction to marine traffic studies. Paper No. 45. Tokyo, Japan: Electronic Navigation Research Institute, Ministry of Transport; 1984.

[2] Fowler TG, Sørgråd E. Modeling ship transportation risk. Risk Analysis 2000;20(2):225–44.

[3] Goodwin E. A statistical study of ship domain. J Navigation 1975.

[4] Fujii Y, Yamanouchi H, Tanaka K, Yamada K, Okuyama Y, Hirano S. The behavior of ships in limited waters. papers, 19. Tokyo, Japan: Electronic Navigation Research Institute; 1978.

[5] Kao S, Lee K, Chang K, Ko M. A fuzzy logic method for collision avoidance in vessel traffic service. J Navigation 2007.

[6] Kuronen J, Tapaninen U, Helminen R, Lehikoinen A. Maritime transportation in the Gulf of Finland in 2007 and in 2015. Turku, Finland: Center for Maritime Studies; 2008.

[7] Ylitalo J, Hanninen M, Kujala P. Accidents probabilities in selected areas of the Gulf of Finland. Espoo, Finland: Helsinki University of Technology; 2008.

[8] Hanninen M. Modeling risks of marine traffic in the Gulf of Finland. Final Seminar of the MS GOF project 2007.

[9] Kujala P, Hänninen M, Arola T, Ylitalo J. Analysis of the marine traffic safety in the Gulf of Finland. Reliability Engineering and System Safety 2009.

[10] Pedersen PT. Collision and grounding mechanics. Copenhagen: The Danish Society of Naval Architects and Marine Engineers; 1995.

[11] Szlapczynski R. A unified measure of collision risk derived from the concept of a ship domain. J Navigation 2006.

[12] Kristiansen S. Maritime transportation: Safety management and risk analysis. Oxford, UK: Elsevier, Butterworth-Heinemann; 2004.

[13] IMO SOLAS. International convention for the safety of life at sea. London: International Maritime Organization; 2003.

[14] Paté-Cornell ME, Murphy DM. Human and management factors in probabilistic risk analysis: The SAM approach and observations from recent applications. Reliability Engineering and System Safety 1996;53:115–26.

[15] Pietrzykowski Z, Uriasz J. The ship domain—A criterion of navigational safety assessment in an open sea area. J Navigation 2009.

CHAPTER 16

Consequences of Failure Modeling for Oil and Gas Spills

Contents

1. Introduction 345
2. Detailed Assessment 346
   Quantitative Risk Assessment 346
   Consequences of Failure 347
      Personnel Consequence *348*
      Environmental Consequence *348*
      Economic Consequence *349*
   Probability of Failure 349
3. Oil Spill Consequences 350
   Oil Spreading Mechanism 351
   Oil Evaporation Mechanism 352
   Oil Emulsification Mechanism 353
4. Gas Spill Consequences 354
   Model for Gas Dissolution 354
   Integration of Gas Dissolution with Jet-Plume Model 356
      Volume Fraction of Gas Bubbles *356*
      Conservation of Liquid Mass *357*
      Gas Mass Loss Due to Gas Dissolution *357*
      Conservation of Momentum *357*
      Conservation of Heat, Salinity, and Oil Mass *357*
      Nonideal Gas Law *358*
      Size of Gas Bubble *358*
5. Example of an Oil Spill 358
References 361

1. INTRODUCTION

The hazards due to the failure of subsea pipeline systems could cause a lot of trouble to the environment including wildlife and sea creatures, also to humans themselves and economical costs. In the last decades, failures of subsea pipelines has become one of the world's worst disasters, because they greatly affect the environment, personnel, and financial aspects. To prevent pipeline failures, a lot of risk assessment inspections are being considered to improve the safety level. A lot of procedures can be used to evaluate the risk

Subsea Pipeline Integrity and Risk Management
ISBN 978-0-12-394432-0
http://dx.doi.org/10.1016/B978-0-12-394432-0.00016-0

and failure consequences, a frequently used method is quantitative risk assessment (QRA). The main purpose of QRA is to determine the target reliabilities for each pipeline system segment. The purpose of consequences of failure (CoF) is to determine the failure consequences, including amount and rate of oil spill and gas spill, affected area, delaying mission, or any other measurement of negative impact. However, this chapter focuses on the determination of oil spill slick and gas spill leakage following a leakage in a pipeline system. Then, a suitable action can be performed, based on these calculations and data, to avoid the consequences of failure, such as number of people affected, production cost affected, and environment area affected.

2. DETAILED ASSESSMENT

Quantitative Risk Assessment

Risk can be described as a term that combines the probability that a specified hazardous event will occur with the severity of the failure consequences. Risk assessment (RA) is the evaluation of the risk aspects of a particular system, whether the risks are from human error, hardware, or software failures, environmental impacts, or a combination of any accidents. In this chapter, risk assessment is used to evaluate the integrity of a pipeline system and take actios to avoid any consequences resulting from the pipeline failures. Generally, the consequences of pipeline failure can exist through leakage, dispersion, fire, explosion, or the like. The risk can be expressed in a mathematical form, as follows [1]:

$$\text{Risk} = \text{Failure frequencies} \times \text{Consequences of failure} \qquad [16.1]$$

Any accident consequences considered may be related to personnel, the environment, and production capacity. Risk has a positive relationship with the event consequences, which means risk increases if the event probability or event consequence increases. The main elements of risk study or analytical risk analysis are those that required to determine the applicable hazards and assess the risk that arises from them. Three principal elements form the analytical process:

1. Identification of the initiating event.
2. Cause analysis.
3. Consequence analysis.

Figure 16.1 shows the quantitative risk acceptance criteria due to the failure consequences. Figure 16.2 shows the methodology of principal steps for risk analyses.

5	$>10^{-2}$					
4	10^{-2} - 10^{-3}			Unacceptable area		
3	10^{-3} - 10^{-4}					
2	10^{-4} - 10^{-5}	Acceptable area				
1	$0\text{-}10^{-5}$					
		A	B	C	D	E
Safety (deaths)		0	0.1	1	10	100
Environmental (recovery period)		0	< 1 year	< 3 year	< 10 year	> 10 year
Economic (relative %)		< 2%	2-5 %	5-10 %	10-20 %	>20 %

FIGURE 16.1 ***Quantitative Risk Acceptance Criteria.*** (For color version of this figure, the reader is referred to the online version of this book.)

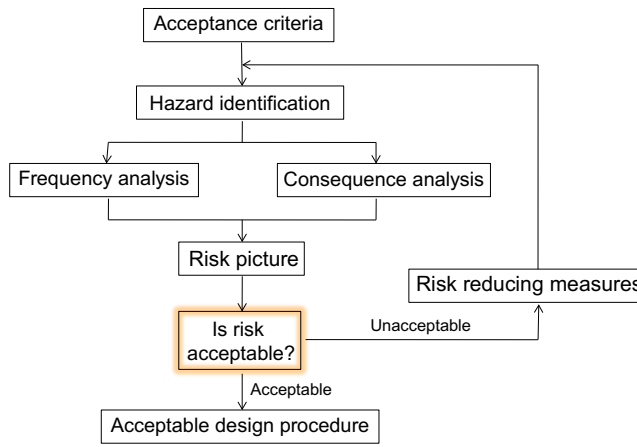

FIGURE 16.2 ***Analysis of Risk Methodology.*** (For color version of this figure, the reader is referred to the online version of this book.)

Consequences of Failure

The consequences of failure can be described as a measurement for the quantification of risk, such as number of people affected due to the accidents (injured or killed), property damage, amount of oil spilled, amount of gas spilled, environment and area affected, or mission delayed. Similar to those of QRA shown in Figure 16.1, the consequences of failure are divided into the three sections of safety, environment, and economic consequences, which are analyzed, respectively, by quantitative assessment [2]:

- **Personnel consequences**: The potential of injured or death caused by explosion, blowout, ignition, pipeline failure, or hazardous happenings.

- **Environmental consequences:** The damage to wildlife creatures, the ecosystem, soil, and water, whether short-term or long-term effects (depending on the hazard).
- **Economic consequences:** The potential of business loss in production interruption and the cost of repairing and recovering the pipeline component that damaged.

The consequence analysis involves a lot of disciplines with several steps [3]:

- Accident scenario analysis of failure consequences.
- Analysis of accidental loads, such as explosion, fire, blowout, and impact on pipeline.
- Analysis of system and equipment response to accidental loads.
- Analysis of final consequences among personnel, the environment, and assets factors.
- Escalation analysis.

In major cases, the potential of consequences depends greatly on the pipeline parameters, such as operating pressure, pipeline length, pipeline diameter and size, and amount of the failure release. The consequences of failure also include the consequences of production losses, cost of repairing the pipeline and various damages, potential fatalities, and cost of negative publicity. However, this chapter does not describe other major consequences, because the three areas of failure consequence shown in Figure 16.1 are the most important ones. In the following sections, the categorization of failure consequence for each area is ranked from class A to class E.

Personnel Consequence

The safety consequences consider the potential personnel injury or fatalities, categorized from A until E in Table 16.1. Safety consequences are usually estimated for failures that lead to ignition, explosion, pollution, or toxic release, but failure of pipeline components containing high-pressure nonhazardous fluids should also be considered [4].

Environmental Consequence

The environmental consequences of failure are concerned with the impact of various types of product releases to the environment nearby, flora and fauna affected, and damages to seawater. The amount and rate of release depends highly on the type of fluid, size of pipeline diameter, flow rate of pipeline, and type of failure, such as leakage or rupture. The environmental consequences are divided according to the product and amount of release,

Table 16.1 Safety Consequence Failure Ranking

CoF Factor	CoF Identification	Description
A	Very low	Personnel injury not likely to happen
B	Low	Potential minor injury, no likely major injury or fatalities
C	Medium	Potential major injury to no more than one or a few people; no potential for fatality
D	High	Potential multiple major injury; potential for one fatality
E	Very high	Potential for multiple fatalities

and the actual impact of the environment is not considered in detail. Table 16.2 ranks the environmental consequences.

Economic Consequence

The economic consequences are calculated as the repair costs and production losses due to the interruption in production, as shown in Table 16.3. The relative throughput has been used as the basis for quantification of the business consequences.

Note that "relative to overall field production" is expressed in terms of a percentage to classify the level of operational critically for each pipeline at the factor stage. The values for the percentage given are for guidance only and can be adjusted following input from the operator.

Probability of Failure

The probability of failure is estimated on the basis of the types of degradation mechanisms operating on the component. Failure probabilities can be estimated by qualitative assessment, from experience data, or by quantitative calculations using more or less refined physical models. For a *qualitative evaluation*, the failure probability is estimated as a rank category; while for a *quantitative evaluation*, the scale for PoF is probability of an event per unit time or probability of an event after a given time.

For a probability of failure study, the safety criteria are commonly expressed as FAR (fatal accident ratio) for an operation. These criteria can be further transformed to a per system requirement in terms of its contribution to the risk. Risk may be expressed in terms of PLL (potential loss of life). Based on the safety requirements, the allowable material utilization factor is less in areas where a failure may be a hazard to personnel. Generally,

Table 16.2 Environmental Consequence Failure Ranking

CoF factor	CoF Identification	Description
A	Very low	None or small impact on the environment; either no release of product or only insignificant release of low toxic or nonpolluting product
B	Low	Minor release of polluting or toxic product; released product will decompose or neutralize rapidly in seawater or air; recovery period <1 year
C	Medium	Minor release of polluting or toxic product or large release of low-polluting or toxic product; released product might take some time to disperse or neutralize or can easily be removed; recovery period <3 years
D	High	Large releases of polluting and toxic product; after some time, product will disperse, decompose; or neutralize, can also be removed; recovery period <10 years
E	Very high	Large releases of high-polluting and toxic product; cannot be removed and takes a long time to disperse or decompose; recovery period >10 years

Table 16.3 Economic Consequence Failure Ranking

CoF Factor	CoF Identification	Costs Relating to Production Loss Relative to Overall Field Production (%)	
A	Very low	<2	Minor flowlines
B	Low	2–5	Small flowlines
C	Medium	5–10	Medium flowlines
D	High	10–20	Important flowlines
E	Very high	≥20	Trunk lines

Zone 1 is for offshore pipeline sections away from platforms, while Zone 2 is for the pipeline sections in the vicinity of the facility [5].

3. OIL SPILL CONSEQUENCES

Oil pollution in seawater has received particular attention over the past years by scientists and governments, as the consequence of serious number accidents involving the release of large amounts of oil at sea. Response measures to an oil spill are enhanced by the capability to forecast the short-term and long-term behavior of the oil spilled. Also known as the fate of oil

at sea: It is determined by several physiochemical properties of the oil as well as by the environmental conditions. Sebastiao and Soares [3] state that the sea state conditions have an important influence on oil spill behavior, but waves and water currents involve different types of mechanism, which are not taken consideration in this chapter. This chapter concentrates on the models that predict the fate of an oil spill in calm weather and without the influence of waves and water currents. The main mechanisms that govern the fate of an oil spill at sea are spreading, evaporation, emulsification, dispersion, and sedimentation. Only the most important mechanisms, oil spreading and oil evaporation, are reviewed in this chapter.

Oil Spreading Mechanism

Much oil spilled on the surface of calm water spreads in the form of a thin continuous layer with a circular pattern, as a result of gravity and net surface tension. The net surface tension, also known as the *spreading coefficient*, is the difference between the air-water surface tension and the sum of air-oil surface tension and oil-water interfacial tension. The most widely used spreading model is the one developed by Fay [6]. Fay developed three phases in the spreading process but the second phase is the most-commonly used spill model. The formula for the second phase is, according to Fay's model as modified by Wang et al. (1975) [7],

$$A_2 = \pi 0.98^2 \left[\frac{\Delta\rho g V^2}{\rho_w \nu_w^{0.5}}\right]^{1/3} t^{1/2} \qquad [16.2]$$

where

A_2 = area of slick [m^2]
g = gravity [ms^{-2}]
V = volume of spill [m^3]
t = time [h]
ρ_w = seawater density
$\Delta\rho$ = density difference between seawater and oil
ν_w = kinematic viscosity of seawater [$m^2\ s^{-1}$]

Since Fay's formula estimates the slick growth, Lehr et al. (1984) [8] developed a Fay-type formula suitable to estimate the initial spill size given the observed spill area:

$$A = 2270\left[\frac{\Delta\rho}{\rho_0}\right]^{2/3} V^{2/3} t^{1/2} + 40\left[\frac{\Delta\rho}{\rho_0}\right]^{1/3} V^{1/3} W^{4/3} t \qquad [16.3]$$

where

A_2 = area of slick [m^2]
W = wind speed [knot]
V = volume of spill [barrel]
t = time [min]
ρ_0 = oil density
$\Delta\rho$ = density difference between seawater and oil

Mackay et al. (1980) [9] modified the formula rate of change of surface area, based on the gravity viscous formulation of Fay (1969) [6] and Hoult (1972) [10], which is useful for oil spill models that have many variables changing simultaneously. The rate of spreading is calculated as

$$\frac{\partial A}{\partial t} = K_1 A^{1/3} \left[\frac{V}{A}\right]^{4/3} \qquad [16.4]$$

where

A = area of slick [m^2]
K = defaulted to 150 s^{-1}
V = volume of spill [m^3]
t = time [s]
ρ_0 = oil density
$\Delta\rho$ = density difference between seawater and oil

Oil Evaporation Mechanism

Evaporation can be described as the initial process involved in the removal of oil spilled on the sea. Evaporation rate is determined by the physio-chemical behaviors of oil and can be increased by high water temperatures, spreading strong winds, and rough seas. Evaporation can rapidly remove the low-boiling components, thus reduce the volume of oil slick. The rate of evaporation of lighter components is influenced by the lighter component in oil itself, oil temperature, thickness of oil, and the physical forces of wind and waves [3].

Reed. (1989) [11] characterizes that the mass transfer rate for oil evaporation is given by

$$\frac{\partial m_i}{\partial t} = \frac{K_2 P_i A f_i M_i}{RT} \qquad [16.5]$$

where

m_i = mass of ith constituent
t = time

A = spill area
f_i = fraction of spill that is constituent i
R = gas constant
P_i = vapor pressure of the particular component
T = temperature;
M_i = molecular weight
while the coefficient K_2 is the mass transfer coefficient given by Mackay and Matsugu (1973) [12] as

$$K_2 = 0.029W^{0.78}D^{-0.11}S^{0.67} \quad [16.6]$$

where
K_2 = mass transfer coefficient for evaporation [ms^{-1}]
W = wind speed [mh^{-1}]
D = spill diameter [m]
S = Schimidt number

Oil Emulsification Mechanism

Emulsification of crude oils and refined products involves the dispersion of water droplets into the oil medium. It is generally agreed that a critical factor is the amount of natural surfactant present in the spilled oil with respect to the potential for emulsification of oils and emulsion stability [10].

The incorporation of water into oil may be derived, as by Mackay et al. (1980), through the following equation:

$$Y = C_3\left[1 - \exp\left(\frac{-2 \times 10^{-6}}{C_3}(1 + W)^2 t\right)\right] \quad [16.7]$$

where
Y = fractional water content
C_3 = mousse viscosity constant
W = wind speed
Mousse formation causes an increase in viscosity, which may be computed by the Mooney equation:

$$\mu = \mu_0 \exp\left[\frac{2.5Y}{(1 - C_3 Y)}\right] \quad [16.8]$$

where μ_0 = parent oil viscosity. Buchanan and Hurford (1988) [13] state that the oil viscosity can be estimated by $\mu_0 = 224A^{0.5}$, where A is the percentage of asphalt content.

4. GAS SPILL CONSEQUENCES

Gases in deepwater oil and gas spills can lose considerable amounts of gas phases due to dissolution in water. The major concerns from a deepwater gas spill are fire, toxic hazard to the working people, and loss of buoyancy of ships and any floating installations. Therefore, it is important to know when, where, and how much of gas will surface. This section describes the model flow in a gas-leaking pipeline and gas dissolution [14]. Figure 16.3 shows a scenario of a deepwater gas blowout. Initially, spilled gas mixture rises as a jet or plume, which may gradually lose its momentum and buoyancy due to the entrainment of ambient fluid in a stratified ocean environment. Note that gas expands as it rises because of the pressure drop and thus increases the buoyancy of the jet or plume.

Model for Gas Dissolution

Gases in deepwater oil and gas spills can lose considerable amounts of gas phases due to the dissolution in water. Gas dissolution has a significant impact on the behavior of the oil plume because of its impact on the buoyancy force. Zheng and Yapa (2002) [15] state that, in deep water, the

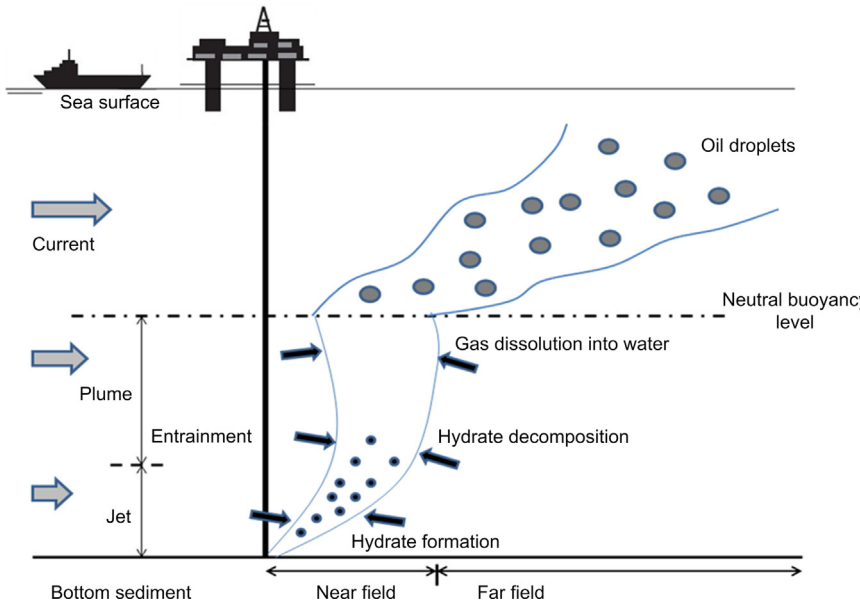

FIGURE 16.3 ***Scenario of a Gas Blowout.*** (For color version of this figure, the reader is referred to the online version of this book.)

high pressure and low temperature make the behavior of oil and gas spills different from those that occur in shallow water in two respects:

1. Gas may be converted into an icelike solid compound called as *gas hydrate.*
2. Gas bubbles may lose considerable amounts of gas phase through dissolution during their long journey.

Both processes alter the buoyancy of the plume significantly. The dissolution rate for a gas bubble is calculated as

$$\frac{\partial n}{\partial t} = KA(C_S - C_0) \qquad [16.9]$$

where

n = number of moles in a gas bubble
K = mass of transfer coefficient
A = surface area of gas bubble
C_S = saturated value of C_0
C_0 = concentration of dissolved gas

while the dissolution mass transfer rate, $\partial m/\partial t$, for a gas bubble is calculated as

$$\frac{\partial m}{\partial t} = KMA(C_S - C_0) \qquad [16.10]$$

where

m = mass of a gas bubble
M = molecular weight of gas

The key parameters in Eqs. [16.9] and [16.10]) are the solubility, C_S, and mass transfer coefficient, K. The solubility may be affected by the salinity, high pressure, and temperature in seawater. The solubility of gas in water is calculated using Henry's law:

$$P = \mathrm{H}x^l \qquad [16.11]$$

where

P = pressure of gas
H = Henry's law constant
x^l = mole fraction of dissolved gas in water

Zheng and Yapa [15] also stated that the simple form of Henry's law, as in Eq. [16.11], is limited to ideal gas and under low pressure conditions. If the pressure is raised in deep water, the equation is no longer usable.

Integration of Gas Dissolution with Jet-Plume Model

The following assumptions are made for modeling the jet-plume hydrodynamics [16]:

1. The flux of the bubbles' number is kept constant with height; for example, bubble coalescence is neglected.
2. All bubbles are of uniform size at the beginning. If a bubble size spectrum becomes available based on field experiments at a later time, it is possible to replace the number flux of bubbles N by an array, $N(r_1, r_2, \ldots, r_n)$. Then, the fate of the individually sized bubbles can be calculated independently.

The gas portion can be expected to occupy the inner core if a plume consists of a mixture of oil and gas vertically.

Volume Fraction of Gas Bubbles

The volume fraction of gas (ε) within the inner gas bubble core can be defined as

$$\varepsilon = \frac{\rho_1 - \rho}{\rho_1 - \rho_b} \qquad [16.12]$$

Figure 16.4 is a schematic diagram of the gas plume from a pipeline leakage. In the figure,

H = height of control volume
ρ = density of the plume bubble-water mixture
ρ_b = density of gas
ρ_1 = density of liquid part of a plume

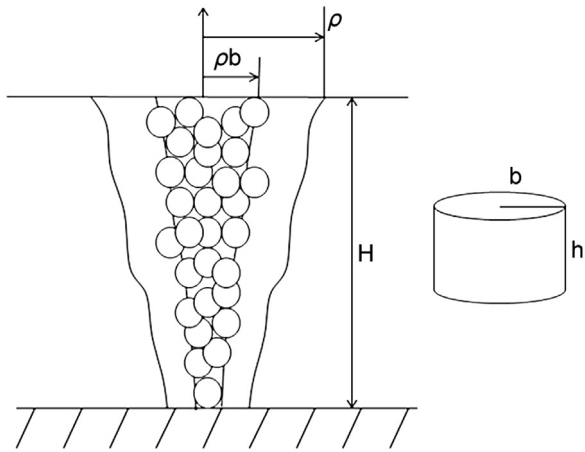

FIGURE 16.4 *Oil or Gas Plume.*

Conservation of Liquid Mass

$$\frac{\partial m_1}{\partial t} = \rho_a Q_e \tag{16.13}$$

where

m_1 = mass of liquid of a control volume
ρ_a = density of the ambient fluid
Q_e = entrainment rate for ambient water

Gas Mass Loss Due to Gas Dissolution

$$\Delta m_b = \frac{Nh}{w + w_b}\frac{\partial n}{\partial t} M_g \Delta t \tag{16.14}$$

where

M_g = molecular weight of gas
Δt = time step
w = vertical velocity of liquid part of plume
w_b = bubble slip velocity

Conservation of Momentum

$$\frac{\partial}{\partial t}[m_1 w + m_b(w + w_b]$$

$$= w_a \rho_a Q_e + (\rho_a - \rho_1) g\pi b^2 \left(1 - \beta^2 \varepsilon\right) h + (\rho_a - \rho_b) g\pi b^2 \beta^2 \varepsilon h \tag{16.15}$$

where

w_a = vertical velocity of ambient fluid

The first term of the right-hand side represents the momentum from the liquid mass, while the second term is related to the vertical force acting on liquid, and the last term represents the vertical force acting on the gas bubbles.

Conservation of Heat, Salinity, and Oil Mass

$$\frac{\partial (m_1 I)}{\partial t} = I_a \frac{\partial m_1}{\partial t} \tag{16.16}$$

where I_a = property such as heat content, salinity, or oil mass, while the subscript *a* represents to the conditions in the ambient water.

Equation [16.16] shows the change of heat, salinity, or oil mass in the control volume due to the entrained mass.

Nonideal Gas Law

$$PM_g = \rho_b ZRT \qquad [16.17]$$

where

Z = compressibility factor

R = the universal gas constant

T = ambient temperature

In deepwater scenarios, the gas can deviate from ideal gas behavior under high pressure.

Size of Gas Bubble

Using the nonideal gas law as in Eq. [16.17], the size of bubbles can be calculated as

$$P_\infty \frac{4}{3}\pi r_b^2 = nRZT_\infty \qquad [16.18]$$

where,

P_∞ = hydrostatic pressure of surrounding water

The solubility of gas in water depends highly on the temperature, ambient pressure, and salinity; and the gas bubbles may experience the variations of shape and size due to gas expansion and dissolution. The compressibility factor, Z, is described as the deviation of a real gas from the ideal gas and is expressed as

$$Z = \frac{PV}{nRT} \qquad [16.19]$$

where

P = ambient pressure

V = gas volume

$Z \equiv 1$ is used for an ideal gas

5. EXAMPLE OF AN OIL SPILL

In this section, the analysis results of the proposed algorithms for spreading and evaporation of the oil spill in the last section are compared with the limited amount of data available [17]. In the example, the oil-water

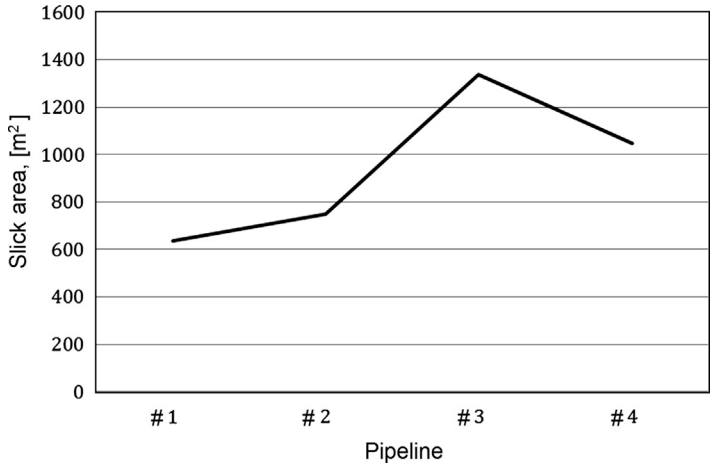

FIGURE 16.5 *Slicked Areas for Four Pipelines.*

interfacial tension is 20 mN/m. Generally, the typical range for oil-water interfacial tension is between 20 and 30 mN/m. The final water constant of emulsion is 75%. Seawater has a density of 1.025 g cm^{-3} at 25°C and a default kinematic viscosity of seawater is 0.682.

The expected leakage pipelines at four sites have been investigated. The analysis results of slick area [m^2] are plotted in Figure 16.5 for different leakage pipelines.

The slicked areas at different pipelines over 2 to 10 hours have been calculated and listed in Table 16.4. The analysis results are also plotted in Figure 16.6, which defines the relationship between the slicked area and the time over 2 to 10 hours for the four leaked pipelines. The calculated slicked area of pipeline 3 is highest, followed those of pipelines 4, 2 and 1. The higher density of oil may also affect the oil spreading to the area nearby.

Table 16.4 Variation of Slicked Area with Time in Different Pipelines

Time	Area Slick (m^2)			
(hours)	Pipe 1	Pipe 2	Pipe 3	Pipe 4
2	183.7	215.8	386.4	302.2
4	259.8	305.2	546.4	427.3
6	318.2	373.8	669.2	523.3
8	367.3	431.6	772.7	604.3
10	410.7	482.5	8643.0	675.6

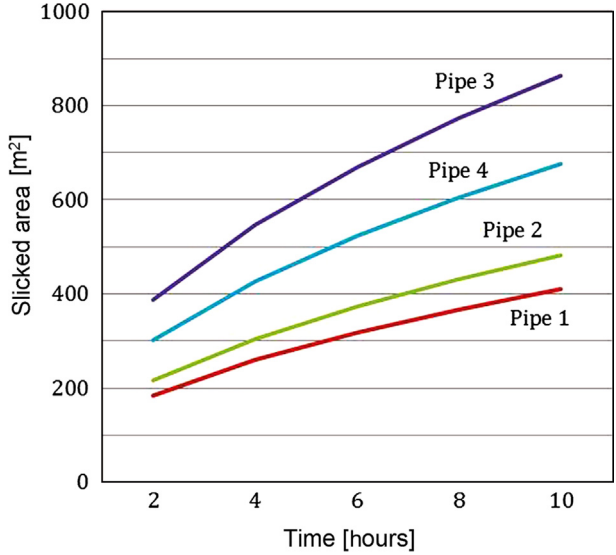

FIGURE 16.6 ***Variation of Slicked Areas with Time of Four Pipelines.*** (For color version of this figure, the reader is referred to the online version of this book.)

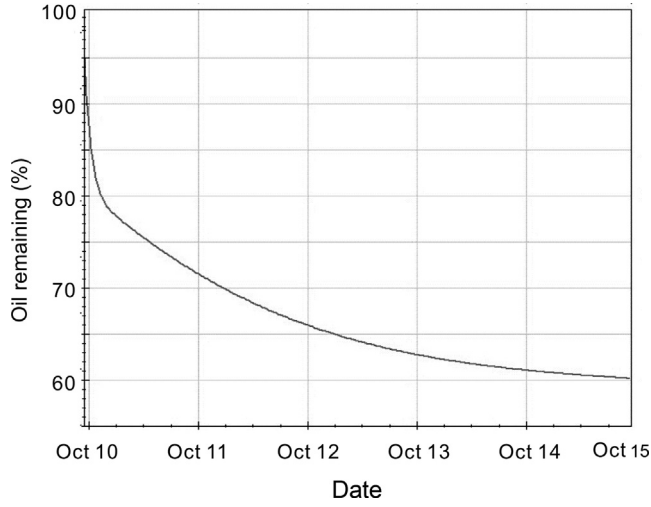

FIGURE 16.7 ***Oil Remaining at Wind Speed of 15 m/h^{-1}.***

Figure 16.7 shows the analysis results of the remaining oil after the spillage. The oil budgets for both evaporated oil and remaining oil are shown in Figure 16.8.

The models for oil and gas spills in a leakage pipeline system are developed for the analyses of oil and gas spill consequences. The oil spill

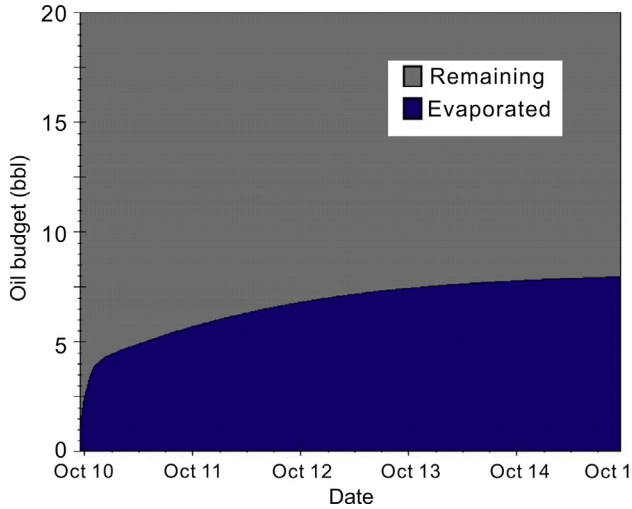

FIGURE 16.8 ***Oil Budgets for Evaporated Oil and Remaining Oil.*** (For color version of this figure, the reader is referred to the online version of this book.)

model is used to calculate the oil spill volume and oil slicked areas at four crude oil pipeline systems with a defaulted spill volume size of 50 m^3. The variations in oil budgets for evaporated and remaining oil with time are calculated based on the developed model, and these results may be used to reduce failure consequences.

REFERENCES

[1] Vinnem JE. Offshore risk assessment – Principles, modeling & applications of QRA studies. Springer series in reliability engineering. Dordrecht, The Netherlands: Kluwer Academic Publishers; 1996.
[2] Kirchkoff D, Doberstein B. Pipeline risk assessment and risk acceptance criteria in the state of Sao Paolo, Brazil. Impact Assessment and Project Appraisal, September 2006;24(3):221–34. Beech Tree Publishing, 10 Watford Close, Guildford, Surrey GU1 2EP, UK.
[3] Sebastiao P, Soares CG. Modeling the fate of oil spills at sea. Oxfor5d, UK: Elsevier Science Ltd; 1995. vol. 2.
[4] Bai Y, Bai Q. Subsea pipelines and risers. Oxford, UK: Elsevier Science Ltd; 2005.
[5] Kolluru RV. Risk assessment and management. In: Environmental strategies handbook: A guide to affective policies and practices. New York: McGraw Hill; 1994.
[6] Fay JA. The spread of oil slicks on a calm sea. pp, 53–63. New York: Plenum Press; 1969.
[7] Wang H, Campbell JR, Ditmas JD. Computer modeling of oil drift and spread in Delaware Bay. Newark, Delaware: Ocean Engineering, University of Delaware; 1975.
[8] Lehr WJ, Fraga RJ, Belen MS, Cikerge HM. A new technique to estimate initial spills size using a modified Fay-type spreading formula. Marine Pollution Bulletin 1984;15(9):326–9.

[9] Mackay D, Buist I, Mascarenhas R, Petersen S. Oil spill processes and models. Toronto, Ontario, Canada: Environmental Protection Service; 1980.
[10] Hoult DP. Oil spreading on the sea. Cambridge, MA: Massachusetts Institute of Technology; 1972.
[11] Reed M. The physical fates component of the natural resource damage assessment model system. Oil Chemical Pollution 1989;5:99–123.
[12] Mackay D, Matsugu RS. Evaporation rates of liquid hydrocarbon spills on land and water. Canadian J Chemical Engineering 1973:434–9.
[13] Benkherouf A, Allidina AY. Leak detections and location in gas pipeline. IEE Procedings 1988;135:142–8.
[14] Liu M, Zhang S, Zhou DH. Fast leak detection and location of gas pipelines based on an adaptive particle filter. International Journal of Applied Mathematics and Computer Science 2005;15:541–50.
[15] Zheng L, Yapa PD. Modeling gas dissolution in deepwater oil/gas spills. Journal of Marine Systems 2002;31(4).
[16] Zheng L, Yapa PD, Chen FH. A model for simulating deepwater oil and gas blowouts—Part 1. Theory and model formulation. Journal of Hydraulic Research 2002:41.
[17] Bai Y, Abu Bakar S, He S, Bakar Mohd Arif A. Consequences of failure estimation for oil and gas spills. Rio de Janeiro, Brazil: OMAE2012–83098; 2012.

CHAPTER 17

Environmental Impact Assessment

Contents

1. Introduction 363
2. The Motivation and Object of EIA 364
3. The EIA Process 365
   Guideline Principles of EIA 365
   Performing an EIA 366
4. Impact Analysis Methodology of Oil Spills 368
   Environmental Effects 368
   Effects on Wildlife *368*
   Effects on the Ocean *369*
   Cleanup and Recovery 369
   Theory of Oil Spills 369
   Oil Dispersion *370*
   Oil Spreading *371*
   Oil Evaporation *371*
5. Environmental Impacts 373
   Direct Impacts 374
   Secondary Impacts 374
   Indirect Impacts 374
   Cumulative Impacts 374
6. Example of Assessment 374
References 376

1. INTRODUCTION

An environmental impact assessment (EIA) is a process to predict the environmental consequences of a project's development. By evaluating the project through the EIA, we can assess the environmental effects of each plan and select the plan that will suit our needs the most. Since nature's well being is a key aspect in maintaining the world balance, the EIA has gained prominence, especially in the petroleum industry [1], for helping limit the human footprint on the natural world. Well planned developments aided by the EIA will greatly reduce risks associated with the

Subsea Pipeline Integrity and Risk Management
ISBN 978-0-12-394432-0
http://dx.doi.org/10.1016/B978-0-12-394432-0.00017-2

petroleum industry, helping to avoid disasters such as the BP oil spill that contaminated much of the Gulf of Mexico and the surrounding coastlines in 2010.

In decades, oil slicks could become one of the world's worst environmental disasters. Due to such factors as oxygen reduction and petroleum toxicity, oil spills threaten hundreds of species of fish, birds, any living beings including humans. A lot of species of wildlife have been threatened by the spills, including three basic elements: land, water, and air. Birds become easy prey, as their feathers , matted by oil, make them less able to fly away. Marine mammals lose body weight when they cannot feed due to contamination of their environment by oil.

Once an area is contaminated by oil, the whole character of the environment should be considered. While the oil spills freely, a lot of consequences can occur. One of them is the spread by wind and wave, which is discussed in this chapter. The oil spills that float on the ocean surface might evaporated through air and sun, it might also spread through water flow and combine with air and sun. The oil spills can affect the ambient environment, especially the wildlife through air and water. Therefore, this chapter emphasizes the potential environmental impacts and the consequences taken to manage the environmental risk.

2. THE MOTIVATION AND OBJECT OF EIA

The EIA is a formal process used to predict the environmental consequences of any development project [2]. It foresees the potential problems at an early stage in the project's planning and design to prevent, reduce, and compensate for any adverse impact. The EIA also attempts to give an accurate account of the total environmental risk to society arising from all phases of a process designed for the manufacturing of the product or provision of a service.

The objective of the EIA is to identify and evaluate the impacts on the environment of an initiative and alternative in the decision making process. The EIA focuses on the environmental problems that can be recognized, which need the most thorough attention. Moreover, it also identifies those unlikely to need detailed study. The main

task of the environmental impact assessment for a subsea pipelines follow:

- To identify any potential environmental impacts, issues, and concerns throughout the project life cycle.
- To describe the steps taken to manage and mitigate the environmental, social, and health risks related to the project.
- To optimize the project and avoid serious technical and economic constraints.

3. THE EIA PROCESS

Guideline Principles of EIA

The EIA consists of few processes. The EIA procedure is to decide whether the EIA is necessary in a particular case and where it is going. The EIA procedure is also intended to make the most potential benefit of EIA while keeping the process as simple and flexible and avoiding duplication of existing planning procedures.

Figure 17.1 shows the eight guideline principles that might be used in the EIA. Descriptions of each of the guideline principles follow [3]:

1. **Transparency:** All kind of assessment bases and decisions have to be accessible and open.
2. **Certainty:** The timing and the process of the project or assessment should be agreed on in advance and followed by all participants.

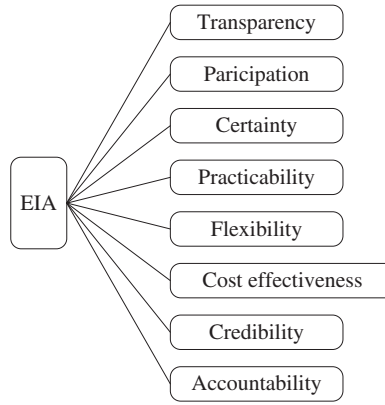

FIGURE 17.1 ***The EIA Concept and Eight Guideline Principles.*** *Source: Mackay and Matsugu [3].*

3. **Participation:** Timely and an appropriate access to the process for all sites.
4. **Practicability:** The output and information should be provided by the project or the assessment process and should be ready to use in decision making and planning.
5. **Flexibility**: The project or assessment process should be able to adapt and, at the same time, deal efficiency with any proposal and the decision making situation.
6. **Cost-effectiveness:** The project or assessment process and its outcomes will ensure environmental protection at a minimum cost to society.
7. **Credibility:** The assessment is undertaken and should be brought out with professionalism and based on the objective.
8. **Accountability:** The team leader or the decision maker is responsible to all parties and sites for the actions and decisions under the assessment process.

Performing an EIA

The important stages in the environmental impact analysis and its important keys are listed as follows:

1. **Scoping:** This is a process that helps determine the coverage or the scope itself of the EIA. Scoping also is a process that identifies the key issues of the EIA before the detailed studies. Scoping should be carried out in the earliest stage of the project planning, and it should be an open and involving practice. A scoping practice can identify the main issues quickly by the planning authorities. Figure 17.2 illustrates the methods of scoping.
2. **Baseline studies:** A baseline study is an important reference point from which to conduct the EIA. The term *baseline* refers to a collection of background information of the social, economic, and biophysical settings for the proposed project area. Baseline data are collected for two main purposes:
   - To provide a description of the status and trends of environmental factors against predicted changes that can be compared and evaluated in terms of importance.
   - To provide means of detecting actual change by monitoring.
3. **Predicting and assessing impacts:** This is to cover and consider the impact prediction, uncertainties, and comparison of alternatives for impact prediction. The prediction should be based on the available environmental baseline of the project data. The prediction can be described in quantitative terms or even in qualitative terms.

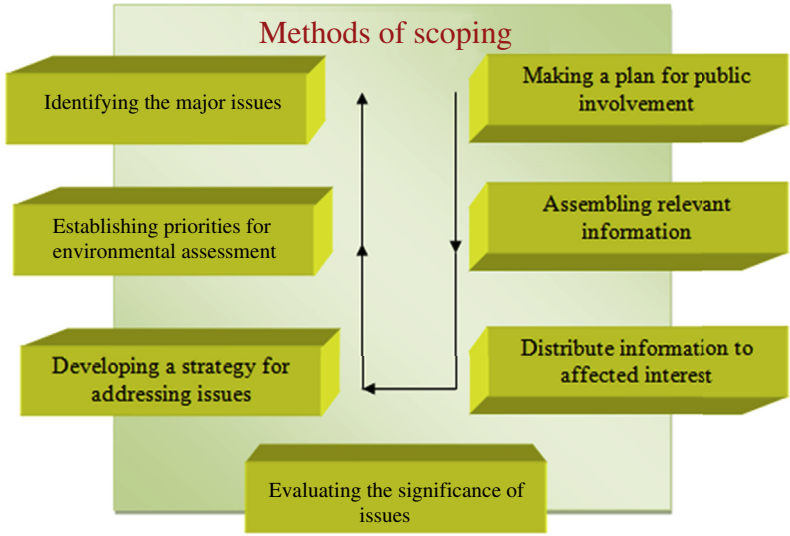

FIGURE 17.2 ***Methods of Scoping.*** (For color version of this figure, the reader is referred to the online version of this book.)

4. **Mitigation:** This briefly describes the concept, objectives, and types of mitigation measures. It also prevents adverse effects. Mitigation includes three important measures, each of them has a different meaning:
   - *Prevent:* The most effective approach toward the adverse effects. It is a better solution than trying to ballast their effect through specific mitigation measures.
   - *Reduce:* If the adverse effects cannot be prevented, the steps that should be taken are the methods to reduce the adverse effects.
   - *Offset:* When the effects cannot be prevented or reduced, they may be offset by remedial or compensatory actions.
5. **Monitoring:** This is the most important issue of an EIA. Monitoring comes along with some explanations on monitoring principles, types, and institutional aspects. It also involves checking that the development proceeds in accordance with the planning permission. There are three types of monitoring: baseline monitoring, impact monitoring, and compliance monitoring. Monitoring should be permanent and performed for a long period. Interruptions in monitoring may result in an inaccurate conclusion for the project impact.

4. IMPACT ANALYSIS METHODOLOGY OF OIL SPILLS

Impact assessment is the process to identify the future repercussion of a current action. Oil spills are really dangerous to the ambient environment. Oil spills are caused by the petroleum hydrocarbon from tankers, offshore platforms, wells, and drilling rigs or by refined petroleum products, such as diesel and gasoline. Like the previous oil spills, the BP oil spill spilled about 780,000 cubic meters, with a huge impact to the environment. All oil spills affect the environment, and wise responses are needed.

As shown in Figure 17.3, the environment impact assessments of an EIA are categorized by three types of impacts: ecological impact, social impact, and economic impact.

Environmental Effects

An oil spill contaminates the environment and destroys a life cycle not only for animals but also human beings. It affects the wildlife, even the ocean [5].

Effects on Wildlife

A lot of wildlife are covered by black, sticky oil after, an oil spill. This is very common for birds attacked by the oil spills. It is usually thought that only birds are attacked; this is not true. Other marine life also is threatened.

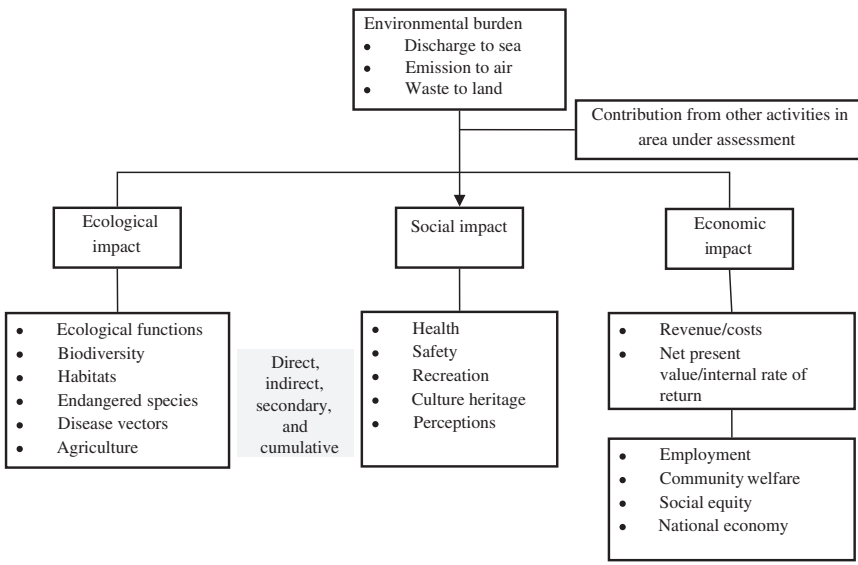

FIGURE 17.3 ***Framework of Environment Impact Assessment.*** *Source: Bai and Zukifli [4].*

When the oil spills float on the surface of the water, they can affect many marine animals and sea birds. The thick oil layer of oil spills coats the birds and wildlife bodies. As the oil becomes stickier over time, it adheres to wildlife even more.

The animals first covered with oil may be affected differently than the animals covered with oil later. The oil spill at the earlier time might be more poisonous, so the wildlife that encountered it earlier will be more poisoned. The impact of an oil spill on wildlife is also affected by where spilled oil reaches.

Effects on the Ocean

The oil spills not only wastes natural resources but also waste the ocean from many sources. It could be from an accidental leak or the results of chronic and careless habits in using oil and oil products. When oil starts to mix up with water, the composition becomes mousse, which is a sticky substance. Half of the oil waste may sink with suspended particulates, and the remainder eventually congeals into sticky tar balls.

Cleanup and Recovery

Cleanup and recovery from an oil spill or leakage is difficult and depends on many factors. The techniques used to clean up an oil spill depend on characteristics of the oil and the type of environment involved. Pollution-control measures include containment and removal of the oil.

The removal of the oil involves dispersing it into smaller droplets to limit immediate surface and wildlife damage, biodegradation, and normal weathering processes. Individuals of large-sized wildlife species are sometimes rescued and cleaned, but micro-sized species are usually ignored.

The countermeasures of an oil spill to clean up and remove the oil are selected and applied on the basis of many interrelated factors, including ecological protection, socioeconomic effects, and health risk. It is important to have contingency plans in place in order to deploy pollution control personnel and equipment efficiently.

Theory of Oil Spills

The environmental burden usually consists of the discharges to the sea, emission to the air, and waste to the land. Therefore, the calculations of oil spills in this chapter include the dispersion of oil into water, oil spreadable, and oil evaporation through the air and sun, which are illustrated in Figure 17.4.

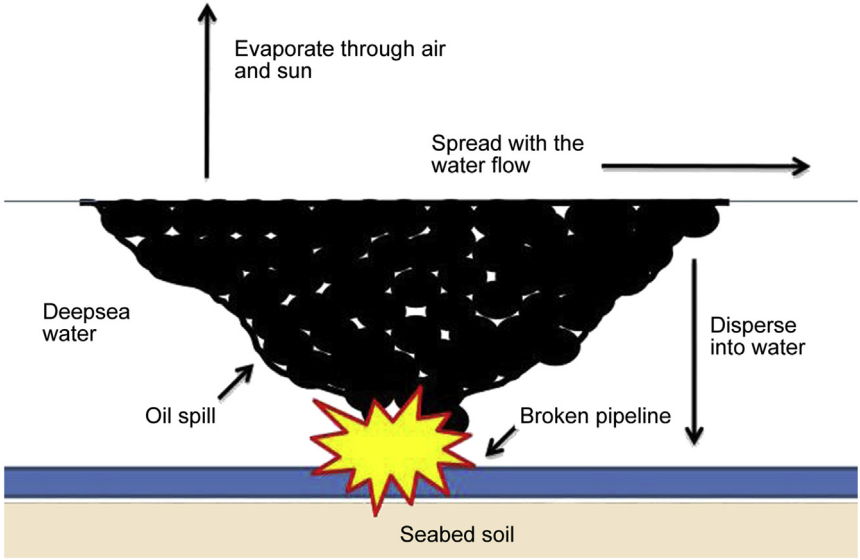

FIGURE 17.4 ***Oil Spreading, Dispersion, and Evaporation into Water.*** (For color version of this figure, the reader is referred to the online version of this book.)

Oil Dispersion

The normal oil spill is of crude oil, which forms small droplets of oil that merge in the water column after spillage. The natural dispersion can inspire the environment to remove oil from the sea surface, because the rate of natural dispersion has a huge impact on the life of oil slicking on the sea surface. Reed [6] used an approach based on the formulation by Mackay and Matsugu [3] to compute the dispersion of surface oil into the water column. The lost fraction of sea surface oil per hour is calculated in the following equation:

$$D = D_a D_b \tag{17.1}$$

where

$$D_{\mathrm{a}} = 0.11(u + 1)^2 \tag{17.2}$$

$$D_{\mathrm{b}} = \left(1 + 50\mu^{1/2}\delta s_{\mathrm{t}}\right)^{-1} \tag{17.3}$$

D = fraction sea surface of oil spill dispersion
D_{a} = fraction of sea surface dispersed per hour

D_b = fraction of dispersed oil not returning to the slick
u = wind speed
μ = viscosity
δ = slick-thicknes
s_t = oil-water interfacial tension.

Oil Spreading

The oil release is a continuous, time-varying release, in which the release rate typically decreases with time, especially for gravity spreading. This type failure comes from punctures in pipelines.

Shaw and Briscoe (1978) [1] wrote equations for the increase in area on land and water of unconfined spills. Equation [17.4] is suitable for the gravitational phase of spreading for instantaneous spills, while Eq. [17.5] shows the continuous spills in water. For Instantaneous spills,

$$r = \left[\left(\frac{8g(\rho_w - \rho_1) V_0}{\pi \rho_w} \right)^{1/2} t + r_0^2 \right]^{1/2} \quad [17.4]$$

For continuous spills,

$$r = \sqrt{\frac{2}{3}} \left(\frac{8g(\rho_w - \rho_1) B_1}{\pi \rho_w} \right)^{1/4} t^{3/4} \quad [17.5]$$

where

r = pool radius
g = acceleration due to gravity
V_0 = volume of instantaneous spill
t = time after initial spill
r_0 = initial radius of contained liquid
B_1 = continuous liquid spill rate
ρ_w = density of water
ρ_1 = density of spilled liquid, which is less than the density of water

Equations [17.4] and [17.5] ignore viscosity and surface tension effects and expect that the spreadable of pool is due to the conversion of gravitational potential energy into the kinetic energy.

Oil Evaporation

When the normal boiling point of a liquid is below the environment temperature, the fluid pours out faster and more easily on the ground,

and it transforms into a large, cold liquid pool. The allowing gas results in a cold, dense gas cloud that hovers over the boiling liquid pool. Any heat transfer into the liquid pool evaporates to produce more gas, at a rate that depends on its input of heat transfer rate and heat of vaporization of the liquid.

Most oil spills have been controlled by crude oil viscosity. Generally, the evaporation rate for crude oil may be controlled by meteorological variables. Since the temperature of oil is very important to the variable, to calculate the evaporative emission rate, it is very important that the heat balance of a liquid pool be known. The variables and parameters for oil temperature and heat balance can be used to determine the evaporation rate of oil spills and the nonboiling liquid pools. Figure 17.5 illustrates the general heat balance of a liquid spill, as described by Shaw and Briscoe [1].

Fleisher [7] illustrates how to estimate the evaporation rate for single component liquid, which also is used in the Shell spills model:

$$Q_a = \frac{k_g A_p p_s M}{R T_a} \qquad [17.6]$$

where

T_a = ambient temperature
Q_a = evaporative emission rate to the air
A_p = pool area
p_s = vapor pressure of the compound
M = molecular weight
R = gas constant
k_g = mass transfer coefficient

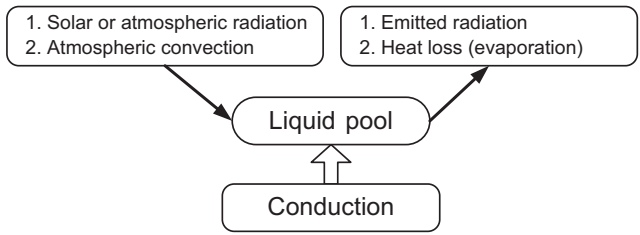

FIGURE 17.5 ***Heat Budget of an Evaporating Pool.*** *Source: Shaw and Briscoe [1].*

To calculate the mass transfer coefficient, k_g, in Eq. [17.6], a general relationship of chemical engineering approach by Perry et al. [8] is used:

$$k_g = \frac{N_{Sh} D_m}{d_p} \quad [17.7]$$

where

D_m = molecular diffusion

d_p = pool diameter

and the Sherwood number, N_{Sh}, and the Schmidt number, N_{Sc}, are expressed as follows:

$$N_{Sh} = 0.037 N_{Sc}^{1/3} \left[N_{Re}^{0.8} - 15,200 \right], \qquad N_{Re} > 320,000 \quad [17.8]$$

$$N_{Sh} = 0.664 N_{Sc}^{1/3} N_{Re}^{1/2}, \qquad N_{Re} < 320,000 \quad [17.9]$$

$$N_{Sc} = \frac{\nu}{D_m} \quad [17.10]$$

the Reynolds number can be calculated from the formula that follows:

$$N_{Re} = \frac{u d_p}{\nu} \quad [17.11]$$

where

ν = kinematic viscosity

u = ambient wind speed

5. ENVIRONMENTAL IMPACTS

Subsea pipelines, offshore oil drilling rigs, coastal storage facilities, and refineries all have the potential to accidentally release crude oil into water**.** All these are considered when the environment is affected [7]. *Environmental impact* is defined as any change to the environment, whether adverse or beneficial, wholly or partially resulting from an organization's activities, products, or services. An impact may be sudden and acute but it may also occur indirectly. The gradual buildup of a pollutant may cause a wider impact, experienced over a long period of time, perhaps through human generations. The environmental impacts are classified in the following subsections.

Direct Impacts

Direct impacts are associated with the actual installation of a structure, chemical spillage, or emission of a gas. They are acute impacts, short lived, sudden, and significant.

Secondary Impacts

Secondary impacts arise as a consequence of direct impacts. These are consequences of the direct impact, such as the decrease of a species, as a result of high sudden mortality, on the ecosystem.

Indirect Impacts

Indirect impacts are the effects on environmental quality and public opinion arising from related activities and may be associated with development outside the physical extent of the field development.

Cumulative Impacts

These are the resultant impacts from a number of different sources within a particular development or the impacts arising from more than one development in a region. These are chronic effects, which result from a continual discharge or emission, buildup over time, and resulting in progressive damage on environmental quality.

6. EXAMPLE OF ASSESSMENT

Back to the oil spills, all the equations are used especially to calculate the spreadable oil and its evaporation. The continuous liquid spill rate can be calculated from a revision of Eq. [17.5]:

$$B_1 = \frac{9}{32}\rho_w \left[\frac{\pi r^4}{gt^3}\left(\frac{1}{\rho_w - \rho_1}\right)\right] \qquad [17.12]$$

Table 17.1 lists the input parameters for the oil spill evaporation and spread analysis.

The continuous liquid spill rate of 2.19×10^{-5} [m^3s^{-1}] is calculated with Eq. [17.12] using the input parameters listed in Table 17.1. The oil spills evaporation is calculated by using Eq. [17.6]. To find the mass transfer coefficient of the evaporative emission rate into the air, the Schmidt number used is based on Eq. [17.8], because the pool diameter is lower than assumed based on the laminar to turbulent transition that occurs at Reynolds number of 320,000.

Table 17.1 Parameters for EIA Analysis

Parameter	Symbol	Value and Unit
Molecular weight	M	58.1 $kgmole^{-1}$
Pool area	A_p	331.1 m^2
Vapor pressure of the compound	p_s	37,932 pa
Gas constant	R	8.31 $Jmole^{-1}K^{-1}$
Ambient environment temperature	T_a	303 K
Gravity	g	9.8 ms^{-2}
Initial plume density	ρ_{p0}	2.34 kgm^{-3}
Ambient or environmental density	ρ_a	1.16 kgm^{-3}
Initial volume flow rate	V_{c0}	0.305 m^3s^{-1}
Initial volume	V_{i0}	16.48 m^3
Friction velocity	u^*	0.344 ms^{-1}
Initial cloud width	D_0	20.54 m
Ambient wind speed	u	15 ms^{-1}
Pool diameter	d_p	20.54 m
Kinematic viscosity	ν	1.10×10^{-5} m^2s^{-1}
Molecular diffusion	D_m	1.23×10^{-5} m^2s^{-1}
Volume of instant spills	V_0	780,000 m^3
Time after initial spill	t	600s
Pool radius	r	10.27 m
Density of water	ρ_w	1,000 kgm^{-3}
Density of spilled liquid	ρ_1	788 kgm^{-3}
Viscosity	μ	8.668 cP
Slick thickness	δ	300 cm
Oil-liquid surface tension	s_t	107.76 dyn/cm

Since the mass transfer coefficient, k_g, is 1.905×10^{-2}, the evaporative emission rate to the air, Q_a, is 0.00553 [kgs^{-1}].

Equations [17.1] to [17.3] are used to calculate the fraction of sea surface oil spills dispersion:

$$D = D_a D_b = 2.1 \times 10^{-7}$$

When the wind speed is 15 ms^{-1}, the software ADIOS 2 gives the oil evaporation, oil dispersion, and the oil remaining.

Figure 17.6 shows the variations of oil budget with time from an analysis assessment. The dark area shows the evaporated oil, while the unshaded area shows the remaining oil, and the lightly shaded area represents the oil dispersion from the total amount spilled of 780,000 m^3 or 500,000 barrels. From the results, we can see both the oil dispersion and the oil remaining carry about 30% each while the rest or 40% is the oil remaining.

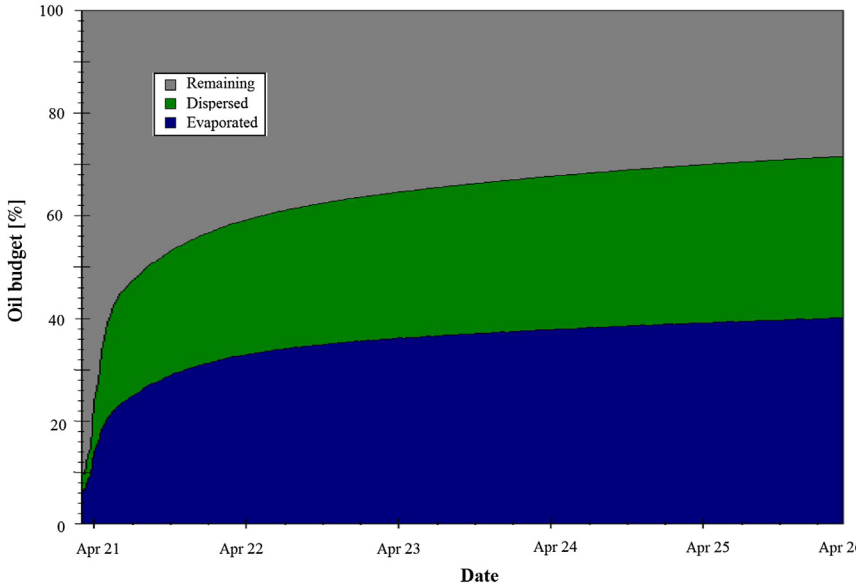

FIGURE 17.6 ***Variations of Oil Budget with Time.*** (For color version of this figure, the reader is referred to the online version of this book.)

REFERENCES

[1] Shaw P, Briscoe F. Evaporation from spills of hazardous liquids on land and water. SRD-R-100. Warrington, UK: UKAEA; 1978.
[2] DETR and The National Assembly for Wales. Environmental impact assessment: A guide to procedures. London: Thomas Telford Publishing; 2000.
[3] Mackay D, Matsugu RS. Evaporation rates of liquid hydrocarbon spills on land and water. Can J Chem 1973.
[4] Bai Y, Zukifli ZA. Environmental impact assessment for offshore pipelines. Rio de Janeiro, Brazil: OMAE; 2012. 2012–83100.
[5] Lantzy RJ, et al. Guidelines for use of vapor clouds dispersion models. 2nd ed. New York: American Institute of Chemical Engineers,; 1996.
[6] Reed M. The physical fates component of the natural resources damage assessment model system. Oil Chemical Pollution 1989;5(2–3):99–123.
[7] Fleischer MT. SPILLS, An evaporation/air dispersion model for chemical spills on land. Houston, TX: Shell Development Company; 1980.
[8] Perry RH, Green DW, Maloney JO. In: Perry's chemical engineers' handbook. New York: McGraw-Hill Book Company; 1984.

CHAPTER 18

Oil Spill Response Plan

Contents

1. Introduction 377
2. Oil Spill Consequences 378
3. Restoration Planning 379
   Compensatory Restoration 382
4. Affected Environment 383
   Effects on Wildlife 384
   Effects on Ocean 385
5. Cleanup Cost and Cleanup Recovery 387
   Control Factors of Cleanup Cost 388
      Location *388*
      Shoreline Oiling *388*
      Effect on Cost of Oil Type *389*
      Spill Size Cost Correlation *389*
      Cost Implication of Cleanup Strategy *389*
   Estimation of Cleanup Cost 389
References 390

1. INTRODUCTION

Pipeline networks for the transportation of crude oil and gas can be found in many places of the world. However, in most developing countries, there is a lack of proper standards and guidelines for the design, construction, and operation of these pipelines and inadequate procedures and regulations for addressing environmental concerns related to oil spills. Furthermore, the poor financial situation in these countries prevents proper maintenance of the pipeline systems and may exacerbate the difficulty to maintain proper contingency facilities to fight oil spills when they occur. Oil spills caused by pipeline ruptures or leakage in these areas are not addressed promptly and efficiently. As a result, they often create major environmental disasters. A ruptured pipeline has the potential to cause serious environmental damage, since most of the products being transported are environmentally hazardous if spilled.

To reduce the frequency of oil spills and minimize their consequences, it is necessary to get the approximate regulations, standards, and risk

Subsea Pipeline Integrity and Risk Management
ISBN 978-0-12-394432-0
http://dx.doi.org/10.1016/B978-0-12-394432-0.00018-4

management procedures and experience in the operation of pipelines in industrialized regions [1]. Although pipeline oil spills cannot be completely eliminated, their frequency and severity can be reduced by using the proper standards, regulations, and pipeline risk management.

Establishment of appropriate and effective methods for better management of the pipeline infrastructure could be facilitated by a thorough understanding of the following items:

- Details of pipeline oil spills.
- Cleanup costs.
- Prevention measures.
- Regulations and guidelines addressing environmental aspects.
- Oil spills emergency response plan.

Government agencies and oil transporters share a keen interest in being able to anticipate an oil spill response plan for cleaning purposes. While the oil spill cleanup depends on a variety of factors, most notably location, type of oil, spill size, and cleanup strategy, all the factors make it difficult to develop a universal per-unit cost. This chapter evaluates the basics of oil spills, restoration planning, a proposed restoration project, environment effects, cleanup costs, and cleanup recovery.

2. OIL SPILL CONSEQUENCES

The basic consequences of oil spills include the spreading of oil through water, the spreading of evaporated oil through the air, and the dissolving of oil into seawater. When oil is spilled freely on seawater, several consequences may come about due to the spillage. The oil may be spread by wind and waves, and the remaining oil that floats on the seawater might be evaporated by the sun and wind. In some cases, a certain amount of oil may spread through the water and be dissolved into it naturally. Figure 18.1 illustrates the oil spill consequences with a combination of oil spreading, oil evaporating, and oil dissolution through the seawater.

The environment surrounding the oil spill determines the algorithms used in each case since the fate of oil differs whether the spills occurs at open sea or close to a coastal zone. Table 18.1 summarizes the dominant processes after an oil leakage occurs, including different stages of oil spill and importance, dominant time, dependency, and ability [2]. The qualitative scale of understanding and ability to write descriptive equations, as presented by Mackay & McAuliffe is also included.

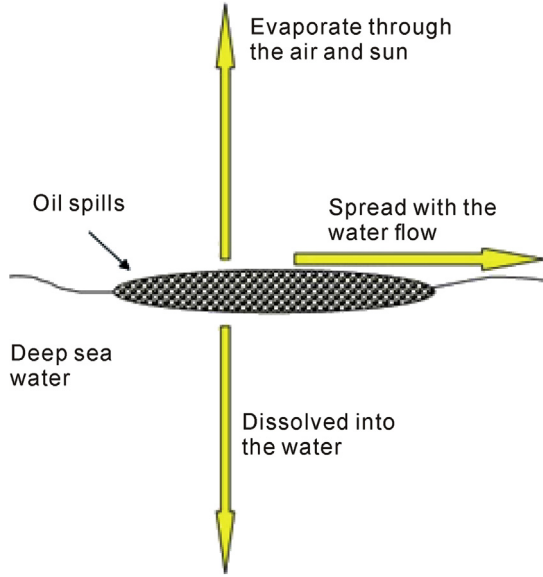

FIGURE 18.1 ***Oil Spill Consequences.*** (For color version of this figure, the reader is referred to the online version of this book.)

3. RESTORATION PLANNING

Oil spills may cause serious problems, especially to the ambient environment. It is hard to recover and even takes years to fully recover if it has happened. One of the processes to recover an oil spills is restoration [4]. The restoration has its own criteria, which evaluate alternatives to achieve the restoration requirements. Following is a list of the general criteria of evaluation:

- **Effectiveness:**
  - Primary restoration is used to extend each alternative that can return the injured natural resources to the baseline.
  - Compensatory restoration recovers the environment for the interim lost services provided by the resources.
- **Protectiveness:** Extends the implementation of alternatives and gets rid of the additional injury to the environment.
- **Technical feasibility:** The level of uncertainty in the success of each alternative.
- **Cross benefits:** The alternative benefits to more than one resource with or without services.
- **Collateral effects:** Concurrent effects of each alternative on the environment.

Table 18.1 Summary of Dominant Oil Spills Processes

Process	Importance	Dominant Time	Dependency	Ability*
Spreading	Area extent		Gravity, surface tension, inertia, viscosity, shear diffusion	F/F
Drifting	Passage over larger area/volumes of water		Wind and water currents	G/G
Evaporation	Loss of 20–40% mass, density and viscosity increase	First few hours	Spill area, slick thickness, pressure of oil composition and temperature, mass transfer co-efficient	E/G
Dissolution	Loss of ~1% mass, may be important from a toxicological viewpoint	Shortly after spill	Dissolution mass transfer coefficient, solubility	E/F
Dispersion	From 10–15 $\mu g\, l^{-1}$ up to 1–2 $mg\, l^{-1}$ in the top 10 m water column		Sea state (wind shear and breaking waves)	P/VP
Emulsification	Uptake of up to 80% water into oil, viscosity and volume increases, density becomes similar to seawater		Turbulence, temperature and oil composition (presence of constituents that favor mousse formation)	P/VP

Photolysis	Slow formation of oxygenated polar water soluble species which affect spreading and mousse formation	May become noticeable after a week or more	Presence of sunlight or clouds, interrupted by night	F/VP
Sedimentation	Rarely expected through weathering alone in cold water, temporary submergence in the top meters may occur in consequence of high seas and overwashing by waves		Increased density as a result of weathering process, association with suspended particulate matter or fecal pellets	F/P
Biodegradation	May be the ultimate fate of much of the dissolved and dispersed oil	After 3 months and may persist for years	Hydrocarbon dilution and degradability, water contents of nutrient and O_2, location of the spill	G/P

* The qualitative scale presented by Mackay and McAuliffe [3]: F = fair; G = good; E = excellent; P = poor; VP = very poor.
Source: Sebaqstiao and Soares [2].

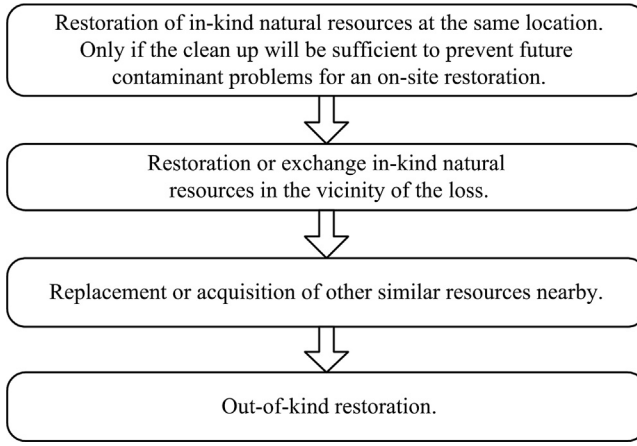

FIGURE 18.2 ***Flowchart of Restoration Projects.***

- **Consistency:** Moves with policies and compliance with federal, state, and local law.
- **Cost considerations.**

The primary goal of restorations is to compensate for natural resources and hospitality that were lost or adversely affected by the release of hazardous substances. Figure 18.2 shows a flowchart of restoration projects. The flowchart of restoration includes returning the injured resource to its prior condition as well as the acquisition of other resources to compensate for those that were lost.

The term *in-kind* in the flowchart means that the work focuses on habitats and species comparable to those that were hurt or injured, destroyed, or lost. Further, the term *out-of-kind* means that the work focuses on resources different from those that were hurt or injured, destroyed, or lost.

Compensatory Restoration

The restoration has a lot of alternatives to consider for replacing or acquiring the same ecological resources and lost services that are not restored. Restoring the equivalent or ecologically similar habitat at a site near the injured wetland can occur in compensation for the loss of ecological services.

These restoration alternatives can be identified by the desired characteristics for the potential projects, such as

1. Habitat restored must be similar to the habitat affected and provide similar services.

2. Project must be in the same watershed as the affected wetland.
3. Project must provide long-term benefits to resources that are known as potentially affected, including fish and wildlife.

The factors that can affect the success of the project are such ones as the physical and logistic factors or the ability of the project to compensate for the natural resources and service that were lost. A restoration that could not be protected would be disfavored over one when future land use is restricted. The following list has five potential restoration alternatives [5]:

1. **No action:** This restoration is an alternative to all others that are compared in the environmental assessment. This means that no restoration, no rehabilitation, no replacement, and no acquisition action would occur. This alternative gives the minimum cost because no action is taken, but it is potentially loss recovery for sure.
2. **Restoration of "in-kind" natural resources at the same location:** Restoration of natural resources whether "in kind" or "out of kind" cannot be implemented or is potentially less viable than restoration because of a lack of intertidal habitat and growth.
3. **Restoration or replacement of "in-kind" natural resources in the vicinity of the loss.**
4. **Replacement or acquisition of similar resources within estuary watershed.**
5. **Restoration or replacement of "out-of-kind" natural resources in the watershed.**

All these alternatives can be evaluated with the environmental consequences. The relevant considerations are listed as

- Technical feasibility.
- Relationship between the expected cost of the proposed actions and the expected benefits.
- Results of any actual or planned response actions.
- Potential for extra injury from the proposed actions (long-term and indirect effects).
- Natural recovery period of the injured resources.
- Ability of the resources to recovery.
- Potential effects of the action on human health and safety.

4. AFFECTED ENVIRONMENT

Oil spills are a serious matter because they can result in both immediate and long-term environmental damage; the damage from some oil spills can even

last for decades after the spill. The environment is really in a dangerous situation if it is contaminated. Deepwater oil spills usually affect the marine undersea life, marine mammals, and even wildlife habitats and breeding grounds. They also may affect human beings who live on land and use water almost every minute. This makes water one of the most important natural resources [6].

Effects on Wildlife

Too much wildlife is covered with black and sticky oil after spills, which usually affects birds and other marine life living in and around the sea. The thick, sticky layer of oil spill coats the birds and wildlife's bodies; and the condition becomes worse if the weather is humid, which causes the oil to become stickier over time and adhere to the wildlife even more.

The deadly damage can take several forms. The oil sometimes clogs the animals respiratory tract, especially, whales and dolphins, making it impossible for the animals to breathe properly and disrupting their ability to communicate with each other. Some fish are attracted to oil because it looks like food to them.

Crude and bunker oils usually cause a lot of problems, because this kind of oil sticks to bird's feathers and affects the marine life. Some possible problems follow:

- Birds become dehydrated and starve due to the oily water that is undrinkable, and they give up on diving and swimming to look for food.
- Hypothermia in birds and fur seal pups is caused by destroying the insulation and waterproofing properties of their fur and feathers.
- Marine mammals and birds become easy prey because the oil sticks their flippers and wings to their bodies, making it hard for them to escape predators.
- Oil causes damage to the inside of animals and birds' bodies, such as ulcers or bleeding in the stomach.

Not only the animals but humans and other living beings are also affected. The oil usually not only sticks to birds and other animals, it is poisonous. The possible problems that ingested oil can cause follow:

- Making the animal too ill to breed.
- Poisoning the animal's food chain.
- Damage to marine mammals that can cause irritation, ulceration of skin, mouth, or nasal cavities.
- Damage to marine mammal's immune system; bacterial or fungal infections.

FIGURE 18.3 ***Oil Spill's Impact on Wildlife.*** (For color version of this figure, the reader is referred to the online version of this book.)

- Decrease in egg shell thickness.
- Poisoning young through the mother.

The oil spill's effects on wildlife also occurs wherever the spilled oil reaches. Figure 18.3 shows some of the examples of how badly the oil spill affects the wildlife and the environment.

Effects on Ocean

The initial spread of oil spills or leakage in water depends on the oil's relative and composition. The oil slick formed remains cohesive or breaks up in the case of rough seas. Oil spills usually have three consequences. If the oil spill reaches the shoreline or coast, it interacts with sediments, which may cause erosion as well as contamination. When the oil spill starts to mix with water, the composition becomes mousse. This composition is a sticky substance that clings even more to whatever it comes in contact with.

Oil waste or leakage from offshore may occur during various stages of well drilling, workover, and repair operations. These stages may happen while oil is being produced from the offshore wells, handled, and provisionally stored. This occurs either when the oil is being transported offshore by subsea flowline or tanker. The amount of oil spilled or leaked during offshore production operations is relatively nonnotable. The oil leak from offshore drilling operations may come from disposal of oil-based drilling fluid wastes, deck runoff water, pipeline leaks, or well failures or blowouts. Offshore production waste can also pollute the ocean, as can deck runoff water, leaking storage tanks, pipeline leaks, and the wells themselves. Oil spills from ships and tankers include the transportation fuel

used by the vessels themselves or their cargos. Whether the oils leak and spread all over the ocean or on the surface depends on the relative density and composition.

The oil slick formed may remain cohesive or break up in the case of rough seas. Waves, water currents, and wind, force the oil slick to drift over large areas, affecting the open ocean, coastal areas, and marine and terrestrial habitats in the path of the drift. Oil leaks that contain volatile organic compounds partially evaporates, losing a quarter of its mass and becoming denser and more viscous. Only a small percentage of oil dissolves in water. The oil residue also can disperse almost invisibly in the water or form a thick mousse with the water. Half of the oil waste may sink with suspended particulate matter, and the remainder eventually congeals into sticky tar balls. Meanwhile, oil waste weathers and disintegrates by means of photolysis and the decomposition due to microorganisms and biodegradation. The rate of biodegradation depends on the availability of oxygen, nutrients, microorganisms, and temperature. Figure 18.4 shows the affected ocean caused by the oil spills.

FIGURE 18.4 ***Affected Coast after Oil Spills Disaster.*** (For color version of this figure, the reader is referred to the online version of this book.)

5. CLEANUP COST AND CLEANUP RECOVERY

The costs associated with cleaning up an oil spill are strongly influenced by the circumstances surrounding the spill, including the type of product spilled, the location and timing of the spilling, sensitive areas affected, liability limits in place, and cleanup strategy. The most important factors determining a per-unit amount (either per gallon or per ton) cost are location, type of oil, and possibly total spill amount. The complex interrelationships of these factors and the manner in which they are influenced by other factors are shown in Figure 18.5.

The following are the main methods used to solve the problem of oil spills:

- Leave the oil alone to let it break down by natural means. If there is no possibility to clean up the oil polluting coastal regions or marine industries, the best method is to leave the oil to disperse by natural means. A combination of wind, sunlight, current, and wave action may rapidly disperse and evaporate most oils. However, light oils may disperse faster than heavy oils.

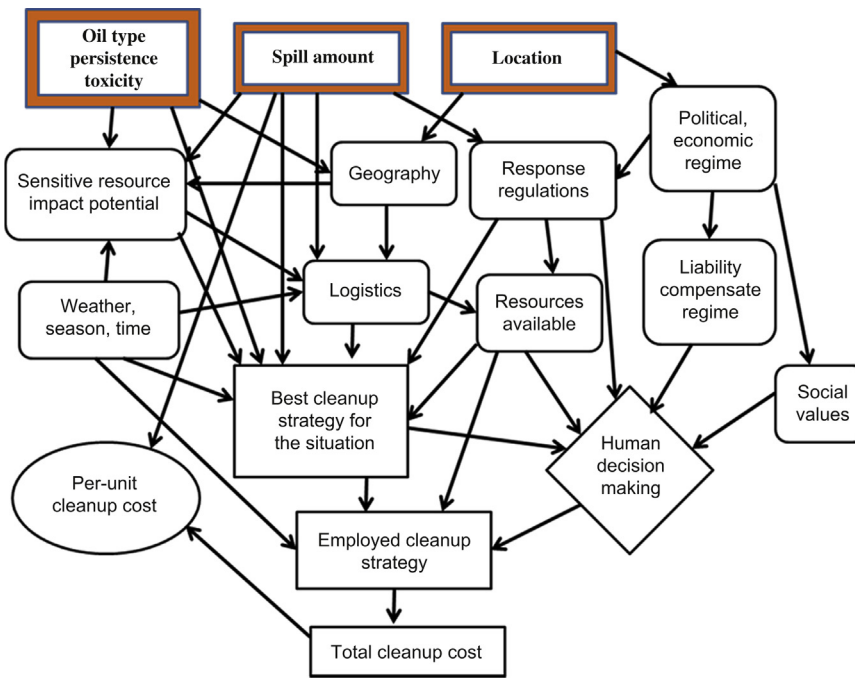

FIGURE 18.5 ***Factors determining Per Unit Oil Spills Cleanup Costs.*** *Source: Etkin [7].* (For color version of this figure, the reader is referred to the online version of this book.)

- Control the oil spill with booms and collect it from the water surface using skimmer equipment. Spilled oil floats on water and initially forms a slick that is a few millimeters thick. Various types of booms are used either to surround or isolate a slick or to block the passage of a slick from vulnerable areas, such as the intake of a desalination plant, fish-farm pens, or other sensitive locations.
- Use dispersants to break up the oil and speed its natural biodegradation. Dispersants act by reducing the surface tension that stops oil and water from mixing.
- Introduce biological agents to the spill to hasten biodegradation. Most of the oil components washed up along a shoreline can be broken down by bacteria and other microorganisms into a harmless substance. This action is called *biodegradation*.

Control Factors of Cleanup Cost

Some control factors that may affect the cleanup cost of oil spill follow:

- Location of spillage and regional cost differences.
- Shoreline of oiling.
- Cost impact of oil type.
- Spill size for cost correlation.
- Cost implications of cleanup and effectiveness of cleanup.

Location

The most important determinant of cleanup costs is the location, which is a complex factor involving geographic, political, and legal considerations. Oil spills that occur near shore or in ports are significantly more expensive than spills in offshore areas, due to the higher probability of shoreline impact.

Another factor in determining the impact and oil response costs for an oil spill is the region and nation. Generally, spills in more highly developed nations with high labor costs, complex regulations for spill response, and high standards for environmental protection rank among the most expensive.

Shoreline Oiling

The proximity of the oil spill to a shoreline is one of the most important factors affecting the cleanup costs. When an oil spills occurs, the most important geographical factors to consider are

- Did the oil spill in a location where it is likely to hit any shoreline? Is the oil spill close enough to shore or under an influence that makes it likely the oil will affect the shoreline?

- What type of shoreline is involved?
- How close is the shoreline to inhabited areas?

Effect on Cost of Oil Type

The type of oil spilled significantly affects the cleanup cost and determines the direct environmental impact of the spill incident. Toxicity factors heavily in a gasoline or lighter refined fuel spills, due to the higher proportion of lighter end hydrocarbon components. The heavier oils and crudes presents the greatest challenge to cleanup crews. Diesel fuel and light crude oil are less expensive to clean up than heavy crude or heavier fuel oil. [7].

Spill Size Cost Correlation

An analysis of 96 oil spills (Etkin [8] and Monnier [9]) showed that the cleanup cost per tonne was significantly negatively correlated with spill size. Monnier found that the spills under 10 tonnes had average per-unit cleanup costs of $345,000/tonne, whereas the spills of over 50 tonnes had costs of $12,000/tonne. Smaller spills are more expensive to clean up than larger spills because of the costs associated with the cleanup response, mobilizing the equipment and personnel, as well as bringing in the experts to evaluate the spill response and damages.

Cost Implication of Cleanup Strategy

The selection of cleanup strategies and its decision process can significantly affect the cleanup cost. The cleanup costs are mostly directly correlated with the spill's impact and shoreline impact. The amount of money used on an effective cleanup can significantly reduce later natural resource and property damage claims.

When oil spills near a potentially sensitive coastline, the most cost-effective approach to a cleanup operation is to invest as much equipment, personnel, and energy into keeping the oil away from the shoreline or sensitive coastline.

Estimation of Cleanup Cost

The following equation and methodology integrate all factors into a single algorithm:

$$C_{\mathrm{ui}} = C_{\mathrm{li}} t_{\mathrm{i}} o_{\mathrm{i}} m_{\mathrm{i}} s_{\mathrm{i}}$$

$$C_{\mathrm{li}} = r_{\mathrm{i}} l_{\mathrm{i}} C_{\mathrm{n}}$$

$$C_{\mathrm{ei}} = C_{\mathrm{ui}} A_{\mathrm{i}} \qquad [18.1]$$

where

C_{ui} = response cost per unit for scenario i
C_{li} = cost per unit spilled for scenario i
C_n = general cost per unit spilled in nation n
C_{ei} = estimated total response cost for scenario i
t_i = oil type modifier factor for scenario i
o_i = shoreline oiling modifier factor for scenario i
m_i = cleanup methodology modifier factor for scenario i
s_i = spill size modifier factor for scenario i
r_i = regional location modifier factor for scenario i
l_i = local location modifier for scenario i
A_i = specified spill amount for scenario i

This cost estimation model integrates the cost data on the most important cost factors, such as location, shoreline oiling, cleanup strategy, and spill amount. However, the circumstances surrounding a spill incident are complex and unique. One universal per-unit cost is meaningless in the face of these complex factors.

REFERENCES

[1] API. Fate of spilled oil in marine waters. Washington, DC: American Petroleum Institute; 1999. Publication number 4691.
[2] Sebastiao P, Soares CG. Modeling the fate of oil spills at sea. Spill Science and Technology Bulletin 1995;2(2/3):121–31.
[3] Mackay D, McAuliffe CD. Fate of hydrocarbons at sea. Oil and Chemical Pollution 1988;5:1–20.
[4] Ralof J J. Valdez spill leaves lasting impacts. Sci News February 1995;102(143).
[5] Carl MG, et al. Persistence of oiling in mussel beds after the Exxon Valdez oil spill. Mar Environ Res 2011;51(2):167–90.
[6] National Oceanic and Atmospheric Administration, US. Fish and Wildlife Service, New York State Department of Environmental Conservation. Final restoration plan and environmental assessment applied environmental services superfund site, hazardous substances release. http://www.darrp.noaa.gov/northeast/shorerealty/; 2002.
[7] Etkin DS. Estimating cleanup costs for oil spills. International Oil Spill Conference 1999.
[8] Etkin DS. Worldwide analysis of marine oil spills cleanup cost factors. Arctic and Marine Oil Spill Program Technical Seminar June 2000.
[9] Monnier I. The costs of oil spills after tanker incidents. DNV Research A/S. Høvik, Norway: Det Norske Veritas; 1994.

INDEX

Note: Page references followed by "f" indicate figure, "t" indicate table, and by "b" indicate boxes.

A

Acceptance criteria, 173–176
  for environmental risk, 174–175, 175t
  for financial risk, 175–176
  general information on, 173
  for individual risk, 174
  for societal risk, 174, 174f
Accidental damage, as flexible pipe failure mechanism, 114–115
Acoustic emission, 118t, 121, 133–134
Acoustic pigs, 86
Airborne dispersion, 194
Aluminum polyethylene laminate (APL), 161
Amorphous fluorinated polymer (CYTOP), 159
Anode sledges, CP and, 91–92
Anti-Stokes light, 152–153
API 2A-LRFD safety index, 296–298
APL, *see* Aluminum polyethylene laminate
ATMOS Pipe, 138–141, 140f
AutoReaGas, 295
Axial force, moment capacity effect of, 34f, 35
Axial stress, maximum allowable, 63

B

B31G criterion, 19–21, 298
  evaluation of, 21
  maximum allowable defect length and depth in, 20
  maximum allowable design pressure in, 19
  problems with, 21
  safe maximum pressure level in, 20–21
  for spiral corrosion, 22, 22f
Baseline studies, in EIA, 366
Bathtub curve, of failure rate, 272–273, 273f
Bayes method, for MTRA PoF assessment, 337–338
BCA, *see* Burial and coating assessment
Bend stiffener, failure modes of, 109
Bending moment capacity, 31–32
  bending stress and, 38
  corrosion in compression and, 31–32
  as defect depth function, 41f
  as defect width function, 42f, 44f
  for dented pipes burst pressure with longitudinal notch, 60–61
  maximum allowable, 45–49
    collapse pressure for external overpressure cases and, 47
    limit bending moment for external overpressure cases, 45–46
    limit bending moment for internal overpressure cases, 47–49
    safety factors for, 45, 46t
  pressure interaction with, 39–49
    analytical compared to FE results for, 39–44, 40f, 41f, 42f, 44f
  strength calculation guidelines for, 44–45
Bending stress, bending moment capacity and, 38
Bernoulli equation, 135–137, 312
Bias, influence of, 179, 179t
Bilby-Cottrell-Swinden dislocation model, 57–58
Biodegradation, 388
Biological leak detection methods, 127–128, 127f
Birdcaging, 107, 108f
Blockage, pipe, 114
Blockage risk assessment, 311–314, 329
  CoF for, 313–314, 314t
  PoF for, 312–313, 313t
Bore fluid parameter monitoring, for flexible pipes, 118t, 122
BOTDA, *see* Brillouin optical time-domain analysis

BOTDR, *see* Brillouin optical time-domain reflectometry
Brillouin optical time-domain analysis (BOTDA), 155–157
Brillouin optical time-domain reflectometry (BOTDR), 155–156, 156f
Brillouin scattering, 152–157, 153f, 154f, 156f
British Gas, 84–86
Buckling, 38, 55–56
Burial and coating assessment (BCA), 86
Burn-in phase, 272–273
Burst pressure, of dented pipes with longitudinal notch, 57–61
  bending moment and uniaxial tensile stress in, 60–61
  compliance modification for, 58–59
  flow stress modification for, 61
  geometry correction factors for, 59–60
  toughness modification for, 58
Burst strength criteria, for dented pipes, 61
Bursting criterion, for dented pipes, 53–54

C

Caliper pigs, 85
Capital expenditure (CAPEX), 135
Carbon dioxide (CO_2), 3–4
  composition of, 5
  sweet corrosion, 4–6
    chemical additives and, 15
    free spans and, 17–18, 18f
    H_2S and, 13–14
    inhibitors and, 14–15, 16f
    multiphase flow and, 16
    pH and, 14, 14f
    prediction models compared for, 10–11, 10f
    sensitivity analysis for, 11–18, 11t
    Shell model for predicting, 8–11, 10f
    single-phase flow and, 16, 17f
    temperature and, 12–13, 13f
    total pressure and CO_2 partial pressure and, 11, 12f
    water cut and, 16–17
Carcass collapse, 105–106, 106f
Cathodic protection (CP), 74, 75t
  anode sledges and, 91–92
  repairs, 90–92
Cause analysis, 176–177
  ETA for, 177
  FTA for, 177
  purposes of, 176–177
  risk analysis example for dropped object and quantitative, 201–203
    basic data and assumptions for, 203, 203t
    energy absorbed by steel pipe in, 202–203
    flow line or spool hit probability in, 202
    probability cones in, 201–202
  risk analysis example for subsea gas pipeline and, 196–198, 199t
Circumferential cracks, fracture of pipes with, 62–63
  fracture condition and critical stress, 62
  material toughness and, 62
  maximum allowable axial stress and, 63
  net section stress and, 62–63
Cleanup and recovery, of oil spills, 369, 387–390, 387f
Clustering, 107, 108f
CO_2, *see* Carbon dioxide
Coefficient of variation (COV), 297
CoF, *see* Consequence of failure
Coherent optical time-domain reflectometry (COTDR), 150–150
Collapse
  allowable corrosion depth based on, 260
  dented pipes, moment criterion for, 55
  from external pressure, 35–38, 36f
    as function of defect depth, 40f
    as function of defect width, 41f
  local buckling and, 44
  pressure for external overpressure cases, 47
  strength, 43
Collision, 335, 335f
Combined loads, 27–35, *See also* Moment capacity, under combined loads

Combustion, in consequence modeling, 188f, 190
Compatibility, 251
Compensatory restoration, 382–383
Compliance modification, 58–59
Compression
  corrosion in, 28–30
    bending moment capacity and, 31–32
  definition of, 29
Conceptual engineering, 253
Concrete sleeve installation, 89, 90f
Consequence analysis, 188–192
  consequence modeling for, 188–191, 188f
    combustion in, 188f, 190
    damage and loss in, 188f, 190
    discharge in, 188f, 189
    dispersion of gas in, 188f, 189
    dispersion of liquid in, 188f, 189
    ignition in, 188f, 189–190
    uncertainty in, 191
  for failure, 191–192, 192f, 193f
  risk analysis example for dropped object and, 205
  risk analysis example for subsea gas pipeline and, 198, 199t
Consequence of failure (CoF), 216, 347–349
  for blockage risk assessment, 313–314, 314t
  detailed assessment, 226–227
  economic consequences, 219, 224–225, 225t, 281, 282t, 348–349, 350t
  environmental consequences, 219–220, 220t, 224, 226t, 280–281, 281t, 348–349, 350t
  financial risk and, 254–256
  gas spills and, 354–358, 354f
    gas dissolution and jet-plume models integrated for, 356–358
    gas dissolution model and, 354–355
  introduction to, 345–346
  MTRA and, 340–342
    assessment methodology for, 340–341
    cost-efficiency analysis for, 341
    human reliability analysis for, 342
  oil spills and, 350–353, 378, 379f, 380t
    emulsification mechanism and, 353
    evaporation mechanism and, 352–353
    example of, 358–361, 359f, 359t, 360f, 361f
    spreading mechanism and, 351–352
  personnel consequences, 347–348, 349t
  purpose of, 345–346
  for QRA and target reliability, 294–295
  QRA for, 346
  QRBI and, 275, 280–281, 280t, 281t, 282t, 285, 286t
  quantitative risk acceptance criteria for, 346, 347f
  risk assessment, 229–230
  safety consequences, 219, 224, 225t, 280, 280t
Constant failure zone, 272–273
Construction vessels, 181, 198
Corning Glass Works, 145
Corroded pipe, 18–24
  B31G strength criterion for, 19–21
    evaluation of, 21
    maximum allowable defect length and depth in, 20
    maximum allowable design pressure in, 19
    problems with, 21
    safe maximum pressure level in, 20–21
    for spiral corrosion, 22, 22f
  defect width effect on, 24, 24f
  groove interactions with, 23
  NG-18 strength criterion for, 18–19
  pits interactions with, 23
  RBIM example and inspection frequency of, 207–210, 207t, 208t, 209f, 210f
  requalification criteria for, 4
  types of, 21–24, 21f
  weld interactions with, 23–24, 23f
Corrosion, *See also* Sour corrosion; Sweet corrosion
  collapse and allowable depth of, 260
  in compression, 28–30
    bending moment capacity and, 31–32
  defect prediction, 4–18
    growth and, 7–8
    inspection for, 7
    introduction to, 4–5

Corrosion (*Continued*)
parameters for, 8
reliability-based design for, 4
Shell model for, 8–11, 10f
for sour corrosion, 6–7
for sweet corrosion, 5–6
sweet corrosion models compared for, 10–11, 10f
definition of, 3
dry fatigue compared to, 111, 111f
external sheath damaged by, 109–110, 109f
as flexible pipe failure mechanism, 109–110, 109f
hoop stress and allowable depth of, 259–260
internal influences of, 3–4
reliability-based strength design for, 236–245, 236–237
CRs determined for, 258–259
design examples for, 239–243
dry gas line example for, 239–241, 240t, 241t, 242f
LSF for, 237, 238f
maximum allowable defect depth in, 239
model for, 237–239
recommendations for, 244–245
trends in, 243–244
wet liquid line example for, 241–243, 242f, 240t, 242t, 243t
spiral, B31G criterion for, 22, 22f
types of, 4, 21–24, 21f
width of, 24, 24f
Corrosion coating repair, 88
Corrosion rate uncertainty factor, 238–239
Corrosion rates (CRs), 258–259, 300
Cost of consequences, 265, 265t
Cost-efficiency analysis, for MTRA CoF assessment, 341
COTDR, *see* Coherent optical time-domain reflectometry
Coupon sampling and analysis, for flexible pipes, 122
COV, *see* Coefficient of variation
CP, *see* Cathodic protection
Cracks
dented pipes reliability-based assessment and size of, 66–70
fracture criterion for dented pipes with, 54
with longitudinal cracks, 56–61
fracture of pipes with circumferential, 62–63
fracture condition and critical stress, 62
material toughness and, 62
maximum allowable axial stress and, 63
net section stress and, 62–63
intelligent pigs for detection of, 84–85
longitudinal
failure pressure of pipes with, 56–57
fracture of pipes with, 56–61
CRs, *see* Corrosion rates
Cumulative impacts, 374
CYTOP, *see* Amorphous fluorinated polymer

D

Damage
accidental, 114–115
in consequence modeling, 188f, 190
definition of, 103
detailed assessment, 228
environmental, 256
event-based damage, 217
generic hazard and pipeline damage list, 182–183
screening assessment, 223
time-based damage, 217
DAS, *see* Distributed acoustic sensing
DDS, *see* Distributed disturbance sensor
de Waard model, *see* Shell model, for corrosion prediction
Deepwater pipe laying, flood prevention in, 98
Deepwater pipeline repair, 93–98
diverless repair research and development for, 95–96
introduction to, 93–95
midline replacement and, 97–98, 97f
pipeline replacement in, 94–95, 95f
SmartPlug for, 96–98, 96f, 97f

Defect depth, 258–259, 262, 263f
bending moment capacity as function of, 41f
collapse pressure as function of, 40f
in reliability-based strength design for corrosion, 239–239
Defect prediction, corrosion, 4–18
growth and, 7–8
inspection for, 7
introduction to, 4–5
parameters for, 8
reliability-based design for, 4
Shell model for, 8–11, 10f
for sour corrosion, 6–7
for sweet corrosion, 5–6
sweet corrosion models compared for, 10–11, 10f
Defect width
bending moment capacity as function of, 42f, 44f
collapse pressure as function of, 41f
corroded pipe effect of, 24, 24f
moment capacity reduction and, 33f, 34–35
Dented pipes
burst pressure with longitudinal notch in, 57–61
bending moment and uniaxial tensile stress in, 60–61
compliance modification for, 58–59
flow stress modification for, 61
geometry correction factors for, 59–60
toughness modification for, 58
causes of, 52
design examples with, 64–70
case description and input data for, 65, 65t
parameter measurements for, 65, 65t
reliability assessments for, 65–66, 66f, 67f, 68f
safety factors and, 66–70, 69t, 70f
sensitivity study for, 66–70, 69t, 70f
introduction to, 52
leakage and, 52
limit-state based criteria for, 52–56
burst pressure with combined dent and longitudinal notch, 57–61
burst strength criteria, 61
bursting criterion, 53–54
failure pressure of pipes with longitudinal cracks, 56–57
fatigue criterion, 54
fracture criterion for dented pipes with cracks, 54
general information on, 52–53
moment criterion, buckling and, 55–56
moment criterion, collapse, 55
out of roundness as serviceability limit state, 53
reliability-based assessment of, 63–64
crack sizes and, 66–70
design examples and, 65–66, 66f, 67f, 68f
design format for, 63–64
LSF for, 64
uncertainty measure in, 64
structural integrity of, 52, 64
Detailed assessment
acceptable annual failure probability, 230, 230t
data collection, 228
degradation mechanisms, 227–228
failure modes identification, 229
flowchart of, 226–227, 227f
internal corrosion, 228
pipeline segmentation, 229, 229f
in QRBI, 272
risk assessment, 229–230
safety classes, 230
Deterministic LCC model, 249
Direct impacts, 374
Discharge, in consequence modeling, 188f, 189
Dispersion of gas, in consequence modeling, 188f, 189
Dispersion of liquid, in consequence modeling, 188f, 189
Displacement-controlled situations, local buckling and, 44–45
Distributed acoustic sensing (DAS), 150–151

Distributed disturbance sensor (DDS), 150
Distributed fiber optic sensors, 148–157, 149f
  Brillouin scattering and, 152–157, 153f, 154f, 156f
  Raman scattering and, 151–152, 151f
  Rayleigh scattering and, 149–151
Distributed temperature sensing (DTS), 151–152, 151f
Diverless repair, 95–96
DNV ORBIT software, 271–272
DNV RP F101, 304–305
DNV-RP-H101, 309
Drift grounding, 340
Dropped object risk analysis, *see* Risk analysis example, for dropped object
Dry gas line example, for reliability-based strength design, 239–241, 242f, 240t, 241t
DTS, *see* Distributed temperature sensing
Durability, 251
Dynamic model-based system, 131

E

ECL, *see* ELF communication link
Economic consequences, 219, 224–225, 225t, 281, 282t, 348–349, 350t
Economic value analysis (EVA), 249–250
Eddy current inspection, for flexible pipes, 118t, 119–120, 119f
EGP, *see* Electronic gauging pig
EIA, *see* Environmental impact assessment
Elastic compliance factor, 58–59
Elastic wave inspection vehicle, 84–85
Electronic gauging pig (EGP), 85
ELF communication link (ECL), 96, 96f
ELF waves, *see* Extremely low-frequency waves
Emulsification mechanism, oil, 353
End fitting, failure modes of, 105
Engineered backfill installation, 89, 91f
"Engineering, procurement, and construction" (EPC), 253
Environmental consequences, 219–220, 220t, 224, 226t, 280–281, 281t, 348–349, 350t
Environmental damage, 256
Environmental impact assessment (EIA)
  example of, 374–375, 375t, 376f
  guidelines principles of, 365–366, 365f
  introduction to, 363–364
  motivation and object of, 364–365
  oil spill methodology for, 368–373, 368f
    cleanup and recovery in, 369
    environmental effects in, 368–369
  oil spill theory and, 369–373, 370f
    oil dispersion in, 370–371
    oil evaporation in, 371–373, 372f
    oil spreading in, 371
  stages of, 366–367, 367f
    baseline studies in, 366
    impact prediction and assessment in, 366
    mitigation in, 367
    monitoring in, 367
    scoping, 366, 367f
Environmental impacts, 373–374
Environmental risk, 174–175, 175t, 181–182
EPC, *see* "Engineering, procurement, and construction"
Erosion, 112, 112f
ETA, *see* Event tree analysis
EVA, *see* Economic value analysis
Evaporation mechanism, oil, 352–353, 371–373, 372f
Event tree analysis (ETA)
  for cause analysis, 177
  for gas release, 192f
  uses of, 311
Expected costs, calculating, 264f, 265–266, 266t
Explosion, 190, 335
External leak detection systems, 128–130
  fiber optic cables, 129–130
  hydrocarbon vapor sensing systems, 129
  vacuum annulus monitoring, 129
External sheath
  corrosion damaging, 109–110, 109f
  failure modes of, 107–108, 108f
  material selection of, 115

Extremely low-frequency waves (ELF waves), 96, 96f
Exxon Production Research, 95–96

F

Fabrication tolerance example, using LCC model, 257–267
  analysis procedure steps in, 258–267
    cost of consequence for, 265, 265t
    expected costs calculation for, 264f, 265–266, 266t
    failure modes considered for, 258
    initial costs for, 266, 266t
    life cycle costs compared for, 266–267, 267f
    limit state equations for, 258–261
    parameters and variables defined for, 261–263
    quality aspect considered for, 258
    reliability analysis for, 264, 264f
    structure definition for, 258
  background for, 257–258
  common input parameters for, 263, 264t
  defect length for, 262, 263f
  LSF in, 260–261
  operational data for, 261, 262t
  pipeline and environmental data for, 261, 262t
  wall thickness uncertainty in, 262–263, 263t
FAD, *see* Failure assessment diagram
Failure
  bathtub curve of, 272–273, 273f
  consequence analysis of, 191–192, 192f, 193f
  definition of, 103
  flexible pipes drivers and mechanisms of, 109–115
    accidental damage as, 114–115
    corrosion as, 109–110, 109f
    erosion as, 112, 112f
    fatigue as, 110–111, 111f
    pipe blockage or flow restriction as, 114
    pressure as, 113
    production fluid composition as, 114
    service loads as, 114
    temperature as, 112–113, 113f
  immediate, 257
  PARLOC database rates of, 278–279
  probability of, 217–218, 217t, 218f
  random, 182, 198
  time dependent, 257
  time independent, 257
Failure assessment diagram (FAD), 61
Failure modes, *See also* Consequence of failure; Probability of failure
  in fabrication tolerance example, using LCC model, 258
  of flexible pipes, 105–109
    of bend stiffener, 109
    of end fitting, 105
    of external sheath, 107–108, 108f
    of internal carcass, 105–106, 106f
    of internal pressure sheath, 106, 107f
    of pressure armor, 107
    risk management for, 104
    of tensile armor, 107, 108f
  reliability-based strength design identification of, 234
  risk analysis and qualitative review of, 182–185
    example of, 183–185
    generic hazard and pipeline damage list for, 182–183
  risk analysis with SRA estimating, 185–188
    simplified calculations of, 186, 186f
    strength and resistance model and, 187
    strength uncertainties evaluation for, 187–188
Failure pressure, of dented pipes with longitudinal cracks, 56–57
Failure statistics, for flexible pipes, 103–104, 104f
Fatal accident rate (FAR), 349–350
Fatalities, potential, 191–192
Fatigue
  corrosion fatigue compared to dry, 111, 111f
  dented pipes criterion for, 54
  as flexible pipe failure mechanism, 110–111, 111f
  wet compared to dry, 110

Fault tree analysis (FTA), 177, 311
FBG sensor, *see* Fiber Bragg Grating sensor
FDEMS, *see* Frequency-dependent electromagnetic sensing
FE, *see* Finite element
FEED, *see* Front end engineering design
FFS, *see* Fitness for service
Fiber Bragg Grating sensor (FBG sensor), 147–148, 148f
Fiber optic sensor techniques, 147–157
  BODTA and, 155–157
  BODTR and, 156f, 155–157
  DAS, 150–150, 150–151
  distributed fiber optic sensors, 148–157, 149f
    Brillouin scattering and, 152–157, 153f, 154f, 156f
    Raman scattering and, 151–152, 151f
    Rayleigh scattering and, 149–151
  DTS and, 151–152, 151f
  FBG sensor, 147–148, 148f
Fiber optics, *See also* Optical fibers
  for external leak detection, 129–130
  introduction to, 145–147
  subsea RTP monitoring with, 159–164
    fiber survival and, 163–164, 164t
    layout and integration for, 162, 162f, 163f
    objectives of, 160
    optical fiber choice for, 160
    optical fiber geometric structure for, 161, 161f
    pipe joint crossing solutions for, 162
  types of sensing, 158–159
    PCF, 158–159, 159f
    POF, 159
    telecommunication optical fiber, 158, 158f
Financial risk, for LCC model, 254–256
  CoF in, 254–256
  human loss in, 255–256
  PoF in, 254
Financial risk acceptance criteria, 175–176
Finite element (FE), 39–44, 40f, 41f, 42f, 44f
Fire, 336
FIREX, 295
First party individual risk, 180–181
Fishery resources study, 333
Fishing interaction, risks from, 181
Fitness for service (FFS), 289–292, *See also* Risk- and reliability-based FFS
Flexible pipes
  failure drivers and mechanisms of, 109–115
    accidental damage as, 114–115
    corrosion as, 109–110, 109f
    erosion as, 112, 112f
    fatigue as, 110–111, 111f
    pipe blockage or flow restriction as, 114
    pressure as, 113
    production fluid composition as, 114
    service loads as, 114
    temperature as, 112–113, 113f
  failure modes of, 105–109
    of bend stiffener, 109
    of end fitting, 105
    of external sheath, 107–108, 108f
    of internal carcass, 105–106, 106f
    of internal pressure sheath, 106, 107f
    of pressure armor, 107
    risk management methodology for, 104
    of tensile armor, 107, 108f
  failure statistics for, 103–104, 104f
  integrity management of, 103
    acoustic emission for, 118t, 121
    bore fluid parameter monitoring for, 118t, 122
    coupon sampling and analysis for, 122
    in design stage, 115–116
    eddy current inspection for, 119–120, 119f, 118t
    general and close visual inspection for, 117–119, 118t
    inspection and monitoring methods for, 117, 118t
    in installation and commissioning stages, 116–117
    in manufacturing stage, 116
    radiography for, 118t, 120

RAMS and MAPS for, 118t, 121
strategy for, 115–117
testing and analysis measures for, 122
ultrasonic techniques for, 118t, 120–121
vacuum testing of riser annulus for, 123
introduction to, 102–104, 102f
risk analysis of, 102–103
Flood prevention, in deepwater pipe laying, 98
Flooded member detection (FMD), 74, 75t
Flow rate, internal leak detection with change of, 132–133
Flow restriction, 114
Flow stress modification, 61
FMD, *see* Flooded member detection
Fracture
dented pipes criterion for
with cracks, 54
with longitudinal cracks, 56–61
of pipes with circumferential cracks, 62–63
fracture condition and critical stress, 62
material toughness and, 62
maximum allowable axial stress and, 63
net section stress and, 62–63
Free spans
intelligent pigs for detection of, 86
sweet corrosion sensitivity analysis and, 17–18, 18f
Frequency-dependent electromagnetic sensing (FDEMS), 122
Front end engineering design (FEED), 311
FTA, *see* Fault tree analysis
Fully plastic neutral axis, 30–31, 30f, 33f, 34
Funicular curve, 36–37

G

Gas bubbles, 356, 356f, 358
Gas dissolution model, 354–358
Gas hydrates, 315, 355
Gas mass loss, from gas dissolution, 357
Gas pipelines, PoF for, 314–322
hydrate formation curve for, 315–316, 316f
hydrate formation probability for, 317–322
main data parameters in, 317t
temperature distribution in, 318f
inlet pressure and temperature analysis in, 317–319, 322, 320f, 321f, 319t
pressure comparisons in, 318f
Gas spill consequences, 354–358, 354f
gas dissolution and jet-plume models integrated for, 356–358
gas dissolution model and, 354–355
General imaging (GI), 74, 75t
General visual imaging (GVI), 74, 75t
Generic hazard and pipeline damage list, 182–183
Geometry correction factors, 59–60
Geopig, 85–86
Gere, J. M, *see* Timoshenko and Gere's equations
GI, *see* General imaging
Glycol, 15, 259
Gradient intersection method, for leak detection, 135–137, 138f
Grooves, corroded pipe interactions with, 23
Grounding, 334–335, 334f
Grout bags, 89, 90f
Grouting methods, 93, 94f
Gulf of Mexico, oil spill in, 363–364
GVI, *see* General visual imaging

H

H Rosen Engineering (HRE), 85–86
H_2S, *see* Hydrogen-sulfide
Hardware-based leak detection methods, 127f, 128
Hazard identification, 176
in MTRA, 334–336
collision, 335, 335f
explosion, 335
fire, 336
grounding, 334–335, 334f
marine traffic accidents, 336, 337f
structural failure, 336
for risk analysis and qualitative review of failure modes, 182–183
risk analysis example, for subsea gas pipeline and, 195–196

HDPE, 115
Heat, conservation of, 357–358
HEGADA-S, 194
High-frequency eddy current (HFEC), 82–83
  applicability of, 83
  capabilities and limitations of, 83
  principle of, 82–83
High-pressure and high-temperature applications (HPHT), 102
HOE, *see* Human or organization error
Hoop stress, 29, 34–35, 37–38, 259–260
HPHT, *see* High-pressure and high-temperature applications
HRE, *see* H Rosen Engineering
Human loss, cost associated with, 255–256
Human or organization error (HOE), 178–180, 179t, 180f, 251–252
Human reliability analysis, for MTRA CoF assessment, 342
Hydratight, 94–95
Hydrocarbon vapor sensing systems, 129
Hydrogen-sulfide (H_2S), 3–4
  odor of, 6
  sour corrosion and, 4, 6–7
  sources and presentation of, 6
  sweet corrosion sensitivity analysis and, 13–14
Hydrostatic collapse, 113
Hydrotech, 94–95

I

IA, *see* Inhibitor availability
ICCP, *see* Impressed current cathodic protection
Identification of initial events, 176
IE, *see* Inhibitor efficiency
Ignition, in consequence modeling, 188f, 189–190
Immediate failure, 257
IMO, *see* International Marine Organization
Impact prediction and assessment, in EIA, 366
Indirect impacts, 374
Individual risk
  acceptance criteria for, 174
  first party, 180–181
  risk analysis example for subsea gas pipeline and, 196
Infant mortality phase, 272–273
Inhibitor availability (IA), 15, 16f
Inhibitor efficiency (IE), 15, 16f
Inhibitors, 14–15, 16f
Initial assessment
  CoF
    economy ranking, 225, 225t
    environmental ranking, 224, 226t
    safety ranking, 224, 225t
  PoF, 224, 224t
  in QRBI, 272
  risk ranking matrix, 225–226, 226t, 227t
Initial cost, for LCC model, 250–253
  design and engineering services in, 252–253
  in fabrication tolerance example, 266, 266t
  management and, 251–252
  marine operations in, 253
  materials and fabrication in, 253
  operation in, 253
  quality in, 250–251
Initial events
  identification of, 176
  probability of, 178–180
    bias' influence on, 179, 179t
    HOE frequency and, 178–180, 179t, 180f
  risk analysis example for subsea gas pipeline and, 197
In-kind restoration, 382–383, 382f
Inspection, *see* Pipeline inspection; Risk-based inspection
Inspection and monitoring methods, 117–122
  acoustic emission, 118t, 121
  bore fluid parameter monitoring, 118t, 121
  eddy current inspection, 118t, 119–120, 119f
  for flexible pipe integrity management, 117, 118t

general and close visual inspection, 117–119, 118t
radiography, 118t, 120
RAMS and MAPS, 118t, 121
ultrasonic techniques, 118t, 120–121
Integrity management, 73–74, *See also* Pipeline inspection
of flexible pipes, 103
acoustic emission for, 118t, 121
bore fluid parameter monitoring for, 118t, 122
coupon sampling and analysis for, 122
in design stage, 115–116
eddy current inspection for, 118t, 119–120, 119f
general and close visual inspection for, 117–119, 118t
inspection and monitoring methods for, 117, 118t
in installation and commissioning stages, 116–117
in manufacturing stage, 116
radiography for, 120, 118t
RAMS and MAPS for, 121, 118t
strategy for, 115–117
testing and analysis measures for, 122–123
ultrasonic techniques for, 120–121, 118t
vacuum testing of riser annulus for, 123
risk-based inspection and, 172–173
for RTP, 159–160
Integrity of pipeline system, 346, *See also* Risk assessment
Intelligent pigs, for pipeline inspection, 74, 84–86, *See also* Magnetic flux leakage; Ultrasonic pigs
caliper pigs, 85
crack detection with, 84–85
free span detection with, 86
general information on, 84
leakage detection with, 86
route survey with, 85–86
Internal carcass, failure modes of, 105–106, 106f
Internal leak detection systems, 128, 130–134
acoustic emission detectors, 133–134
change of flow rate or pressure, 132–133
MBLPC, 130–131
pressure trend monitoring, 131, 133
real-time transient modeling, 131–132, 132f
Internal overpressure, limit bending moment for, 47–49
Internal pressure sheath, 106, 107f, 115
International Convention for the Prevention of Pollution from Ships (MARPOL), 340–341
International Marine Organization (IMO), 340–341
ITU-T G.652 single-mode fiber, 160

J

Jet fire, 190
Jet-plume model, 356–358
Jumper replacement, 98

K

Kao, Charles, 145

L

LCC model, *see* Life cycle cost model
Leak detection algorithm, 139–140
Leak detection systems
biological methods for, 127–128, 127f
complications and challenges of, 126
external, 128–130
fiber optic cables, 129–130
hydrocarbon vapor sensing systems, 129
vacuum annulus monitoring, 129
gradient intersection method for, 135–137, 138f
groups of, 127–134, 127f
hardware-based methods for, 127f, 128
internal, 128, 130–134
acoustic emission detectors, 133–134
change of flow rate or pressure, 132–133
MBLPC, 130–131
pressure trend monitoring, 131, 133
real-time transient modeling, 131–132, 132f

Leak detection systems (*Continued*)
introduction to, 125–127
key attributes of different, 134–135, 136t
mass balance method for, 137–138
monitoring techniques for, 137t
negative pressure wave method for, 141–143, 142f
principles of, 135–143
purpose and principles of, 126
selection of, 127
software-based methods for, 127f, 128
statistical, 138–141
introduction to, 138–139
leak detection algorithm for, 139–140
sequential probability ratio test for, 140–141, 140f
Leakage
consequences of, 125–126
dented pipes causing, 52
intelligent pigs for detection of, 86
QRA identifying, 309
risers or repaired pipelines detection of, 98
of VLCC, 340
LEOS system, 129
Level of magnetism, 76–77
Life cycle cost model (LCC model), *See also* Fabrication tolerance example, using LCC model
benefit of, 248
EVA and, 249–250
financial risk for, 254–256
CoF in, 254–256
human loss in, 255–256
PoF in, 254
initial cost for, 250–253
design and engineering services in, 252–253
in fabrication tolerance example, 266, 266t
management and, 251–252
marine operations in, 253
materials and fabrication in, 253
operation in, 253
quality in, 250–251
introduction to, 248–250
on-bottom stability example using, 267–269
probabilistic compared to deterministic, 249
target reliability and, 290–291, 291f
time value of money for, 256–257
Limit bending moment, 45–49
Limit state function (LSF), 64, 234–234
in fabrication tolerance example, using LCC model, 260–261
in reliability-based strength design for corrosion, 237, 238f
Limit-state criteria, for dented pipes, 52–56
burst pressure with combined dent and longitudinal notch, 57–61
burst strength criteria, 61
bursting criterion, 53–54
failure pressure of pipes with longitudinal cracks, 56–57
fatigue criterion, 54
fracture criterion for dented pipes with cracks, 54
general information on, 52–53
moment criterion
buckling and, 55–56
collapse and, 55
out of roundness as serviceability limit state for, 53
Liquefied natural gas (LNG), 146–147
Liquid mass, conservation of, 357
LNG, *see* Liquefied natural gas
Load-controlled situations, local buckling and, 44–45
Load-resistance factored design (LRFD), 258
Local buckling, 44–45
Longitudinal cracks, 56–61
Longitudinal force, 34f, 35
Longitudinal notch, burst pressure of dented pipes with, 57–61
LRFD, *see* Load-resistance factored design
LSF, *see* Limit state function

M

Magnetic anisotropy and permeability system (MAPS), 118t, 121
Magnetic circuit, 76–77

Magnetic flux leakage (MFL), 76–80
applicability of, 80
capabilities and limitations of, 79–80
data analysis and, 79
magnetism and, 76–78, 77f
principle behind, 76
sensors and resolution for, 77–78
Magnetic reluctance, 76–77
Magnetism, 76–78, 77f
Management, in initial cost, 251–252
MAPS, *see* Magnetic anisotropy and permeability system
Marine operations, 253
Marine Safety Information System (MSIS), 337
Marine traffic accidents, 336, 337f
Marine traffic risk assessment (MTRA)
CoF and, 340–342
assessment methodology for, 340–341
cost-efficiency analysis for, 341
human reliability analysis for, 342
data collection for, 332–333
fishery resources study in, 333
offshore exploration, development, production activities study in, 333
origin, destination, marine traffic volume study in, 333
route, approach characteristics, navigability study in, 333
vessel information in, 332
hazard identification in, 334–336
collision, 335, 335f
explosion, 335
fire, 336
grounding, 334–335, 334f
marine traffic accidents, 336, 337f
structural failure, 336
introduction to, 332
PoF and, 336–340
Bayes method for, 337–338
numerical model method for, 338–339, 339f
ship collision probability in, 339–340
ship grounding probability in, 340
statistics method for, 337
procedure for, 332f
risk assessment methods for, 342–343
Marine traffic volume study, 333
MARPOL, *see* International Convention for the Prevention of Pollution from Ships
Mass balance method, for leak detection, 137–138
Mass balance with line pack compensation (MBLPC), 130–131
Material loss
causes of, 181–182
in consequence modeling, 188f, 190
risk analysis example for subsea gas pipeline and, 199, 200t
Material repair, 255
Material toughness, 62
Materials and fabrication costs, 253
Maximum allowable axial stress, 63
Maximum allowable bending moment, 45–49
collapse pressure for external overpressure cases and, 47
limit bending moment and
for external overpressure cases, 45–46
for internal overpressure cases, 47–49
safety factors for, 45, 46t
Maximum allowable defect length and depth, in B31G criterion, 20
Maximum allowable design pressure, in B31G criterion, 19
MBLPC, *see* Mass balance with line pack compensation
Mechanical damage, 52, 58, *See also* Cracks; Dented pipes
Merchant vessels, 181, 197, 197t
Metal loss inspection techniques, 76–84
general information on, 76
HFEC, 82–83
applicability of, 83
capabilities and limitations of, 83
principle of, 82–83
MFL, 76–80
applicability of, 80
capabilities and limitations of, 79–80
data analysis and, 79
magnetism and, 76–78, 77f
principle behind, 76
sensors and resolution for, 77–78

Metal loss inspection techniques (*Continued*)
RFEC, 83–84
ultrasonic pigs, 80–82, 80f
applicability of, 82
capabilities and limitations of, 82
data analysis and, 81
principle of, 80–81
sensors for, 81
Methanol, 15
MFL, *see* Magnetic flux leakage
Midline repair and tie-ins, 98
Midline replacement, 97–98, 97f
Miller's equations, 35
Mitigation, in EIA, 367
Moment capacity, under combined loads, 27–35, *See also* Bending moment capacity
bending moment capacity, 31–32
bending stress and, 38
corrosion in compression and, 31–32
cases of
corrosion in compression, 28–30
types of, 28f
definition of, 27–28
dented pipes criterion for
buckling and, 55–56
collapse and, 55
equations for, 32–35
axial force and, 34f, 35
defect width and, 33f, 34–35
fully plastic neutral axis and, 33f, 34
longitudinal force effect and, 34f, 35
fully plastic neutral axis and, 30–31, 30f, 33f, 34
general information on, 27–28
Momentum, conservation of, 357
MONA, 295
Money, time value of, 256–257
Monitoring, 367, *See also* Inspection and monitoring methods
Monte Carlo stochastic simulation method, 312
Mooney equation, 353
Mousse formation, 353
MSIS, *see* Marine Safety Information System
MTRA, *see* Marine traffic risk assessment
Multiphase flow, 16

N

Navigability study, 333
NDT, *see* Nondestructive testing
Negative pressure wave method, for leak detection, 141–143, 142f
Net section stress, 62–63
NG-18 criterion, 18–19
Nondestructive testing (NDT), 74, 75t
Nonideal gas law, 358
NORSOK model, 10–11, 10f
Numerical model method, for MTRA PoF assessment, 338–339, 339f

O

Ocean, oil spill's impact on, 385–386, 386f
OFDR, *see* Optical frequency-domain reflectometry
Offshore Pipelines and Risers (OPR), 146–147
Offshore Reliability Data Book, 196
Oil dispersion, 370–371
Oil evaporation, 352–353, 371–373, 372f
Oil mass, conservation of, 357–358
Oil pipelines, PoF for, 322–329
WAT curve and, 322–323, 323f
wax deposition probability calculations and, 323–329
data parameters for, 324t
inlet pressure and temperature analysis for, 324, 326t, 327f, 328f, 329
pressure comparisons for, 325f
temperature distribution for, 325f
Oil spills
cleanup costs and recovery with, 387–390, 387f
consequences of, 350–353, 378, 379f, 380t
emulsification mechanism and, 353
evaporation mechanism and, 352–353
example of, 358–361, 359f, 360f, 361f, 359t
spreading mechanism and, 351–352

cost correlation to size of, 389
dominant processes of, 380t
EIA methodology for, 368–373, 368f
cleanup and recovery in, 369
environmental effects in, 368–369
EIA theory of, 369–373, 370f
oil dispersion in, 370–371
oil evaporation in, 371–373, 372f
oil spreading in, 371
environment affected by, 383–386
ocean impact, 385–386, 386f
wildlife impact, 384–385, 385f
in Gulf of Mexico, 363–364
management of, 377–378
restoration planning for, 379–383, 382f
Oil spreading, 371
OLCR, *see* Optical low-coherence reflectometry
OLGA, 295
On-bottom stability, example using LCC model for, 267–269
Operation costs
initial costs of, 253
RBIM example reducing, 206–211
corroded pipes inspection frequency in, 207–210, 209f, 210f, 207t, 208t
prioritizing tasks in, 210–211, 211f
OPR, *see* Offshore Pipelines and Risers
Optical domain reflectometry (OTDR), 148–149
Optical fibers, *See also* Fiber optics
application of, 146–147
Brillouin scattering and, 152–157, 153f, 154f, 156f
fiber optic monitoring on subsea RTP and
choice of, 160
geometric structure of, 161, 161f
history of, 145–147
light propagation in, 145–146, 146f
PCF, 158–159, 159f
polymer, 159
Raman scattering and, 151–152, 151f
Rayleigh scattering and, 149–151
telecommunication, 158, 158f
temperature and coating of, 164, 164t
Optical frequency-domain reflectometry (OFDR), 148–149
Optical low-coherence reflectometry (OLCR), 148–149
OTDR, *see* Optical domain reflectometry
Out of roundness, 44, 53
Out-of-kind restoration, 382–383, 382f

P

PA-11/12, 115
PARLOC database, 272, 274, 283
failure rates from, 278–279
Pasquill stability, 195
PC, *see* Polycarbonate
PCF, *see* Photonic crystal fiber
PE, *see* Polyethylene
Personnel consequences, 347–348, 349t
pH, sweet corrosion sensitivity analysis for, 14, 14f
PHAST, 295
Photonic crystal fiber (PCF), 158–159, 159f
Pigs, *See also* Intelligent pigs, for pipeline inspection; Magnetic flux leakage
acoustic, 86
BCA, 86
caliper, 85
electronic gauging, 85
ultrasonic, 80–82, 80f
applicability of, 82
capabilities and limitations of, 82
data analysis and, 81
principle of, 80–81
sensors for, 81
Pipe blockage, 114
Pipe toughness, 58
Pipe wall magnetism, 77
Pipeline inspection, 73–86
external, 76
intelligent pigs for, 74, 84–86
caliper pigs, 85
crack detection with, 84–85
free span detection with, 86
general information on, 84
leakage detection with, 86
route survey with, 85–86
internal, 73–74

Pipeline inspection (*Continued*)
introduction to, 73–76
metal loss techniques for, 76–84
general information on, 76
HFEC, 82–83
MFL, 76–80, 77f
RFEC, 83–84
ultrasonic pigs, 80–82, 80f
methods and types of, 74, 75t
Pipeline integrity management, *see* Integrity management
Pipeline repair
deepwater, 93–98
diverless repair research and development for, 95–96
introduction to, 93–95
midline replacement and, 97–98, 97f
pipeline replacement in, 94–95, 95f
SmartPlug for, 96–98, 96f, 97f
general maintenance, 88–93
corrosion coating repair, 88
CP repairs, 90–92
span rectification measures, 92–93, 94f
submerged weight rectification, 88–89, 90f, 91f, 92f
methods, 86–93
conventional, 86–88, 87t
Pipeline replacement, deepwater, 94–95, 95f
Pipeline safety regulations, 73–74, *See also* Safety factors
Pipeline segmentation
for QRA and target reliability, 293
in QRBI, 277–278, 282–283
Pipeline strength uncertainties, 187–188
Pipeline system, integrity of, 346
Pits, corroded pipe interactions with, 23
PLL, *see* Potential loss of life
PMMA, *see* Polymethyl-methacrylate
PoF, *see* Probability of failure
POF, *see* Polymer optical fiber
Poisson's ratio, 36
Polyamide PA-11, 112–113
Polycarbonate (PC), 159
Polyethylene (PE), 161
Polymer optical fiber (POF), 159
Polymethyl-methacrylate (PMMA), 159
Polystyrene (PS), 159
Pool fire, 190
Powered grounding, 340
PPA, *see* Pressure point analysis
Preliminary engineering, 253
Pressure
B31G criterion
maximum allowable design pressure, 19
safe maximum pressure level, 20–21
bending moment capacity interaction with, 39–49
analytical compared to FE results for, 39–44, 40f, 41f, 42f, 44f
collapse from external, 35–38, 36f
as function of defect depth, 40f
as function of defect width, 41f
dented pipes with longitudinal cracks and failure, 56–57
dented pipes with longitudinal notch and burst, 57–61
external overpressure cases
collapse pressure for, 47
limit bending moment for, 45–46
as flexible pipe failure mechanism, 113
gas pipelines PoF analysis of inlet, 317–319, 322, 319t, 320f, 321f
gas pipelines PoF comparison of, 318f
hoop stress induced by, 37–38
internal leak detection with change of, 132–133
limit bending moment for internal overpressure cases, 47–49
longitudinal cracks and failure, 56–57
oil pipelines PoF analysis of inlet, 324, 329, 326t, 327f, 328f
oil pipelines PoF comparisons of, 325f
riser testing of, 98
SRA for risk- and reliability-based FFS and, 295–299, 299f
Pressure armor, failure modes of, 107
Pressure point analysis (PPA), 131
Pressure sheath, *see* External sheath; Internal pressure sheath
Pressure trend monitoring, 131, 133
Probabilistic LCC model, 249
Probability cones, 201–202

Probability of failure (PoF), 216–217, 217t
for blockage risk assessment, 312–313, 313t
damage progression, 218, 218f
detailed assessment, 226–227
estimating, 349–350
financial risk and, 254
of gas pipelines, 314–322
hydrate formation curve for, 315–316, 316f
hydrate formation probability for, 317–322
inlet pressure and temperature analysis in, 317–319, 322, 319t, 320f, 321f
main data parameters in, 317t
pressure comparisons in, 318f
temperature distribution in, 318f
initial assessment, 224, 224t
MTRA and, 336–340
Bayes method for, 337–338
numerical model method for, 338–339, 339f
ship collision probability in, 339–340
ship grounding probability in, 340
statistics method for, 337
of oil pipelines, 322–329
WAT curve and, 322–323, 323f
wax deposition probability calculations and, 323–329
for QRA and target reliability, 293–294
QRBI and, 274, 278–279, 283–285, 283t, 284t, 285t
risk assessment, 229–230
PROBAN, 65
Production activities study, 333
Production fluid, as flexible pipe failure mechanism, 114
Production loss, 255–256
PS, *see* Polystyrene
PTX, 85
PVDF, 115

Q

QA, *see* Quality assurance
QC, *see* Quality control
QRA, *see* Quantitative risk assessment
Qualitative risk acceptance criteria, 277, 277f
Quality, 250–251, 258
Quality assurance (QA), 116
Quality control (QC), 116
Quantitative risk acceptance criteria, 277, 277f, 346, 347f
Quantitative risk assessment (QRA), 272, *See also* Risk- and reliability-based FFS
for CoF, 346
flowchart of, 290f
leakage identified by, 309
methods and process of, 309–311, 312f
objectives of, 289–290, 304, 345–346
target reliability and, 292–295
CoF and, 294–295
pipeline segmentation and, 293
PoF and, 293–294
Quantitative risk assessment based RBI (QRBI)
case study for, 282–288, 283t
CoF identification in, 285, 286t
high-risk location and degradation mechanisms in, 286–287, 287t
inspection plan in, 287
pipeline segmentation in, 282–283
PoF and, 283–285, 283t, 284t, 285t
risk determination in, 285, 286t
CoF determination for, 280–281, 280t, 281t, 282t
definitions for, 272
detailed assessment in, 272
economic consequences in, 281, 282t
environmental consequences in, 280–281, 281t
high-risk locations and failure mechanisms in, 281
information collection for, 276–277
initial assessment in, 272
inspection plan in, 282
introduction to, 271–273
methodology and basic principle of, 273–276
CoF and, 275
PoF and, 274
risk determination and inspection plan for, 276

Quantitative risk assessment based RBI (QRBI) (*Continued*)
motivation and objective of, 272–273
pipeline segmentation in, 277–278
PoF determination for, 278–279
process of, 276–282, 276f
risk acceptance criteria in, 277, 277f
safety consequences in, 280, 280t

R

Radial deflection, 36
Radiography, for flexible pipes, 120, 118t
Raman scattering, 151–152, 151f
Ramberg-Osgood material curve, 39
RAMS, *see* Riser and anchor chain monitoring system
Random failure, 182, 198
RATs, *see* Rope access technicians
Rayleigh scattering, 149–151
RBI, *see* Risk-based inspection
RBIM, *see* Risk-based inspection and integrity management
Real-time transient modeling, 131–132, 132f
Reinforced thermoplastic pipe (RTP), 146–147
fiber optic monitoring on subsea, 159–164
fiber survival and, 163–164, 164t
layout and integration for, 162, 162f, 163f
objectives of, 160
optical fiber choice for, 160
optical fiber geometric structure for, 161, 161f
pipe joint crossing solutions for, 162
installation-related deficiencies of, 159–160
integrity management of, 159–160
Reliability-based assessment, of dented pipes, 63–64
crack sizes and, 66–70
design examples for, 65–66, 66f, 67f, 68f
design format for, 63–64
LSF for, 64
uncertainty measure in, 64
Reliability-based FFS, *see* Risk- and reliability-based FFS
Reliability-based strength design, 4
corrosion allowance in, 236–245, 236–237
CRs determined for, 258–259
design examples for, 239–243
dry gas line example for, 239–241, 242f, 240t, 241t
LSF for, 237, 238f
maximum allowable defect depth in, 239
model for, 237–239
recommendations for, 244–245
trends in, 243–244
wet liquid line example for, 241–243, 242f, 240t, 242t, 243t
failure modes identification for, 234
introduction to, 233–234
safety factor calibration for, 235–236
target reliability levels for, 235–236, 236t
uncertainty measures in, 234–235
distribution functions selected for, 234–235
statistical values determined for, 235
Reluctance, magnetic, 76–77
Remote field eddy current (RFEC), 83–84
Remotely operated towed vehicle (ROTV), 74, 93, 75t
Repair, *see* Pipeline repair
Requalification criteria, 4
Restoration planning, for oil spills, 379–383, 382f
RFEC, *see* Remote field eddy current
Riser and anchor chain monitoring system (RAMS), 118t, 121
Riser annulus, vacuum testing of, 123
Riser replacement or repairs, 98
Risk. *See also specific risks*
definition of, 346
environmental
acceptance criteria for, 174–175, 175t
causes of, 181–182
QRBI determination of, 276, 285, 286t
Risk acceptance criteria

in QRBI, 277, 277f
in risk assessment, 308–309, 310t
Risk analysis, *See also* Consequence analysis
acceptance criteria and, 173–176
for environmental risk, 174–175, 175t
for financial risk, 175–176
general information on, 173
for individual risk, 174
for societal risk, 174, 174f
cause analysis and, 176–177
ETA for, 177
FTA for, 177
purposes of, 176–177
causes of risk, 180–182
construction vessels and, 181
first party individual risk, 180–181
fishing interaction as, 181
merchant vessels and, 181
random failures and, 182
societal, environmental, material loss, 181–182
concepts of, 171, 172f
failure modes qualitative review and, 182–185
example of, 183–185
generic hazard and pipeline damage list for, 182–183
failure modes SRA estimation and, 185–188
simplified calculations of, 186, 186f
strength and resistance model and, 187
strength uncertainties evaluation for, 187–188
of flexible pipes, 102–103
identification of initial events and, 176
initial events probability and, 178–180
bias' influence on, 179, 179t
HOE frequency and, 178–180, 179t, 180f
introduction to, 171–173
objectives of, 171
Risk analysis example, for dropped object, 200–205
acceptable risk levels for, 200–201
consequence analysis in, 205
quantitative cause analysis for, 201–203
basic data and assumptions for, 203, 203t
energy absorbed by steel pipe in, 202–203
flow line or spool hit probability in, 202
probability cones in, 201–202
results of, 204–205
energy absorbed by steel pipe in, 205
probabilities in, 204–205
Risk analysis example, for subsea gas pipeline, 193–200
cause analysis and, 196–197
gas releases in, 193–196
airborne dispersion and, 194
discharge and, 194, 194t
hazard ranges and, 195–196, 196t
Pasquill stability and, 195
representative hole sizes and, 193, 194t
subsea plume and, 194
water depth effect on, 195
wind speeds and, 195, 195t
individual risk and, 196
material loss risk in, 199, 200t
risk estimation in, 200
societal risk and, 197–199
cause and consequence analysis in, 198, 199t
construction vessels in, 198
estimation of, 199
initial incidents in, 197
merchant vessels in, 197, 197t
random failures in, 198
Risk- and reliability-based FFS, 304–305, *See also* Quantitative risk assessment
CR and, 300
data collection requirements for, 292
example of, 300–305
analysis results for, 300–304, 301f, 302f, 303f, 304f, 301t
data of subsea oil pipeline for, 300, 300t
flowchart of, 290f
further study of, 305
introduction to, 289–292
SRA method for, 296–298, 296f, 297t
pressure capacity in, 295–299, 299f

Risk- and reliability-based FFS (*Continued*)
retaining pressure capacity and, 295–299
strength uncertainties evaluation in, 298, 299t
target reliability and, 290–292, 291f, 291t
Risk assessment, 329, *See also* Marine traffic risk assessment; Quantitative risk assessment
blockage, 311–314, 329
CoF for, 313–314, 314t
PoF for, 312–313, 313t
definition of, 346
gas pipelines PoF for, 314–322
hydrate formation curve for, 315–316, 316f
hydrate formation probability for, 317–322
inlet pressure and temperature analysis in, 317–319, 322, 320f, 321f, 319t
main data parameters in, 317t
pressure comparisons in, 318f
temperature distribution in, 318f
introduction to, 307–308
method of, 308–311, 347f
MTRA methods for, 342–343
oil pipelines PoF for, 322–329
WAT curve and, 322–323, 323f
wax deposition probability calculations and, 323–329
probability in, 308t
risk acceptance criteria in, 308–309, 310t
Risk management, for flexible pipes and failure modes, 104
Risk matrix, 310t
Risk-based inspection (RBI), 206, 271–272, *See also* Quantitative risk assessment based RBI
acceptance criteria, 221–222, 222t
CoF, 216
economic consequence, 219
environmental consequence, 219–220, 220t
safety consequence, 219
types, 218–219
detailed assessment
acceptable annual failure probability, 230, 230t
data collection, 228
degradation mechanisms, 227–228
failure modes identification, 229
flowchart of, 226–227, 227f
internal corrosion, 228
pipeline segmentation, 229, 229f
risk assessment, 229–230
safety classes, 230
event-based damage, 231, 232t
failure causes, 217
failure modes, 216
initial assessment, 223–226, 224t, 225t, 226t, 227t
optimized inspection scheme, 215, 215f
PoF, 216
damage progression, 218, 218f
qualitative RBI analysis, 217, 217t
probabilistic risk analysis, 214–215
process of, 214–215, 222
risk estimation, 220–221, 221t
screening assessment, 222–223, 223t
subsea pipeline inspection, 213–214
time-based damage, 231, 231f
Risk-based inspection and integrity management (RBIM), 172–173
operation cost reduction example with, 206–211
corroded pipes inspection frequency in, 207–210, 209f, 210f, 207t, 208t
prioritizing tasks in, 210–211, 211f
Rock dumping, 91f
Rope access technicians (RATs), 74, 75t
ROTV, *see* Remotely operated towed vehicle
Route survey, intelligent pigs for, 85–86
RTP, *see* Reinforced thermoplastic pipe

S

Safe maximum pressure level, in B31G criterion, 20–21
Safety, 251
Safety consequences, 219, 224, 225t, 280, 280t
Safety critical element (SCE), 117
Safety factors

dented pipes design examples and, 66–70, 69t, 70f
for maximum allowable bending moment, 45, 46t
pipeline safety regulations, 73–74
reliability-based strength design calibration of, 235–236
target reliability levels for, 235–236, 236t
Salinity, conservation of, 357–358
SAM, *see* System action management
Sandbags, 89, 90f
SCADA computer, 131, 132f
Scale, 5–6
SCC, *see* Surface control center
SCE, *see* Safety critical element
Scoping, 366, 367f
Screening assessment, 222–223, 223t
Secondary impacts, 374
Segmentation, pipeline, *see* Pipeline segmentation
Sensing fiber optics
PCF, 158–159, 159f
POF, 159
telecommunication optical fiber, 158, 158f
types of, 158–159
Sensors
for MFL, 77–78
for ultrasonic pigs, 81
Sequential probability ratio test, 140–141, 140f
Service loads, as flexible pipe failure mechanism, 114
Serviceability, 251
Serviceability limit-state criteria, 53, 200
Shell, 95–96, 275
Shell model, for corrosion prediction, 8–11, 10f
Ship collision probability, 339–340
Ship grounding probability, 340
Shoreline oiling, 388–389
SIF, *see* Stress intensity factor
Single-phase flow, sweet corrosion sensitivity analysis and, 16, 17f
SmartPlug, 96–98, 96f, 97f
SMYS, *see* Specified minimum yield stress
Snell's law, 145–146
Societal risk
acceptance criteria for, 174, 174f
causes of, 181–182
risk analysis example for subsea gas pipeline and, 197–199
cause and consequence analysis in, 198, 199t
construction vessels in, 198
estimation of, 199
initial incidents in, 197
merchant vessels in, 197, 197t
random failures in, 198
Software-based leak detection methods, 127f, 128
Sour corrosion (H_2S corrosion), 4, 6–7
Span rectification measures, 92–93, 94f
Specified minimum yield stress (SMYS), 19
Spiral corrosion, B31G criterion for, 22, 22f
Spool piece installation, 94–95, 95f
Spreading mechanism, oil, 351–352
SRA, *see* Structural reliability analysis
SSC, *see* Sulfide stress cracking
Stabilization mattresses, 89, 92f
Standard depth of penetration, 119–120
Statistical leak detection systems, 138–141
introduction to, 138–139
leak detection algorithm for, 139–140
sequential probability ratio test for, 140–141, 140f
Statistics method, for MTRA PoF assessment, 337
Stokes light, 152–153
Strength uncertainties, 187–188
Stress intensity factor (SIF), 58
Structural failure hazard, 336
Structural integrity, of dented pipes, 52, 64, *See also* Reliability-based assessment, of dented pipes
Structural reliability analysis (SRA), 172–173, 218, 289–290
for failure mode estimation, 185–188
simplified calculations of, 186, 186f
strength and resistance model and, 187
strength uncertainties evaluation for, 187–188

Structural reliability analysis (SRA) (*Continued*)
flowchart of, 290f
for risk- and reliability-based FFS, 296–298, 296f, 297t
pressure capacity in, 295–299, 299f
strength uncertainties evaluation in, 298, 299t
STRUREL, 65
Submerged weight rectification, 88–89
concrete sleeve installation and, 89, 90f
engineered backfill installation and, 89, 91f
sand or grout bag installation and, 89, 90f
stabilization mattresses and weight saddles installation, 89, 92f
Subsea gas pipeline risk analysis, *see* Risk analysis example, for subsea gas pipeline
Subsea plume, 194
Sulfide stress cracking (SSC), 6
SureFlex JIP, 117
Surface control center (SCC), 96, 96f
Sweet corrosion (CO_2 corrosion), 4–6
prediction models compared for, 10–11, 10f
sensitivity analysis for, 11–18, 11t
chemical additives and, 15
free spans and, 17–18, 18f
H_2S and, 13–14
inhibitors and, 14–15, 16f
multiphase flow and, 16
pH and, 14, 14f
single-phase flow and, 16, 17f
temperature and, 12–13, 13f
total pressure and CO_2 partial pressure and, 11, 12f
water cut and, 16–17
Shell model for predicting, 8–11, 10f
SYSREL, 261, 264, 269
System action management (SAM), 342

T

Target reliability
LCC model and, 290–291, 291f
QRA and, 292–295
CoF and, 294–295
pipeline segmentation and, 293
PoF and, 293–294
risk- and reliability-based FFS and, 290–292, 291f, 291t
Telecommunication optical fibers, 158, 158f
Temperature
DTS and, 151–152, 151f
as flexible pipe failure mechanism, 112–113, 113f
gas pipelines PoF analysis of inlet, 317–319, 322, 320f, 321f, 319t
gas pipelines PoF distribution of, 318f
oil pipelines PoF analysis of inlet, 324, 329, 326t, 327f, 328f
oil pipelines PoF distribution of, 325f
optical fiber coatings and, 164, 164t
sweet CO_2 corrosion sensitivity analysis and, 12–13, 13f
Tensile armor, failure modes of, 107, 108f
Testing and analysis measures
coupon sampling and analysis, 122
for flexible pipe integrity management, 122–123
vacuum testing of riser annulus, 123
Tie-ins, deepwater flow line and pipeline, 98
Time dependent failure, 257
Time independent failure, 257
Time value of money, for LCC model, 256–257
Timoshenko and Gere's equations, 35, 38–39
Toughness, pipe, 58
Traffic accidents, marine, 336, 337f

U

Ultimate limit state, 200
Ultrasonic pigs, 80–82, 80f
applicability of, 82
capabilities and limitations of, 82
data analysis and, 81
principle of, 80–81
sensors for, 81
Ultrasonic techniques, for flexible pipes, 118t, 120–121
Uncertainty measures, 234–235
Unconfined vapor cloud explosion (UVCE), 190

Uniaxial tensile stress, 60–61
UVCE, *see* Unconfined vapor cloud explosion

V

Vacuum annulus monitoring, 129
Vacuum testing, of riser annulus, 123
Valve repairs or change-outs, 98
Very large crude carrier (VLCC), 340
Visual inspection, for flexible pipes, 117–119, 118t
VIVs, *see* Vortex-induced vibrations
VLCC, *see* Very large crude carrier
Von Mises yield criterion, 29
Vortex-induced vibrations (VIVs), 110

W

Wall thickness
  determinations for, 233–233
  in fabrication tolerance example, using LCC model, 262–263, 263t
WAT curve, *see* Wax appearance temperature curve
Water cut, 16–17
Water depth, 195
Wax appearance temperature curve (WAT curve), 322–323, 323f
Weight saddles, 89, 92f
Welds, corroded pipe interactions with, 23–24, 23f
Wet liquid line example, for reliability-based strength design, 241–243, 242f, 240t, 242t, 243t
Width, defect, *see* Defect width
Wildlife, oil spill's impact on, 384–385, 385f
Wind speeds, 195, 195t
WOAD, *see* World Offshore Accident Databank
Work-class remotely operated vehicle (WROV), 74, 75t
World Offshore Accident Databank (WOAD), 337
WROV, *see* Work-class remotely operated vehicle

X

XLPE, 115

Y

Young's modulus, 36